Cooper, Michelle (2024) ***The character, dynamics and sources of sediments in Lake Dalrymple: insights and implications for reservoir management.*** **PhD Thesis, James Cook University.**

The character, dynamics and sources of sediments in Lake Dalrymple: insights and implications for reservoir management

Thesis submitted by
Michelle Cooper B.Sc. (Hons.)

in December 2024
For the degree of Doctor of Philosophy
in the College of Science and Engineering
James Cook University

Acknowledgements

This has been an incredibly long journey, one I often thought I wouldn't see the end of! I am indebted to the guidance and encouragement of my advisors past and present: Prof. Graham Shields, forever supportive and objective; John Faithful; Dr Stephen Lewis, who, before he became my supervisor, was my ever-reliable field hand; Prof. Scott Smithers and Dr Raphael Wust.

This project relied on fieldwork and I had many field hands: Dr Stephen Lewis, Prof. Graham Shields, Kevin Hooper, Dr Diane Jorgensen, Anne Gore (vale), Clive Grant, Timothy Austin, and Andrea Sorbello Lewis. Equipment was supplied or made by the talented Paul Givney, Clive Grant and Matthew Carey. Special thanks go to Tony Bailey, Ron Jordan and Gary Caddies of Sunwater—without them I might still be stranded in the middle of the reservoir!

I spent many hours in the lab. I thank Liz Webber, Bill Pappas, Tara Webster, Simon Webber and Christian Thun, all lab gurus at Geoscience Australia; Gordon Warria, Elvy Grigolato and the team at the Advanced Analytical Centre at JCU; the lab team at TropWATER; and Ross Freeman (vale) who was always ready to discuss the complexities of XRD analysis.

I appreciate and acknowledge the specialist skills of those people around me: my GIS gurus Mirjam Maughan and Steven Ackerly; Dr Thomas Stieglitz who processed my seismic data; Dr David Champion with his encyclopaedic knowledge of Queensland geology, geochemistry and isotopes; and Dr Patrice de Caritat and Helen Arnold for knowing everything about statistics.

I gratefully acknowledge the support of Geoscience Australia, particularly Dr Anthony Budd, Dr Adrian Hitchman and Allison Britt for being supportive bosses and keeping plenty of tissues in their offices.

I have many colleagues I'm proud to call friends; people who didn't give up on me, even when I wanted to give up on myself. Dr Diane Jorgensen, Kirsten Perry and Prof. Jody Webster, I thank you for being supportive, understanding and providing constructive input. Dr Claire Krause, your help and support has been amazing—is there any problem that cannot be solved with cake?! Likewise, Dr Aleks Kalinowski has been an amazing mentor.

Steven Ackerly, thank you and LB for being there for me and doing your best to keep me sane.

Last, but not least I would like to thank my parents Helen and John Whitbourn, who supported me in every way they could. I dedicate this thesis to my mother Helen Whitbourn, who never gave up on me and always accepted me as I am. Her encouragement and support were unwavering. Thank you for believing in me for all these years. I miss you more than I ever thought possible.

Acknowledgement of Country

I acknowledge all the Traditional Custodians of Country where this research was conducted and written up and their continuing connection to land, sea and community. I pay my respects to them, their cultures, Elders and youth; past, present and emerging.

Statement of the contribution of others

Advisors

Professor Graham Shields, Department of Earth Sciences, University College London

Professor Scott Smithers, College of Science and Engineering, and Centre for Tropical Water & Aquatic Ecosystem Research (TropWATER), James Cook University

Dr Stephen Lewis, Catchment to Reef Research Group, TropWATER, James Cook University

Nature of Assistance	Contribution	Contributor
Intellectual support	Proposal writing	Mr John Faithful, Golder Associates Dr Stephen Lewis, JCU
	Data processing & analysis	Dr Thomas Stieglitz, JCU Mr Ross Freeman (vale), Sietronics Dr David Champion, Geoscience Australia
	Statistical support	Ms Helen Arnold Dr Patrice de Caritat, Geoscience Australia
	Cartography & GIS	Ms Mirjam Maughan, Dept of Resources, Qld Mr Steven Ackerly Mr Colin Kimber, Geoscience Australia
	Editorial assistance	Dr Stephen Lewis, JCU Prof. Graham Shields, University College London Prof. Scott Smithers, JCU Mr John Faithful, Golder Associates Dr Patrice de Caritat, Geoscience Australia Dr Claire Krause, Geoscience Australia Dr David Champion, Geoscience Australia Dr Aleks Kalinowski, Geoscience Australia
Financial Support	Fee waiver & stipend	School of Earth Sciences (now College of Science and Engineering), JCU
	Research & travel	Land and Water Australia Contaminants Program grant (Project JCU 18)
	Research	JCU Graduate Research Scheme Geoscience Australia
Data collection and research assistance	Fieldwork	Dr Stephen Lewis, JCU Prof. Graham Shields, University College London Mr Kevin Hooper, JCU

		Dr Diane Jorgensen, Geoscience Australia Ms Anne Gore (vale), JCU Mr Timothy Austin Mrs Andrea Sorbello Lewis Mr Ron Jordan, Sunwater Mr Tony Bailey, Sunwater Mr Clive Grant, JCU Mr Paul Givney, JCU Mr Brett Baker, JCU Mr Matt Carey, Geoscience Australia
	Lab work	Advanced Analytical Centre, JCU, incl. Mr Gordon Warria, Mr Elvy Grigolato, Mr Alan Chappell and Dr Sharon Ness TropWATER, JCU Geoscience Australia laboratories, incl. Mrs Liz Webber, Mr Bill Pappas, Ms Tara Webster, Mr Christian Thun and Mr Simon Webber Centre for Microscopy and Micro Analysis, University of Queensland

Statement of the contribution of co-authors

The following chapters have been published or are being prepared for publication. Below is an overview of each co-author's contributions to the publications.

Chapter	Publication details	Contributions of each author
2	Cooper, M., Lewis, S. E., & Smithers, S. G. (2017). Spatial and temporal dynamics of suspended sediment causing persistent turbidity in a large reservoir: Lake Dalrymple, Queensland, Australia. *Marine and Freshwater Research*, 68(7), 1377–1390. https://doi.org/10.1071/MF16316	The authors co-developed the research question. Cooper undertook field sampling with assistance from Lewis (& others as previously acknowledged). Cooper prepared and analysed all samples (exception some water quality and Total Organic Carbon analyses). Cooper interpreted the data and developed the figures and tables. Cooper and Helen Arnold conducted the statistical analysis. Cooper wrote the first draft of the paper which was revised with editorial input from co-authors and Prof. Graham Shields. Further editorial input was provided by John Faithful, anonymous reviewers, and Natalie Korszniak, Copy Editor, and the Associate Editor, both of *Marine and Freshwater Research*.
3	Cooper, M., Lewis, S. E., Smithers, S. G. & Faithful, J. W. (in prep). Effect of turbid inflow on sediment transport and deposition in a stratified reservoir in the seasonally dry tropics of Queensland, Australia.	Cooper undertook field sampling with assistance from Lewis and others. Cooper prepared and analysed samples, interpreted the data and constructed the figures and tables. Cooper wrote the first draft of the paper and revised it following editorial input from the co-authors, Dr Claire Krause and Prof. Graham Shields.

4	Cooper, M., Lewis, S. E., Smithers, S. G. & Zhao, J-X. (in prep). Geochemistry and particle size of core sediments from Lake Dalrymple: sediment distribution and implications for source.	Cooper designed the field sampling program and conducted sediment coring and grab sampling with the assistance of Lewis and Clive Grant. Cooper sub-sampled cores, and prepared and analysed all sediment samples. Cooper conducted the data analysis with assistance from Dr Patrice de Caritat and Dr David Champion. Cooper constructed the figures and tables. Cooper wrote the first draft of the paper and revised it following editorial input from co-authors Stephen Lewis and Prof. Graham Shields, and Patrice de Caritat, and David Champion.
5	Cooper, M., Lewis, S. E., Stieglitz, T. C., & Smithers, S. G. (2018). Variability of the useful life of reservoirs in tropical locations: A case study from the Burdekin Falls Dam, Australia. *International Journal of Sediment Research*. https://doi.org/10.1016/j.ijsrc.2017.11.002	The authors co-developed the research question in collaboration with Prof. Graham Shields and Mr John Faithful. Cooper and Lewis conducted sediment sampling with the assistance of Clive Grant. Cooper prepared and analysed sediment samples. Lewis provided technical instruction and Stieglitz processed the seismic and bathymetric data. Cooper interpreted the data and constructed the figures and tables. Cooper managed draft preparation with editing input from co-authors. Further editorial input was provided by anonymous reviewers, and Charles Melching, Associate Editor, and the Submission Editor, both of *International Journal of Sediment Research*.

Abstract

This research presents the first detailed study of sediment sources, transport and deposition within Lake Dalrymple, a key component of the extensive Burdekin River system. Dams and their reservoirs are considered vital to ensure water and power supply for growing populations around the world. Minerogenic turbidity in reservoirs may negatively affect aquatic ecology and water infrastructure, and, along with deposited sediment, influences the management and performance of a dam. Lake Dalrymple, a large reservoir formed by the Burdekin Falls Dam (BFD) and located in the seasonally dry tropics of northern Queensland, has suffered from elevated turbidity since its completion in 1987.

The turbidity in Lake Dalrymple, the BFD reservoir, is largely due to suspended sediment, transported into the reservoir during wet-season flow events that carry an average of 2.6 million tonnes of sediment. These high sediment loads also have the potential to shorten the dam's lifespan. To carry out a detailed assessment of sediment characteristics and behaviour within the reservoir under varying flow conditions, water and sediment sampling was conducted over three consecutive median to below-median rainfall and discharge water years (2003–2006), and again five years later. Suspended and benthic sediment samples were then analysed for concentration, particle size, organic content, and mineralogy.

Chapter two examines the cause and variability of the persistent (year-round) turbidity in Lake Dalrymple, by focussing on the characteristics of suspended and benthic sediment samples collected during four dry seasons (May–November; 2004, 2005, 2006 and 2011). Water in the reservoir remained turbid (>45 NTU) throughout the year due to colloidal particles (<0.9 μm) composed of clay and mica minerals remaining in suspension. Benthic sediments ranged from 1 to 30 μm in size indicating that the resuspension of reservoir bottom sediments has little effect on turbidity. This study also found that dry season turbidity levels are strongly affected by the magnitude and duration of inflow waters from the preceding wet season, reflecting the limited availability of suspended particles delivered from the upstream catchment and the ability of large (in magnitude and/or duration) flows to flush the reservoir of suspended sediment. Elevated turbidity in the reservoir and downstream irrigation areas during the dry season is likely to remain a common feature and must be incorporated into all agricultural and wetland management plans.

The research outlined in chapter three focusses on the transport and delivery of suspended sediment to Lake Dalrymple during the wet season (December–April). The reservoir stratifies thermally in the spring and early summer, developing a thermocline between 5 and 15 m that is shallowest in upstream areas of the reservoir. This stratification allows turbid inflows (up to 2080 NTU), which carry an average of 2.6 million tonnes of sediment annually, to form turbidity currents that travel through the reservoir as an interflow. During flow events, turbid interflows in deeper parts of the reservoir (>20 m) were found to transition into underflows, disrupting stratification. These turbidity currents extend through the reservoir all the way to the dam wall, even in years of below-average (mean) flow. Overflow of the dam also occurs during most below-average to average flow events (dependent on reservoir volume prior to each wet season and the frequency of wet season inflow events), discharging turbid water carrying fine-grained sediment (97% of particles <62.5 µm) and limiting the amount of fine sediment deposited in the reservoir. The consistent formation of turbidity currents in Lake Dalrymple allows greater predictability of, and control over, sediment transport behaviour.

An examination of the particle size of turbidity current and benthic sediments from samples collected throughout the reservoir found that sediment >126 µm is largely absent from wet season inflow in below-average flow events and is moved through the reservoir as bedload (a process restricted to the uppermost reaches) or deposited in the reservoir's upper reaches. A substantial increase in particle size was observed in benthic sediment samples from the southern Burdekin, southern Suttor and Central sections of the reservoir collected after above-average inflow events, with peaks shifting from 6–14 µm to 11–400 µm.

Chapter four investigates changes in sediment composition, geochemistry, and particle size over time (the 24 years post-dam construction) and by spatial location to better understand the sources and effect of sediment deposited within Lake Dalrymple. Fifty-one cores and sediment grab samples were collected throughout the reservoir. Sub-samples were analysed for particle size (n=281), major and trace elements, and mineralogy (n=162). The mineralogy of benthic sediment was similar across all sites with sediments composed of quartz, muscovite/illite, kaolinite and smectite group clays. Differences in sediment geochemistry, mineralogy and particle size observed within the reservoir were found to be dominantly spatial and not temporal, with greater differences in geochemistry and size observed between locations rather than with depth. All analyses highlighted two sediment populations that had common characteristics: sediment from the Burdekin and Central sections of the reservoir grouped together, as did sediments from the Suttor and Eastern sections.

The physical and geochemical characters of these two groups of sediment in the reservoir were identified. Coarser (silt and sand sized) particles were found in the North and South Burdekin, South Suttor and Central sections of the reservoir and are attributed to the narrow form of the Burdekin arm, which remains riverine during inflow and carries larger particles further into the reservoir. These sediments also contained higher concentrations of quartz, Sr, Ca and Na, and less Rb and Cs, than samples from the Suttor and Eastern sections. Clay (up to 55%) and fine silt-sized particles dominated in the Eastern and North Suttor sections. A decrease in particle size was seen from the northern point of inflow (North Burdekin) to the dam wall (Eastern Reservoir) and from the southernmost point of inflow. This fractionation and sorting of sediment as it moves through the reservoir is further complicated by in-reservoir sorting. Sr isotope ratios from 26 sub-samples highlighted the presence of Burdekin and Suttor end-members and indicated that the contribution to sediments from the Suttor source increased as samples got closer to the dam wall, with 71%–83% of sediment deposited in the Central Reservoir from the Burdekin River system, and 46%–58% of sediment deposited in the Eastern Reservoir from the Suttor/Belyando/Cape River system. Sediment was observed to preferentially deposit in the relict river channel, particularly in the northern Burdekin section and central to eastern sections of the BFD reservoir, but no sediment has built up immediately behind the dam wall where it could negatively impact on dam operations by blocking water intake structures. The extensive sediment geochemistry dataset created by this study creates an environmental baseline for sediment in the reservoir that can be used in any future evaluations of sediment quality (for example, of heavy metal concentrations) or distribution and will contribute to an appropriate management strategy for this system.

Chapter five details a quantitative assessment of sediment deposition in the reservoir used to estimate the useful life of the BFD and examine that life in a global context. Two independent methods were used to calculate the volume of sediment deposited in Lake Dalrymple since construction. The average annual trapping efficiency of the dam was calculated to be 71% indicating that that 68 million t, or 65 million m^3, of sediment was trapped in the reservoir over the 24 years from construction to 2011. Extrapolating the depth of deposited sediment using data from sediment cores produced a comparable estimate of 61 million m^3 of sediment deposited to 2011. This sediment volume equates to an average of 0.15% of capacity lost per year since construction was completed, from an average deposition rate of 1.2 cm yr^{-1} if spread evenly throughout the dam. If current sediment loads/climate regimes persist, reservoir capacity will be reduced by 50% after 345 years. However, the useful life of the BFD reduces to 276 years when drawdown data are considered, as the reservoir experiences a 60% drawdown return period of 1 in approx. 15 years so its use would be affected once 40% of storage was filled with sediment.

The BFD was found to have a slightly longer useful life than similar large tropical to sub-tropical dams in India and a much longer half-life than for both similar-sized and larger dams in China, Brazil, and Iran. The key reasons for the BFD's longer useful life are the relatively low sediment load entering the reservoir annually, the dam's lower trapping efficiency, limited sediment deposition, particularly behind the dam wall, and the BFD's ability to pass highly turbid annual flood waters.

This thesis has contributed to a broader understanding of the key character and behaviour of sediment entering, transiting, and remaining in Lake Dalrymple and identified the primary sources of that sediment. This research contributes to our understanding of sediment sources and behaviour within large reservoirs situated in seasonally dry (semi-arid) tropical regions and contributes to the limited knowledge base for reservoirs in such regions, informing those responsible for reservoir planning, development and management in similar regions worldwide. The findings are particularly relevant as the dam operators plan to raise the wall of the BFD by 2 m to increase water supply and security, and the Australian Government seeks to build new dams in northern Australia.

Table of contents

List of figures

List of tables

Chapter 1: Introduction

1.1. Reservoirs: their processes, problems and impacts

Humans have long relied on dams to supply water reliably for domestic, agricultural, and industrial uses. Dams were constructed in Egypt to provide water for quarry workmen as early as 2900–2600 BC, in Peru to protect civic/ceremonial centres during the Initial Period (1200–800 BC) and in India for agricultural purposes from the third century BC (Burger, 2003; Jansen, 1980; Shaw & Sutcliffe, 2003). More recently, dams have also been constructed to control floods and to generate electricity, and reservoirs have become important areas for recreation and animal habitat. Despite their benefits, dams and their reservoirs may commonly alter the water quality of waterways downstream, modify the timing, magnitude and frequency of high and low flows, negatively impact on flora, fauna and society, and inhibit the movement of sediment and reduce sediment delivery to the coast (Ansar et al., 2014; Benchimol & Peres, 2015; Friedl & Wuest, 2002; Li et al., 2021; Syvitski et al., 2022; Syvitski et al., 2005; Villacorta-Rath et al., 2022). Undesirable consequences related to water quality and suspended and deposited sediments also occur within reservoirs, impacting dam infrastructure, useful life and ecological function.

The primary purpose of over half of Australia's 564 large dams (>15 m tall) is to pond water for domestic water supply, with most of the remainder built to supply water for irrigation (24%) or generate hydroelectricity (12%; Australian National Committee on Large Dams (ANCOLD), 2010). Many (15%) of Australia's large dams are multipurpose, for example, the Warragamba Dam in NSW (water supply and power generation) and Eungella Dam in Queensland (irrigation and supply) or have been designed with future purposes in mind, such as the Burdekin Falls Dam in Queensland, an irrigation dam for which provision has been made to raise the wall and generate hydropower.

As a result of strict water quality guidelines (ANZECC & ARMCANZ, 2000), much of the research into reservoirs in Australia has focussed on dissolved oxygen concentration, pH and their relationships with physical and biological processes. Parameters such as temperature, electrical conductivity/salinity and dissolved oxygen have been used to identify stratification of the water column and model inflow pathways through reservoirs in a range of climates (Chudek et al., 1998; Dallimore et al., 2004; Marti et al., 2011).

Many Australian reservoirs suffer from algal blooms, particularly of cyanobacteria, which are toxic to humans and can cause anoxia (Burford et al., 2004; Jones & Poplawski, 1998). High water temperatures, thermal stratification, turbidity, high nutrient concentrations and depletion of dissolved oxygen may all contribute to cyanobacterial blooms (Jones & Poplawski, 1998; Rahman et al., 2005). Episodic storm inflows transport large sediment and nutrient loads (Amos et al., 2004; Jones & Poplawski, 1998) and sediments washed into a reservoir from agricultural catchments frequently contain high phosphorus loads from fertilisers (Burford et al., 2012; Rahman & Bakri, 2010). Artificial destratification has been used in some reservoirs to improve chemical water quality and control phytoplankton growth by inducing mixing. It was found to successfully alleviate anoxia in Chaffey Reservoir, NSW (Sherman et al., 2000), reduce evaporation by reducing surface layer water temperature in Googong Reservoir, New South Wales, (Sherman et al., 2010) and reduce cyanobacteria in a small tropical reservoir on an island off North Queensland (Hawkins & Griffiths, 1993).

Inflow may also cause mixing within a reservoir, partially or completely disrupting stratification or displacing resident water, leading to reoxygenation and upwards transport of nutrients as observed in Lake Gordon, Tasmania (Steane & Tyler, 1982) and Prospect Reservoir in New South Wales (Schladow & Hamilton, 1995). Uneven heating may lead to horizontal flow and uneven cooling can lead to stratification and upwelling, as can diurnal heat fluxes (Finlayson et al., 1980; Imberger, 1985b; Wells & Sherman, 2001). Many Australian reservoirs have provided data for modelling the behaviour of inflow and internal currents (Fernandez & Imberger, 2006; Hebbert et al., 1979; Imberger, 1985a; Marti et al., 2011), allowing simulation of plunging flows (Dallimore et al., 2004), identification of factors that may reduce vertical transport and mixing processes (such as warm winters; Bertone et al., 2015), and prediction of algal blooms (Vilhena et al., 2010). Stratification and mixing processes during and after inflow events are important factors to consider when trying to understand the transport and deposition of sediment within a reservoir (Mueller et al., 2013).

1.2. Sediment-related problems in reservoirs

Some of the most common problems within reservoirs may be caused by, or related to, sediment: reduced storage capacity, elevated turbidity, damage to infrastructure, and high nutrient/solute and contaminant loads (such as heavy and trace metals, toxic organics and residual chemicals; de Cesare et al., 2001). Any of these problems can lead to a reservoir becoming unfit for purpose. Hence it is important to understand the key processes that deliver the sediment and influence deposition processes.

Dams can be very effective sediment traps (Olive & Olley, 1997), with large reservoirs (capacity >1 x 10^6 m^3) commonly having a trap efficiency (TE; the percentage of incoming sediment that is retained by the reservoir) of >99% (Williams & Wolman, 1984). The amount and distribution of sediment retained in a reservoir are dependent on: the ratio between storage capacity and inflow; sediment particle size, grading and behaviour; reservoir size, shape and age; inflow and outflow rates and their location; the type of outflow structure and method of operation; stratification; currents and flow patterns within the reservoir; and surface wave action (Brune, 1953; Butt et al., 2010; Heinemann, 1981; Nagle et al., 1999; Raudkivi, 1993; Roca, 2012; Verstraeten & Poesen, 2000). Coarser sediment (coarse silt and sand) often enters as both suspended and bed load and settles out at the upstream end of the reservoir, creating a delta, while finer particles may be deposited throughout the reservoir and some colloidal fractions may not settle at all (Bayram & Kenanoğlu, 2016; Frenette & Julien, 1996; Morris & Fan, 1998; Raudkivi, 1993; White, 1990). However, this pattern of deposition can change over time as a reservoir ages and begins to fill with sediment (Juracek, 2015; Morris & Fan, 1998). If a reservoir receives and traps large sediment loads it may rapidly fill and lose capacity, a problem documented in many reservoirs, large and small, around the world (Carvalho et al., 2000; K. D. Fu et al., 2008; Garg & Jothiprakash, 2008; Lahlou, 1996; Pitt & Thompson, 1984; Rãdoane & Rãdoane, 2005; Roca, 2012; Tamene et al., 2006; Zeng & Zhou, 1989). The useful life of a dam is defined as the length of time over which it is safe and operable (Wieland, 2013), and includes the period where sediment deposition reduces storage capacity but does not hamper operations (Frenette & Julien, 1996; Garg & Jothiprakash, 2008; Sumi & Hirose, 2009). Understanding the useful life of reservoirs and the factors that influence it is critical for optimising dam location, design and management to maximise useful life and economic returns.

Turbidity is a measure of the transmittance of light through water or how clear the water is—the more suspended material in a water sample, then the higher the turbidity. Turbidity may be caused by suspended and colloidal matter such as clay, silt, finely divided organic and inorganic matter, and plankton and other microscopic organisms (APHA, 1998). Minerogenic turbidity is caused by sediment washing or blowing into a reservoir or through resuspension of sediment that has previously entered the reservoir. Such turbidity varies in response to hydrological events and meteorological factors such as storm-driven inflow and strong winds (Akhurst & Breen, 1988; Cossu et al., 2016; Effler et al., 2006b; Filstrup & Lind, 2010; Hu et al., 2006; Valipour et al., 2017) and is therefore often seasonal, associated with specific times of the year, or wet season rain events (Cossu et al., 2016; Lick et al., 1994; Tammeorg et al., 2013). Turbidity usually reduces naturally within weeks to months of elevated inflow ceasing (Chou & Wu, 2010; Effler et al., 2006a; Gelda et al., 2013); however, in some cases sediment persists in the water column year-round (Hart, 1986; Hart, 1999; Lind et al., 1997). Elevated turbidity may be problematic in a number of ways: reducing light penetration, water temperature, and therefore photosynthesis and primary production (Bilotta & Brazier, 2008; Hubble & Harper, 2001; Lei et al., 2018; Tundisi & Tundisi, 2011); limiting the visual range of fish reducing their ability to forage, prey or avoid being preyed upon (Chivers et al., 2013; Kerr, 1995) and smothering benthic surfaces (Davies-Colley & Smith, 2001). Modification of the sediment and turbidity regime can significantly alter the ecology of the impounded stream both in the reservoir and downstream (Batalla & Vericat, 2009; Cattanéo et al., 2021; Espa et al., 2016). These problems are all exacerbated by persistence of turbidity in a reservoir.

Turbid water caused by suspended sediment (SS) can increase the cost of treating water for both municipal and industrial uses (Clark, 1985; Skene & Oades, 1995), cause abrasion of dam intakes, pipes and hydropower turbines (de Cesare et al., 2001; Padhy & Saini, 2011; Tundisi & Tundisi, 2011) and clog aquifer recharge channels by reducing soil infiltration capacity (Bristow et al., 2000). Even moderate turbidity levels (10–50 NTU) may be problematic because of regulatory requirements for many reservoirs to supply low turbidity water (Gelda et al., 2013). Where sediment travels through a reservoir as a turbidity current, with little dilution or loss to deposition (Lee & Yu, 1997; Raudkivi, 1993), it may cause the deposition of sediment immediately behind a dam wall (Annandale, 2006; Samadi & Galay, 2005). If sediment builds up behind the dam wall or in front of water intake structures then the dam may be unable to function properly, particularly if it has deep-water outlets or is used for hydropower (Emamgholizadeh et al., 2018; Oehy & Schleiss, 2007). Identification and monitoring of sediment source, flow pathways and areas of deposition are vital to ensure effective and proactive management of a reservoir to prolong its useful life.

Problems with sediment have been documented in Australian reservoirs. Many of the reservoirs in sub- to tropical regions of Australia have relatively high capacity to inflow ratios (>0.5) and may have high (>70%) sediment TE (Waterhouse et al., 2016), potentially limiting their useful life. However, previous research has often focused on small reservoirs (catchment area <100 km^2) in temperate and grassland locations (Chanson, 1998; Chanson & James, 1999) where extreme reservoir sedimentation has also been documented (Chanson, 2012). Conversely, other studies have discussed the ability of some dams in Queensland to reduce the supply of sediment to the coast, correspondingly limiting beach replenishment and causing coastal erosion (Pringle, 1991; Wolanski & Hopper, 2022). ^{137}Cs has been used to date sediment and estimate sediment accumulation rates in a small reservoir in semi-arid, western New South Wales (Jones et al., 2000), and in South Australia diatom records and radionuclide data have been used for the same purpose (Tibby et al., 2010).

Several studies into the sources of sediment to some Australian reservoirs have been undertaken. For example, to determine why catchment soil conservation methods were failing to reduce sediment supply to the rapidly silting Lake Argyle, Western Australia, Wasson et al. (2002) used sediment yield estimates to quantify sediment transport into Lake Argyle and then tested the findings with strontium, neodymium and caesium tracers, finding that ~96% of the sediment came from rocks and soils that covered less than 10% of the catchment. Magnetic and geochemistry data were used to identify the dominant source of fine sediment, and associated phosphorus, reaching Chaffey Reservoir, allowing reservoir managers to better target sediment reducing practices and reduce the growth of cyanobacteria (CSIRO Division of Water Resources, 1994); geochemical, Nd–Sr isotopic and statistical analyses were used to identify major sources of sediment to Lake Wivenhoe (Douglas et al., 2007); and geochemical modelling using sediment fingerprinting was explored for the Baroon Pocket Reservoir in South East Queensland (Laceby et al., 2015).

There has been limited research on Australian reservoirs in semi-arid to tropical areas and much of that research has focussed on water quality and biology as opposed to sediment behaviour and characterisation (Geddes, 1988; Oliver & Ganf, 1988). Chudek et al. (1998) completed a review of the stratification behaviour of Queensland dams and thermal stratification has also been widely researched to determine reservoir suitability for recreational fisheries, for water offtake management, and to establish the influence of wind and retention time on seasonal circulation (MacKinnon & Herbert, 1996; Russell, 1987; Townsend, 1998). Australia has highly weathered soils that are rich in clay-sized particles that are readily transported into streams and reservoirs where they cause high turbidity (Olive & Walker, 1982). Natural processes like evaporation may then increase the concentration of solutes, colloids and suspended material (Townsend, 2002). Many water bodies in arid and semi-arid Australia are extremely (>90 nephelometric turbidity units (NTU)) and persistently turbid (Geddes, 1984; Townsend, 2002). Although elevated turbidity may be the natural state in some waterbodies, persistent turbidity in reservoirs may damage infrastructure or render the water unfit for purpose.

Acknowledging that sediment is one of the most common river contaminants, the Australian Government's National River Contaminants Program (2001–2005) funded further research to understand large-scale patterns of sediment transport and the potential effects on river ecology to assist catchment and resource managers to predict the hazard of sediment delivery to streams; identify the major river reaches that are impacted by sediment; and to estimate the resultant sediment delivery to estuaries and the coast. Goals of the program included an improved understanding of sediment transport processes down large river systems, especially in sub-tropical and tropical Australia, knowledge of the role of sediment in driving ecological processes within naturally turbid systems, and better sediment management in river catchments (Land & Water Australia, 2002). One of the program's areas of interest was the Burdekin River in northern Australia, including a focus on Lake Dalrymple, the reservoir formed by the Burdekin Falls Dam.

The Burdekin Falls Dam (BFD) in North Queensland is situated on the Burdekin River, the largest supplier of freshwater and SS to the Great Barrier Reef (Kroon et al., 2012; Kuhnert et al., 2018). Many studies have detailed sediment in the river system, transport to the reef and effects on the GBR (reviewed in detail by Bainbridge, 2015). Limited studies of sediment character and behaviour in the BFD reservoir have been conducted and are discussed further in section 1.3 (Faithful & Griffiths, 2000; Griffiths & Faithful, 1996). These studies suggest that more research is required to better understand the sediment-related processes—source, behaviour, transport and deposition—occurring within the BFD reservoir. This thesis addresses these knowledge gaps.

1.3. Significance of the research

This thesis presents the first detailed study of sediment sources, transport and deposition in Lake Dalrymple, a large reservoir located in the seasonally dry tropics of northern Queensland, Australia. Spatially and temporally intensive sampling conducted over three consecutive median to below-median rainfall and discharge water years (1 October to 30 September; Figure 2.2), and again five years later, has produced several new datasets.

These include:

1. Quantitative assessment of sediment causing persistent turbidity in the reservoir
2. Detailed assessment of sediment characteristics and behaviour within the reservoir under varying flow conditions
3. Extensive sediment core and grab sample geochemistry that will contribute to an environmental baseline for the reservoir
4. Quantitative assessment of sediment deposition in the reservoir
5. Bathymetric data that provides a baseline for analysing further sediment deposition using future surveys.

This research contributes to our understanding of SS sources and behaviour within large reservoirs situated in seasonally dry (semi-arid) tropical regions and contributes to the limited knowledge base for reservoirs in such regions. This study has relevance for reservoir managers and ecologists responsible for reservoir planning, development and management in tropical to sub-tropical regions worldwide. The findings are particularly relevant as the Queensland Government has committed funding for a detailed business case for raising the wall of the BFD by at least 2 m to increase water supply and security and the Australian Government looks to build new dams in tropical northern Australia, including at Hells Gate on the Upper Burdekin River.

1.4. The study area—Lake Dalrymple, North Queensland

The Burdekin River catchment is the second largest in Queensland (~130,120 km^2). On average, the Burdekin River transports 3.3 Mt of fine sediment (<63 μm) per year to the coast (McCloskey et al., 2021) but suspended sediment loads are extremely variable, ranging from 0.009 to 15.7 Mt over the 1986–87 to 2009–10 period (Kuhnert et al., 2012). The BFD is located 159 km upstream from the Burdekin River mouth and captures ~88% (114,220 km^2) of the Burdekin River catchment area.

Lake Dalrymple (or BFD reservoir) is the largest lake by volume in Queensland (12th largest in Australia; Australian National Committee on Large Dams (ANCOLD), 2010) with a capacity of 1.86 TL, maximum depth of 40 m and a surface area of 220 km^2 when at full supply level (Sunwater Limited, 2009). The reservoir was formed in 1987 after the completion of the BFD on the Burdekin River in northern Queensland, Australia (Figure 1.1). The dam was constructed primarily to supply water to the downstream Burdekin River Irrigation Area (now part of the Burdekin-Haughton Water Supply Scheme, BHWSS) and the mining industry but is also used to supplement urban and industrial water supply to the city of Townsville. The dam's design also allows for an increase in spillway height to increase storage and support the generation of hydroelectric power. The reservoir is also listed in the Directory of Important Wetlands in Australia due to its important ecological or hydrological functions as part of a major wetland system/complex and provides an important habitat or refuge for key biota (Environment Australia, 2001).

1.4.1. Key issues affecting the BFD reservoir

Most dams are efficient traps of both coarse and fine sediment (Prosser et al., 2001). Despite overflowing during episodic flood events for several weeks almost every wet season (Figure 1.2), the BFD is no exception, having a bed material load trap efficiency (TE) of 100% (Brown and Root, 2001) and overall median calculated TE of 94% (Burdekin Shire Rivers Trust, 2000), although more recent research has suggested an average TE of 66% (Lewis et al., 2013) . Given the large volumes of sediment transported by the Burdekin River every year (average 3.3 Mt of fine sediment <63 µm per year; McCloskey et al., 2021), when the BFD was first constructed it was suggested that it would reduce the movement of sediment through the catchment and prevent sediment aggradation at the coast (Pringle, 1991). This view was supported by Kinhill Cameron McNamara (1996) and by Fleming (1981) who predicted that all bedload and coarse sediment would be trapped by the dam reducing supply to the coast, causing the erosion of the Cape Bowling Green sand spit—an outcome that some researchers believe has occurred (Wolanski & Hopper, 2022), but others dispute (Lewis et al., 2021). Such a high trapping efficiency could also have a significant effect on the life of the dam and has serious implications for the development of management strategies of the reservoir.

Before the BFD reservoir was constructed, Burdekin River water was only turbid during, and shortly after, periods of elevated wet season inflow (e.g. Burrows & Faithful, 2003). Based on this information, the Burdekin Project Assessment Committee (1978) concluded that water within the BFD reservoir would clarify between flow events and that the turbidity of water downstream may even be reduced. In actuality, particulate material remains in suspension within the BFD reservoir maintaining turbidity for most if not all of the year (Burrows & Butler, 2007; Burrows & Faithful, 2003; Griffiths & Faithful, 1996). Turbidity levels in the reservoir exceed the Queensland Water Quality Guidelines trigger value for Central Coast Queensland Region freshwater reservoirs (1–20 NTU; DEHP, 2009) all year round.

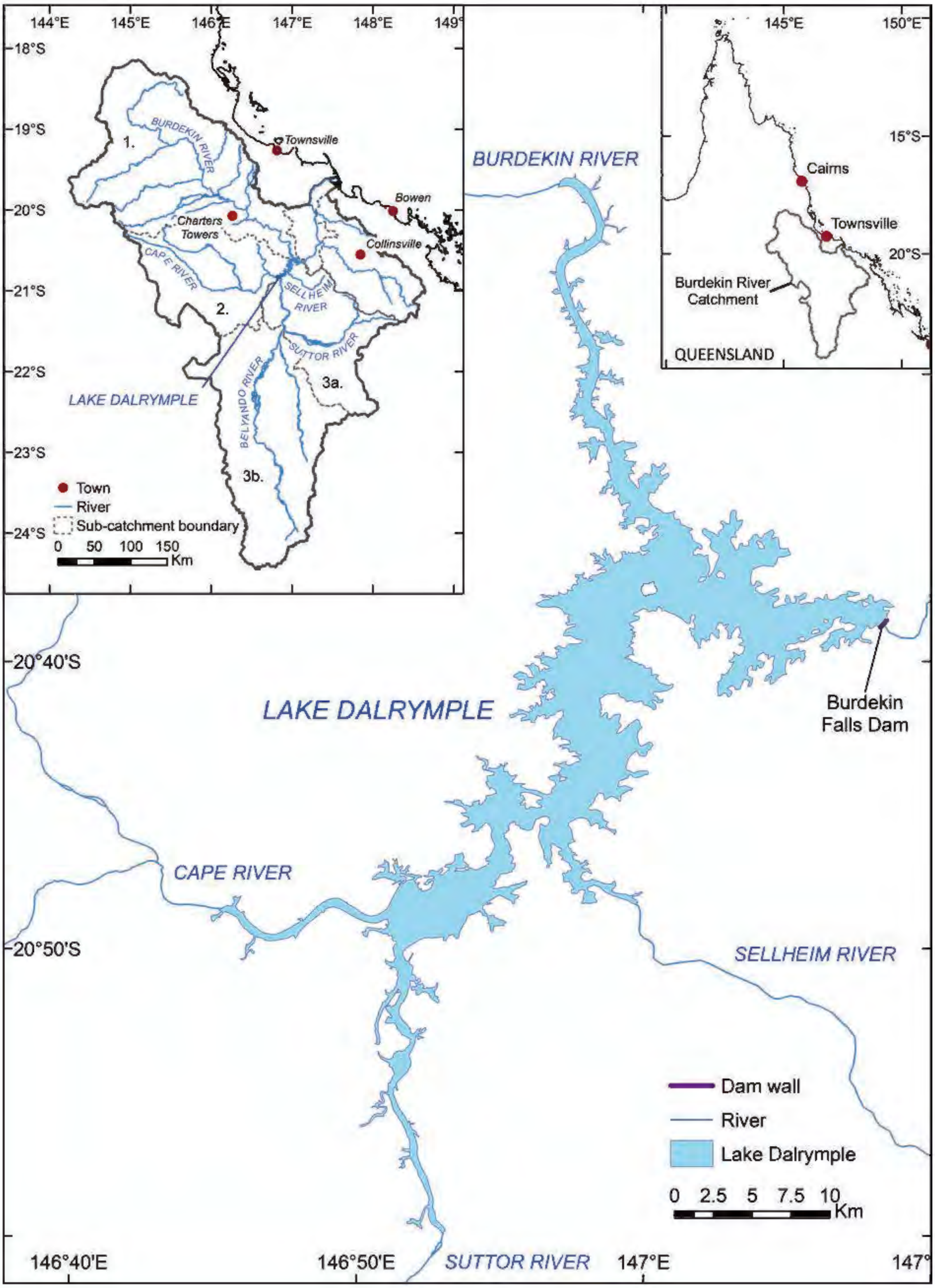

Figure 1.1 Main map: Lake Dalrymple and location of the Burdekin Falls Dam. Small inset: location of the Burdekin River Catchment in northern Queensland, Australia. Large inset: location of Lake Dalrymple within the Burdekin River Catchment. Reservoir sub-catchments are also shown: 1) upper Burdekin River catchment (40,344 km^2); 2) combined Cape River and Campaspe River catchment (20,273 km^2); 3a, b) combined Suttor River and Belyando River catchment (53,477 km^2), includes Sellheim River catchment (1,703 km^2).

This elevated and persistent turbidity has led to the unforeseen consequence of daily irrigation releases being persistently rather than episodically turbid, causing the Burdekin River below the dam to also be persistently turbid (Griffiths & Faithful, 1996; Petheram et al., 2008). Pumping of turbid river water for irrigation into the extensive distributary stream and wetland system of the Burdekin Delta has increased the turbidity of many of these formerly seasonally clear waterbodies (Burrows et al., 2007; Perna & Burrows, 2005). In both wetlands and irrigation channels, turbidity has inhibited the growth of native aquatic plants and promoted the growth of exotic, turbidity-tolerant species in an important fish habitat (Davis et al., 2014), contributing to further decreases in water quality by creating anoxic conditions (Perna & Burrows, 2005). These coastal floodplain wetlands play an important role in improving the quality of water leaving the land and reaching waters of the Great Barrier Reef (Davis et al., 2014). Water released from the BFD reservoir is also used in the downstream Burdekin Delta Artificial Recharge Scheme. Surface clogging of the scheme's groundwater recharge pits by fine sediment has been identified as a major problem and there is a need to determine the physical and chemical characteristics of SS in the Burdekin River in order to assess the required level of pre-treatment before river water is used in the scheme (Bristow et al., 2000).

Figure 1.2 The Burdekin Falls Dam overflowing during the 2003–04 wet season. Mt McConnel, an 'island' in the Central section of the reservoir, can be seen in the top right corner.

Previous studies have examined the SS concentrations and loads that enter, are deposited in, and pass through the reservoir during elevated inflows in the wet season (Bainbridge et al., 2014; Faithful & Griffiths, 2000; Griffiths & Faithful, 1996; Lewis et al., 2013), and the absorption and scattering of light in the reservoir by SS and algae (Campbell et al., 2011a; Campbell et al., 2011b). Despite these advances in our understanding of sediment in the BFD reservoir there are still knowledge gaps relating to sediment sourcing, transport and composition through this key component of the extensive Burdekin River system. Fleming and Loofs (1991) asserted that when the majority of inflow in a season was from the north (Burdekin River) then the dam clears relatively quickly (within 4 months) but it is unclear whether this remains the case two decades after the dam's completion. Limited information exists on the character, source and spatio-temporal dynamics of SS within the reservoir in the dry season (May to November). Although turbidity currents have been identified during previous studies of the reservoir (Faithful & Griffiths, 2000), the consistency of turbidity current formation and variability of the SS present in those currents has not been comprehensively examined over multiple consecutive water years. There is also limited information on sediment deposition within the BFD reservoir and a need to ascertain if and where large-scale deposition occurs and if deposited sediment comes from a dominant source within the catchment. The findings of this investigation will provide additional data to inform the further development of the BFD and the management of the reservoir. Using the BFD reservoir as a case study, this thesis will contribute more broadly to the understanding of persistent turbidity in reservoirs and sediment transport and depositional processes within seasonally dry tropical reservoirs that receive event-driven inflow.

1.4.2. Burdekin Falls Dam reservoir morphology, hydrology and catchment characteristics

The BFD ponds water 50 kilometres up the Burdekin River (Sunwater Limited, 2024b) forming a dendritic reservoir with a Y-shaped morphology and two primary inflow sources: the Burdekin River to the north and the Suttor and Cape Rivers to the south (Figure 1.1). The northern 'Burdekin' arm of the reservoir is a narrow (~0.4–1 km wide), well-defined open channel, with distinct banks lined with living and dead trees and is riverine in nature. The southern 'Suttor' arm is much wider (2–4 km) with two thirds of the channel obscured along the edges by dead trees and much shallower banks creating a riverine to transitional (zone of change from riverine to limnetic dominance) character. The two arms meet in the central section of the reservoir which is wide and open (>1.4 km) although bays or inlets to the north and south, like large sections of the reservoir outside of the relict river channels, are filled with dead trees. The eastern section of the reservoir is lacustrine: wide (>1.2 km), open and deep (>28–32 m towards the dam wall; Figure 1.1).

The BFD reservoir receives water from three major sub-catchments: the Upper Burdekin River in the north and the Suttor/Belyando and Cape/Campaspe river systems in the south (Figure 1.1). The minor Sellheim River also flows directly into the reservoir (Figure 1.1). The geology and geomorphology of the sub-catchments of the reservoir are highly variable (Figure 1.3a, b) but all are intensely weathered. The Upper Burdekin catchment comprises a mix of various igneous, metamorphic and sedimentary rocks, including Cenozoic basalts in the north-west of the sub-catchment and large areas of Silurian to Carboniferous granite and granodiorite outcrops in the north, north-central and eastern sections (Fergusson & Henderson, 2013; Raymond et al., 2012). Extensive areas of erodible red duplex soils, black and red soils of basaltic origin, sands and sodic duplex soils have developed in this sub-catchment (Roth et al., 2002). In contrast, Cenozoic to Holocene sand, gravel and soil alluvial deposits dominate the Suttor/Belyando and Cape/Campaspe sub-catchments. Neoproterozoic to Early Cambrian sandstones, siltstones, and schists, and Carboniferous tuffs and rhyolitic rock are also common in the Suttor/Belyando, and a ridge of Triassic sandstone, siltstone, and mudstone runs along its western fringe (Raymond et al., 2012). Cracking clay soils produced from basic igneous rocks and clay-containing sedimentary rocks, including grey/brown clays and red/yellow earths, are the dominant soil types in both the Cape/Campaspe and Suttor/Belyando (Roth et al., 2002).

Steep-sided mountain ranges (peaks up to 1065 m) and strongly undulating terrain characterise the Upper Burdekin (Roth et al., 2002), where incised river channels produce greater sediment availability and transportability (Bainbridge et al., 2014) than in the Suttor/Belyando and Cape/Campaspe sub-catchments, which are dominated by more gently sloping alluvial plains and lowlands with lower peak elevations, 300–450 m (Croke et al., 2015; Roth et al., 2002). Grazing is the primary land use in the reservoir's sub-catchments (Figure 1.3c; Newham et al., 2017) which, together with land clearing and grain-growing, has contributed to degradation of stream channel stability and widespread erosion (Faithful & Griffiths, 2000; Fleming & Loofs, 1991).

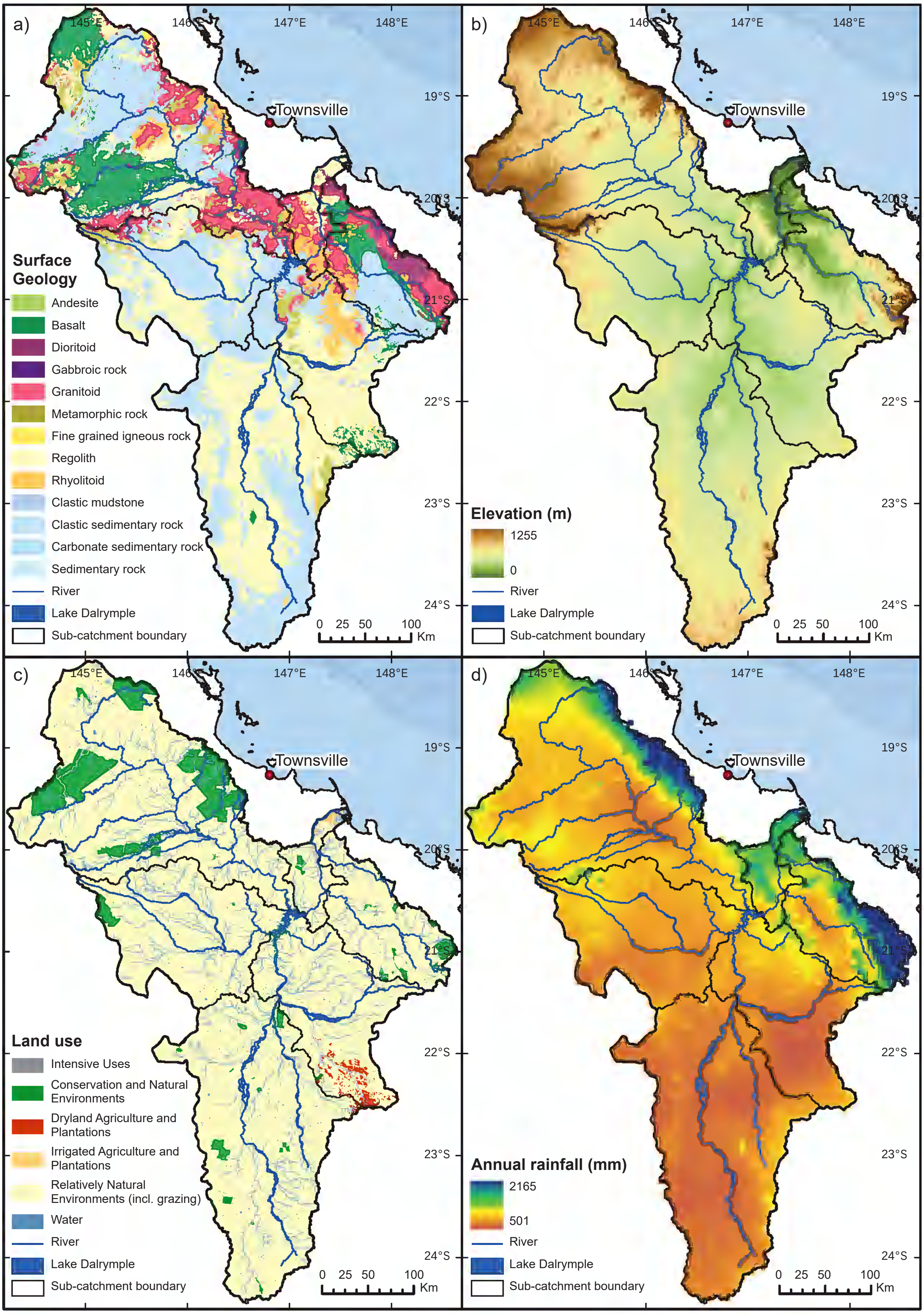

Figure 1.3 Burdekin River catchment a) surface geology, b) elevation, c) land use (ALUM 2021 classification) and d) annual rainfall. Data sourced from a) Geoscience Australia, b) Geoscience Australia, c) Queensland Department of Environment and Science, and d) Bureau of Meteorology.

Most of the area draining into the BFD reservoir is classified as hot semi-arid using the Köppen-Gieger classification (Peel et al., 2007). The climate has a well-defined wet season from December to April, with a dry season from May to November. Rainfall is mostly in the form of short-duration, intense episodes associated with tropical cyclones, tropical depressions and monsoonal troughs (Alexander et al., 2020). Rainfall also varies temporally and spatially within both the catchment and sub-catchment and may be localised or widespread (Figure 1.3d; Alexander et al., 2020; Roth et al., 2002): in the Upper Burdekin coastal ranges mean rainfall is >1500 mm yr^{-1}, while in parts of the Suttor/Belyando sub-catchment it is only 500 mm yr^{-1} (Bainbridge et al., 2014).

The Burdekin River is one of Australia's largest rivers by average annual discharge volume (9.18 million ML yr^{-1}) with very high intra- and inter-annual variability, ranging from 0.25 to 54.03 million ML yr^{-1} (Bainbridge et al., 2014; Roth et al., 2002), and greater than 80% of annual rainfall and river discharge occurring during the wet season (Lewis et al., 2006; Lough, 1991). The BFD reservoir in turn receives highly variable inter-annual and intra-annual inflows, ranging from 0.2 to 26.8 million ML yr^{-1} (DRDMW, 2021), also concentrated in the wet season months (Lewis et al. 2006). Discharge is recorded for water years, which run from 1 October to 30 September. Reservoir water heights reach a minimum late in the dry season–early in the wet season then it fills rapidly (1–2 days) during wet season inflow. Since construction the reservoir has rarely been below 50% capacity (see Figure 2.3); it fills, and has overflowed every year but two since its completion (capacity to average annual inflow ratio = 0.24; Bainbridge et al., 2014).

Rainfall produces rapid runoff with very fast flood-wave speeds (estimated at over 5 $m \cdot s^{-1}$ in the upper to middle sections of the river; Alexander et al. 1997) capable of dislodging and transporting significant amounts of both coarse and fine sediment (Alexander et al., 1999a; Mitchell et al., 2006), such as the 1.5 Mt of sediment transported over six days during a flow event in 2017 (Waterhouse et al., 2018). A large portion of this sediment (average 66%) is trapped in the reservoir (Lewis et al., 2013). The volume of sediment transported into the reservoir each year varies (12%–280% of the average annual yield in the water years from 2005–06 to 2009–10; Bainbridge et al., 2014) and is can be supply or hydraulically limited (Amos et al., 2004). The relative proportions of sediment exported from the catchments above the BFD remain consistent despite variable flow contributions with >75% of the annual mean sediment load delivered from the steep upper Burdekin catchment (average 147 t km^{-2} y^{-1})

and <25% contributed by the southern lowland catchments (averages range from 9 to 17 t km^{-2} y^{-1}; Bainbridge et al., 2014; Lewis et al., 2013; Roth et al., 2002).

1.5. Thesis aims and objectives

The primary aim of this thesis is to investigate the character, dynamics and sources of suspended and benthic sediment in the BFD reservoir (Lake Dalrymple) to better understand the causes and management challenges of such persistently turbid lake systems. Sediment characterisation and sourcing techniques are applied to sediment from this large reservoir, situated in a seasonally dry tropical region, to examine and quantify sediment sources and identify the transportation and depositional processes affecting sediment within this environment. The effects of sediment deposition and distribution on the life of the BFD reservoir are also investigated. The specific research objectives of this study include:

Objective one: Physically and chemically characterise suspended and benthic sediment from the BFD reservoir and describe any intra- and inter-annual variability.

Objective two: Determine the cause of persistent turbidity in the BFD reservoir and identify the processes contributing to the intra- and inter-annual variability of minerogenic turbidity.

Objective three: Examine the effect of thermal stratification on turbid inflow and investigate the influence of turbidity currents on sediment transport and deposition in the BFD reservoir.

Objective four: Examine the potential of geochemical and physical characteristics of sediment deposited in the BFD reservoir to identify discrete sediment sources within a large, geologically complex catchment.

Objective five: Spatially and temporally quantify sediment deposition in Lake Dalrymple to determine the useful life of the BFD and identify where that life sits in a global context.

1.6. Overview of research methods

Sediment and water sampling was conducted in the BFD reservoir from December 2003 to October 2006 and again in September 2011. Data from an initial sampling trip in December 2003 were used to select four water sampling sites that captured representative inflows from the major tributary rivers and transformations through the reservoir and to provide an understanding of the physical properties of SS as it moves through the reservoir (Chapter 2). The three years of data collection from 2004 to 2006 focussed on establishing water quality in both the wet and dry seasons (November to April and May to October respectively) and sampling in September 2011 was designed to examine sediment characteristics following a large wet season. Water quality parameters—temperature, electrical conductivity and turbidity—were measured both in situ and in the laboratory. Dissolved oxygen was also measured in situ.

Water samples containing SS were collected during periods of little inflow in the dry season in June and December 2004, August 2005, October 2006 and September 2011, and during periods of inflow over three consecutive wet seasons (from December 2003 to April 2006). Samples were collected from multiple depths within the reservoir and were used to measure total suspended solids (TSS) concentrations. Benthic sediment samples (n=37) were collected using a van Veen grab from sites throughout the reservoir in areas both in and out of the relict river channel. Grab samples were primarily collected in December 2003 and August 2005 with additional samples collected in September 2011. These samples were used to investigate the character of sediments being deposited in the reservoir and examine the differences between sediment deposited before and after above-average (mean) flow events (Chapter 3). In August and September 2011 sediment cores were collected from 31 locations throughout the reservoir. Both gravity and push cores were collected (Chapter 5). Coring was conducted to investigate how the character of deposited sediment had varied over time and extrapolate the volume of sediment retained by the dam. A bathymetric survey was conducted in February 2004 to examine sediment accumulation along the pre-dam river channels, providing validation for the gravity core data. The area surveyed was limited to the central and eastern sections of the reservoir by slow vessel speed and equipment availability, so it was not possible to use this technique to estimate the volume of sediment in the dam.

All SS and benthic sediment samples were analysed for sediment particle size using laser diffraction (Malvern Mastersizer 2000; n = 447) to examine particle-size distribution patterns. A comprehensive mineralogical and geochemical dataset of suspended and benthic sediment samples was also produced using X-ray diffraction (XRD; n = 318), X-ray fluorescence (XRF n = 181), and inductively coupled plasma mass spectrometry (ICP-MS, n = 162) to further characterise and quantify reservoir sediments and their sources. Additional information on sediment provenance was gained from Sr and Nd isotopic analyses carried out on 26 sediment samples. Sub-sets of sediment samples were analysed for loss on ignition (LOI; n=181) and TOC (n=12) to examine the proportion of organic material and carbonate content present. The density of trapped sediment was measured using the dry mass of 10 grab samples spaced throughout the reservoir and used in sediment volume calculations (Chapter 4).

1.7. Thesis outline

This thesis is presented as a series of research chapters formatted for journal publication. Two chapters have previously been published. As a result, some repetition of background, methodology, and discussion may occur across chapters. This overlap is intentional, as each paper addresses different aspects of the overall research question but is presented in the context of its specific journal submission. The aim is to provide clarity and coherence within each chapter while contributing to the overall research. Supplementary figures and tables relevant for each data chapter are provided as appendices.

Chapter two examines the cause and variability of persistent (year-round) turbidity in the BFD reservoir, specifically investigating the concentration, particle size, organic content and mineralogy of suspended and benthic sediment samples. Samples of SS were collected from the reservoir during four dry seasons (2004, 2005, 2006 and 2011) to examine the characteristics of material that remains in suspension when reservoir inflow is minimal. Benthic sediment samples from the top 15 cm were also collected from throughout the reservoir allowing for comparison with suspended material and to examine the potential for resuspension. The cause of persistent turbidity in tropical reservoirs is variable and under-researched and this chapter seeks to address this research gap. This chapter identifies the key processes causing the persistent turbidity observed in the BFD reservoir and quantifies the characteristics of SS present in the dry season. This chapter is presented in the format of a scientific research paper and has been published in the journal *Marine and Freshwater Research* (Cooper et al., 2017 – Chapter 2).

Chapter three uses water-quality data to examine the development of stratification within the water column of the BFD reservoir and discuss the resultant effect on sediment transport through, and deposition in, the reservoir. Water-quality data, including temperature, electrical conductivity and turbidity, were collected in situ from key sites within the reservoir during the wet seasons of three consecutive water years, 2003–04, 2004–05 and 2005–06. Benthic sediments and core samples were collected during the dry/pre-wet season in December 2003, August 2005 and September 2011. These data are used to examine the inter-annual variability in the formation of a stratified water column and turbidity currents within the reservoir and understand the extent to which the currents affect the reservoir. Particle-size and mineralogical data for SS and benthic sediments are used to investigate the relationship between sediment size and mineralogy, and hydrology, and their potential controls on transport and deposition. Previous studies had observed turbid interflows within the BFD reservoir. This chapter builds on that knowledge by identifying whether turbidity currents will form annually and how interflows effect sediment behaviour and water mixing within the reservoir. This chapter also characterises the SS entering the BFD reservoir in wet season inflow and examines the intra- and inter-annual variability of sediment characteristics and inflow over multiple consecutive water years. The conclusions provide insight into the behaviour of turbid flows in a reservoir that receives highly variable inflow, providing important context for dam operators in tropical regions and worldwide. This chapter is presented in the format of a scientific research paper and will be submitted for publication in a peer-reviewed journal.

Chapter four documents the differences in composition, geochemistry, and particle size of sediment deposited within the BFD reservoir, both over time and by spatial location. Fifty-one cores and sediment grab samples from throughout the reservoir, representing up to 24 years of deposition, were analysed for particle size, major and trace elements, and mineralogy. Twenty-six samples were also analysed for Sr isotopic composition. Data for sediments from single locations (individual cores) are used to investigate changes in sediment character over time. Sediments from multiple locations are compared to identify the physical and geochemical characters of the two primary sources of sediment to the reservoir: the Burdekin River system and the Suttor/Belyando/Cape River system. The data collected for this chapter are used to discuss depositional environmental changes and catchment inputs. Sedimentary evidence of large flow events was also sought. This chapter is presented in the format of a scientific research paper and will be submitted for publication in a peer-reviewed journal.

Chapter five uses two independent methods to calculate the volume of sediment that has been deposited in the BFD reservoir to estimate its useful life. Many dams built after 1950 have filled with sediment and no longer perform to their original design specifications. Given an average of up to 6 million tonnes of sediment per year can enter the BFD reservoir (Bainbridge et al., 2014), the potential exists for the dam to silt up and become unfit for purpose. This chapter uses data from core sampling and density of sediment samples as well as measured sediment loads from upstream gauges and the trapping efficiency method of Lewis et al. (2013) to estimate the volume of sediment that has been deposited in the reservoir in the 24 years of operation through 2011. A limited bathymetrical survey was also undertaken to examine evidence of deposition within the eastern reservoir. The useful life calculations also take water usage into consideration, noting that the reservoir experiences a 60% drawdown return period of 1 in 15 years, meaning that reservoir use would be affected once 40% of storage was filled with sediment. The useful life of the BFD is compared to similar large tropical to sub-tropical reservoirs in Asia, the Middle East and South America, examining properties such as trap efficiency, annual sediment load delivery, and sediment transport and deposition mechanisms, and highlighting the properties of the BFD that promote a longer useful life. This chapter is presented in the format of a scientific research paper and has been published in the *International Journal of Sediment Research* (Cooper et al., 2018).

Chapter six summarises the major findings of this study, placing each in the context of the research objectives outlined in this introduction. The implications of these findings for Australian tropical reservoirs and wider reservoir science are discussed and opportunities for further research are suggested.

Chapter 2: Spatial and temporal dynamics of suspended sediment causing persistent turbidity in a large reservoir: Lake Dalrymple, Queensland, Australia

Published as: Cooper, M., Lewis, S. E., & Smithers, S. G. (2017). Spatial and temporal dynamics of suspended sediment causing persistent turbidity in a large reservoir: Lake Dalrymple, Queensland, Australia. *Marine and Freshwater Research, 68*(7), 1377–1390. http://dx.doi.org/10.1071/MF16316

Minor changes have been made for clarity and to modernise some references. Reviewers will encounter some repetition of information included in the introduction section of this thesis, particularly in the introduction and methods sections.

Abstract

High turbidity in reservoirs may negatively affect aquatic ecology and water infrastructure. Although many reservoirs are turbid, the origin and intra- and interannual variability of turbidity is not well understood. To examine the cause and variability of turbidity, I measured the concentration, particle size, organic content and mineralogy of suspended and benthic sediment samples from Lake Dalrymple, a large reservoir in northern seasonally dry tropical Queensland. Samples were collected during the dry season (May–November) in 2004, 2005, 2006 and 2011. Water in the reservoir is turbid (>45 nephelometric turbidity units (NTU)) throughout the year, predominantly due to colloidal particles (<0.9 µm) composed of clay and mica minerals. Benthic sediments range from 1 to 30 µm in size, suggesting that resuspension of reservoir bottom sediments has little effect on turbidity. Dry season turbidity levels are strongly affected by the magnitude and duration of inflow waters from the preceding wet season, reflecting the limited availability of suspended particles delivered from the upstream catchment. Elevated turbidity in the reservoir and downstream irrigation areas during the dry season is now a common feature and must be incorporated into all agricultural and wetland management plans. These findings demonstrate that managers of turbid reservoirs in seasonally dry tropical regions should not rely on natural flushing and should develop reservoir operating procedures that maximise sediment transfer during flow events to reduce turbidity. Consideration should also be given to catchment management activities that can reduce the availability of fine sediment, such as remediation of large alluvial gullies.

Keywords: Burdekin Falls Dam, particle size, tropical reservoir.

2.1. Introduction

High turbidity levels in reservoirs can reduce light penetration, photosynthesis and primary production (Hubble & Harper, 2001), with negative consequences for the aquatic ecology of impounded lakes (Davies-Colley & Smith, 2001; Donohue & Garcia Molinos, 2009; Zhang et al., 2016). Turbidity caused by suspended sediment or colloidal particles (SS) strongly affects the composition of algae and plankton communities (Davis & Koop, 2006; Lind et al., 1992) and limits the visual acuity of fish, reducing their ability to forage, prey or avoid being preyed upon (Chivers et al., 2013). Suspended sediments in turbid water can increase the cost of treating water for both municipal and industrial uses (Clark, 1985), cause abrasion of dam intakes and hydropower turbines (Padhy & Saini, 2011) and clog aquifer recharge channels by reducing soil infiltration capacity (Bristow et al., 2000). In contrast, persistent (year-round) turbidity may also play a positive role by reducing blue–green algae blooms in lakes and reducing weed growth in irrigation channels (Geddes, 1984; Sabbatini et al., 1998). The causes of turbidity in rivers and lakes, which include SS and biological material such as phytoplankton (Bilotta & Brazier, 2008; Geddes, 1988; Gilvear & Petts, 1985), and the characteristics and behaviours of turbid inflows to reservoirs have been well studied (e.g. de Cesare et al., 2001; Effler et al., 2006a). However, the physical and mineralogical composition of SS that cause persistent turbidity in tropical reservoirs and the how and why the levels of persistent turbidity in a reservoir may vary over time with inflow variability have rarely been described in detail.

Many water bodies in arid and semi-arid Australia are extremely (>90 nephelometric turbidity units (NTU)) and persistently turbid (Geddes, 1984; Townsend, 2002). Previous investigations of persistently turbid reservoirs have focused on the relationship between turbidity and biology (Geddes, 1988; Hart, 1986; Hart, 1999; Oliver & Ganf, 1988). Lake Dalrymple, a reservoir in the seasonally dry tropics of northern Queensland, Australia, is persistently turbid (>45 NTU) due to high concentrations of fine clays suspended in the water column (Faithful & Griffiths, 2000; Griffiths & Farrell, 1991). Prior to construction, the Burdekin Project Assessment Committee (1978) concluded that water within the reservoir would clarify between flow events and that the turbidity of water downstream may even be reduced. However, a small portion of suspended particulate material of both mineral and organic origin transported during flow events (Bainbridge et al., 2014; Faithful & Griffiths, 2000) remains in suspension within the reservoir, maintaining high turbidity all year round (Brizga et al., 2006; Burrows & Butler, 2007; Lymburner et al., 2016). This has led to the unforeseen consequence of irrigation releases being persistently rather than episodically turbid (Griffiths & Faithful, 1996; Petheram et al., 2008). Surface clogging of groundwater recharge pits in the Burdekin River Delta downstream of the dam by fine sediment is a major problem (Bristow et al., 2000) Formerly clear creek and wetland systems on the lower Burdekin River floodplain are now turbid due to river water pumped into them during the dry season (Perna & Burrows, 2005). Elevated turbidity inhibits the growth of native aquatic plants and promotes the growth of exotic, turbidity-tolerant species in an important fish habitat (Davis et al., 2014), further reducing water quality through organic loading and dissolved oxygen deprivation (Perna & Burrows, 2005).

Previous studies have discussed the SS concentrations and loads that enter, are deposited in and pass-through Lake Dalrymple during elevated wet season inflows (Bainbridge et al., 2014; Faithful & Griffiths, 2000; Griffiths & Faithful, 1996; Lewis et al., 2013), and Campbell et al. (2011a) described the variations in absorption and scattering of light by SS and algae. However, the character, source and spatiotemporal dynamics of SS within the reservoir in the dry season (May–November) have not been investigated.

In this study the concentration, particle size and mineralogy of suspended and benthic sediment samples within Lake Dalrymple during the dry season in 2004–06 and 2011 were analysed to characterise and determine the causes of persistent turbidity. This study is one of the first to characterise the persistent SS in a reservoir over several years using a variety of techniques to understand the intra- and interannual variability of minerogenic turbidity. The significance of our findings is discussed with regard to the primary downstream uses of the turbid water and, as such, should assist reservoir managers and ecologists responsible for reservoir planning and management.

2.2. Lake Dalrymple and its catchment

Lake Dalrymple (Figure 2.1) was formed by the Burdekin Falls Dam (BFD) and is turbid (>45 NTU) all year (Burrows & Butler, 2007; Burrows & Faithful, 2003; Griffiths & Faithful, 1996). The dam was constructed primarily to supply the Burdekin River Irrigation Area (BRIA) and was completed in 1987. At full capacity, Lake Dalrymple holds 1.86 TL, covers an area of 220 km^2 and has a maximum depth of 40 m (Sunwater Limited, 2009). The Burdekin Dam is located 159 km upstream from the river mouth and captures ~88% (114,220 km^2) of the Burdekin catchment area (~130,120 km^2). The reservoir is listed in the Directory of Important Wetlands in Australia because of its important ecological or hydrological functions as part of a major wetland system or complex and provides an important habitat or refuge for key biota (Environment Australia, 2001).

Lake Dalrymple receives highly variable inter- and intra-annual inflows, ranging from 0.2 to 26.8 TL yr^{-1} (Figure 2.2). These flows are concentrated in the wet season months: December–April (Lewis et al., 2006; Figure 2.3). Reservoir water heights reach a minimum late in the dry season–early in the wet season before wet season inflows. Sampling was conducted in two below-median, one median and one above-median water years (Figure 2.2).

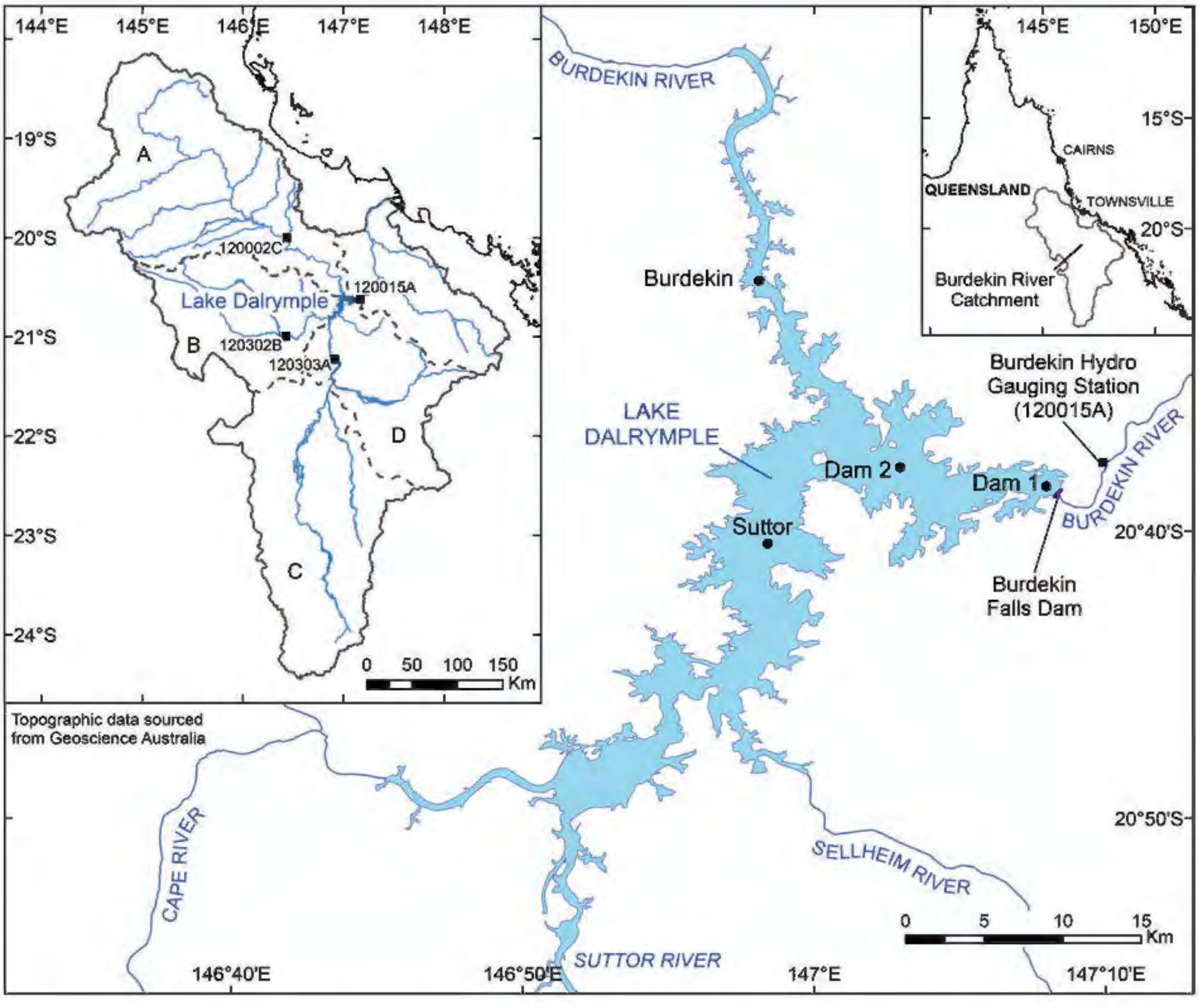

Figure 2.1 Main map: Lake Dalrymple and locations of sampling sites. Small inset (top right-hand corner): location of the Burdekin River catchment within Queensland, Australia. Large inset (top left-hand corner): location of Lake Dalrymple within the Burdekin River catchment and the water gauging stations 120002C (Burdekin River at Sellheim), 120303A (Suttor River at St Anns), 120302B (Cape River at Taemas) and 120015A (Burdekin River at the Hydro Site). Reservoir sub-catchments are also shown and indicated by uppercase letter: A) Upper Burdekin River (40,344 km^2); B) Cape/Campaspe rivers (20,273 km^2); C) Belyando River (35,334 km^2); D) Suttor River (18,143 km^2).

2.3. Materials and methods

2.3.1. Selection of sampling sites

Four sites were selected to best capture key locations within the reservoir that were safely navigable by boat (Figure 2.1). These four sites are listed below:

1. Burdekin, within the northern arm of the reservoir, representative of the inflowing Burdekin River (water depth ~18 m)
2. Suttor, representative of the inflowing Suttor River and Cape Rivers (water depth ~22 m)
3. Dam 2 (central), downstream of the confluence of the northern (Burdekin) and southern (Suttor) arms within the reservoir and representing an area of potential mixing (water depth ~24 m)
4. Dam 1 (eastern), 800 m from the dam wall, representative of water that has travelled furthest through the reservoir (~26 km from the Burdekin site and 24 km from the Suttor site; water depth ~31 m).

Sites were selected to complement previous research sites in the reservoir (Faithful & Griffiths, 2000) and because they allowed for samples to be collected within 1 day (24 h). Samples were collected in the middle of the relict river channels at all locations. Although additional samples could have been collected from closer to the bank in the Burdekin and Dam locations, dead trees fill the non-channel regions of the reservoir in the southern arm, making navigation difficult. Distances from sampling sites to the dam wall, river inflow point, and water monitoring gauges are provided in Appendix A (Table A1).

2.3.2. Suspended sediment sample collection and water quality observation

Reservoir water samples were collected from Lake Dalrymple during the dry season in June and December 2004, August 2005, October 2006 and September 2011. Surface water samples were collected directly into clean 1-L polypropylene bottles. Subsurface water samples were collected using a Van Dorn water sampler (December 2003) or with a peristaltic pump using 6-mm diameter plastic tubing attached to a weight (June 2004 onwards). Tubing was thoroughly rinsed between samples and water was pumped directly into the bottles. Samples were kept cool and were refrigerated within 24 h of collection. In June and December 2004, samples were collected from the surface and at 5 m depth intervals. From February 2005, turbidity was measured in situ (field turbidity) using a Hach Hydrolab Quanta (Hydrolab Corporation), which was calibrated using Milli-Q water and formazin according to the manufacturer's instructions (Hydrolab Corporation, 2002). Readings were taken every 1 m down the water column at the four sample sites (Figure 2.1). August 2005 and October 2006 samples were only collected from three or four depths because probe data indicated that turbidity and electrical conductivity were consistent down the water column. Fewer samples were collected in September 2011 because of equipment failure.

Temperature was recorded in situ using a Hach Hydrolab Datasonde (Hydrolab Corporation) in December 2004 and the Hydrolab Quanta from February 2005 onwards. Measurements were taken every 1 m down the water column allowing thermal stratification of the water column to be identified. Sampling occurred early–late morning at the Burdekin site (mid-afternoon in December 2004), at the middle of the day at the Suttor site (late afternoon in December 2004), in the morning to mid-afternoon at the Dam 2 site (early morning in December 2004) and in the morning at the Dam 1 site (late afternoon October 2006). Collection dates and times for all samples are provided in Appendix A (Table A2).

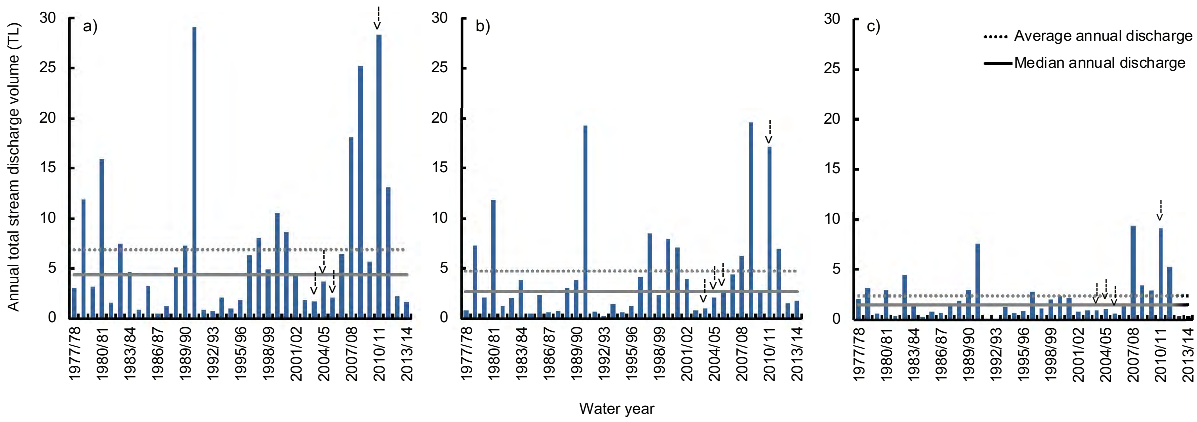

Figure 2.2 Annual discharge at the flow gauges at the a) Burdekin River at the Hydro Site, b) Burdekin River at Sellheim and c) combined Suttor River at St Anns and Cape River at Taemas. Arrows indicate the 2003–04, 2004–05, 2005–06 and 2010–11 water years sampled. Average (mean) and median annual discharge are calculated for the period from the water year of gauge installation (1977–78 for the Burdekin River at Hydro Site, 1968–69 for the Burdekin River at Sellheim and 1968–69 for the combined Suttor River at St Anns and Cape River at Taemas, based on the Cape River gauge date) to the end of the 2013–14 water year (Data source: https://water-monitoring.information.qld.gov.au/, accessed 22 August 2016). Mean ± s.d. discharge was 6.9 ± 7.6 TL (median 4.4 TL) for the Burdekin River at the Hydro Site, 4.7 ± 5.6 TL (median 2.7 TL) for the Burdekin River at Sellheim and 2.4 ± 2.7 TL (median 1.5 TL) for the combined Suttor River at St Anns and Cape River.

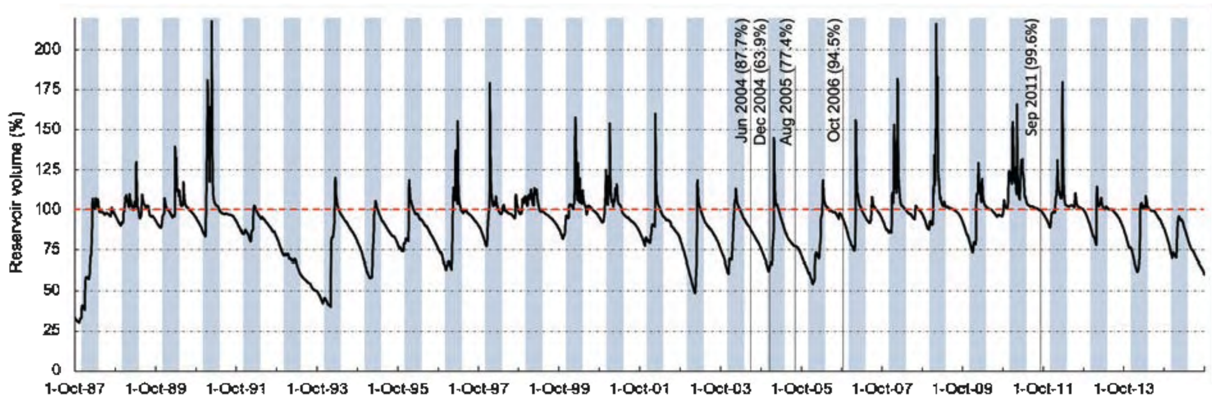

Figure 2.3 Burdekin Falls Dam reservoir volume over time. Sampling dates and corresponding percentage reservoir volume are marked by black vertical lines and wet season months are shaded grey. Data obtained from the then Queensland Department of Natural Resources and Mines (V. Manley, pers. comm., 1 August 2016; October 1987–July 2002) and Sunwater Limited ACN 131034985 (M. Ali, Bureau of Meteorology, pers. comm., 25 July 2016; July 2002–July 2016).

2.3.3. Benthic sediment sample collection

Benthic sediment samples were collected in December 2003 (Burdekin and Dam 1 sites), August 2005 (all sites) and September 2011 (Burdekin and Suttor sites) using a Van Veen grab sampler. Two to three grabs were made at each location and sediment was combined in a bucket from which a >1 kg sample was collected into a zip-lock bag and kept cool. Composite samples increase the representativeness of the sample and mitigate potential heterogeneity issues (International Atomic Energy Agency, 2003; Lietman, 1997). The grab sampler and bucket were thoroughly rinsed with reservoir water between samples. Grab samples were collected after water samples at each location to avoid contamination of the water by resuspended benthic sediments.

2.3.4. Laboratory turbidity and measurements of total SS

The turbidity of water samples was measured in the laboratory using standard methods (APHA, 1998). Laboratory turbidity was measured using a 2100P Hach turbidimeter calibrated using three gel standards covering specific turbidity ranges, namely 0–10 NTU, 0–100 NTU and 0–1000 NTU, and Milli-Q water.

Water samples were analysed for total suspended solids (TSS) using a standard gravimetric filtration method (APHA, 1998). Known volumes of sample were vacuum filtered onto pre-weighed Whatman GF/C filter papers (nominal pore size 1.2 μm) and dried overnight in a 103°C–105°C oven. The filter papers were then weighed again and TSS calculated. This method may underestimate the 'true' SS concentration where a large proportion of the particles are <1.2 μm. However, Hickel (1984) found that Whatman GF/C glass-fibre filters retain not only all particles >1 μm, but also particles down to 0.4 μm. This includes much of the colloidal fraction defined as 0.001–1 μm in size.

2.3.5. Sediment mineralogy

X-Ray diffraction (XRD) analysis was performed using a Siemens D-5000 X-ray diffractometer or a Siemens D500/D501 series X-ray diffractometer. Benthic sediment samples were dried at 40°C and then ground before glass smear mounts were prepared. XRD analysis of SS samples was performed on the dried filter papers used for TSS analysis. Samples were scanned from 5°2θ to 70°2θ, then removed and placed overnight in an ethylene–glycol atmosphere at 40°C before being analysed again. Glycol solvation assisted in identifying smectite group clays that consequently expanded and shifted to a basal peak of ~17 Å. After glycolated samples were analysed, the samples were heated to 400°C for 1 h to distinguish clay assemblages that share the same basal peaks (e.g., smectite and chlorite at ~14 Å). Glycolated and heated slides were run at scan lengths of 5°2θ–35°2θ. Mineral identification and quantification were performed using Bruker AXS Diffrac.Suite *EVA* (version 3.0.0.9) and Bruker AXS Diffrac.Suite *TOPAS* (version 4.2) software respectively. Diffractograms shifted for samples presented on filter papers and were corrected by aligning each plot to the well-crystallised 3.5 Å quartz peak. A cross-check of the mineralogical results using software developed by de Caritat et al. (1994) indicated that the identified mineralogy and calculated mineral percentages were appropriate. Compared with XRF (X-ray fluorescence) major oxide data (data not shown), the quantified mineralogy matched the generated mineral percentages well, although iron was often unable to be fully accounted for.

2.3.6. Total organic carbon

Six SS and six benthic sediment samples were analysed for total organic carbon (TOC) on a RockEval 6 Turbo analyser (Vinci Technologies) using established analytical methods (Espitalie et al., 1985) to examine the proportion of organic material. The furnace was programmed as follows: first, for the pyrolysis phase, hold at 300°C for 3 min, after which the temperature was increased at a rate of 25°C min^{-1} to a maximum of 650°C; and, second, for the oxidation phase, hold at 300°C for 1 min, after which the temperature was increased at a rate of 20°C min^{-1} to a maximum of 850°C.

2.3.7. Sediment particle-size analysis

Particle-size distributions for benthic and SS samples were determined using a Malvern Instruments Mastersizer 2000 laser diffraction particle-size analyser with a lens range of 0.02–2000 µm. Benthic sediment samples were prepared by wet sieving each sample through a 1.4-mm sieve. All sediment samples passed wholly through the sieve with the exception of a small number of samples that contained larger (2–3 mm) organic fragments. Complete (1 L) water samples containing SS were poured directly into the sampling chamber. Applying the methodology of Sperazza et al. (2004), samples were run manually to ensure appropriate dilution and were treated ultrasonically for 1 min while in the sample chamber to ensure that any flocs were disaggregated. No chemical dispersant was used. A laser obscuration of >5% was targeted for water samples, but this was unachievable for most samples (89% of samples were <5% obscuration). The low level of laser obscuration during the analysis of these samples may mean that these data are less precise (Sperazza et al., 2004). Optimal obscuration of 15%–20% (Sperazza et al., 2004) was achievable for benthic sediment analysis. Three measurements were determined for each aliquot, with two aliquots of each sample analysed and an average distribution determined.

Correction to the index of refraction (RI) used in processing by the Mastersizer software was applied based on mineralogical input. RI is one of the parameters used in the Mie Theory calculations for development of the theoretical diffraction pattern that is compared against the actual diffraction pattern by the Mastersizer software (discussed in detail by Sperazza et al., 2004). The default RI for the software was 1.52, the RI for glass beads. When values similar to those for kaolinite (RI = 1.533 or 1.55) were applied, lower weighted residual values were achieved for all samples, indicating a better fit between the theoretical and actual diffraction patterns and hence providing a more reliable particle-size distribution.

2.3.8. Rainfall and hydrological data

Hydrological data were obtained from the Queensland Government's Water Monitoring Data Portal (https://water-monitoring.information.qld.gov.au/, accessed 22 August 2016). Annual and daily discharge data (ML) were downloaded for the gauging stations closest to the reservoir: Burdekin River at Sellheim, Suttor River at St Anns, Cape River at Taemas and Burdekin River at Hydro Site (Figure 2.1). Rainfall records for the same locations as the hydrological gauges (excluding the Suttor River at St Anns) were downloaded from the Bureau of Meteorology website (http://www.bom.gov.au/climate/data/, accessed 11 Jul 2016, see Appendix A, Table A4) and water monitoring station details are provided in Appendix A (Additional methods section).

Daily discharge data were used to calculate the number of days since discharge returned to base flow levels and the duration of discharge above base flow. Base flow is stream flow that is maintained by seepage of groundwater into a channel slowly over time and, for the present study, was quantified as the mean daily discharge from May to November at each site for the full period of gauged data (gauge installation date to 30 November 2015). Discharges for the Cape and Suttor River gauges were combined to give the total inflow entering the southern arm of the reservoir.

2.4. Results

2.4.1. Turbidity and TSS

Field and laboratory turbidity of dry season samples from Lake Dalrymple reveal a strong linear relationship with $R^2 = 0.91$ (Figure 2.4a). Laboratory measurements provided the most extensive record of turbidity across multiple sampling years.

Turbidity remained constant throughout the water column at all sites during the dry season (Figure 2.5a–d) and ranged from 75 to 105 NTU at the Suttor, Dam 1 and Dam 2 sites and from 62 to 91 NTU at the Burdekin site. At each site, similar turbidity ranges were recorded in June 2004, August 2005 and October 2006 (e.g., 100–102, 92–99 and 84–98 NTU

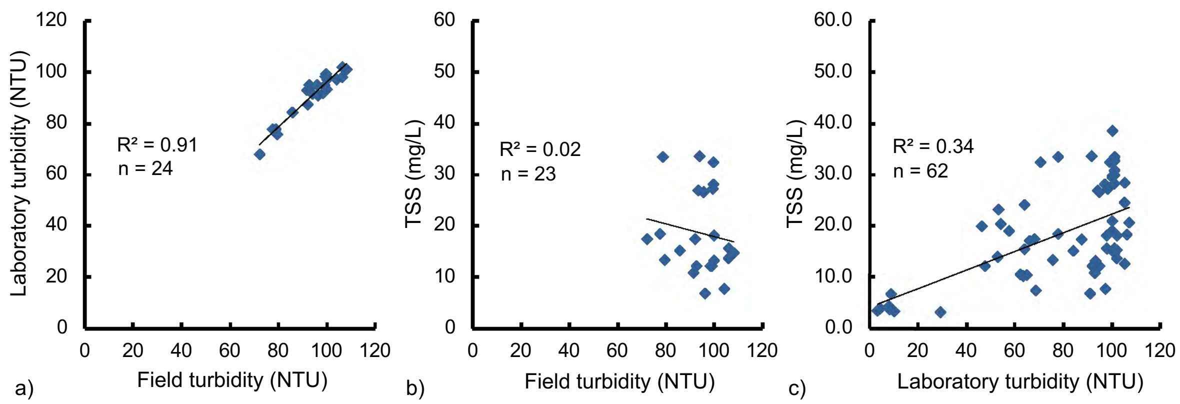

Figure 2.4 (a) In situ turbidity v. turbidity measured in the laboratory, (b) in situ turbidity v. total suspended solids (TSS) and (c) laboratory turbidity data v. TSS. In situ turbidity was not recorded in September 2011 because of equipment failure. Regression statistics for all graphs are included in Appendix A, Figure A1. NTU, nephelometric turbidity units. December 2004 samples from the Burdekin site have been omitted because turbidity was extremely high in these samples because of localised rainfall in the days before sampling. Turbidity and TSS graphs including these highly turbid samples are included in Appendix A, Figure A2.

respectively at the Dam 2 site; Figure 2.5c). Lower values of 46–71 NTU were recorded for samples from the Suttor, Dam 1 and Dam 2 sites in December 2004. Samples collected at the Burdekin site in December 2004 have been excluded from further analysis because they were extremely turbid (1020 NTU in surface water) owing to localised rainfall in the days before sampling and were not considered representative of dry season conditions (for further information on these results, refer to Appendix A, Additional results and discussion section). In the 10 days before sampling in the reservoir, 68 mm rain fell at Sellheim, close to the Burdekin River at Sellheim water monitoring station (Figure 2.1, 120002C), equivalent to the median rainfall for December at this site (67.8 mm; Bureau of Meteorology, 2016). Much lower low turbidities (3–29 NTU) were observed at all four sample sites in September 2011.

TSS did not exhibit a strong linear relationship with turbidity (Figure 2.4b, c) and was rarely consistent through the water column (Figure 2.5e–h). At all sites, TSS ranged from 10 to 34 mg L^{-1} in samples collected in June 2004, December 2004, and August 2005, but in October 2006 this range dropped to 6.8–17 mg L^{-1}. The lowest TSS concentrations at all sites were recorded in September 2011 (3.2–6.6 mg L^{-1}).

2.4.2. Water temperature

Water temperatures at each site covered a narrow range (18°C–23°C) through the water column during the dry season (May–November). Temperature decreased with depth at all sites (Figure 2.5i–l). The temperature difference between surface and bottom waters increased as the dry season progressed, from 1°C in August 2005 to 1°C–5°C in September 2011 and October 2006 as the reservoir began to stratify thermally. In December 2004, the reservoir was clearly stratified, with surface temperatures of 25°C–30°C and bottom temperatures of 19°C–21°C (Figure 2.5j–l).

2.4.3. Sediment mineralogy and TOC

SS samples collected from Lake Dalrymple all contained the same minerals: quartz, muscovite and illite, kaolin group clays (kaolin) and smectite group (expandable) clays. Kaolin (average >54%) and micas (muscovite and illite; >21%) dominated the composition of SS at all four sites (Figure 2.6a). Smectite group clays made up, on average, >12% of all SS. The mineralogical composition of SS also remained consistent across sampling years: the quartz content remained low (3%–6%), rising slightly in samples from 2011 (7%–10%); the kaolin content remained between 46% and 60%; and the content of micas and smectite group clays (average 11%–33% and 6%–25% respectively) was also relatively stable, although samples from all four sites in August 2005 showed a decrease in micas (11%–15%) and a corresponding increase in smectite group clays (19%–22%).

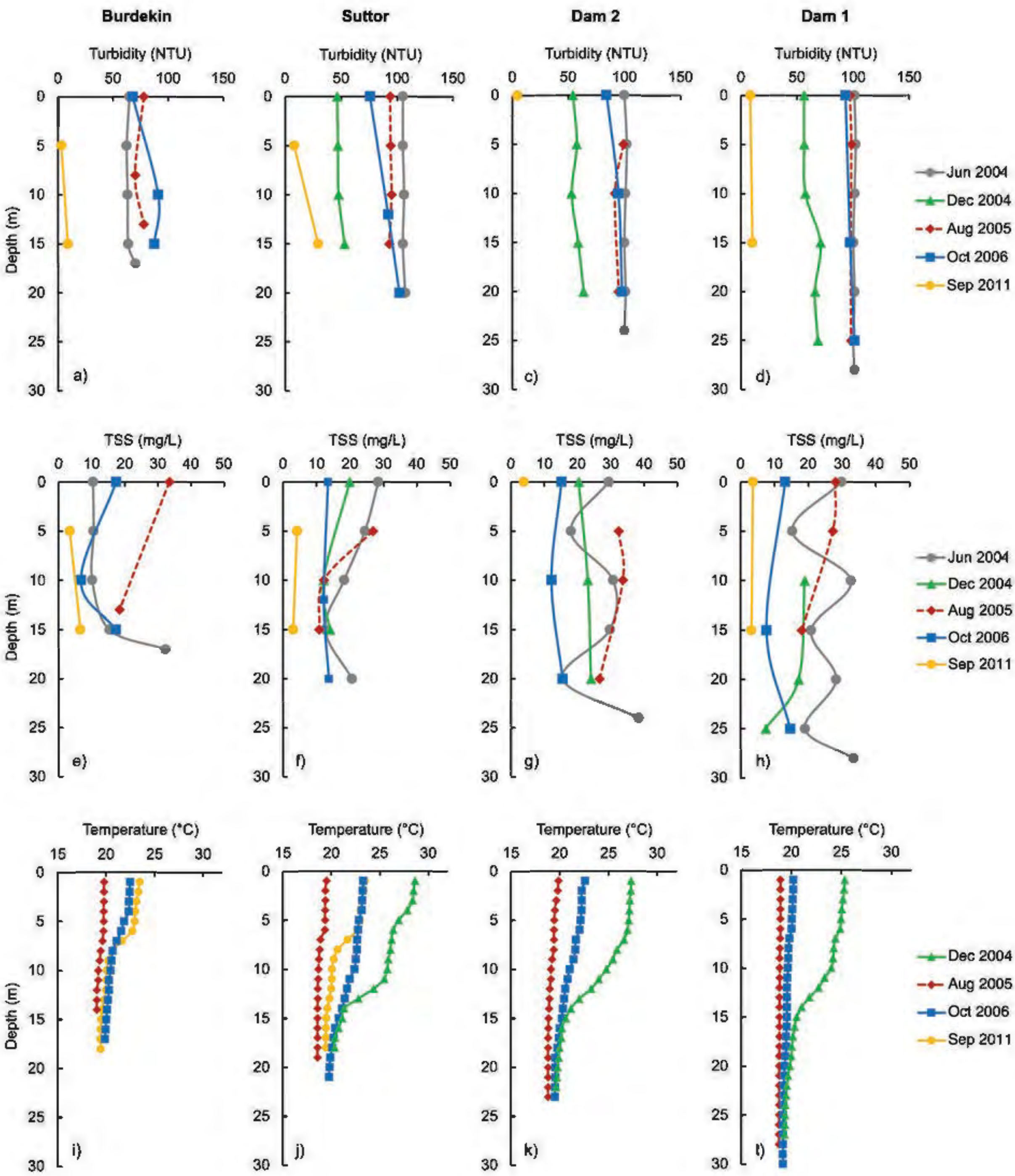

Figure 2.5 Dry season (a–d) turbidity, (e–h) total suspended solids (TSS) and (i–l) water temperature with depth at each of the four sites, namely Burdekin (a, e, i), Suttor (b, f, j), Dam 2 (c, g, k) and Dam 1 (d, h, l). December 2004 samples from the Burdekin site have been omitted because turbidity was extremely high in these samples because of localised rainfall in the days before sampling. Turbidity and TSS graphs for the Burdekin site including these highly turbid samples are included in Appendix A, Figure A2.

Benthic sediments contained kaolin (22%–60%) in proportions similar to SS samples, but higher percentages of quartz (11%–28%; Figure 2.6b). Benthic sediments were composed of 2%–10% feldspar minerals, whereas feldspars were present in just a few of the SS samples (and total <1% of those samples). Compared with benthic sediment from the other three sites, benthic sediment samples from the Burdekin site contained, on average, less kaolin (~30% vs >50%) and more micas (>25% vs <1%; Figure 2.6b).

Suspended sediment samples had higher percentages of TOC (range 2.63%–3.18%) than benthic sediment samples (range 0.61%–0.87%). The limited number of samples available for analysis meant that variations in TOC between dry seasons or sampling locations could not be investigated.

2.4.4. Particle-size distributions

An increase in laser obscuration, caused by increased dispersion of particles due to breaking up of flocs by ultrasonication (Malvern Instruments Ltd., 1999), was not observed during analysis of SS samples indicating minimal flocculation.

SS samples were dominated by colloidal, clay and silt-sized particles (0.05–63 µm). The particle-size distributions of SS at all four sites were bimodal, with dominant fractions centred on 0.1–0.2 µm (range 0.04–1 µm) and smaller secondary peaks at 4–10 µm (Figure 2.7a–d). Secondary peaks at 4–10 µm were larger in samples collected in December 2004 from the Suttor and Dam 2 sites (Figure 2.7a–c). Larger peaks at 10–70 µm (Suttor, Dam 1, Dam 2) and at 10 and 1500 µm (Burdekin) were observed in samples collected in September 2011

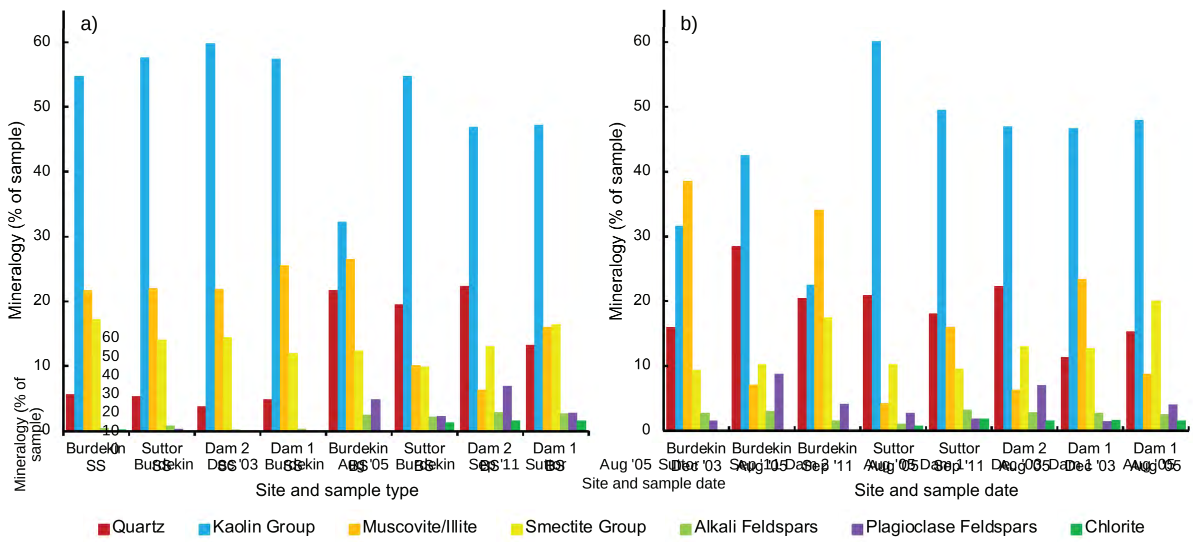

Figure 2.6 (a) Average mineral composition (crystalline component) of suspended (SS) and benthic (BS) sediment from each site. (b) Mineralogy of BS samples.

when water in the reservoir was unusually clear (Figure 2.7a–d). Samples from Dam 1 produced an almost unimodal distribution with a peak at 0.1–0.2 µm (except September 2011 samples; Figure 2.7d). The particle-size distributions of samples collected at Dam 1 in December 2004, June 2004, August 2005, and October 2006 were similar despite differences in the length of time since flow returned to base flow conditions (>259 days for December 2004 vs 89–164 days for June 2004, August 2005, and October 2006).

Benthic sediments were largely composed of clay and silt-sized particles (1–63 µm). Particle-size distributions were predominantly unimodal across the sampled years with a distribution peak centred on 8–10 µm (ranging from 1 to 280 µm) at the Dam 2 site and 4–6 µm (ranging from 1 to 90 µm) at the Suttor and Dam 1 sites. Particle-size distributions for benthic sediment from these three sites were consistent between years at each site (Figure 2.7f–h). Samples from the Burdekin site were variable: two samples exhibited unimodal distributions with a peak at 8–15 µm (ranging from 1 to 225 µm; December 2003, September 2011), whereas a third, collected in August 2005, had a bimodal distribution, with peaks at 15 and 150 µm, and was extremely broad, ranging from 1 to 1000 µm (Figure 2.7e). The minimum particle size of benthic sediment at all sites was 0.9 µm.

2.4.5. Hydrology

A negative linear relationship was found between dry season turbidity levels in the reservoir and the length of time since discharge returned to base flow (Figure 2.8a). A negative linear relationship was also found between dry season turbidity and inflow volume and duration in the preceding wet season (Figure 2.8b). At both the upstream and BFD gauging stations, annual discharge in the 2003–04, 2004–05 and 2005–06 water years was below average (mean; Figure 2.2a–c). Conversely, the second largest total annual discharge recorded at the Burdekin River Hydro Site gauge since the dam was constructed occurred in the 2010–11 water year (28 TL; Figure 2.2a). This was also true for the combined discharge from the Suttor and Cape rivers (Figure 2.2b). Annual discharge at the Burdekin River at Sellheim was the third highest since dam construction (Figure 2.2c). The 2010–11 wet season flow event was also longer in duration than usual, with inflow (above base flow volumes) received over 10 months compared with 3–6 months for the 2003–04, 2004–05 and 2005–06 flow events (Figure 2.8b).

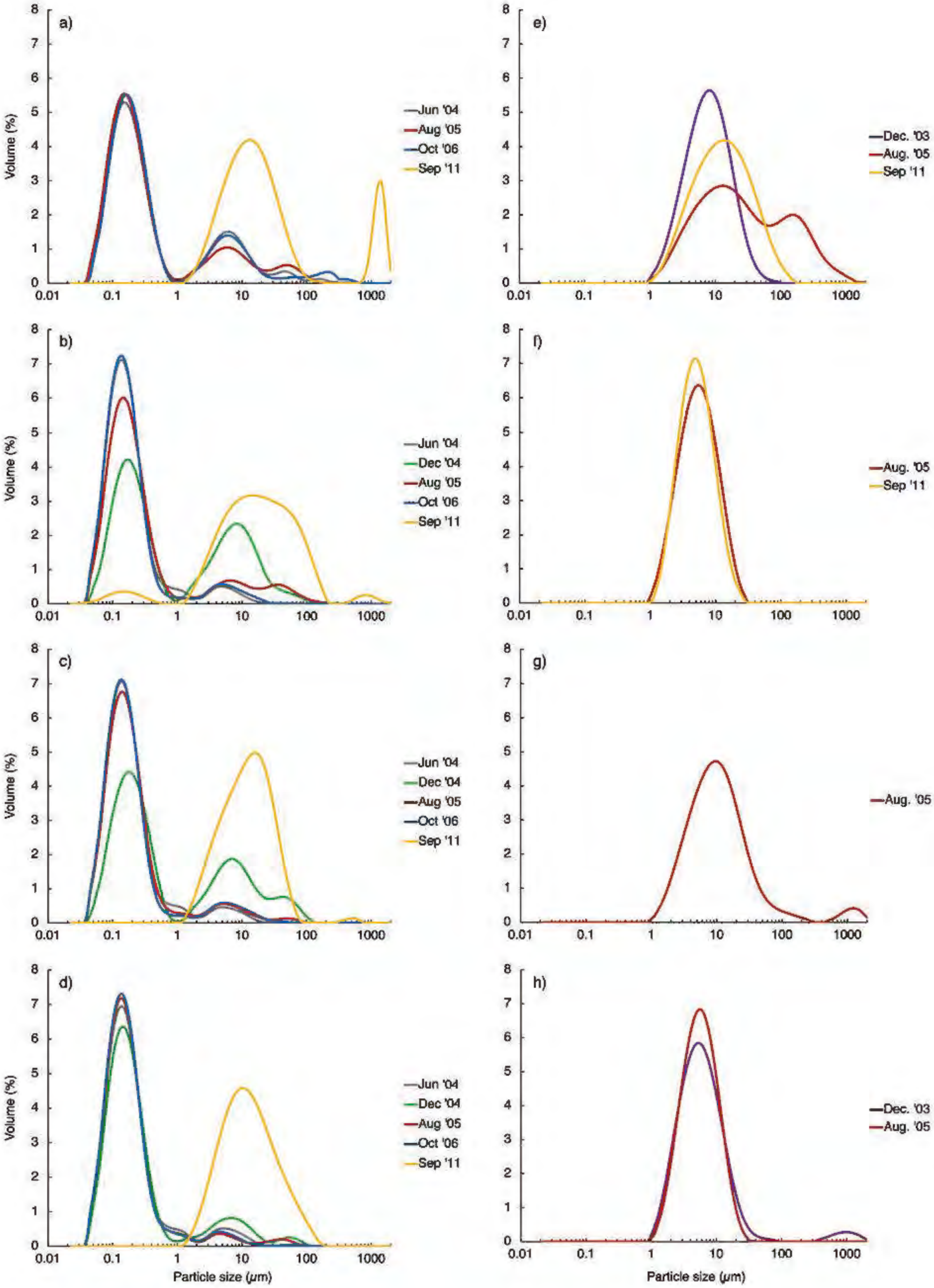

Figure 2.7 Average particle-size distributions for dry season suspended sediment (SS; a–d) and benthic sediment (BS; e–h) samples from the Burdekin (a, e), Suttor (b, f), Dam 2 (c, g) and Dam 1 (d, h) sites.

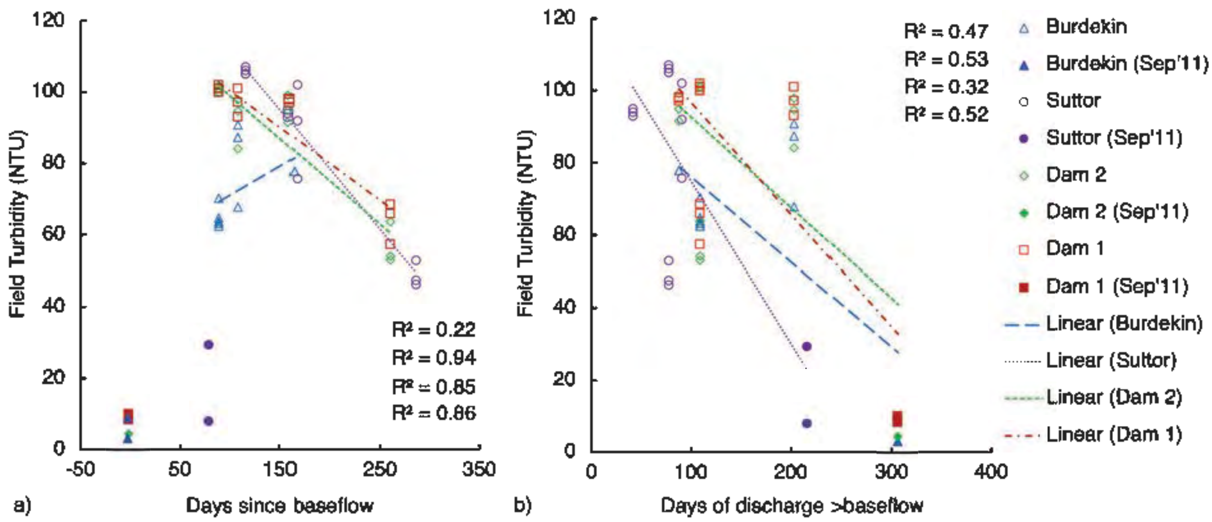

Figure 2.8 (a) Number of days since base flow was last reached plotted against turbidity at each location. September 2011 samples were excluded from the regression calculations as outliers whose turbidity values were greatly affected by the above-average discharge and low flow duration of the 2010–11 water year. (b) Duration of discharge recorded above base flow plotted against turbidity at each location. Regression statistics for both graphs are included in Appendix A (Figure A3).

2.5. Discussion

2.5.1. Turbidity patterns within Lake Dalrymple and the relationship between turbidity and TSS

Minimum values for turbidity in Lake Dalrymple are high (46–105 NTU) compared with other reservoirs in tropical to subtropical locations. For example, 29 formazin nephelometric units (FNU; 1 FTU = 1 NTU) in dry season samples from Aiba Reservoir, Nigeria (Atobatele & Ugwumba, 2008), <5 FTU in Liuxihe Reservoir, China (Wang et al., 2011), and commonly <40 NTU in lakes and reservoirs throughout the US (Shoup & Wahl, 2009). Higher turbidity in water entering reservoirs after high rainfall or streamflow events is common because the water carries elevated sediment concentrations (De Cesare et al., 2006; Georgoulas et al., 2012). However, in most reservoirs, high turbidity caused by SS usually decreases quickly as the SS is deposited as flows wane (Effler et al., 2006a; Wang et al., 2011). This also occurs in the BFD reservoir, where wet season inflows have turbidities of >600 NTU (Faithful & Griffiths, 2000); however, rather than becoming completely clear as flows cease, they typically remain at >46 NTU.

Persistent turbidity of similar magnitude to Lake Dalrymple's has been documented in only a few reservoirs of comparable volume in subtropical environments. Spioenkop Reservoir, South Africa, is affected by seasonal summer rainfall and has a turbidity of between 90 and >145 NTU, with the primary cause of turbidity identified as fine suspended clay particles (Hart, 1999). Similarly, turbidity ranging from 30 to 100 NTU occurs at Lake Le Roux, South Africa (Hart, 1986), and is also attributed to suspended silts and clays (Allanson & Jackson, 1983).

The high (>46 NTU) turbidities recorded in Lake Dalrymple during the dry season are comparable to turbidity values more commonly attributed to resuspension in shallow lakes (<4 m mean depth; Atobatele & Ugwumba, 2008; Geddes, 1984). The consistency of turbidity readings down the water column in the reservoir during the dry season at all sites (Figure 2.5a–d) indicates that no turbid inflows (density currents) were present, as are observed in the wet season (Faithful & Griffiths, 2000). Sediment resuspension is possible in deeper water (>28 m; Tammeorg et al., 2013), but would be expected to increase turbidity close to the substrate (Bloesch, 1994; Effler & Matthews, 2004). The absence of increased turbidity at the bottom of the reservoir suggests that sediment is not being resuspended at the sites monitored in this study. Reservoir drawdown can increase sediment resuspension and turbidity (Effler & Matthews, 2004) when previously submerged areas are uncovered and bottom sediments in the shallower reservoir margins can be resuspended by waves. In Lake Dalrymple, the lowest drawdown levels are often observed late in the dry season (Figure 2.3), but turbidity did not increase with a decrease in reservoir capacity. Between June 2004 and December 2004, reservoir capacity dropped from 87.7% to 63.9%, but turbidity decreased over the same period from 100–107 to 46–71 NTU, further indicating that resuspension is not the dominant process causing persistent turbidity in the reservoir. However, this study sampled sites within the relict river channel, in relatively deep water (17–31 m). Near-shore sediment resuspension, transport and redeposition in deeper water are common in large, deep lakes (Bloesch, 1995) but we did not examine this possibility and cannot rule out resuspension proximal to the shoreline contributing to reservoir turbidity.

Development of thermal stratification in Lake Dalrymple suggests that late in the dry season complete mixing of the water column by wind or currents is weak or non-existent (Tundisi & Tundisi, 2011). The BFD reservoir is strongly stratified and monomictic (Chudek et al., 1998), with variable stratification developing in the dry season. Like other tropical reservoirs, Lake Dalrymple is likely to undergo some daily lateral and vertical mixing because of overnight cooling of surface waters and surface winds (Finlayson et al., 1980; Imberger, 1985a). This mixing in the epilimnion contributes to the uniformity of turbidity in the reservoir, particularly when thermal stratification is weak. In months where air temperatures were low and conditions were windy, stratification was weak. However, thermal stratification consistently developed by December each year (Figure 2.5i–l; Chudek et al., 1998). Strong stratification was observed at the Dam 1 and Dam 2 sites sampled early in the morning (before 08:45 hours) in December 2004, indicating that stratification was not disrupted overnight. This stratification suggests that late in the dry season mixing does not extend beyond the thermocline, an observation also recorded by Chudek *et al.* (1998).

Turbidity–TSS relationships are system specific and often weak (Davies-Colley & Smith, 2001). Faithful and Griffiths (2000) found a correlation between turbidity and suspended particulate material concentration for wet season SS samples from Lake Dalrymple at <600 NTU, but field and laboratory turbidity and TSS were poorly correlated in this study (r^2=0.02 (field) and 0.34 (lab); Figure 2.4b, c). This may indicate that material <1.2 µm was not completely captured by the filter papers. Although TSS is a commonly used measure of sediment concentration, further studies should also undertake analysis of suspended sediment concentrations (SSC; evaporation of a known volume of mixture; Method D 3977-97, ASTM, 2000) to ensure that all SS is captured and improve the accuracy of sediment concentration data (Gray et al., 2000).

2.5.2. Influence of particle size and mineralogy on turbidity

The persistence of turbidity in Lake Dalrymple is predominantly due to the extremely fine particle size (<1 µm) and mineralogy of the sediment. The particle-size data in the present study suggest that sediment resuspension is not the primary factor affecting turbidity in the reservoir because SS falls within the range 0.04–0.9 µm and particles of this size are not found in benthic sediment samples. Although clay particles may be resuspended and removed by large inflow events (Effler et al., 1998), it is unlikely that no particles <0.9 µm would be found in benthic grab samples that represent multiple years of deposition and were collected in dry seasons following below-average flow events (December 2003, August 2005). Calculations using Stokes' Law show that it would take a 0.9-µm particle of average density (2.65×10^3 kg m^{-3}) 15.8 days to settle 1 m under non-turbulent conditions (assuming constant density, 1 kg m^{-3}, and viscosity, 1×10^{-3} N·s m^{-2}, of the water), so it is unsurprising that particles <0.9 µm remain in suspension in the reservoir. Montmorillonite (smectite) clay particles that make up >12% of the SS in the reservoir can have a specific gravity as low as 2.00×10^3 kg m^{-3} (Mindat.org, 2023) and take over 26 days to settle 1 m. Furthermore, experimental analysis by Gomboš et al. (2018) demonstrated that for plate-shaped clay particles <2 µm, Stoke's Law loses its validity as the particles begin to form a colloidal dispersion. In the relatively calm water of a laboratory settling column clay particles eventually reach sedimentation equilibrium (no longer settle out) at a particle size of d(90) = 0.27 µm (Gomboš et al., 2018). This finding supports Lewis et al. (2013) who found that the <1-µm fraction is not trapped by the dam during floods that overtop the spillway. Organic material only makes up a small fraction of SS (TOC 2.63%–3.18%) but this component will also reduce the settling velocity of particles due to its low density (Droppo, 2001).

The secondary particle-size fraction centred on 4–10 µm present in SS from Lake Dalrymple is unlikely to represent sediment flocs because samples were treated with ultrasonication before analysis. The source of this coarser fraction may be related to organic matter, and microscopic analysis would be required to determine the composition. An increase in the volume of larger (4–10 µm) particles at the Suttor and Dam 2 sites in December 2004 (Figure 2.7b, c) may indicate increased growth of freshwater phytoplankton (Bellinger & Sigee, 2010; Griffiths & Faithful, 1996) in the water column as the turbidity decreased (46–64 NTU) and the water temperature increased (Figure 2.5c).

The mineralogy and particle size of the SS causing turbidity in Lake Dalrymple is similar to that causing extreme turbidity in other waterbodies. Colloidal (<1 µm) quartz, nontronite (smectite) and kaolinite cause turbidities as high as ~1000 NTU (S. Townsend, pers. comm.) in the Longreach Waterhole in a semi-arid region of Australia (Townsend, 2002). Although similar in character to the SS causing turbidity in Lake Dalrymple, the turbidity of Longreach Waterhole is exacerbated by its shallowness and lack of drainage, which causes turbidity to increase during the dry season as evaporation reduces the water depth from 3 to 2 m. Similarly, in shallow Lake Alexandrina, South Australia (mean depth 2.9 m), turbidities of 25–155 NTU (mean 92.7 NTU) are caused by colloidal (<2 µm) montmorillonite with minor amounts of kaolinite and illite and maintained by resuspension (Geddes, 1988; Woodyer, 1978). In other regions, persistent turbidity is driven by a single clay type. For example, in Lake Chapala, Mexico, elevated year-round turbidity (24–285 NTU) is produced primarily by smectite group clays (90%, Lind et al., 1997). The mean ± s.d. size of the SS in Lake Chapala is 0.5 ± 0.1 µm (Macías & Lind, 1990), similar to the size of SS in the BFD reservoir. Lake Chapala has a maximum depth of only 10 m (mean <7.2 m) and is susceptible to wind-driven sediment resuspension via wave action coupled with the presence of phytoplankton. Although these turbid waterbodies share similar sediment mineralogy and particle-size characteristics with Lake Dalrymple, the drivers behind their persistent turbidity are different: Longreach Waterhole, Lake Alexandrina and Lake

Chapala are all shallow and have high resuspension potential, whereas Lake Dalrymple is relatively deep and has less reservoir area susceptible to resuspension.

2.5.3. Drivers of changes in turbidity

Limited sediment deposition occurs in the reservoir during the dry season. Turbidity was lower in samples collected in December 2004 relative to samples collected in June 2004, August 2005, and October 2006 (Figure 2.5) because of the increased time (>89 days longer) since significant inflow. The decrease in turbidity with an increase in time since base flow was reached (Figure 2.8) indicates that some sediment is being removed from the water column via deposition.

Dry season turbidity in Lake Dalrymple will remain high in all years except those following above-average flow events regardless of which river is the dominant water source. The observation that turbidity in the dry season remained high (>46 NTU) in the three below-median to median water years examined accords with the findings by Fleming and Loofs (1991), who showed that the reservoir remained turbid (>25 NTU; Griffiths & Faithful, 1996) year-round in the three (below-median to median) water years following dam construction (1987–90; Figure 2.2a). Fleming and Loofs (1991) argued that the reservoir's turbidity was produced primarily by fine sediments delivered from the southern (Suttor River) arm of the reservoir and because they expected the Burdekin River (northern arm) to supply about half the inflow to the reservoir, they expected that lower turbidity would occur except in periods 'below normal flow'. This assertion has generally held true for years of above-average flow, with low (<30 NTU) dry season turbidities recorded in 1990–91 Fleming and Loofs (1991) and in 2010–11 (present study). However, in years of median to average discharge (1988–89, 1996–97, 2005–06) the reservoir has remained turbid (>30 NTU, Chudek et al., 1998; Fleming & Loofs, 1991; this study) even when reservoir inflow was greater from the northern Burdekin arm (62%, 60% and 81% for each year respectively; https://water-monitoring.information.qld.gov.au/, accessed 21 June 2021). In years of well below median flow (1994–95 and 1995–96), higher turbidity (60–300 NTU) was observed even when >50% of inflow was from the Burdekin River (Chudek et al., 1998). Similarly, data for the 2004–05 and 2005–06 water years demonstrate that the reservoir remained turbid throughout the year when the northern Burdekin arm contributed two- and four-fold more water than the combined Suttor and Cape rivers respectively (Figure 2.2). The Burdekin River contributed >50% of reservoir inflow in 22 of the 27 water years since dam construction was completed (from 1987–88 to 2013–2014; https://water-monitoring.information.qld.gov.au/, accessed 21 June 2021), but turbidities <30 NTU are only observed after above-average discharge into and through the reservoir. These results indicate that reservoir managers and BRIA stakeholders should expect turbid discharge from the reservoir in all but above-average flow years and develop management strategies accordingly.

A significant relationship exists between dry season turbidity in the reservoir and inflow volume and duration in the preceding wet season (Figure 2.8b; for slope statistics, see Appendix A, Figure A3), confirming that above-average flows may flush SS from, or dilute SS within, the reservoir. Comparatively lower turbidity (3–29 NTU) was observed in the BFD reservoir in the dry season in the 2010–11 water year following an above-average inflow event. The sediment load of the Burdekin River is dependent on sediment availability (Amos et al., 2004) and sediment supply was depleted after 2 years of above-average discharge in 2007–08 and 2008–09 (Figure 2.2; Bainbridge et al., 2014). The high discharge of the 2010–11 flow event, coupled with the longer inflow duration, filled the reservoir with water that will have initially carried large volumes of SS, much of which would have flowed over the dam wall. As the event continued, water with relatively low concentrations of SS flowed through the reservoir, flushing it of finer particles and diluting the amount of sediment remaining after flow ceased. The reservoir previously became clear following a large discharge event in early 1991 (Burrows & Butler, 2007; Fleming & Loofs, 1991), the largest flow volume to discharge from the reservoir since the completion of the dam (29 TL in the 1990–91 water year; Figure 2.2). The data from this study support the suggestion of Burrows and Butler (2007) that the reservoir only clarifies when post-event and dry season base flow volumes entering the reservoir are very high and have a high dilution capacity, because the only time they had observed the dam to clarify to any degree was in the 1990–1991 water year.

2.5.4. Implications for ecosystem management

The Australian & New Zealand Guidelines for Fresh & Marine Water quality (https://www.waterquality.gov.au/anz-guidelines) provide draft toxicant default guideline values that have informed site-specific guideline values developed under Queensland's Environmental Protection (Water and Wetland Biodiversity) Policy 2019. Environmental values and water quality objectives (WQOs; including for turbidity and TSS) for the surface and ground waters of the Burdekin Basin were approved in 2022 but there was insufficient data to establish local aquatic ecosystem objectives for lakes/reservoirs, including Lake

Dalrymple (https://environment.desi.qld.gov.au/management/water/policy/burdekin-basins). The maximum TSS recorded across the reservoir in the dry season (28.4–38.4 mg L^{-1}) approaches the upper limit for the protection of freshwater fish (<40 mg L^{-1}). Further, turbidity in the reservoir exceeds the Queensland trigger value for Central Coast Queensland Region freshwater reservoirs (1–20 NTU, DEHP, 2009) all year round. Turbidity is likely to exceed the trigger value for tropical Queensland reservoirs (200 NTU) during the wet season each year (Chudek et al., 1998; Faithful & Griffiths, 2000), but does drop below the threshold in the dry season (105 NTU). However, because WQOs for the Burdekin River downstream of the dam are lower (50 NTU; https://environment.desi.qld.gov.au/__data/assets/pdf_file/0034/273598/burdekin-bowen-river-basins.pdf), the downstream Burdekin River is likely to exceed that trigger value for much of the year because of regular releases of turbid reservoir water (>45 NTU) for irrigation.

The high turbidity of surface waters strongly limits phytoplankton productivity in the reservoir (Griffiths & Faithful, 1996). Phytoplankton biomass (using chlorophyll-*a* in the surface water as a surrogate biomass indicator) in the reservoir is low (median 3.2 µg L^{-1}; n = 192; collected 1987–96) when turbidity is high (median TSS 136 mg L^{-1} (n = 216); median Secchi depth 17 cm (n = 214)) and increases approximately twofold when water in the reservoir clarifies, as it can do very briefly over the late winter period when inflows to the reservoir are minimal (J. Faithful, unpubl. data). Despite the low phytoplankton biomass, there are high concentrations of zooplankton, which would provide a substantial source of food for fish present in the reservoir. The zooplankton community assemblage is selected out on the basis that the species present are capable of ingesting organic material associated with the SS (J. Faithful, pers. comm.).

Conversely, elevated turbidity in water released from the BFD reservoir is maintaining the health of key coastal wetlands in the lower Burdekin River by decreasing their vulnerability to other human pressures, for example by supressing aquatic macrophyte growth in nutrient-rich agriculture run-off (Burrows & Butler, 2007). Given that water from the reservoir is likely to remain turbid except in years of above-median and extended inflow, treatments to accelerate sediment deposition, such as adding a flocculent to the reservoir to reduce turbidity, may be considered, as is common in drinking water supply reservoirs (NHMRC & NRMMC, 2011; Perkins et al., 2007). However, clearer water could lead to an increased incidence of algal blooms in both the reservoir and irrigation channels, as well as increased weed growth in irrigation channels (Geddes, 1984; Sabbatini et al., 1998). Although not a natural state, elevated turbidity in the reservoir and BRIA is now a common feature, and actions such as water spreading (using river water that is too turbid for artificial recharge as surface water for farm irrigation) are used to manage turbid water (Davis et al., 2014).

2.6. Conclusions

The findings of this study highlight the importance of a thorough examination of SS, taking sediment characteristics and hydrological conditions into consideration, in order to understand the drivers of persistent turbidity and develop appropriate sediment management strategies. Lake Dalrymple exhibits elevated (>46 NTU) turbidity year-round throughout the water column in below-median to median water years. Dry season turbidity in the reservoir is caused primarily by SS <0.9 µm in size and composed largely of kaolin and smectite group clays and micas. The mineralogy of dry season SS is consistent throughout the reservoir. Clay-sized particles (<3.9 µm) are being supplied by both the Burdekin and the Suttor and Cape rivers (Bainbridge et al., 2014), but the lack of mineralogical distinction between SS from the sites sampled means that the hypothesis that the southern arm of the river catchment is supplying the clays causing the persistent SS and resultant turbidity (Fleming & Loofs, 1991) could not be confirmed. Geochemical tracing of the SS was attempted as part of this PhD project to better constrain its catchment origin and is presented in Chapter 4. Resuspension is unlikely to be the dominant cause of turbidity in the reservoir because the SS causing the turbidity falls within the range 0.04–0.9 µm and particles of this size are not found in benthic sediment samples.

This study emphasises the importance of reservoir flushing by extended periods of high flow as a major control of turbidity and provides evidence that even a persistently turbid reservoir may clarify naturally under very specific circumstances. Persistent turbidity caused by colloidal SS (<0.9 µm) that does not settle out will be reduced by prolonged and above-average reservoir inflow that has depleted its sediment sources continuing to move through the reservoir. Turbidity in the dry season will remain elevated in years where wet season flow events are in the below median to median range. Because turbidity is likely to remain elevated in most years, the present study provides useful information on sediment particle size and mineralogy for water users and irrigation managers downstream. Managers of this and other turbid reservoirs in seasonally dry tropical regions should not rely on natural flushing but may want to develop reservoir operating procedures to maximise sediment transfer during flow events to reduce turbidity.

Chapter 3: Effect of turbid inflow on sediment transport and deposition in a stratified reservoir in the seasonally dry tropics of Queensland, Australia

This paper is in preparation. Reviewers will encounter some repetition of information included in the preceding sections of this thesis, particularly in the introduction and methods sections.

Abstract

Turbidity currents are often the dominant contributor to sediment transport and deposition within lakes and reservoirs. This study examines the effect of thermal stratification on turbid inflow and its influence on sediment transport and deposition in the Burdekin Falls Dam reservoir (Lake Dalrymple) in the seasonally dry tropics of Queensland, Australia. The reservoir is located on the Burdekin River and stratifies thermally in the spring and summer, developing a thermocline between 5 and 15 m depth below the surface that is shallowest in upstream areas of the reservoir. Every wet season (November to April) turbid inflows containing an average of 2.6 million tonnes of sediment enter the reservoir and form turbidity currents that travel through the reservoir as an interflow. During these events, turbid interflows in deeper parts of the reservoir (>20 m) transition into underflows, temporarily disrupting stratification. Turbidity was found to be a reliable proxy for suspended sediment concentration ($r^2 = 0.97$), allowing the spatial and temporal relationships between turbidity, particle size and mineralogy to be investigated. Particle-size data from turbid inflow and benthic sediments from sample sites located throughout the reservoir show that sediment >126 μm is largely absent from wet season inflow in below-average flow events and moves through the reservoir as bedload (a process restricted to the uppermost reaches) or is deposited in the upper reaches of the reservoir. Overflow of the dam occurs even during most below-average to average flow events (dependent on reservoir volume prior to each wet season and the frequency of wet season inflow events), discharging turbid flows carrying fine-grained sediment (97% of particles <62.5 μm) that progress through the reservoir to and over the dam wall, limiting the amount of fine sediment deposited in the reservoir. An increase in the particle size of benthic sediments collected after above-average inflow events indicates that these events transport larger particles from the northern Burdekin sections of the reservoir further into the impoundment. Quartz and feldspars were associated with coarse sediment and deposited in greater percentages upstream while smectite and kaolinite group clays were found in greater proportions in the fine sediment (<62.5 μm) deposited in sections of the reservoir closest to the dam wall. These data provide insight into the behaviour of

turbid flows in reservoirs that receive highly variable inflow, providing important context for dam operators in tropical regions and worldwide.

Keywords: Seasonally dry tropics, turbidity current, density current, particle size, water reservoir.

3.1. Introduction

The physico-chemical limnological character of a reservoir and the primary stratification and mixing processes occurring during elevated streamflow events are important factors to understand the transport and deposition of sediment within a reservoir (Mueller et al., 2013). Sediment-laden flows entering a reservoir will form turbidity currents due to the difference in density between the incoming water and water already in the reservoir (De Cesare et al., 2006). Water density differences are driven by temperature, electrical conductivity and suspended sediment (SS) concentration (Griffiths & Faithful, 1996; Uhlmann et al., 2011). These currents transport sediment into, through, and out of a reservoir and usually propagate as either overflow (surface), interflow (intrusion) or underflow (bottom) depending on the density of the inflowing and resident waters (An & Julien, 2014; Lee & Yu, 1997). Turbidity currents may cause problems in reservoirs such as reducing storage capacity, blocking intake structures and damaging hydropower infrastructure (de Cesare et al., 2001; Majoro et al., 2020; Oehy & Schleiss, 2007).

Previous studies have examined the characteristics of turbid inflows to reservoirs, including turbid flow behaviour (Effler et al., 2006a; LaBounty & Horn, 1997; McCullough et al., 2007) and the impact of turbidity currents on sedimentation (de Cesare et al., 2001; Samadi Boroujeni et al., 2009). Models have been created to describe the development and behaviour of turbidity currents in reservoirs in a range of temperate to tropical environments (e.g. Chung et al., 2009; Gelda et al., 2013; Liu & Chen, 2013; Wang et al., 2012), focussing on water temperature, salinity and SS concentration. Researchers have also generated models to predict the effect of potential turbidity current control measures such as dredged guiding channels and obstacles (Imtiyaz et al., 2024; Marosi et al., 2015). Other studies focus on the relationship between reservoir stratification and water quality (temperature, dissolved oxygen, salinity, turbidity; Bertone et al., 2015; Chudek et al., 1998; Marti et al., 2011; Townsend, 1998). Several studies discuss turbidity as a marker of inflow (Elçi, 2008) but the impact of turbid flows on the transport and deposition of sediment in these environments is not described. The variability of sediment composition within turbidity currents in reservoirs situated in seasonally dry tropical locations characterised by highly seasonal and inter-annually variable flow regimes has rarely been described.

The Burdekin Falls Dam (BFD) reservoir is a large (220 km^2, 1.86 TL), strongly stratified reservoir in the seasonally dry tropics of northern Queensland, Australia (Figure 3.1; Chudek et al., 1998). Water impounded in the reservoir is persistently turbid throughout the year (>45–100 NTU in the dry season) due to abundant fine clays suspended in the water column (Cooper et al., 2017 – Chapter 2). Annual rainfall variability in the reservoir's catchment is 'moderate' to 'moderate-high' (Bureau of Meteorology, 2017). Greater than 80% of mean annual rainfall and discharge occurs during the wet season (November to April; Lewis et al., 2006; Lough, 2007) and inflow volumes are largely dominated by flood events (Bainbridge et al., 2014). As a result, inflow is highly variable with an interannual CV of 119% (1991–2020; Lewis et al., 2021). Previous studies have examined three separate inflow events early in the life of the reservoir and found that water temperature gradients and sediment loads (through their contribution to flow density) determine where in the water column turbidity currents will flow (Faithful & Griffiths, 2000; Griffiths & Faithful, 1996). Lewis et al. (2013) identified key sediment particle-size classes trapped by the reservoir (5.0–>30 μm sized particles) and catchment-wide sediment budgets (Bainbridge et al., 2014) show that an average of 2.1 million tonnes of sediment is exported from the reservoir annually. However, no study has presented a comprehensive characterisation of the SS present in turbidity currents or benthic sediment within the BFD reservoir nor examined the variability over multiple consecutive water years.

This paper will discuss the impact of reservoir stratification on the development of turbidity currents and its influence on sediment transport and deposition within the seasonally dry tropics context. This study analysed the concentration, particle size, and mineralogy of suspended and deposited (benthic) sediment samples collected during the wet season in three below-mean average water years (<6.6 TL discharge at the downstream Burdekin River Hydro Site water monitoring station) to characterise turbid flows that enter the BFD reservoir during wet seasons and their relationship to benthic sediments. This is one of the first studies to characterise the SS entering a seasonally dry tropical reservoir over several years using water quality and particle-size data to understand the intra- and inter-annual variability of turbid inflow. Our results demonstrate that a thorough examination of SS, including particle size, mineralogy, and limnological and hydrological conditions is necessary to understand the behaviour and fate of sediment in seasonally dry tropical reservoirs.

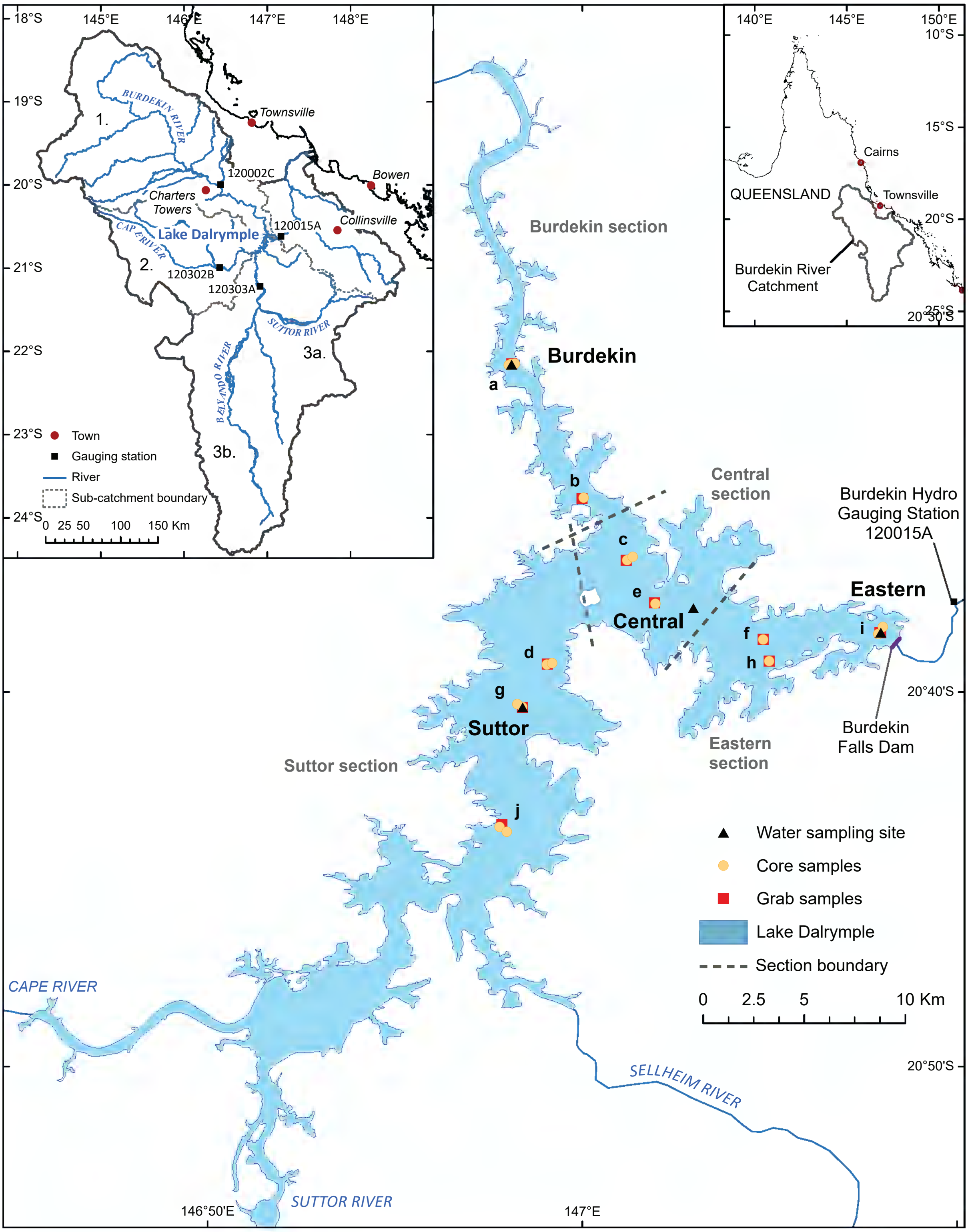

Figure 3.1 Map of the BFD reservoir showing water and benthic sediment sampling sites. For this study, the reservoir is divided into Burdekin, Suttor, Central and Eastern reservoir sections. Small inset: Location of the Burdekin River catchment in Queensland, Australia. Large inset: Location of the BFD reservoir (Lake Dalrymple), major rivers and water monitoring stations: 120002C Burdekin River at Sellheim, 120303A Suttor River at St Anns, 120302B Cape River at Taemas, and 120015A Burdekin River at Hydro Site. Reservoir sub-catchments marked by numbers: 1) Upper Burdekin River, 2) Cape River, 3a) Suttor River and 3b) Belyando River.

3.2. Background

The Burdekin River catchment is a large (>130,000 km^2) coastal catchment situated in the seasonally dry tropics of northern Queensland, NE Australia. The Burdekin River is one of Australia's largest rivers as measured by discharge volume (Mitchell et al., 2006) and transports 3.3 Mt of fine sediment (<63 µm) per year to the coast on average (McCloskey et al., 2021). 114,220 km^2 (~88%) of the Burdekin catchment lies upstream of the BFD (Figure 3.1).

The BFD was completed in 1987. Its reservoir, Lake Dalrymple, is the largest by volume in Queensland, Australia (ANCOLD, 2010). At full supply level the BFD reservoir holds 1.86 TL of water and covers an area of 220 km^2. The maximum depth of the reservoir is 40 m (mean depth 8.45 m) and it is 50 km in length from the dam wall to the furthest inflow channel (Sunwater Limited, 2009, 2024b). The BFD was constructed to supply irrigation water to downstream cropping lands and the mining industry. Provisions were made at the time of construction to allow for vertical extension of the dam wall to increase storage and support the generation of hydroelectric power.

The reservoir has three major sub-catchments: The Upper Burdekin River, Cape River, and Belyando-Suttor rivers (Figure 3.1). Bainbridge *et al.* (2014) describes the physical geography of these sub-catchments in detail, and grazing is the primary land use in each (Roth *et al.,* 2002). Most of the area draining into the BFD reservoir is classified as hot semi-arid using the Köppen-Gieger classification (Peel et al., 2007). The climate has a well-defined wet season from November to April, with a dry season from May to October. Rainfall varies temporally and spatially within both the catchment and sub-catchments (Roth et al., 2002). In the Upper Burdekin coastal ranges mean rainfall is >1500 mm/yr, while parts of the Suttor and Belyando sub-catchments receive only 500 mm/yr (Bainbridge et al., 2014). The reservoir fills rapidly (1–2 days) during wet season inflow and, since construction, has rarely been below 50% capacity; it fills, and has overflowed every water year but two (1992–93 and 2014–15; capacity to average annual inflow ratio = 0.24; Bainbridge et al., 2014). Highly turbid inflows carry high concentrations of fine SS (>150 mg/l TSS; Faithful & Griffiths, 2000; Griffiths & Faithful, 1996) which remain in suspension and cause persistent turbidity in the reservoir (Cooper et al., 2017 – Chapter 2). The Upper Burdekin River contributes >50% of water inflow into the BFD reservoir in four out of five years (Figure B1) and is also the dominant sediment source to the reservoir under all streamflow conditions (contributing 76–95% of sediment in the water years from 2005–06 to 2009–10; Bainbridge et al., 2014).

3.2.1. Reservoir morphology

The BFD reservoir is a warm monomictic, dendritic reservoir with a Y-shaped morphology and two primary inflow sources: the Burdekin River to the north and the Suttor and Cape rivers to the south (Figure 3.1). Reservoirs are characterised by three regions: riverine (inflows dominate lake characteristics), transition (zone of change from riverine to limnetic dominance) and lacustrine (limnetic processes dominate; Uhlmann et al., 2011). The Burdekin section of the reservoir (Figure 3.1) is a narrow (~0.4–1 km wide) open channel, with distinct banks lined with living and dead trees and is classed as riverine. The Suttor River was originally much narrower than the Burdekin River (<200 m wide), but the Suttor section of the reservoir is much wider (2–4 km) with two thirds of the channel obscured along the edges by dead trees and much shallower banks. This section of the reservoir is riverine to transitional. The former confluence of the two rivers occurs in the Central section of the reservoir; this transitional section is wide and open (>1.4 km) although bays or inlets to the north and south are filled with dead trees. The lacustrine Eastern section is wide (>1.2 km), open and deep (28–32 m deep at the Eastern site; Figure 3.1).

3.3. Methods

3.3.1. Selection of water sampling sites

Four sites were selected to capture key locations within the reservoir that capture inflow from the Burdekin and Suttor/Cape sources and its progress through the reservoir and were safely navigable by boat (Figure 3.1):

1. Burdekin, within the northern arm of the reservoir, representative of the inflowing Burdekin River (water depth ~18 m)
2. Suttor, representative of the inflowing Belyando-Suttor rivers and Cape River (water depth ~22 m)
3. Central, downstream of the confluence of the northern (Burdekin) and southern (Suttor) arms within the Central section of the reservoir and representing an area of potential mixing (water depth ~24 m)

4. Eastern, 800 m from the dam wall in the Eastern section of the reservoir, representative of water that has travelled furthest through the reservoir (~26 km from the Burdekin site and 24 km from the Suttor site; water depth ~31 m).

Sites were strategically located to take advantage of data collected in previous studies (Faithful & Griffiths, 2000). Samples were collected in the middle (or within ~30 m) of the relict river channels at all locations. Distances from sampling sites to the dam wall (as measured along the channel), river inflow point and water monitoring gauges, plus water depths, are provided in Appendix B (Table B1).

3.3.2. Hydrology

Hydrological data were obtained from the Queensland Government's Water Monitoring Data Portal (https://water-monitoring.information.qld.gov.au/, accessed 2 February 2017). Annual and daily discharge data were downloaded for the gauging stations closest to the reservoir: Burdekin River at Sellheim (site ID 120002C), Suttor River at St Anns (120303A), Cape River at Taemas (120302B) and Burdekin River at Hydro Site (120015A; Figure 3.1). Discharges for the Cape and Suttor River gauges were combined to give the total inflow entering the southern arm of the reservoir. Water monitoring station details are provided in Appendix B, p 183. Daily reservoir capacity data were obtained from the then Queensland Department of Natural Resources and Mines (V. Manley, pers. comm., 1 August 2016; October 1987–July 2002) and Sunwater Limited ACN 131034985 (M. Ali, Bureau of Meteorology, pers. comm., 25 July 2016; July 2002–July 2016).

This study covers three consecutive water years (1 Oct. to 30 Sept. each year)—2003–04, 2004–05 and 2005–06—with additional data collected in 2011. At the upstream and BFD water monitoring stations, annual discharge in those water years was below the mean (<6.6 TL at the Burdekin River Hydro Site 5 km downstream of the dam wall; Appendix B, Figure B1). Median annual discharge was recorded at the Hydro Site gauge in 2004–05 (3.7 TL) and just slightly above median discharge at the Burdekin Sellheim gauge in 2005–06 (2.7 TL, median 2.3 TL). Despite the below-mean discharge, reservoir overflow occurred each year (Appendix B, Figure B2). In comparison, three well above-mean water years were recorded at the Hydro Site gauge between 2006 and 2011: 18 TL total discharge in 2007–08, 25 TL in 2008–09 and 28 TL in 2010–11 (Appendix B, Figure B1).

3.3.3. *Timing of sampling*

In situ physico-chemical water-quality data and water samples were collected from the BFD reservoir during the wet season in: February 2004; December 2004, January and February 2005; and March and April 2006 (Table 3.1). Excluding December 2004, sampling was carried out during periods of inflow into the reservoir (as reservoir volume increased; Figure B2), once heavy rainfall was recorded in the reservoir's catchment. In December 2004, inflow related to localised rainfall was observed at the Burdekin site but samples from the other three sites were collected prior to inflow and provide a comparison with late dry-season water conditions.

Benthic sediments and core samples were collected during the dry/pre-wet season in December 2003, August 2005 and September 2011. The 2003 and 2005 samples were collected before the three well above-average water years in 2007–08, 2008–09 and 2010–11 and the 2011 samples were collected after. Further sample collection details are provided in Appendix B (Table B3).

Table 3.1 Water sampling timing in relation to peak reservoir overflow.

Water year	Sample day	Relation to peak overflow
2003–04	17–19 February 2004	1-3 days after
2004–05	16–17 December 2004	40-41 day prior
	12 January 2005	14 days prior
	26 January 2005*	Same day
	2 February 2005	7 days after
2005–06	29 March 2006	17 days prior
	11 April 2006	2 days prior
	14 April 2006	Same day

*On 26 January 2005 conditions were too dangerous to remain on the reservoir, so sampling was limited to shallow depths (<15 m) from two locations.

3.3.4. *Physico-chemical water quality*

Water temperature and electrical conductivity (EC) provide a reliable indication of the physico-chemical structure of the water column of a reservoir, in particular whether the water column is thermally stratified or mixed, or if the stratification is disrupted (De Cesare et al., 2006). EC is a measure of the water's ability to conduct electricity that is often directly related to the concentration of ions in the water. It may also act as a marker of recent inflow where the inflowing water has lower EC than the resident water in the reservoir (Faithful & Griffiths, 2000). Temperature and EC were recorded in situ at 1 m intervals through the water column using a Hach Hydrolab Datasonde® from February 2004 to January 2005 and a Hach

Hydrolab Quanta® from February 2005 onwards. EC was calibrated using prepared standards within the range anticipated during the study according to the manufacturer's instructions (Hydrolab Corporation, 2002). Shallow sites (Burdekin, Suttor) were usually sampled in the morning to middle of the day, followed by the deeper sites (Central, Eastern), reducing the potential effect of diurnal warming on results as observed in the Australian tropical Darwin River Reservoir and Manton River Reservoirs (Townsend et al., 1997). Collection dates and times for all samples are provided in Appendix B (Table B3).

From February 2005, turbidity was measured in situ (field turbidity) at 1 m intervals using the Hach Hydrolab Quanta supplemented by a turbidity sensor with a measurement range of 0–2000 NTU. The Quanta was calibrated using Milli-Q water and formazin standards according to the manufacturer's instructions (Hydrolab Corporation, 2002). Readings were taken every 1 m down the water column at the four sample sites (Figure 3.1).

3.3.5. Suspended sediment sample collection

Surface water samples were collected directly into clean 1-L polypropylene bottles. Subsurface water samples were collected following the method outlined in Cooper et al. (2017 – Chapter 2), using a 6 L Van Dorn water sampler (February 2004) or a peristaltic pump (December 2004 onwards). In February and December 2004 samples were collected from the surface and at 5 m depth intervals. From January 2005, when turbidity was also measured in situ, samples were collected from depths above, within and below the turbid water layer (when present), as delineated by the probe data (turbidity, EC and temperature). Samples were immediately stored on ice until they were returned to the laboratory for analysis.

3.3.6. Benthic sediment sample collection

Benthic sediment samples were collected using a Van Veen grab sampler, gravity corer or push corer on three occasions:

1) December 2003 – grab samples were collected throughout the reservoir to allow the surficial benthic sediments to be examined
2) August 2005 – grab samples were collected to cross-check bathymetric data collected in 2004
3) August/September 2011 – a series of cores were collected as part of a more extensive study of deposited sediment within the reservoir, with additional grab samples collected where cores failed and at previous water sampling sites. Details for each sample,

including core lengths and sampling locations, are shown in Table 5.2. Core collection and transport methods are described in detail in Cooper et al. (2018 – Chapter 5).

Thirty-eight benthic sediment (grab) samples were collected using a Van Veen grab sampler. Water depths for sampling locations varied from 11.8 to 30 m. Sediment samples obtained using the Van Veen sampler represented a sample depth of 0 to 15 cm. Sediment from two to three grabs collected in proximity to each other (within approximately 50 m^2) was placed in a bucket and thoroughly mixed to ensure homogeneity before an approximate 1 kg (wet weight) sample was collected. Use of composite samples increased the representativeness of each sample and mitigated potential heterogeneity issues (International Atomic Energy Agency, 2003).

Twenty-nine sediment cores were collected using either a gravity or push corer throughout the BFD from water depths from 3.7 to 32 m. Core lengths ranged from 2.5 to 88 cm. Cores were transported upright and frozen on return to the laboratory. The length of each core was recorded before it was split using a rock saw. Each core was photographed and sediments sub-sampled every 5-cm using plastic tools. Sub-samples were a slice up to 1 cm thick, centred on the depth marker being sampled (e.g., 4.5–5.5 cm for the 5-cm depth sample). Samples were taken more frequently based on notable changes in physical/visual characteristics through the core length (e.g., Munsell soil colour or particle size changed, or laminations were observed).

A sub-set of core and grab samples that spatially overlapped at 10 sites within the reservoir (n = 58; Figure 3.1, Table 3.2) were selected to allow comparison between sediment deposited in the reservoir before and after above-average flow events. The particle size and mineralogical data for sediments from the top 15 cm of each core was combined to allow comparison of core samples with grab samples.

3.3.7. Laboratory turbidity and total suspended sediment

The turbidity of water samples was measured in the laboratory using standard methods (APHA 1998). Laboratory turbidity was measured using a 2100P Hach turbidimeter calibrated using three gel standards (0–10 NTU, 0–100 NTU and 0–1000 NTU) and Milli-Q water according to the manufacturer's instructions (Hach Company, 2004). Laboratory measurements provided the most complete record of turbidity across multiple sampling years (including samples over 2000 NTU); therefore, laboratory turbidity measurements will be the

Table 3.2 Details of core and grab samples collected in the BFD reservoir.

Site	Location/ section	Co-ordinates (decimal degrees)		Date collected	Water depth (m)	Sample type	Core length (cm)	Relation to channel
a	Burdekin	-20.521060	146.968630	Aug 2005	14.5	Grab	*15	In
a	Burdekin	-20.521076	146.968335	Aug 2011	19.4	Gravity	30	In
a	Burdekin	-20.520975	146.969949	Aug 2011	6.5	Gravity	67	In
a	Burdekin	-20.521620	146.967300	Aug 2011	6.2	Push	25	Out
a	Burdekin	-20.521001	146.968072	Sep 2011	17.9	Grab	*15	In
b	Burdekin	-20.581000	146.999880	Dec 2003	18.0	Grab	*15	In
b	Burdekin	-20.580224	147.000916	Aug 2011	20.0	Gravity	16	In
b	Burdekin	-20.579542	147.000407	Sep 2011	19.4	Grab	*15	In
j	Suttor	-20.726030	146.964190	Dec 2003	15.0	Grab	*15	In
j	Suttor	-20.727156	146.963174	Sep 2011	18.6	Gravity	N/A	In
j	Suttor	-20.729289	146.966423	Sep 2011	3.7	Push	43	Out
g	Suttor	-20.674020	146.973360	Aug 2005	19.8	Grab	*15	In
g	Suttor	-20.673772	146.973312	Sep 2011	22.2	Gravity	31	In
g	Suttor	-20.672494	146.971075	Sep 2011	8.4	Push	43	Out
g	Suttor	-20.674087	146.973097	Sep 2011	22.3	Grab	*15	In
d	Suttor	-20.654650	146.984470	Dec 2003	20.0	Grab	*15	In
d	Suttor	-20.654864	146.984225	Sep 2011	22.9	Gravity	33	In
d	Suttor	-20.654287	146.986602	Sep 2011	8.3	Push	30[#]	Out
c	Central	-20.608510	147.019530	Aug 2005	19.0	Grab	*15	In
c	Central	-20.608466	147.019929	Aug 2011	18.6	Gravity	85	In
c	Central	-20.606885	147.022430	Aug 2011	21.0	Gravity	82	In
e	Central	-20.627480	147.032060	Aug 2005	20.4	Grab	*15	In
e	Central	-20.627840	147.032496	Sep 2011	22.0	Gravity	41	In
f	Eastern	-20.643650	147.080410	Aug 2005	11.8	Grab	*15	Out
f	Eastern	-20.643734	147.080419	Aug 2011	13.0	Gravity	2.5	Out
h	Eastern	-20.653330	147.083110	Aug 2005	25.8	Grab	*15	In
h	Eastern	-20.653348	147.083097	Aug 2011	27.5	Gravity	88	In
i	Eastern	-20.640680	147.132690	Dec 2003	30.0	Grab	*15	In
i	Eastern	-20.640580	147.132310	Aug 2005	28.8	Grab	*15	In
i	Eastern	-20.641274	147.131612	Aug 2011	32.0	Gravity	71	In
i	Eastern	-20.638194	147.133828	Sep 2011	23.0	Grab	*15	Out

*Approximate depth of sediment sampled.
[#] Core length was adjusted to remove inferred pre-dam sediment (see section 5.3.2).
Burdekin = the Burdekin (northern) section of the reservoir, Suttor = the Suttor (southern) section of the reservoir, Central = the central section of the reservoir, Eastern = the eastern section of the reservoir (see Figure 3.1).
Site name corresponds to locations as marked in Figure 3.1.

primary turbidity data referenced in this paper. Laboratory turbidity was not recorded in April 2006 due to operator error. In situ turbidity data offers additional insight into storm inflow depths within the BFD reservoir and was used to supplement laboratory turbidity data.

Total suspended solids (TSS) in water samples were determined using a standard gravimetric filtration method (APHA 1998) after samples were prepared using the method outlined in Cooper et al. (2017 – Chapter 2). The Whatman GF/C filter papers (nominal pore size 1.2 µm) used in this method may underestimate the 'true' SS concentration where a large proportion of the particles are <1.2 µm. However, Hickel (1984) found that Whatman GF/C glass-fibre filters retain not only all particles >1 µm, but also particles down to 0.4 µm. This includes much of the very fine fraction (particles <1 µm in diameter) known to be present in event flow through the BFD reservoir (Faithful & Griffiths, 2000).

3.3.8. Sediment particle-size analysis

Particle-size distributions for benthic and SS samples were determined using a Malvern Instruments Mastersizer 2000 laser diffraction particle-size analyser with a lens range of 0.02–2000 µm. Ninety-seven water column (SS) and 58 benthic sediment samples were analysed. Samples were wet sieved through a 1.4-mm sieve prior to analysis to remove coarser particles that would damage the Mastersizer. All samples passed completely through the sieve with only occasional organic fragments removed, however particle-size distributions may include sizes up to 2 mm because elongate particles, with a short axis less than the sieve-size, may pass through the sieve (Matthews, 1991). Samples were run manually, as per Sperazza et al. (2004), to ensure appropriate dilution and were treated ultrasonically for 1 min while in the sample chamber to ensure disaggregation of flocs. No chemical dispersant was used. An optimal laser obscuration of 15–20% for particle size analysis (Sperazza et al., 2004) was achieved for benthic sediment analysis through dilution with filtered water. Due to the lower TSS in the water samples, a lower laser obscuration of >5% was targeted for water samples. This lower target was unachievable for 13% of water samples with low SS concentrations (n = 10), which implies that the particle-size data for these samples may be less precise (Sperazza et al., 2004). Three measurements were determined for each sample aliquot, with two aliquots of each sample analysed and an average distribution determined. Correction to the index of refraction (RI) used in processing by the Mastersizer software was applied based on mineralogical input (Cooper et al., 2017 – Chapter 2). Sediments were classified as one of three size classes based on the Udden-Wentworth sediment grain size scale (Blott & Pye, 2012): clay (<3.9 µm), silt (3.9–62.5 µm), or sand (62.5–2000 µm).

3.3.9. Sediment mineralogy

The mineral composition of suspended and benthic sediment was determined using X-ray diffraction (XRD) analysis to identify the minerals present in the sediment and allow comparison between sediment being transported and sediment being deposited. Analysis was performed using a Siemens D-5000 X-ray diffractometer or a Siemens D500/D501 series X-ray diffractometer. Samples were prepared and analysed using the methods described in Cooper et al. (2017 – Chapter 2). Both benthic and SS samples were analysed, glycolated, re-run, heated to 400°C and run a third time to distinguish between clay assemblages that share the same basal peaks (e.g., smectite and chlorite at ~14 Å). Mineral identification and quantification were performed using Bruker AXS Diffrac.Suite EVA and TOPAS software respectively. Diffractograms shifted for samples presented on filter papers and were corrected by aligning each plot to the well-crystallised 3.5 Å quartz peak.

XRD analysis was performed on all SS samples from February 2004 to February 2005, and samples from 14 April 2006. A sub-set of core samples (n = 39) was analysed for XRD. Sample selection was based on particle-size results and other physical properties e.g., colour. Where sections of core were considered homogenous, every second sample down core was analysed.

3.4. Results

3.4.1. Water quality observations

3.4.1.1. <u>Turbidity</u>

Field and laboratory measurements of wet season water turbidity are highly consistent within and over multiple wet years ($r^2 = 0.97$; Figure 3.2a) and demonstrate a strong, linear correlation with TSS ($r^2 = 0.97$; Figure 3.2) a relationship not observed in a companion study using dry season samples (Cooper et al., 2017 – Chapter 2). The strong relationship between turbidity and TSS allows turbidity to approximate sediment concentration in this study (Gippel, 1995).

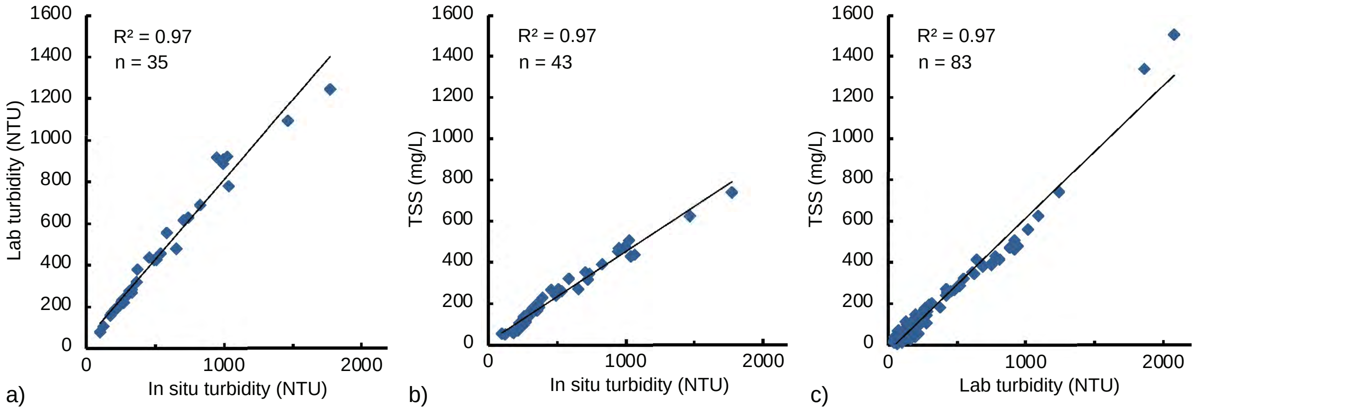

Figure 3.2 (a) Turbidity measured in the laboratory v. in situ turbidity (three separate sampling trips two water years, 2004–05 and 2005–06), (b) in situ turbidity v. total suspended solids (TSS; four separate sampling trips covering two water years, 2004–05 and 2005–06), (c) laboratory turbidity data v. TSS (six separate sampling trips covering three water years, 2003–04, 2004–05 and 2005–06). Multiple samples were collected down the water column at each of the four locations on every sampling trip. In situ turbidity measurements that exceeded the probe maximum of 2000 NTU were excluded.

The turbidity of wet season samples ranged from 46–2080 NTU (Figure 3.3a–t). Laboratory turbidity ranged from 49–2080 NTU at the Burdekin site, 46–812 NTU at the Suttor site, 53–1092 NTU at the Central site, and 56–886 NTU at the Eastern site. Samples collected at the beginning of the wet season (December 2004) prior to inflow were least turbid (46–71 NTU; Figure 3.3a, f, k, p). At the Burdekin site turbidity was only 49–64 NTU in samples from below 10 m, however turbidity was extremely high (1020 NTU, Figure 3.3a) in surface water due to localised rainfall in the days prior to sampling (Cooper et al., 2017 – Chapter 2; discussed in Appendix A). The highest turbidity and TSS values (2080 NTU and 1507 mg/L respectively) were recorded at the Burdekin site in January 2005. Field turbidity maximums of 2000 NTU were recorded at the Burdekin and Central sites in April 2006 (Figure 3.3e, o).

Turbidity increased with depth at the Burdekin site in all three wet seasons (Figure 3.3b–e). The turbidity difference between surface and bottom water ranged from 410 NTU (March 2006) to 1180 NTU (January 2005). Turbidity varied less with depth at the Suttor site, measuring 170–300 NTU, but rose sharply (by 610–660 NTU) below 17 m in the 2004–05 and 2005–06 water years (Figure 3.3f–j). In January 2005, turbidity at the Suttor site peaked at ~15 m (812 NTU; Figure 3.3g) while turbidity above and below this depth was lower (133–193 NTU). Turbidity at the Central site showed a similar mid-depth (10–15 m) peak in all three wet seasons, ranging from 640 to 690 NTU in February 2004 and January 2005 with much lower turbidity above and below (<280 NTU; Figure 3.3l, m). Later in February 2005 and in 2006 turbidity increased sharply by up to 950 NTU in the water column below 10–15 m (Figure 3.3m–o). A mid-column layer of high turbidity water (475–944 NTU) of varying thickness (4–13 m) and at varying depths (12–28 m) formed at the Eastern site closest to the dam wall in February 2004 and March/April 2006 (Figure 3.3r–t).

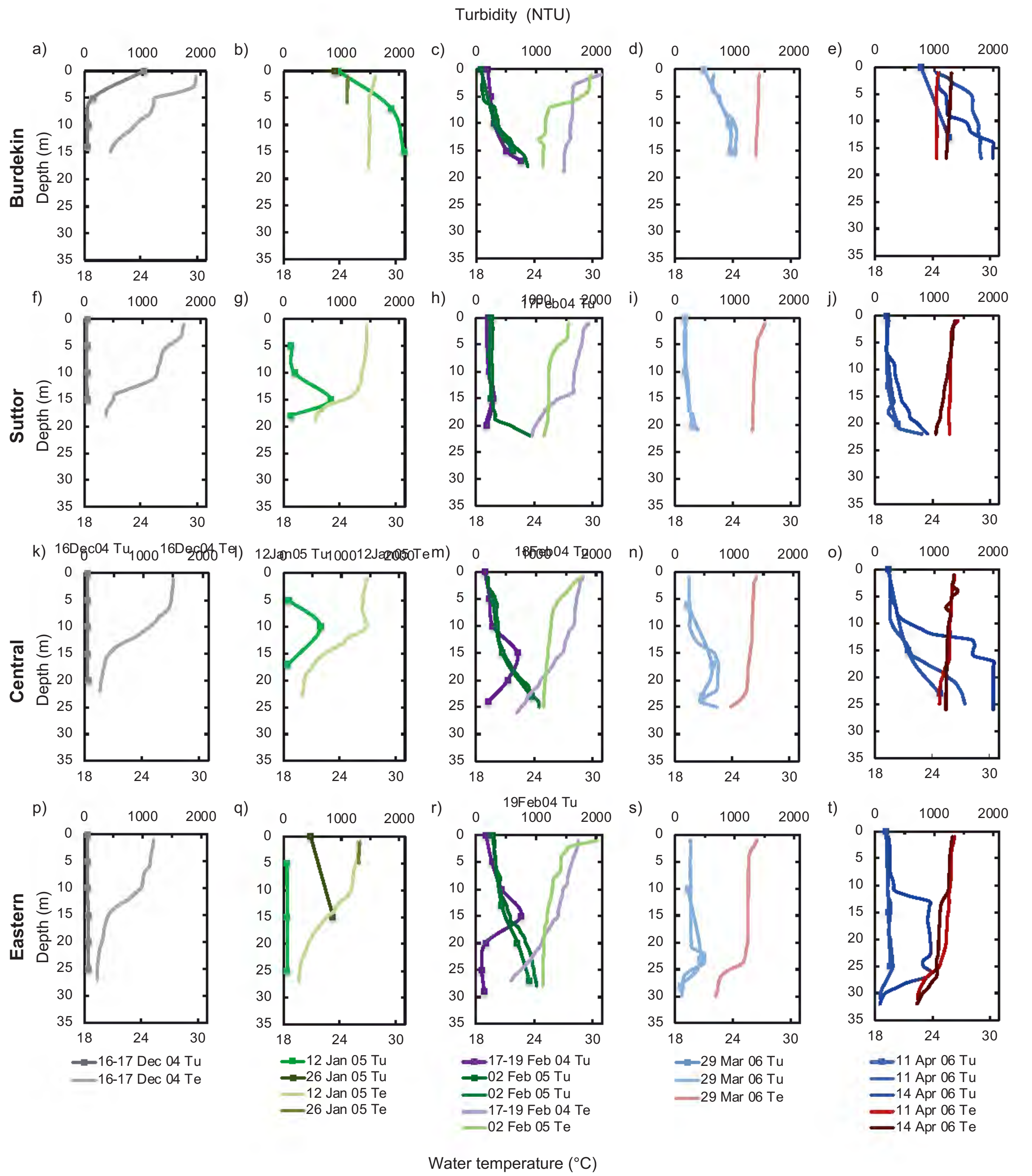

Figure 3.3 Turbidity and water temperature data for each sampling site: Burdekin = a–e, Suttor = f–j, Central = k–o, Eastern = p–t. Markers indicate laboratory data and smooth lines indicate in situ measurement. Tu = turbidity and Te = temperature. Note that the field turbidimeter maximum was 2000 NTU.

3.4.1.2. Temperature

Water temperatures indicated that the reservoir was thermally stratified early in the wet season each year, with surface temperatures of 25°C–30°C and temperatures of 19°C–21°C within 1 m of the bottom (Figure 3.3a, f, k, p). Higher surface temperatures (29°C–30°C) were recorded at the shallower Burdekin and Suttor sites (14–19 m and 18–23 m respectively). In this study, the shallower sites were sampled first (the Burdekin and then the Suttor) so the warmer temperatures are not attributable to a daytime warming effect.

Thermal stratification was observed in December, January and February (Figure 3.3) with the thermocline present in the upper 15 m of the water column at all sites except the Burdekin site in January 2005 where temperature remained constant with depth (Figure 3.3b). Temperatures measured in the 2005–06 wet season were constant with depth at most sites, except at the Eastern and Central sites where cooler water occurred below 25 m and 20 m respectively (Figure 3.3n, o, s, t).

3.4.1.3. Electrical conductivity

EC values were constant down the water column in December 2004 (prior to inflow), ranging from 162–187 µS/cm at all sampling sites (Figure 3.4a, f, k, p). Chemical stratification, as denoted by sharp shifts in electrical conductivity through the water column, was evident at the Burdekin site with lower EC values observed in surface waters (162–164 µS/cm to 3 m below the surface, compared to 175–183 µS/cm below 4 m; Figure 3.4a). In January and February of the same wet season (Figure 3.4b, c), stratification was still evident. although EC was found to be highest in surface waters (>176 µS/cm above 4 m c.f. 117–131 µS/cm below 7 m, Figure 3.4b, and >124 µS/cm above 4 m c.f. <92 µS/cm below 7 m, Figure 3.4c).

The difference between maximum and minimum EC within the water column at each site varied between, and within, wet seasons. For example, at the Central site the difference was 63 µS/cm in February 2004, <33 µS/cm in January/February 2005, and varied from 28 to 72 µS/cm in the observations from the March/April 2006 (Figure 3.4l–o).

In many instances, EC decreased as turbidity increased: at the Burdekin and Suttor sites in January 2005 (Figure 3.4b, g) and at the Central and Eastern sites in February 2004 and March/April 2006 (Figure 3.4m, r, n, s, t). On other occasions EC did not closely relate to turbidity. For example, EC increased at 15 m depth at the Central site in January 2005, the same depth at which an increase in turbidity was observed (Figure 3.4l). However, in March and April 2006 EC was constant down the water column at the Burdekin site (80–94 µS/cm) even though turbidity increased by over 440 NTU (Figure 3.4d, e).

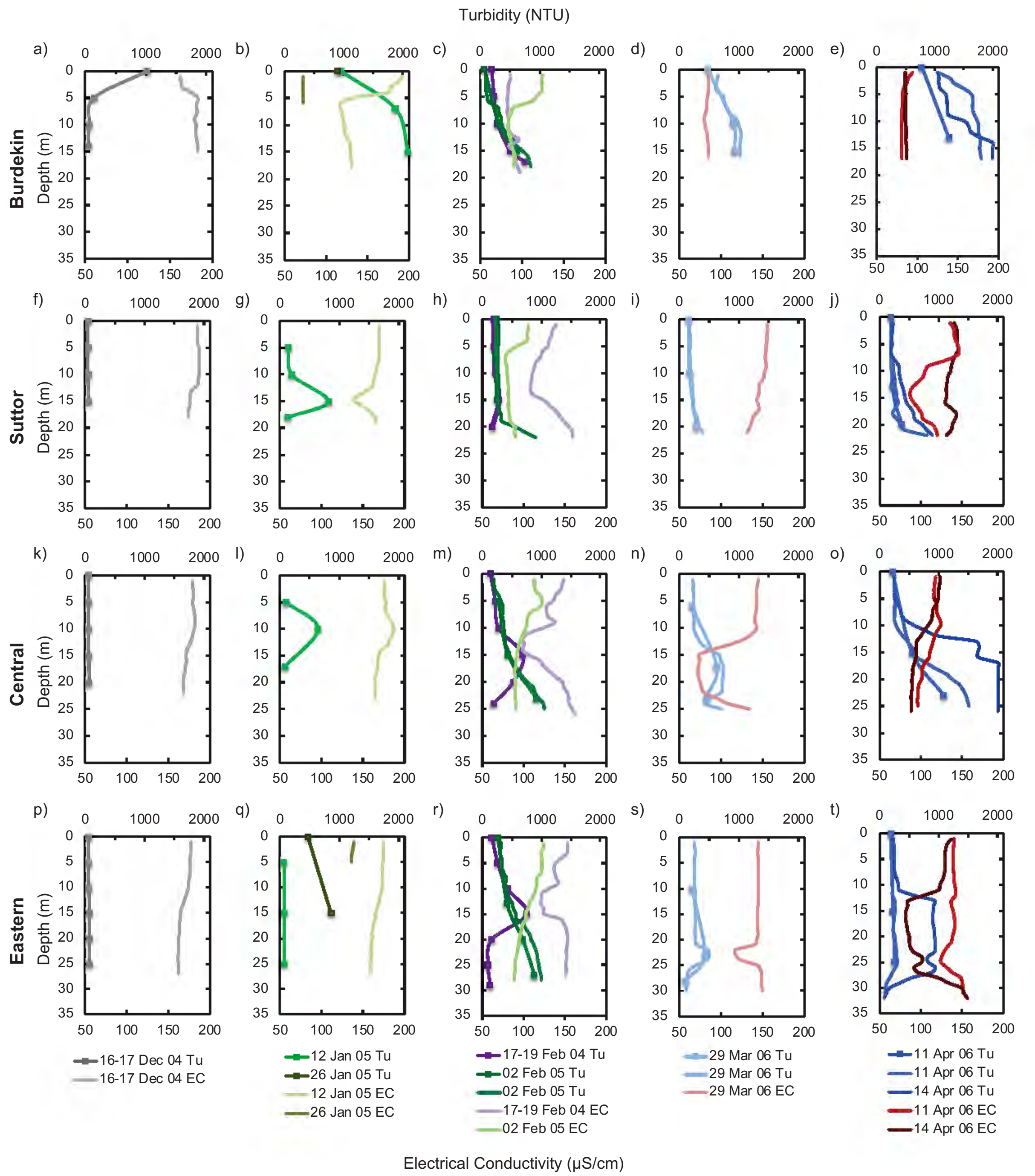

Figure 3.4 In situ electrical conductivity profile data for each sampling site: Burdekin = a–e, Suttor = f–j, Central = k–o, Eastern = p–t. Markers indicate laboratory data and smooth lines indicate in situ measurement. Tu = turbidity and Te = temperature. Note that the field turbidimeter maximum was 2000 NTU.

3.4.2. Sediment particle-size analysis

The particle-size data for SS samples collected at all four sites display mostly bimodal (occasionally trimodal) distributions due to distinctive fine (0.04–0.9 µm with a peak at 0.1–0.3 µm) and coarser (0.9–126 µm with a peak at 2–6 µm) fractions (Figure 3.5). The coarser silt–clay fraction dominated Burdekin site SS samples collected in the 2003–04 and 2005–06 water years (composing an average of >80% of the sample; Figure 3.5a, c), but dropped to an average of only 64%, and contained a larger proportion of finer particles (average 36% 0.04–0.9 µm) in the 2004–05 water year. Conversely, a finer clay-silt fraction dominated Suttor site SS (average 68%) in all years sampled (Figure 3.5d–f). Most SS samples exclusively contained sediments <62.5 µm in diameter. Where particles >62.5 µm diameter occurred, they comprised <3% of those samples. Less than 1.3% of SS was >126 µm in diameter.

Samples from depths where turbidity data indicated turbid inflow typically contained more of the coarser silt–clay sediment (e.g., samples from >10 m depth at the Central site in April 2006 contained 55%–99% 0.9–126 µm particles, Figure 3.5i). The average particle-size fractions for the inflow sediments over the monitored years are presented in Table 3.3. Particle-size data suggest that a greater proportion of silt entering the BFD reservoir is delivered from catchments upstream of the Burdekin site than the Suttor site (average 36% c.f. 16%), with the southern catchments contributing a greater proportion of clay-sized particles (average 84% at the Suttor site; Table 3.3).

The particle-size distribution of benthic sediments varies from unimodal to bimodal. The minimum particle size of almost all samples is 0.9 µm (3 samples have less than 0.2% particles <0.9 µm; Figure 3.6); the maximum particle size is 710 µm. Samples from the Burdekin and southern Suttor sections of the reservoir (Figure 3.6a, b, j) are the most variable in distribution ranging from 0.9 µm to 1416 µm and with peaks from 7 µm to 400 µm. Conversely samples from the northern Suttor and Eastern sections of the reservoir (Figure 3.6d, g–i) have very uniform distributions, with ranges from 0.7 µm to 2000 (although <3.5% of each sample is >62.5 µm) and peaks at 4–8 µm.

Benthic sediments collected in December 2003 and August 2005 (prior to above-average flow events in the 2007–08, 2008–09 and 2010–11 water years) range from 0.9 µm to 2000 µm but generally have dominant peaks at 4–14 µm, except at the northernmost

Burdekin site where a second peak is observed at 159 µm. Samples collected in September 2011 are coarser, with modal peaks between 4–447µm and total ranges of 0.7 µm–1415 µm.

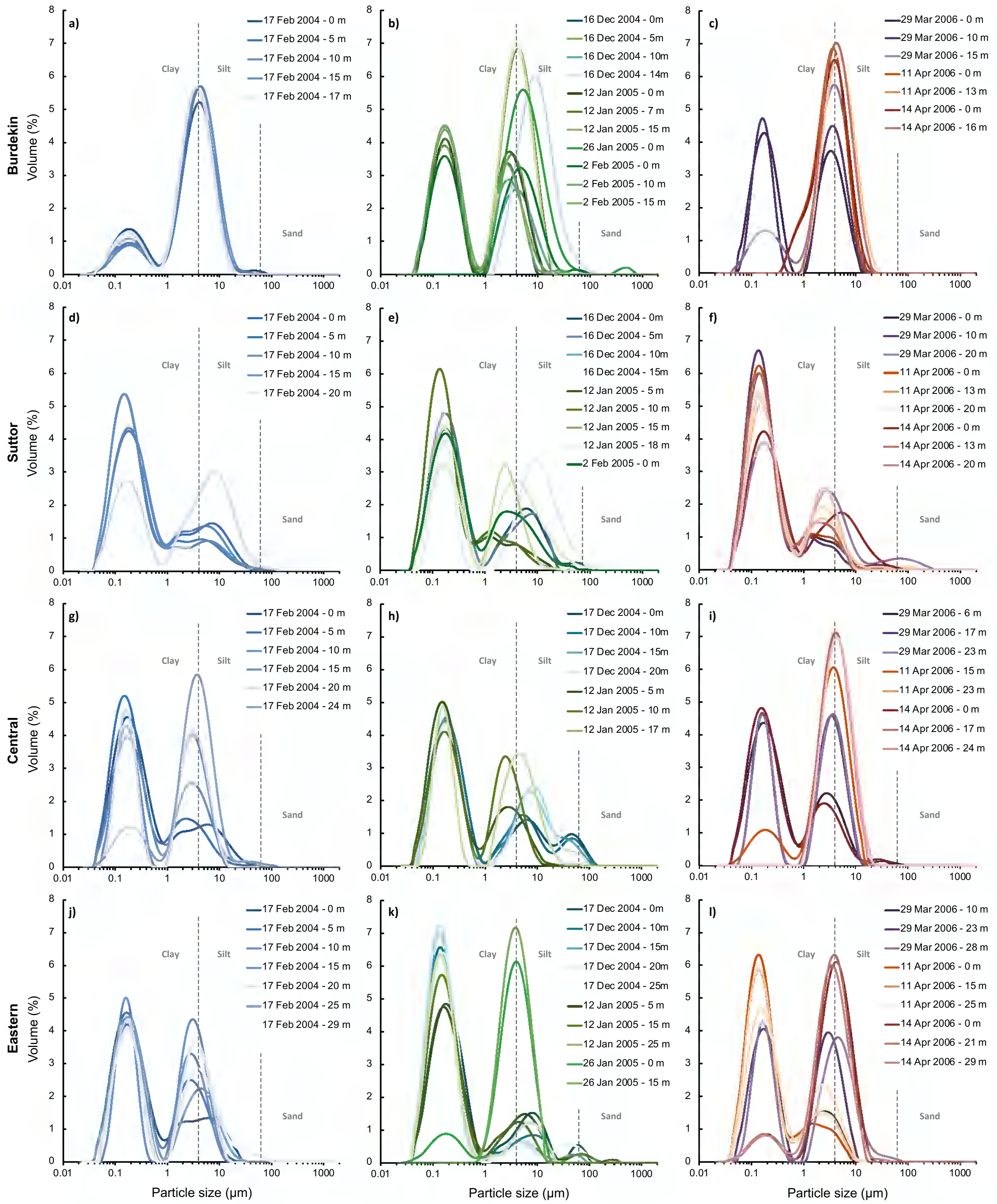

Figure 3.5 Particle-size distributions for wet season SS samples from the a–c) Burdekin, d–f) Suttor, g–i) Central and j–l) Eastern sites. Wet season 2003/2004 data are shown in blue, 2004/2005 in green, and 2005/2006 in purple/orange. Particle-size data from February 2005 for the Suttor, Central and Eastern sites were corrupted and not able to be used.

Table 3.3 Average particle size and mineralogy of SS samples (mean ± standard deviation, SD).

		SS particle size (mean ±1 SD)				Mineralogy (mean ±1 SD)							
Location	**Date**	**n**	**Clay (%)**	**Silt (%)**	**Sand (%)**	**n**	**Qtz (%)**	**Kaol (%)**	**Musc/ Ill (%)**	**Smec (%)**	**Fsp (%)**	**Amp (%)**	**Chl (%)**
Burdekin	17 Feb 2004	5	59±4	41±4	0.0	5	9±1	53±4	11±3	22±5	2±2	0	2±2
	16 Dec 2004	4	67±35	32±35	0.2±0.5	4	8±5	54±16	22±13	13±5	3±3	0	1±1
	12 Jan 2005	3	61±19	39±19	0.0	3	6±1	61±4	19±5	12±3	2±2	0	0
	26 Jan 2005	1	35	63	2	1	7	38	49	4	2	0	0
	2 Feb 2005	3	82±11	18±11	0.1±0.2	3	4±1	58±2	20±4	16±3	0	0	1±2
	29 Mar 2006	3	75±9	25±9	0.0		-	-	-	-	-	-	-
	11 Apr 2006	2	54±16	46±16	0.0		-	-	-	-	-	-	-
	14 Apr 2006	2	55±9	45±9	0.0	2	10±1	53±7	8±2	18±4	4±0	0	7±4
	All samples	**23**	**64±19**	**36±19**	**0.1±0.4**	**18**	**8±3**	**55±9**	**18±11**	**16±6**	**2±2**	**0**	**2±3**
Suttor	17 Feb 2004	5	80±13	20±13	0.1±0.2	5	5±1	57±1	12±4	26±5	0±1	0	0
	16 Dec 2004	4	66±15	33±14	1±1	4	6±3	66±5	15±2	10±4	2±3	0	0
	12 Jan 2005	4	87±12	13±12	0.1±0.2	4	8±1	53±4	5±6	14±4	1±1	0	0
	2 Feb 2005	1	84	16	0.0	3	2±1	68±1	18±1	12±1	0	0	0
	29 Mar 2006	3	91±8	8±6	1±2		-	-	-	-	-	-	-
	11 Apr 2006	3	94±2	5±1	0.1±0.2		-	-	-	-	-	-	-
	14 Apr 2006	3	90±9	10±9	0.0	3	6±2	67±7	9±2	17±6	1±1	0	0
	All samples	**23**	**84±14**	**16±13**	**0.4±0.7**	**19**	**5±2**	**61±9**	**16±6**	**17±7**	**1±2**	**0**	**0**
Central	19 Feb 2004	6	81±10	19±10	0.1±0.2	6	6±2	52±8	17±5	23±3	1±1	0	2±2
	17 Dec 2004	4	70±6	28±6	2±1	4	3±2	58±19	22±9	17±17	0	0	0
	12 Jan 2005	3	83±13	17±13	0.0	3	3±1	60±6	31±5	6±0	0	0	0
	2 Feb 2005		-	-	-	3	3±0	65±1	20±1	12±0	0	0	0
	29 Mar 2006	3	81±6	19±6	0.0		-	-	-	-	-	-	-
	11 Apr 2006	2	58±9	42±9	0.0		-	-	-	-	-	-	-
	14 Apr 2006	3	63±25	37±25	0.0	3	10±3	56±3	14±4	17±3	2±2	0	1±0.5
	All samples	**21**	**74±14**	**25±14**	**0.3±0.7**	**19**	**5±3**	**57±10**	**20±8**	**16±9**	**1±1**	**0**	**1±2**
Eastern	18 Feb 2004	7	82±4	18±4	0.0	7	5±2	55±5	15±3	23±5	0	0	2±2
	17 Dec 2004	5	89±6	11±5	1±1	6	3±1	57±16	33±20	7±4	0.4±1	0	0
	12 Jan 2005	3	86±4	13±3	1±1	3	9±4	53±7	23±4	16±6	0	0	0
	26 Jan 2005	2	57±3	43±3	0.0	2	6±0	54±6	32±8	6±1	1±0	0	0
	2 Feb 2005		-	-	-	4	4±0	66±2	18±1	13±1	0	0	0
	29 Mar 2006	3	82±14	18±14	0.0		-	-	-	-	-	-	-
	11 Apr 2006	3	95±2	5±2	0.0		-	-	-	-	-	-	-
	14 Apr 2006	3	60±4	40±4	0.0	3	13±6	58±5	10±4	15±1	3±0	0	1±2
	All samples	**26**	**81±13**	**19±13**	**0.2±0.5**	**25**	**6±4**	**57±9**	**21±13**	**14±7**	**1±1**	**0**	**1±1**

Note: Clay = <3.9 µm, Silt = 3.9–62.5 µm, sand = 62.5–2000 µm. Qtz = Quartz, Kaol = Kaolinite Group, Musc/Ill = Muscovite/Illite, Smec = Smectite Group, Fsp = Feldspars, Amp = Amphiboles, Chl = Chlorite.

3.4.2.1. Sediment mineralogy

Suspended sediment was predominantly composed of kaolinite group clays (average 55%–61%; henceforth referred to as ‘kaolinite’), micas (muscovite/illite; 18%–21%), smectite group clays (14%–17%; ‘smectite’) and quartz (Table 3.3). Feldspar minerals (<4% on average) and chlorite (up to 7% in Burdekin samples, <4% at Dam sites and absent from Suttor samples; Table 3.3) were present in minor amounts. The SS composition remained relatively consistent across sampling years (Table 3.3) although all samples collected in February 2004 contained more smectite than average (22%–26% c.f. 14%–17% avg.). The mineralogy of most samples from turbidity currents (e.g., at 10–15 m at the Suttor, Central and Eastern sites, >280 NTU; Figure 3.3g, l, m, r, o, t) was not substantially different from samples collected from less turbid water (<200 NTU) above and/or below. Turbid water from 21–29 m at the Eastern site in April 2006 (up to 940 NTU) contained above-average quartz (15%–17%) and below-average micas (7%).

All benthic sediments (grab and core samples) contained the same minerals as SS with addition of small amounts of amphiboles (<2%) and occasional vermiculite and goethite (<1.4 %). Feldspars were more abundant in benthic sediment (2%–16%), particularly in samples from the Burdekin section of the reservoir (Table 3.4). The range that each mineral contributed to benthic sediment samples for each section of the reservoir was generally similar to the SS samples (Table 3.4), with the following exceptions: 1) average smectite content in the Suttor section was lower (3%–8% c.f. 8%–16%); 2) the mica content in samples from the Burdekin and Suttor sections (7%–42%) was higher than Central and Eastern section site samples (3%–19%); and 3) samples from the Central and Eastern sections contained more chlorite (up to 6% c.f. <1%).

The minerals represented in benthic sediments collected in 2011 were the same as those present in the December 2003 and August 2005 samples (Table 3.4), but the proportional contribution of each mineral changed from 2003–05 to 2011. For example, the proportions of quartz and feldspar were higher in samples from 2011 from the Burdekin, southern Suttor and Central sections of the reservoir (13%–17% and 3%–10% more, respectively; Table 3.4) and kaolinite decreased in samples from the Burdekin and Central sections (0%–25% less). Proportions of each mineral in samples from the Eastern section were approximately the same at sites h and i (easternmost) but quartz abundance was lower (16% less) and an increase in kaolinite occurred at site f (+21%; Table 3.4).

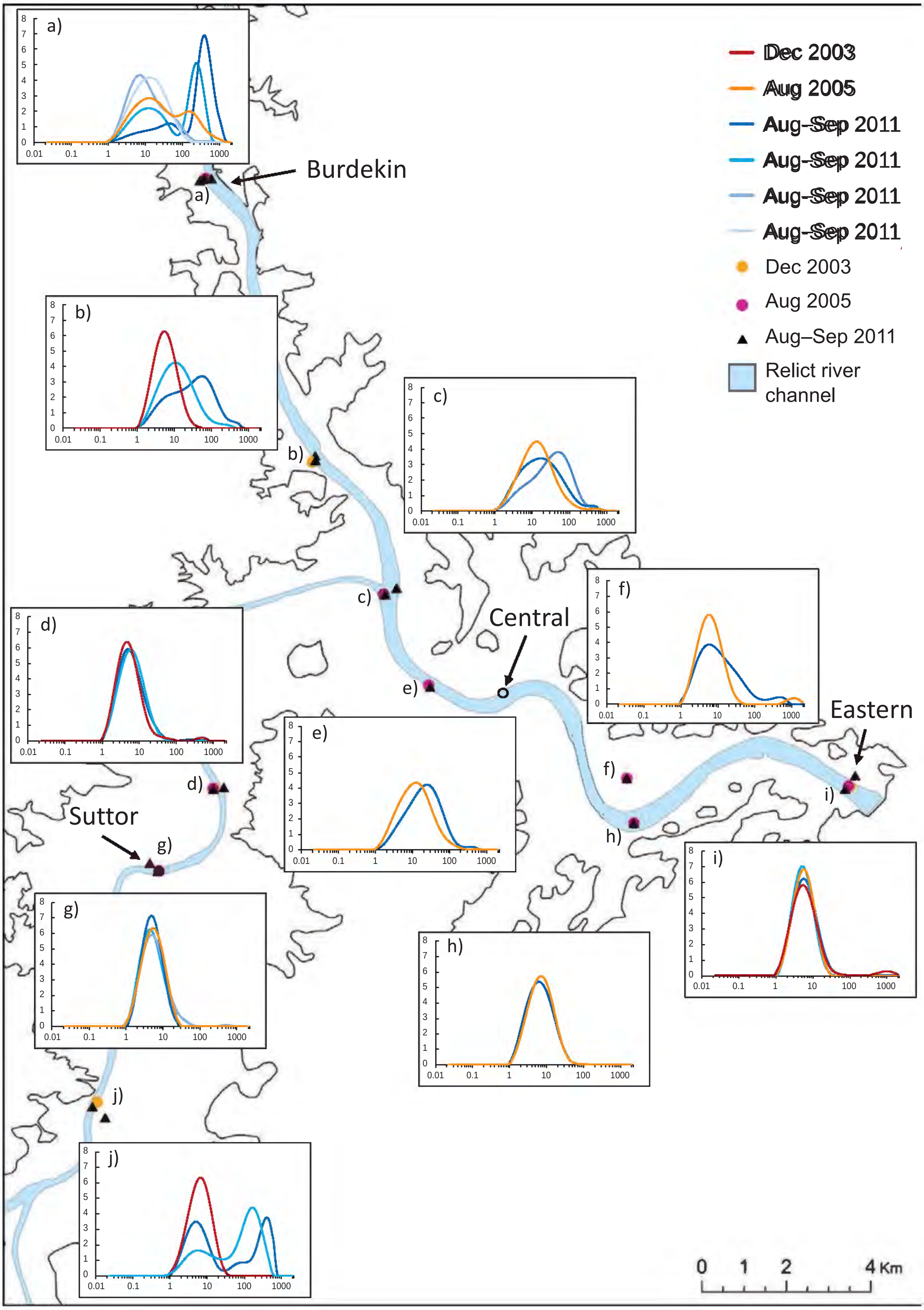

Figure 3.6 Particle size of benthic sediment samples from the BFD reservoir and the location of the samples in the reservoir. Samples in red were collected prior to above-average flow events in 2008, 2009 and 2011, samples in blue were collected after those events. Water sampling sites are also marked for reference.

Table 3.4 Average (mean ± standard deviation, SD) benthic sediment particle size and mineralogy for samples from 10 sites within the reservoir that were collected both before (2003–2005 samples) and after (2011 samples) above-average discharge events in 2007–08, 2008–09 and 2010–11.

			Benthic sediment particle size (mean±1 SD)				**Mineralogy (mean ±1 SD)**								
Site	**Reservoir section**	**Date**	**n**	**Clay (%)**	**Silt (%)**	**Sand (%)**	**n**	**Quartz (%)**	**Kaolinite Group (%)**	**Muscovite/ Illite (%)**	**Smectite Group (%)**	**Feldspars (%)**	**Amphiboles (%)**	**Chlorite (%)**	**Other (%)**
a	Burdekin	2003–2005 sample	1	11	58	31	1	28	42	7	10	12	0.0	0.0	0.0
		2011 samples	11	9 ± 9	46 ± 33	44 ± 40	8	42 ± 14	19 ± 13	13 ± 10	8 ± 6	16 ± 8	0.2 ± 0.5	0.1 ± 0.3	0.3 ± 0.6
b	Burdekin	2003–2005 sample	1	34	66	0	1	14	36	37	10	3	0.0	0.0	0.0
		2011 samples	2	13 ± 4	70 ± 11	17 ± 15	2	31 ± 13	26 ± 3	25 ± 13	8 ± 7	9 ± 5	0.7 ± 1.0	0.9 ± 1.2	0.2 ± 0.3
c	Central	2003–2005 sample	1	13	80	7	1	18	60	4	13	4	0.0	1.2	0.0
		2011 samples	6	10 ± 5	68 ± 13	21 ± 16	3	31 ± 9	38 ± 10	11 ± 5	8 ± 1	10 ± 5	1.4 ± 2.4	0.5 ± 0.4	0.2 ± 0.2
d	Suttor	2003–2005 sample	1	40	58	2	1	15	43	29	5	7	0.0	0.0	0.0
		2011 samples	6	33 ± 4	66 ± 3	0.5 ± 1.1	2	11 ± 0.1	41 ± 0.1	36 ± 0.4	7 ± 1	4 ± 1	0.0	0.0	0.0
e	Central	2003–2005 sample	1	16	79	5	1	18	56	3	12	3	2.0	6.0	0.0
		2011 samples	3	9 ± 1	80 ± 3	12 ± 2	1	28	31	19	8	13	1.0	0.0	0.0
f	Eastern	2003–2005 sample	1	31	66	4	1	39	35	11	10	5	0.0	0.0	0.0
		2011 samples	1	24	67	9	1	23	56	5	11	5	0.0	0.0	0.0
g	Suttor	2003–2005 sample	1	36	64	0	1	14	30	42	11	2	0.0	0.0	0.3
		2011 samples	7	38 ± 3	61 ± 3	0.3 ± 0.8	4	15 ± 2	42 ± 8	29 ± 11	8 ± 3	5 ± 2	0.0	0.5 ± 0.9	0.4 ± 0.7
h	Eastern	2003–2005 sample	1	25	74	<1	1	19	56	5	10	5	0.0	5.0	0.0
		2011 samples	3	30 ± 16	70 ± 15	0	2	16 ± 0.2	54 ± 3	11 ± 0.2	13 ± 4	4 ± 0.2	0.0	0.9±1.2	0.6 ± 0.0
i	Eastern	2003–2005 samples	2	34 ± 1	65 ± 3	1 ± 2	2	13 ± 3	47 ± 1	16 ± 10	16 ± 5	5 ± 1.6	0.0	1.6 ± 0.2	0.0
		2011 samples	4	33 ± 2	67 ± 2	0	2	18 ± 3	51 ± 2	15 ± 2	10 ± 3	5 ± 0.1	0.5 ± 0.7	0.0	0.6 ± 0.4
j	Suttor	2003–2005 sample	1	28	72	0	1	21	33	32	8	6	0.0	0.0	0.0
		2011 samples	4	13 ± 10	34 ± 17	53 ± 27	3	38 ± 25	32 ± 14	18 ± 11	3 ± 3	9 ± 3	0.0	0.0	0.0

Clay = <3.9 µm, Silt = 3.9–62.5 µm, sand = 62.5–2000 µm. ‘Other’ includes vermiculite and goethite.

3.5. Discussion

3.5.1. Stratification and turbidity current pathways

Elevated SS in inflows to the BFD reservoir from the Burdekin and Suttor river catchments travelled in a turbidity current that moved through the reservoir as either an interflow or underflow. The location of turbid flows within the water column through the reservoir is dependent on the density of the inflow and the density of the water column in the BFD reservoir. Inflow denser than the reservoir water will form an underflow, or will enter the reservoir as an interflow where water density between the inflow and the reservoir water column are equivalent (Lee & Yu, 1997). Temperature is usually the dominant control on inflow density (Chung et al., 2009), and this is true for the BFD reservoir where 60% of the density difference between the top and bottom of the water column can be attributed to the temperature gradient (Griffiths & Faithful, 1996). Water profile sampling indicated that turbid water (>280 NTU) flowed through the Burdekin section of the BFD reservoir as an underflow at 10–19 m depth (Figure 3.3a–e) and along the thermocline (at 10–15 m or 25 m depth) in the Suttor, Central and Eastern sections of the BFD reservoir (e.g., Figure 3.3g, l, m, r). Observation of the turbidity current at the Eastern site indicates that SS are reaching the dam wall.

Turbidity currents in the Central and Eastern sections of the BFD reservoir transformed from an interflow into an underflow as inflow events continued. The formation of underflows was due to an increase in SS concentration (turbidity increase of 250–1260 NTU; Figure 3.3), causing an increase in density. Turbid inflow at the Central site initially formed a mid-column layer (at 10–20 m depth) before changing to an underflow later in each event (below 15 m). A similar pattern of interflow was seen at the Eastern site in the 2003–04 and 2004–05 water years, but in April 2006 the interflow layer became thicker (14 m) but did not reach the bottom of the reservoir (Figure 3.3). It is common for inflow to travel along the bottom of upstream sections of a reservoir as an underflow and then separate from the bottom further downstream and continue as an interflow (Chung et al., 2009; Gelda & Effler, 2007; Gu et al., 1996). There are only few examples in the literature of interflow transitioning to underflow as inflow continues, as seen in this study. De Cesare et al. (2006) described turbidity currents in thermally stratified Lake Lugano, Switzerland where inflow initially formed an interflow, but increased sediment concentration as inflow continued raised inflow density causing it to plunge and form an underflow. However, Lake Lugano is very deep (288 m), and the interflow and underflow were separated by >60 m of clearer, resident water. Unlike Lake Lugano, no separation of flows was observed in the BFD reservoir.

The transition to an underflow at the Central and Eastern sites disrupts stratification in the BFD reservoir (Figure 3.3) and results in mixing in both the epilimnion and hypolimnion, an effect seen in other stratified reservoirs (Huang et al., 2014; Li et al., 2024; Rueda et al., 2010). Inflow occurs when the BFD reservoir is strongly stratified, however, in the tropics the stability of stratification is low relative to higher latitude lakes. This is because of the disturbance caused by wet season inflow during summer when stratification is strongest and the lower temperature range within the water column once it has been disrupted (Lewis, 1987; Townsend, 1998). In the 2004–05 water year a decrease in turbidity at the depth of the original interflow (− >200NTU, 10-20 m; Figure 3.3h, m) and increase in turbidity below 20 m (+ >250 NTU) indicated that mixing (dilution) and/or sediment settling was occurring. When a turbidity current reaches a dam, it may create a return current, or it may form a muddy layer near the dam and promote sediment settling (Cao et al., 2015; Marosi et al., 2015; Schleiss et al., 2016; Yu et al., 2000). The increase in flow thickness from 4 to 14 m at the Eastern site in 2005–06 suggests pooling of turbid water once it reaches the dam wall, only 800 m downstream of this site. Deposition of sediment from the turbidity current may also have caused an increase in buoyancy which can increase the thickness of the turbid layer (Gladstone & Pritchard, 2010). Mixing allows for the cycling of nutrients and dissolved oxygen (Helfer et al., 2012). This is observed in the BFD reservoir where dissolved oxygen concentrations measured in the deepest sections increase from <5% to >55% (Eastern site, below 25 m, March and April 2006). The breakdown of stratification in the BFD reservoir is brief and is rapidly re-established (over <6 months) once flow from the Burdekin River has passed (Brizga et al., 2006; Chudek et al., 1998).

Electrical conductivity was not always a reliable indicator of the location of turbid inflow in the BFD reservoir. A decrease in conductivity compared to the reservoir's resident water can be used as a marker of recent inflow (Effler et al., 2008; Faithful & Griffiths, 2000; Steane & Tyler, 1982). Turbidity clearly delineated water flow into the reservoir during the wet season (Figure 3.4) and was often an order of magnitude larger than in the dry season (max 812–2080 NTU at the four sites c.f. <100 NTU; Cooper et al., 2017 – Chapter 2). A synchronous decrease in EC was observed for inflow at some sites including at the Eastern site in March/April 2006 (Figure 3.4t). During the same event, turbidity data indicated inflow below 10 m at the Burdekin and Central sites, but corresponding EC observations remained consistent down the water column (Figure 3.4e, o).

3.5.2. Tracking the movement of suspended sediment

The consistent formation of turbidity currents in the BFD reservoir allows greater predictability of, and control over, sediment transport behaviour. Turbidity currents do not always form regularly in reservoirs that experience them (Chamoun et al., 2016). Turbidity currents form consistently in the BFD reservoir, even during below-average flow events (1.9– 3.3 TL total inflow; Faithful & Griffiths, 2000; Griffiths & Faithful, 1996). The behaviour of above-average (mean) inflow was not documented due to the nature of events during this study but limited data for inflow in April 1997 (Chudek et al., 1998), an average water year (6.3 TL), shows a turbid baseflow within the reservoir at a depth below 15 m. Accurate prediction of turbidity current behaviour is key in reservoirs that are managed to release those currents and reduce problematic sedimentation (Lee et al., 2014) or to prevent turbid flow into water supply intakes (Lai et al., 2015).

Turbidity currents transport sediment up to 50 km through the BFD reservoir to the dam wall where it has the potential to be deposited or damage dam infrastructure. High turbidity (>640 NTU) and an increase in SS particle size (average 70% 0.9–126 µm particles in turbidity current samples c.f. 33% in water above or below) recorded each year at the Eastern site indicates that SS travels through the reservoir to the dam wall. Turbidity currents in other reservoirs have been observed to travel long distances along the original river channel: 100 km in Lake Mead, USA and >80 km in Sanmenxia Reservoir, China (Fan, 1986). In both of these reservoirs the turbidity currents are subsequently vented through the dam outlets (Fan, 1986) reducing the amount of sediment available for deposition but potentially damaging dam infrastructure via sediment abrasion (Wang et al., 2005). Sediments deposited within reservoirs close to the dam may accumulate and hamper outlets and reduce capacity, as observed in the Dez Dam, Iran, Tarbela Reservoir, Pakistan, and the Luzzone Dam, Switzerland (de Cesare et al., 2001; Khakzad & Elfimov, 2015; Mazhar et al., 2021). The ability of turbidity currents to transport sediment to the BFD indicates the potential for sediment to be deposited in an area of the reservoir where it may cause damage, for example, near to the dam wall where it might block lower-level water intake structures (discussed (Discussed further in Cooper et al., 2018 – Chapter 5).

Turbid flows exit the reservoir when the BFD overflows, transporting sediment downstream and reducing deposition within the reservoir. This occurs even during below-average wet seasons due to the low capacity/inflow ratio of the reservoir (0.24). Water overflowed the BFD for >40 days in each water year examined in this study changing the reservoir from a lacustrine to riverine environment. In April 2006 reservoir overflow was sampled daily for TSS by Bainbridge et al. (2006b). The reservoir began to overflow on 9 April, before the turbidity current reached the Eastern site, indicating that initial overflow from the reservoir is ambient water being displaced as the reservoir fills (Dallimore et al., 2004; Marti et al., 2011). Sediment concentration in this overflow was 147 mg/L on 11 April (Bainbridge et al., 2006b), similar to TSS measured at depth at the Eastern site (143 mg/L, 304 NTU at 25 m, c.f. 71 mg/L and 217 NTU at the surface). Sediment concentrations in dam overflow measured by Bainbridge et al. (2006b) on 17 April were similar to those recorded in the turbidity current at the Eastern site on 14 April (342 mg/L, peak particle size 3.55 µm c.f. 452 mg/L, 944 NTU, 3.5–5 µm at 21 m depth), but surface samples contained much less SS (105 gm/L and 230 NTU), indicating that sediment carried in the turbidity current was flowing over the spillway. Overflow reducing the sediment available for deposition increases the life of the BFD.

The exit of turbid flow from the BFD reservoir in dam overflow decreases sedimentation within the reservoir. Allowing sediment to exit the reservoir as soon as it arrives at the dam wall, done in an uncontrolled manner in the BFD reservoir, reduces the opportunity for sedimentation and accumulation in the reservoir (Müller et al., 2017). Faithful and Griffiths (2000) found that at a site close to the BFD wall, the turbidity current travelled at a depth of 5–20 m and the bulk of highly turbid inflow overflowed the spillway. The turbid flows observed in this study were deeper (13–27 m) but still overflowed the spillway. Turbid inflow will continue to move through a reservoir until its velocity is reduced to zero and its sediment load is deposited, or the dam halts it (Raudkivi, 1993). Once it reaches the wall, turbid water will accumulate, increasing in volume as long as the turbid flow continues (Fan, 1986). Once the BFD reservoir has filled and begun to overflow, the barrier to turbid flow is removed and SS is transported out of the reservoir. Reservoirs with bottom outlets commonly discharge turbid flows to discharge sediment and reduce sedimentation that could limit the useful life of the dam (de Cesare et al., 2001; Fan, 2008; Wang et al., 2005).

This understanding of turbidity current behaviour in the BFD reservoir will allow dam managers to manipulate water releases in the future to discharge turbid water from targeted depths and facilitate sediment removal should sedimentation near the dam wall become a problem or if turbidity currents threaten to damage proposed hydroelectric infrastructure (Queensland Government, 2017).

3.5.3. Sediment deposition and the fate of coarse particles

Benthic particle-size data suggests that most very coarse particles (>500 µm) are deposited prior to entering the BFD reservoir. Fielding and Alexander (1996) showed that the Upper Burdekin riverbed around Big Bend (~142 km upstream of the BFD reservoir) is characterised by coarse-grained to very fine-grained sands (62.5–2000 µm) and gravels (>2mm). Peak flood wave speeds of >5 $m \cdot s^{-1}$ are experienced in the Burdekin River channel even during some below-average flow events and these are capable of mobilising gravels (Alexander & Fielding, 1997). Some dry season flows are also capable of local transport of sand and small gravel (Fielding & Alexander, 1996). The BFD reservoir has a bed load trapping efficiency of 100% (Brown and Root, 2001) and will preferentially trap 95% of particles >30 µm (Lewis et al., 2013). Our results establish that <3% of SS is >62.5 µm indicating that, in below-average flow years, negligible coarse sediment is transported through the reservoir. Coarse sand (>500 µm) makes up <9% of benthic sediment samples at all sites (<4% in pre-2011 samples) except in the northern Burdekin section (Figure 3.6a) where samples contain up to 28% coarse sand. These data suggest that coarse sand is only deposited in the upper reaches of the BFD reservoir, where the initial reduction in flow velocity leads to the deposition of this coarser sediment fraction (Csiki & Rhoads, 2010; Tarela & Menéndez, 1999).

Coarse particles >126–500 µm may be transported into the BFD reservoir by wet season flow events or as bedload. Increased discharge velocity during wet season events may allow the transport of coarser particles if available (Walling & Moorehead, 1989; Walling et al., 2011). Coarse particles were present in benthic sediments from the BFD reservoir, but they only constituted <1.3% of SS samples. Although >126 µm particles were rare in SS samples from this study (in <5 samples), they were reported in dam overflow during the 2005–06 water year (0.28–564 µm; Bainbridge et al., 2006b) and the 2007–08 water year (10.04 to 710 µm; Lewis et al., 2009) confirming regular transport of coarse particles in SS as far as the dam wall. Bedload transport is likely to be minimal and mainly occur in the Burdekin section of the BFD reservoir where sandy deposits have formed. Sediment deltas form in the upstream sections of reservoirs where inflow velocity decreases and bed load and coarse particles are deposited (Chaudhuri, 2017; Morris & Fan, 1998). In-channel benthic samples from the

Burdekin site (Figure 3.6a) were found to have 20%–72% >126 μm particles, indicating the formation of a delta in this section of the BFD reservoir. Further downstream, in the Burdekin and Central reservoir sections (Figure 3.6b, c) up to 10% of samples are composed of particles >126 μm, decreasing to <6% in the Eastern section of the BFD reservoir. While larger flow events will transport larger particles further into the reservoir, underflow turbidity currents such as those observed at the Burdekin site may also transport sediment, particularly less cohesive coarse particles, as bedload along the delta deposits (Morris & Fan, 1998; Wildman Jr. et al., 2011).

Quartz, feldspar and chlorite are likely to be present as larger particles carried by wet season flow and a greater proportion of these particles are likely to be sourced from the Upper Burdekin River sub-catchment. The much larger percentage of quartz and feldspars found in benthic sediment than in SS (11%–42% and 2%–16% c.f. 2%–13% and <4%; Table 3.3, Table 3.4) suggests that these two minerals are present as larger particles that settled out while finer particles were preferentially exported from the dam in overflow or remained in suspension (Cooper et al., 2017 – Chapter 2; Lewis et al., 2013). Chlorite composes 1%–7% of wet season SS samples from the Burdekin, Central and Eastern sites (Table 3.3), but was only found in trace amounts in SS from the Burdekin site in the dry season (average 0.2% of samples; Cooper et al., 2017 – Chapter 2), clearly showing that this mineral is transported by flow events. Amphiboles were present in trace amounts in benthic sediment samples (≤2%) from 2011 only, and were not found in any SS samples, suggesting that these minerals may be associated with rarer, very coarse particles transported into the BFD reservoir during above-average flow events. Samples of SS from the turbidity currents at the Burdekin site were dominated by the >0.9 μm fraction (average 82%) while samples from the Suttor site only contained 32% of particles >0.9 μm on average, pointing to the Burdekin River as the dominant source of coarser sediment. Some contribution of coarse particles from the banks of the BFD reservoir is also likely, particularly given the relative narrowness of the Burdekin section of the reservoir and therefore proximity to sampling sites. Larger smectite fractions in benthic sediment from the Central and Eastern section sites (average 8%–16%, c.f. 8%–10% in Burdekin samples and 3%–8% in Suttor) are likely to be present as fine particles that are preferentially transported into these areas of the reservoir every year, regardless of the strength of inflow, increasing their proportion in benthic sediment through deposition during the dry season.

3.5.4. *Effect of above-average discharge events on sediment particle size and composition*

The above-average discharges that passed through the reservoir prior to the collection of core and grab samples in 2011 altered the proportions of minerals present in benthic sediments but did not alter the type of minerals present. Increases in quartz and feldspar were observed in sediments from the Burdekin (+14%–15% and +4%–6% respectively), upstream Suttor (+17% quartz, +3% feldspars) and the Central sections of the reservoir (+8%–9% quartz, +2%–3% feldspars) further confirming that these minerals are associated with the larger particles, as was observed in Lake Powell (Wildman Jr. et al., 2011), and would have been transported further into the reservoir by these events. Kaolinite decreases of 10%–25% at the Burdekin and Central section sites are attributed to the dilution effect of the increased deposition of quartz and feldspar.

The above-average discharge events between 2008 and 2011 transported coarser particles further into the reservoir but did not greatly affect the particle-size distribution of sediments in the northern Suttor or Eastern sections of the reservoir (Figure 3.6). Particle-size distribution in the southern Burdekin, southern Suttor and Central section sediments show a coarsening in samples collected after the above-average flow events (peaks shift from 6–14 μm to 11–400 μm, Figure 3.6b, c, e) indicating that coarser material has been transported into the dam. Coarsening was also observed in 2011 samples from the shallow Eastern section at site f (Figure 3.6f). No change was seen in the size distribution of northern Suttor section sediments, despite the combined discharge from the Suttor and Cape Rivers being the highest in 2007–08 (9.3 TL) and 2010–11 (9.1 TL) since the construction of the reservoir in 1987 (in 2007–08 the Suttor and Cape rivers contributed 60% of total flow into the reservoir).

3.6. Conclusion

Griffiths and Faithful (1996) concluded that the highly turbid nature of inflows to the BFD reservoir is likely to be a continuing feature of the system and this is true even 28 years after the dam was built. It is therefore essential to understand these turbid flows and the impact they are likely to have on sediment transport and deposition in the reservoir. This study has contributed to that understanding by carefully examining the physico-chemical characteristics of the water column and mixing processes that occur within the BFD reservoir during wet-season inflows and the resultant effect on the movement of sediment. This study also documents the relationships between turbidity, particle size and mineralogy in a seasonally dry tropical reservoir.

Suspended sediment in the BFD reservoir was found to travel in a turbidity current that moves through the reservoir as either an interflow or underflow. Upon reaching the dam wall, turbid flows are discharged in overflow, even during below-average discharge events. Particles >126 µm are transported into the reservoir by wet season flow events or as bedload and are mainly deposited in the upper reaches of the reservoir. Quartz and feldspars were found to be more abundant in coarser sediment and as a result occur mainly in sediment deposited upstream only. Because of these processes, sediment deposition in the Central and Eastern sections of the reservoir is minimal (26%; Cooper et al., 2018 – Chapter 5) and restricted to fine <62.5 µm, kaolinite- and smectite-rich particles, prolonging the useful life of the reservoir. Extreme (1-in-11 to 1-in-22 year at the Burdekin Hydro Site) discharge events between 2008 and 2011 transported coarser particles further into the BFD reservoir altering the particle-size distribution in some, but not all, sections of the reservoir.

The results of this study provide insight into the behaviour of turbid flows in stratified reservoirs that receive highly variable inflow, providing important context for dam operators in tropical regions and worldwide. Dam owners Sunwater Limited plan to raise the dam wall by 2 m to increase water supply and bring the dam in line with modern engineering design standards (Sunwater Limited, 2024a). The Australian Government is considering building new dams in tropical northern Australia, and dam construction continues in tropical to sub-tropical regions in Asia. These are all regions that can expect large turbid inflows into any reservoir, so it will be important for dam planners to consider the ability of turbidity currents to form and transport sediment through a reservoir and ensure that turbid flows can be vented when needed to avoid problematic sedimentation. Although turbidity currents travel through the BFD reservoir in the same way in most years, changes to the reservoir's dimensions, as would be the case with the potential expansion of the BFD, could change the future stratification and sediment transfer and depositional characteristics of the reservoir. Should the reservoir be maintained with the capacity to trap all but the largest event flows, to maximise water storage, then the reservoir would no longer overflow each year, leading to additional backflow within the reservoir and a greater amount of sediment being trapped annually.

Chapter 4: Geochemistry and particle size of core sediments from Lake Dalrymple: sediment distribution and implications for source

This paper is in the final stages of development. Reviewers will encounter some repetition of information included in the preceding sections of this thesis, particularly in the introduction and methods sections.

Abstract

Undisturbed benthic sediments archive environmental changes and catchment inputs to lake systems. This study examined the characteristics of sediments in cores collected throughout Lake Dalrymple, a reservoir on the Burdekin River in north-eastern Australia, to examine the sedimentological processes that fractionate the sediment in the dam and to distinguish the catchment inputs. Sediment samples collected using gravity/push cores or grabs and representing up to 24 years of sediment influx and deposition were analysed for particle size, major and trace elements, strontium (Sr) isotopes and mineralogy. Sediment has preferentially deposited in the relict river channels which tend to be relatively deep compared to the surrounding lake bathymetry. This is particularly so in the northern Burdekin arm and central to eastern sections of the reservoir. Coring attempts indicate no sediment has built up immediately behind the dam wall. Even though sediment is largely delivered to the reservoir in seasonal, highly sediment-laden inflow, core sediments do not preserve a recognisable record of discrete above-average flow events. Mineral composition was dominated by quartz, muscovite/illite, kaolinite and smectite, reflecting the variable geology of the upper river catchments: igneous, metamorphic and sedimentary rocks in the Upper Burdekin and more heavily weathered sedimentary rocks and clay soils in the Suttor/Belyando/Cape river catchments. Greater differences in sediment geochemistry, mineralogy and particle size were observed between locations within the reservoir rather than with depth, indicating that these differences are predominantly spatial and not temporal. The physical and geochemical characteristics of the two primary sources of sediment to the reservoir were identified. Sr isotopic ratios indicated that most of the sediment deposited in the Central Reservoir came from the Burdekin River system (71%−83%), while approximately half the sediment deposited in the Eastern Reservoir came from the Suttor/Belyando/Cape river systems (46%−58%). The geochemical data collected as part of this study provides an environmental baseline for sediment in the BFD reservoir. This understanding of the influence of particle

size on sediment distribution and character contributes to our knowledge of the processes affecting sediment geochemistry and sediment transport within reservoirs.

Keywords: Burdekin Falls Dam, reservoir, sediment core, particle-size distribution, sediment source.

4.1. Introduction

Sedimentation is a common problem in reservoirs around the world. Dams routinely trap sediment resulting in loss of reservoir storage and reduced usable life (Ajaaj et al., 2024; Guo et al., 2020; Kondolf et al., 2014; Palmieri et al., 2001; Perera et al., 2023; Pitt & Thompson, 1984; Tamene et al., 2006; Yao et al., 2023). Knowing the type of sediment being deposited, where it is being deposited, and the timeframe of deposition, is therefore crucial for the long-term management of reservoirs (Simms et al., 2008). The spatial and temporal distribution of deposited sediment in a reservoir also provides insights into the sediment sources and sedimentological processes occurring throughout the reservoir. Studying how particle size and composition influences the fractionation and deposition of sediment allows targeted management of sediment types and sources within the upstream catchment area, especially when sediment may deposit in places that are problematic for dam operation, e.g., near the dam wall (Oehy & Schleiss, 2007; Samadi Boroujeni et al., 2009). The major and trace element composition of lake sediments can also provide historical environmental information and create a baseline for further investigations (Gao et al., 2015; Ra et al., 2011; Routh et al., 2007).

While many studies on major and trace element geochemistry of sediments have been conducted in lakes, less research has been carried out in reservoirs (Abraham, 1998) despite the potential differences in the limnological response of reservoirs c.f. lakes (Thornton, 1984). Differences may include astatic shorelines, high flushing rates, high turbidity and sedimentation rate, and variable water release level (Thornton et al., 1990). Water bodies with extensive sediment records, some dating back as far as 7,700 years, have provided an insight into climate change (Fukumoto et al., 2015; Wang et al., 2015) and anthropogenic impacts (Gao et al., 2014; Liu et al., 2014). More commonly, geochemical research has focussed on those reservoirs and lakes that trap industrial runoff or windblown sediments (Duan et al., 2014) and become sinks for heavy metals (Souza & Wasserman, 2015; Zhao et al., 2022), which may negatively affect fauna and primary production in the water body (Long et al., 1995; Moore & Ramamoorthy, 2012; Szyczewski et al., 2009). Work in Australian reservoirs and lakes has focussed on analyses of heavy metal concentrations in surface sediments (Roach, 2005); the use of lead and caesium isotopes to assess sediment source processes, such as the contribution from subsoils, and deposition rates (Simms et al., 2008; Wasson et al., 1987); and the identification of sediment sources (Douglas et al., 2003; Rahman & Bakri, 2010; Wasson et al., 2002). Few studies have examined the broader geochemistry of reservoir sediments with a focus on sediment distribution and none have been conducted in tropical Australian reservoirs. This study attempts to address this gap by considering Lake Dalrymple, a reservoir in Queensland.

Lake Dalrymple, the reservoir of the Burdekin Falls Dam (BFD; Figure 4.1), is situated in the seasonally dry tropics of northern Queensland. A large (1.86 TL, 220 km^2 area) reservoir that receives seasonal, highly sediment-laden inflow, the dam traps incoming water and sediment from three major river systems: the upper Burdekin River, which enters the reservoir from the north, and the Suttor/Belyando and Cape/Campaspe river systems, which enter from the south (Figure 4.1). The reservoir loses 0.15% of capacity due to sediment deposition per year and bathymetric data show that in the 24 years after the dam's construction (1987–2011) little of the channel has been infilled (Cooper et al., 2018 – Chapter 5). Although sediment exits the reservoir by flowing over the dam during wet season flow events (Faithful & Griffiths, 2000), fine sediment <0.9 μm remains in suspension year-round (Cooper et al., 2017 – Chapter 2) and >95% of coarser sediments (>30 μm) are trapped (Lewis et al., 2013).

The objective of this study is to characterise the spatial and temporal variability of the benthic sediments in the BFD reservoir, including their mineralogy, geochemistry and particle size, to examine the sedimentological processes that fractionate the sediment in the dam. This study incorporates the data from gravity and push cores and grab samples spread throughout this large reservoir. Characteristics that relate sediments to their major catchment source were investigated and evidence of known large flow events was sought. The geochemical and physical information obtained in this study will serve as a baseline for future evaluations of sediment composition in this reservoir and enable reservoir managers to better understand where sediments are deposited. Improved understanding of sediment sources and distribution will inform an appropriate management strategy for this system and for other tropical reservoirs with multiple flow sources.

4.1.1. Study area

Lake Dalrymple formed in 1987 after the completion of the BFD on the Burdekin River in north-eastern Queensland, Australia (Figure 4.1). The Burdekin River drains a catchment >130,000 km^2 and is one of Australia's largest rivers as measured by discharge volume (Mitchell et al., 2006), transporting 3.3 Mt of fine sediment (<63 µm) per year to the coast on average (McCloskey et al., 2021). A catchment area of 114,220 km^2 (~88% of the total Burdekin catchment) lies upstream of the BFD (Figure 4.1). At full supply level, the BFD reservoir holds 1.86 TL of water and covers an area of 220 km^2. The maximum water depth is 40 m (average 8.45 m) and it is 50 km in length (Sunwater Limited, 2024b). The BFD was constructed to supply water for irrigation and the mining industry, but provisions were made at the time of construction to allow for vertical extension of the dam wall to increase storage and support hydroelectric power generation. Inflow fills the reservoir during the November to April wet season and it has overflowed every year but two (capacity to average annual inflow ratio = 0.24; Bainbridge et al., 2014).

The BFD reservoir receives inflow from three major sub-catchments: the Upper Burdekin River, Cape/Campaspe rivers, and Suttor/Belyando rivers (Figure 4.2). Rainfall produces rapid runoff with very fast flood-wave speeds (estimated at over 5 $m \cdot s^{-1}$ in the upper to middle sections of the river; Alexander & Fielding, 1997) capable of displacing and transporting significant amounts of both coarse and fine sediment (Alexander et al., 1999a; Mitchell et al., 2006), a large portion of which (average 66%) is trapped in the reservoir (Lewis et al., 2013). Rainfall varies temporally and spatially within both the sub-catchments but occurs mostly during the wet season (Alexander et al., 2020; Roth et al., 2002). In the Upper Burdekin coastal ranges mean rainfall is >1500 mm $year^{-1}$ but parts of the Suttor and Belyando sub-catchments receive only 500 mm $year^{-1}$ (Bainbridge et al., 2014). The volume of sediment transported into the reservoir each year varies—12%–280% of the average annual yield in the water years from 2005–06 to 2009–10 (Bainbridge et al., 2014)—and may be supply or hydraulically limited (Amos et al., 2004). The Upper Burdekin River consistently contributes >75% of the total sediment load delivered to the reservoir while the remaining sub-catchments contribute <25%, despite variable flow contributions (Bainbridge et al., 2014; Lewis et al., 2013). Fine SS (<1 µm) transported in inflow contributes to persistent turbidity in the reservoir (Cooper et al., 2017 – Chapter 2; Faithful & Griffiths, 2000; Griffiths & Faithful, 1996).

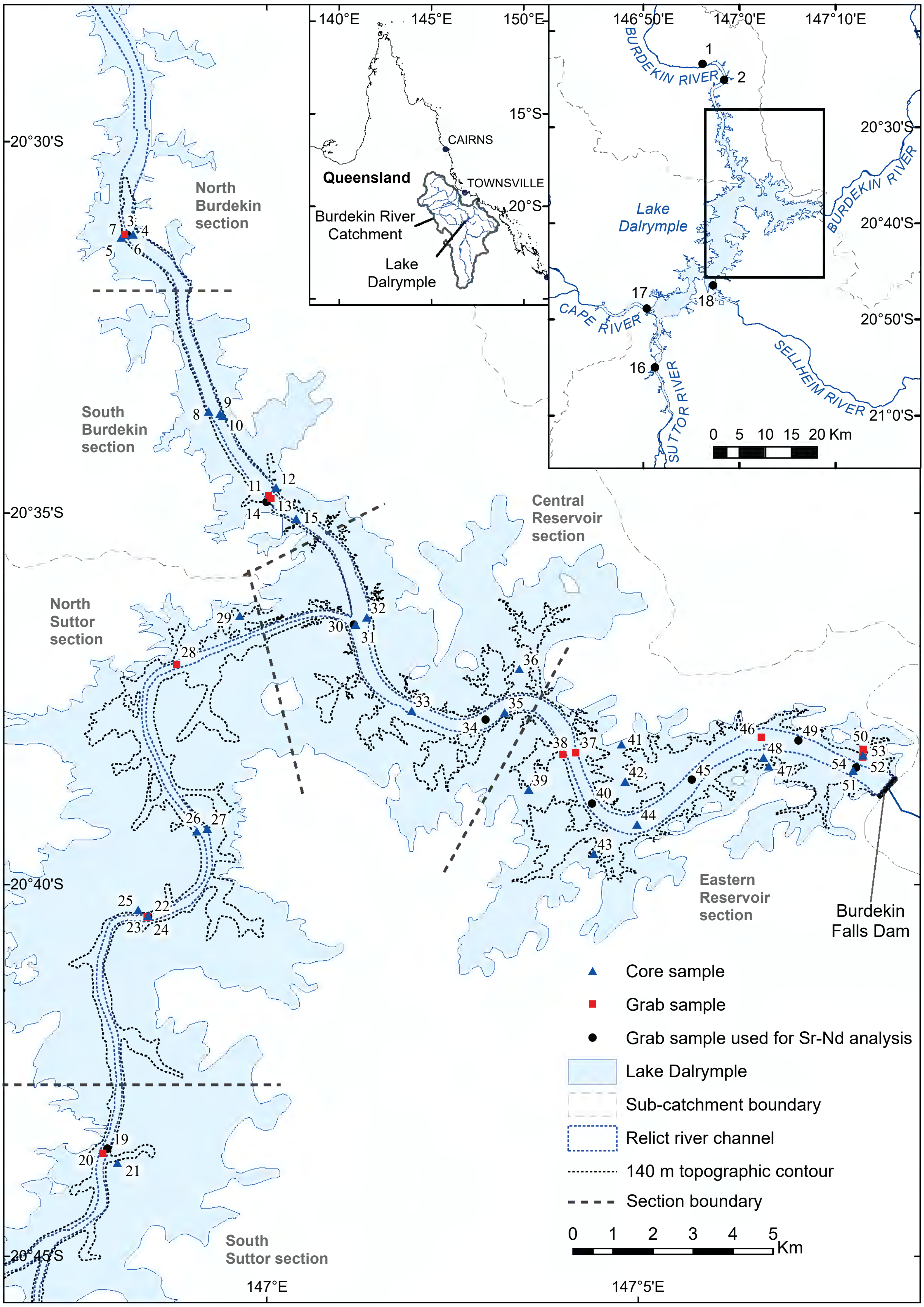

Figure 4.1 Small inset: Location of the Burdekin River catchment and Lake Dalrymple in northern Queensland, Australia. Large inset: Rivers entering the BFD reservoir (Lake Dalrymple) and location of additional samples. Main map: Location of cores and grab samples in the BFD reservoir. Sample details provided in Table 4.1.

The geology and geomorphology of the sub-catchments of the reservoir are highly variable (Figure 4.2) but all are intensely weathered. The Upper Burdekin catchment comprises a mix of various igneous, metamorphic and sedimentary rocks, including Cenozoic basalts in the north-west of the sub-catchment and large areas of Silurian to Carboniferous granite and granodiorite outcrops in the north, north-central and eastern sections (Fergusson & Henderson, 2013; Raymond et al., 2012). Extensive areas of erodible red duplex soils, black and red soils of basaltic origin, sands and sodic duplex soils have developed in this sub-catchment (Roth et al., 2002). In contrast, Cenozoic to Holocene sand, gravel and soil alluvial deposits dominate the surficial geology of the Suttor/Belyando and Cape/Campaspe sub-catchments (Figure 4.2). Neoproterozoic to Early Cambrian sandstones, siltstones, and schists, and Carboniferous tuffs and rhyolitic rock are also common in the Suttor/Belyando, and a ridge of Triassic sandstone, siltstone, and mudstone runs along its western fringe (Raymond et al., 2012). Cracking clay soils produced from basic igneous rocks and clay-containing sedimentary rocks, including grey/brown clays and red/yellow earths, are the dominant soil types in both the Cape/Campaspe and Suttor/Belyando (Roth et al., 2002).

Steep-sided mountain ranges (peaks up to 1,065 m) and strongly undulating terrain characterise the Upper Burdekin (Roth et al., 2002), where relatively steep and incised river channels produce greater sediment availability and transportability (Bainbridge et al., 2014) than in the Suttor/Belyando and Cape/Campaspe sub-catchments which have more gently sloping channels, flatter alluvial plains and lowlands, and lower peak elevations, 300–450 m (Croke et al., 2015; Roth et al., 2002). Grazing is the primary land use in the reservoir's sub-catchments (Newham et al., 2017) which, together with land clearing and grain-growing, has contributed to degradation of stream channel stability and widespread erosion (Faithful & Griffiths, 2000; Fleming & Loofs, 1991).

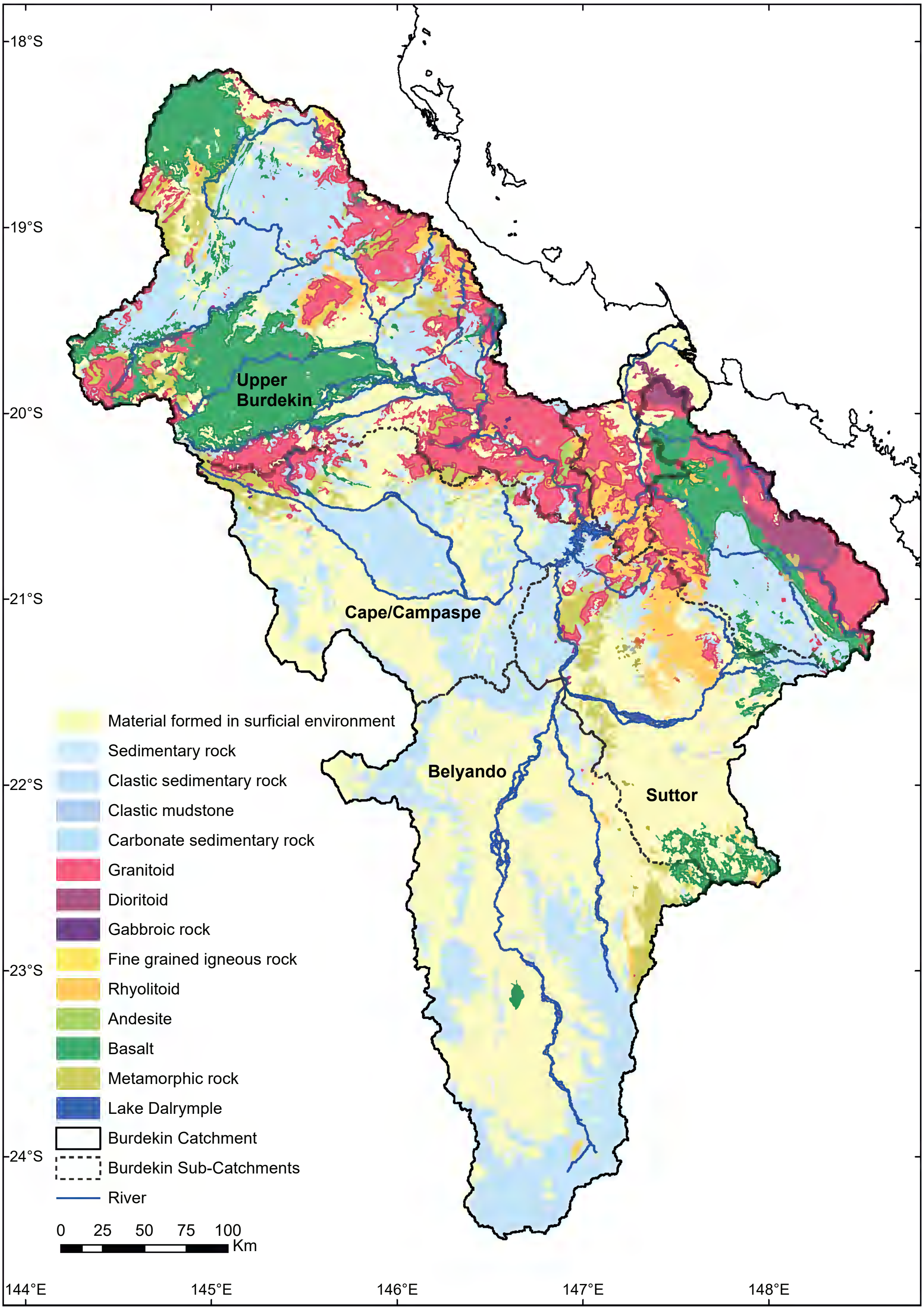

Figure 4.2 1:1 million surface geology of the Burdekin River catchment (Raymond et al., 2012). Reservoir sub-catchment boundaries are also shown. The Belyando River flows into the Suttor River upstream of the BFD reservoir so they are referred to as the Suttor/Belyando sub-catchment for the purposes of this study.

4.2. Methods

The reservoir was divided into the following sections for this study: North Burdekin (where the Burdekin River enters the reservoir), South Burdekin, South Suttor (where the Suttor/Belyando and Cape/Campaspe river systems enter the reservoir), North Suttor, Central Reservoir and Eastern Reservoir as shown in Figure 4.1. A range of analytical methods were performed on core and grab sediment samples to investigate the composition and particle size of sediment deposited in the BFD reservoir including: granulometry, X-ray diffraction (XRD), loss on ignition (LOI), X-ray fluorescence (XRF), and inductively coupled plasma mass spectrometry (ICP-MS).

4.2.1. Selection of sampling sites

Benthic sediment samples were collected from the BFD reservoir using a grab sampler, gravity corer or push corer. Sampling sites were selected to represent a range of depositional environments including from both in and out of the relict river channel (henceforth referred to as the channel), in a variety of water depths (2.7–32 m), and in areas of interest such as the confluence of the Burdekin and Suttor arms of the reservoir and behind the dam wall. Sampling locations were also influenced by the need to: a) provide a broad spatial coverage of the reservoir within the allocated fieldwork period; b) allow for comparison with previous studies (e.g. Faithful & Griffiths, 2000); c) correspond with water sampling sites (e.g. Cooper et al., 2017 – Chapter 2); and d) sample specific zones, such as areas of deposition as highlighted by a bathymetric survey (Cooper et al., 2018 – Chapter 5). A grab sample was collected when attempts to collect a core failed. Potential sampling sites closer to the shore in some Burdekin and Dam locations were explored, however abundant dead trees filled the non-channel regions of the reservoir particularly in the Suttor sections, making navigation difficult. Sample site co-ordinates and sampling dates are provided in Appendix C, Table C4. Sediments were classified as in or out of the channel using water depth at the core site, bathymetry data (Cooper et al., 2018 – Chapter 5) and pre-dam topographic data (Figure 4.1).

4.2.2. Core collection and sediment sampling

Twenty-three sediment samples were collected using a Van Veen grab sampler in December 2003, March 2004, August 2005, and September 2011 (Figure 4.1; Appendix C, Table C4). The grab sampler collected sediment from up to 15 cm below the benthic surface. Composite sediment samples were produced by combining the sediment from two to three grabs from a location (approximately 50 m^2) in a bucket and collecting approximately 1 kg of well-mixed sediment into a zip-lock bag. Creating composite samples increased the representativeness of each sample and mitigated potential heterogeneity issues (International Atomic Energy Agency, 2003; Lietman, 1997). Grab samples were kept cool and refrigerated on return to the laboratory.

Gravity and push cores were collected from 31 locations within the BFD reservoir in August and September 2011 (Figure 4.1, Table 4.1). Core collection methods are described in detail in Cooper et al. (2018 – Chapter 5). Gravity cores were collected using an 80 kg Ewing Piston Corer mounted on a twin-hulled boat from locations with water depths >3.5 m. The core catcher and barrel of the gravity corer were constructed from stainless steel and were lined with a polycarbonate tube which retained the sediment core. Push cores were collected with a manual push corer that used plastic tubing directly to capture sediment. Push cores were collected in water <10 m deep. Three gravity core tubes collected material that was unable to be preserved as a core and were instead treated as grab samples (Table 4.1).

Cores were stored and transported in an upright position. On return to the laboratory, the cores were frozen (upright), photographed, measured and then split using a rock saw. Half of each core was photographed and sampled, and the other half was archived. Samples were collected by taking a 1-cm thick slice centred on the depth being sampled (e.g., 9.5–10.5 cm for a 10-cm depth sample). Cores were subsampled every 5 cm using plastic tools, with additional samples taken more frequently if visual changes in sediment composition were noted (e.g., colour or particle size changed, or laminations were observed). Samples were labelled by ‘site - sample depth’ (e.g., *4 - 04 cm* is a sample from site 4, depth 4 cm). A total of 266 core sub-samples were collected as well as 15 grab samples. All core and grab samples underwent particle-size analysis (n=281).

A sub-set of 162 core/grab sediment samples was selected based on particle-size results and other physical properties (e.g., colour changes or fine laminations) for geochemistry and mineralogy analyses. Every second sample down core was analysed when sections of a core were considered homogenous. These sub-samples were analysed using X-Ray diffraction (XRD), X-Ray fluorescence (XRF) and inductively coupled plasma mass spectrometry (ICP-MS).

Table 4.1 Details for cores and grab samples collected in the BFD reservoir.

Site ID	Location	Water depth (m)	Sample Type	Sediment depth (cm)	Relation to channel	Corer reached pre-reservoir surface
1	Burdekin River	1.2	Grab	15*	In	N/A
2	North Burdekin	2.0	Grab	15*	In	N/A
3	North Burdekin	19.4	Gravity core	30	In	Undetermined
4#	North Burdekin	6.5	Gravity core	67	Edge	Undetermined
5	North Burdekin	6.2	Push core	25	Edge	Undetermined
6	North Burdekin	14.4	Grab	15*	In	N/A
7	North Burdekin	17.9	Grab	15*	In	N/A
8	South Burdekin	19.0	Gravity core	66	In	Undetermined
9#	South Burdekin	13.5	Gravity core	82	Edge	Undetermined
10	South Burdekin	3.5	Gravity core	60	Edge	Undetermined
11	South Burdekin	19.4	Grab	15*	In	N/A
12	South Burdekin	2.7	Push core	43	Out	Undetermined
13^	South Burdekin	20.0	Gravity core (failed)	Mixed core sed. ~16cm	In	N/A
14	South Burdekin	18.0	Grab	15*	In	N/A
15	South Burdekin	20.0	Gravity core	44	In	Undetermined
16	Suttor River	2.0	Grab	15*	In	N/A
17	South Suttor	6.0	Grab	15*	In	N/A
18	South Suttor	8.0	Grab	15*	In	N/A
19	South Suttor	15.0	Grab	15*	In	N/A
20^	South Suttor	18.6	Gravity core (failed)	Mixed core sed. ~15cm	In	N/A
21#	South Suttor	3.7	Push core	43	Out	Undetermined
22	North Suttor	19.8	Grab	15*	In	N/A
23	North Suttor	22.3	Grab	15*	In	N/A
24#	North Suttor	22.2	Gravity core	31	In	Undetermined
25#	North Suttor	8.4	Push core	43	Out	Undetermined
26#	North Suttor	22.9	Gravity core	33	In	Undetermined
27	North Suttor	8.3	Push core	37	Out	Yes
28	North Suttor	24.0	Grab	15*	In	N/A
29	North Suttor	7.0	Push core	22	Out	Yes
30	Central Reservoir	19.0	Grab	15*	In	N/A
31#	Central Reservoir	18.6	Gravity core	85	In	Very likely
32#	Central Reservoir	21.0	Gravity core	82	In	Undetermined
33	Central Reservoir	22.0	Gravity core	41	In	Undetermined
34	Central Reservoir	23.3	Grab	15*	In	N/A
35#	Central Reservoir	25.0	Gravity core	81	In	Undetermined
36	Central Reservoir	6.4	Push core	35	Out	Yes
37	Eastern Reservoir	27.0	Grab	15*	In	N/A
38	Eastern Reservoir	15.2	Grab	15*	Edge	N/A
39	Eastern Reservoir	13.0	Gravity core	24	Out	Yes
40	Eastern Reservoir	25.7	Grab	15*	In	N/A
41	Eastern Reservoir	7.0	Push core	22	Out	Very likely
42	Eastern Reservoir	13.0	Gravity core	2.5	Out	Very likely

Site ID	Location	Water depth (m)	Sample Type	Sediment depth (cm)	Relation to channel	Corer reached pre-reservoir surface
43	Eastern Reservoir	9.2	Push core	26	Out	Yes
44#	Eastern Reservoir	27.5	Gravity core	88	In	Undetermined
45	Eastern Reservoir	27.1	Grab	15*	In	N/A
46	Eastern Reservoir	29.0	Grab	15*	In	N/A
47	Eastern Reservoir	8.1	Push core	27	Out	Very likely
48	Eastern Reservoir	18.5	Gravity core	22	Edge	Yes
49	Eastern Reservoir	26.2	Grab	15*	In	N/A
50^	Eastern Reservoir	N/A	Gravity core (failed)	Core catcher only	Out	N/A
51#	Eastern Reservoir	32.0	Gravity core	71	In	Undetermined
52	Eastern Reservoir	23.0	Grab	15*	Edge	N/A
53	Eastern Reservoir	19.0	Gravity core	2	Edge	Yes
54	Eastern Reservoir	28.8	Grab	15*	In	N/A

Note: Location refers to reservoir sections marked in
*Approximate depth of grab samples; estimate based on the size of the Van Veen grab sampler used
# Indicates 'long' cores referred to in the text
^ Samples from sites 13 and 20 consist of combined material from the top 15–16 cm of deposited sediment (equivalent to a grab sample) as the core sediment slipped out of the corer on recovery and was bagged. Material was only recovered from the core catcher for Sample 50.
N/A = not applicable

4.2.3. Hydrological data

Hydrological data were obtained from the Queensland Government's Water Monitoring Data Portal (https://water-monitoring.information.qld.gov.au/, accessed 2 February 2017). The mean and median annual discharges were calculated for gauging stations closest to the reservoir (Burdekin River at Sellheim, 120002C; Suttor River at St Anns, 120303A; Cape River at Taemas, 120302B; and Burdekin River at Hydro Site, 120015A) for the period from the water year of gauge installation (between 1977–78 and 1968–69) to the end of the 2015–16 water year. Daily discharge is presented in Appendix C, Figure C3a–f.

4.2.4. Particle-size analysis

Particle-size analysis was conducted on 281 sediment samples. Particle-size distributions were determined using a Malvern Instruments Mastersizer 2000 laser particle-size analyser (range 0.02–2000 µm) using the method described in Cooper et al. (2017 – Chapter 2). Samples were wet sieved using a 1.4 mm sieve prior to analysis to remove any coarse particles that would damage the Mastersizer. Twelve percent of samples (n=34) contained organic or inorganic fragments >1.4 mm that were removed from the aliquot (Appendix C, Table C5), all other samples exclusively contained material that passed through the sieve. Particle-size distributions may include sizes up to 2 mm because elongate particles, with a short axis less than the sieve-size, may pass through the sieve (Matthews, 1991). Samples were run manually to ensure suitable dilution and were treated ultrasonically for one minute while in the sample chamber to ensure disaggregation of flocs. No chemical dispersant was used. Optimal laser obscuration of 15–20% (Sperazza et al., 2004) was achieved for sediment analysis via dilution with filtered water. Three measurements were produced for each sample aliquot and two aliquots of each sample were analysed and an average distribution obtained.

Correction was applied to the index of refraction (RI) used in processing by the Mastersizer software based on mineralogical input (Cooper et al., 2017 – Chapter 2). Sediments were classified into one of four size classes based on the Udden-Wentworth particle-size scale (Blott & Pye, 2012): clay (<3.9 μm), fine silt (3.9–15.6 μm), medium to coarse silt (15.6–62.5 μm; referred to as coarse silt) and sand (>62.5 μm). The fine and coarse silt size fractions were combined for use in ternary plots (silt; 3.9–62.5 μm).

4.2.5. X-Ray diffraction

Mineral composition was determined for 162 samples using a Siemens D-5000 X-ray diffractometer or a Siemens D500/D501 series X-ray diffractometer. Samples were prepared using the Smear Mount method described by Moore and Reynolds (1997) and mineral assemblages were determined using the methods detailed in Moore and Reynolds (1997). Three diffraction patterns were run for each sample: untreated and air-dried; ethylene–glycol solvated at 40°C for 24 hours; and heated to 400°C for a minimum of 1 h. Scans were run over the range 5°2θ to 70°2θ for air-dried samples and at the shorter range of 5°2θ– 35°2θ for glycolated and heated slides. Mineral identification and quantification were performed using Bruker AXS Diffrac.Suite EVA (ver. 3.0.0.9) and Bruker AXS Diffrac.Suite TOPAS (ver. 4.2) software respectively.

4.2.6. X-Ray fluorescence and inductively-coupled plasma mass spectrometry

After LOI analysis (method in supplementary data Appendix C, p 187), samples were ground and glass beads were prepared for XRF and ICP-MS analyses using either LM100 or 12-22 flux, following the method documented in de Caritat et al. (2010). XRF analysis was performed using a Philips PW2404 4kW sequential wavelength dispersive spectrometer fitted with a rhodium X-ray tube (PANalytical B.V.) calibrated using three international standards (certified reference materials, CRM): JLk-1 (sediment from Lake Biwa, Geological Survey of Japan), STSD-4 (stream sediment, Geological Survey of Canada) and NIM-G (granite, South Africa's Bureau of Standards). XRF data were obtained for 11 major elements (Al, Ca, Fe, K, Mg, Mn, Na, P, S, Si and Ti; reported as oxides in %), 23 trace elements (As, Ba, Ce, Cl, Cr, Cs, Cu, F, La, Mo, Nb, Nd, Ni, Pb, Rb, Sc, Sr, Th, U, V, Y, Zn, Zr; reported as elements in ppm) and calculated LOI. Fe was reported as Fe_2O_3Tot (total). To remove uncertainty or bias caused by the presence of organic material or loosely bound water and directly compare the geochemistry of samples, calculated LOI was subtracted from each sample and XRF data were normalised to 100%.

ICP-MS analysis for trace elements was performed on the fused samples previously analysed for XRF (see Pyke, 2000). Samples were prepared and analysed with an AGILENT 7500ce ICP-MS using the methods documented in de Caritat et al. (2010). The instrument was calibrated using synthetic standards with an internal standard solution added online. The calibrations obtained were verified against a range of blanks and CRMs (detailed in the Supplementary material). ICP-MS data were obtained for 43 elements, reported in ppm: Ag, As, Ba, Be, Bi, Cd, Ce, Co, Cr, Cs, Cu, Dy, Er, Eu, Ga, Gd, Ge, Hf, Ho, La, Lu, Mo, Nb, Nd, Ni, Pb, Pr, Rb, Sb, Sc, Sm, Sn, Sr, Ta, Tb, Th, U, V, W, Y, Yb, Zn and Zr. Analytical precision and bias for both the XRF and ICP-MS analyses were calculated from repeat analyses of CRM and are presented in Appendix C (Table C6).

The two methods for trace elements analysis (XRF and ICP-MS) show high correlations among the elements (e.g., r^2 = >0.94 for Ba, Rb, Sr, V, Zn and Zr). ICP-MS data were used preferentially in this study. The 54 elements on which statistical and spatial analysis were carried out included: Ag, Al, As, Ba, Be, Bi, Ca, Cd, Ce, Co, Cr, Cs, Cu, Dy, Er, Eu, Fe, Ga, Gd, Ge, Hf, Ho, K, La, Lu, Mg, Mn, Mo, Na, Nb, Nd, Ni, P, Pb, Pr, Rb, S, Sb, Sc, Si, Sm, Sn, Sr, Ta, Tb, Th, Ti, U, V, W, Y, Yb, Zn and Zr.

4.2.7. Strontium/Neodymium isotopic analysis

Sr and Nd isotopic analyses were carried out on 26 sediment samples (15 grab and 11 suspended) at the Centre for Microscopy & Microanalysis (CMM) at the University of Queensland. Suspended sediment samples collected during three sampling trips during the March/April 2006 wet season inflow event (Chapter 3) were combined to create samples representative of SS being transported into the reservoir. One sample was created for each of the following reservoir areas: North Burdekin, North Suttor, Central Reservoir and Eastern Reservoir. Composite samples representing the same four areas were created from SS samples collected in the 2006 dry season (Cooper et al., 2017 – Chapter 2). The final three SS samples were collected during wet season inflow in the North Burdekin, Eastern Reservoir and the Suttor River in December 2003, February 2004, and March 2004 respectively.

Sediments were dried in non-metallic containers in a 40°C oven. Samples were dissolved in Teflon beakers by conventional digestion methods, using concentrated HF-HNO_3 mixtures on a hot plate following the method of Eggins et al. (1997). A 10-mL aliquot was generated. Six samples contained material that was resistant to dissolution in acid. These samples were placed into thermoresistant glass beakers with lids on and ashed at 550°C for one hour before being prepared using the method above. Sr and Nd isotopic analysis was performed on a 7–8 mL aliquot, which was dried before being redissolved in hydrochloric acid. That solution then underwent standard cation exchange and the resulting purified sample was analysed using a VG-Sector-54 WARP-filtered high-abundance-sensitivity thermal ionisation mass spectrometer (TIMS) as described in Li et al. (2006) and Tonguç Uysal et al. (2007).

4.2.8. Simple mixing model

Examination of the geochemical data identified elements that produced lines of mixing with distinct end-members. A simple mixing model was used to estimate the potential contribution of sediment at any given site from each source (Faure & Mensing, 2005):

$$X_M = X_A f_A + X_B(1 - f_A)$$

Where: X_M = concentration of element X in the mixture M

X_A, X_B = concentration of element X in components A and B

f_A = contribution of component A in %

[Note: To solve using $^{87}Sr/^{86}Sr$ ratios, concentrations of element X were replaced with the respective ratio for mixture M and components A and B.]

Solving for f_A provided an estimate of the contribution from source A. Values for individual samples were used to solve the equation for both Sr isotope and other geochemical data. Eight grab samples collected in 2005 were used in this analysis: six from sites 30, 34, 40, 45, 49, and 54, with samples from the North Burdekin (site 6) and South Suttor (site 22) designated as components A and B.

4.3. Results

4.3.1. Hydrological background

Sediment grab samples from December 2003 to August 2005 were collected in water years of below-average (mean) annual discharge (<6.6 TL at the Burdekin River Hydro Site 5 km downstream of the dam wall; Appendix B, Figure B1) at the upstream and BFD water monitoring stations. Cores and extra grab samples collected in September 2011 post-dated three well above-average water years: 18 TL total discharge in 2007–08, 25 TL in 2008–09 and 28 TL in 2010–11 (all recorded at the Hydro Site gauge; Appendix B, Figure B1). The largest post-dam water year (for discharge) occurred in 1990–91 when a total discharge of 29 TL was recorded at the Hydro Site gauge.

4.3.2. Core characteristics

Gravity cores ranged from 2.5–88 cm in length (median 52 cm) while push cores were shorter overall at 10–43 cm (median 26 cm). The longest cores (>82 cm) were collected from within the channel in the Central and Eastern reservoir and South Burdekin sections of the reservoir. Cores collected from outside of the channel were shorter (median 26 cm) than cores collected from the edge of, or within, the channel (medians of 60 cm and 55 cm respectively). Details for each of the cores and grab samples, including general location within the reservoir and the water depth at the coring site, are summarised in Table 4.1.

Eleven cores were determined to have reached the pre-reservoir surface. This includes seven cores that reached gravel or larger-sized material and/or hard, sticky clay or were collected from drowned riverbanks and contained a dense layer of leaf material at their base, interpreted as material deposited as flooded trees died and dropped all their leaves (described in Cooper et al., 2018 – Chapter 5). Distinct changes in particle-size and/or geochemistry of sub-samples suggested that four more cores were likely to have reached pre-reservoir sediment. The remaining 17 cores and grabs contained only material <2 mm and/or showed no clear evidence of having struck pre-dam material and were interpreted to contain only sediment deposited since the construction of the dam.

Core sediments were not dated, and it was not possible to draw correlations between cores based on particle sizing or distinctively coloured layers. Occasional dark laminations were visible in cores (Figure 4.3c), particularly in organic-rich sediments, but almost all cores were visually homogenous with regards to colour (Figure 4.3b, d), with only large changes in

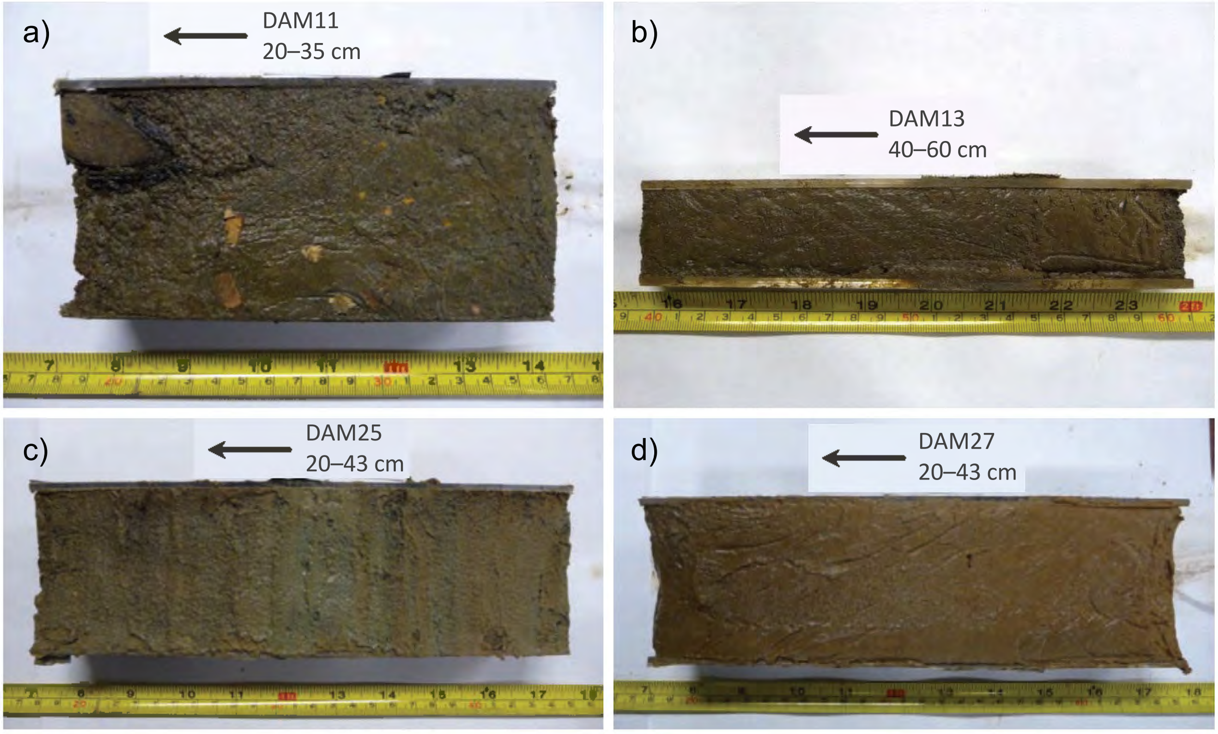

Figure 4.3 Photos of split sections of core from the BFD reservoir: a) push core from site 36, Central Reservoir; b) gravity core from site 32, Central Reservoir; c) push core from site 25, North Suttor; d) push core from site 21, South Suttor. Arrow indicates direction to top of core.

particle size visible. Sandy layers were preserved in a handful of cores but did not produce down-core distribution patterns consistent with a series of large inflow events (see section 4.4.2).

4.3.3. Particle-size analysis

Particle-size distributions of sediment from the BFD reservoir were predominantly unimodal to bimodal (Figure 4.4). The secondary population in bimodal samples was mostly minor, contributing a peak with a mode <4%. Most sediment particles were >0.9 µm and 17% of samples contained particles <0.9 µm; in all but two samples the <0.9 µm component was <3% of the total (core samples *51 - 40 cm*, 10.5% and *44 - 85 cm*, 15.6%). Particles <0.5 µm were found in only six core samples and comprised <0.5% of all but two of those samples (the two exceptions contained 8%–12% of <0.5 µm particles and were from the Eastern Reservoir).

Sediment samples from the North and South Burdekin reservoir cores displayed variable particle-size distributions (Figure 4.4a, b) with the primary modes of sediment from both in and out of the channel varying from 8 to 251 µm. In and out of channel samples from the South Suttor produced distributions with coarse modes (126–400 µm) in all but the shallowest samples (<15 cm, primary mode at 6–8 µm, Figure 4.4c). Core sediments from the North

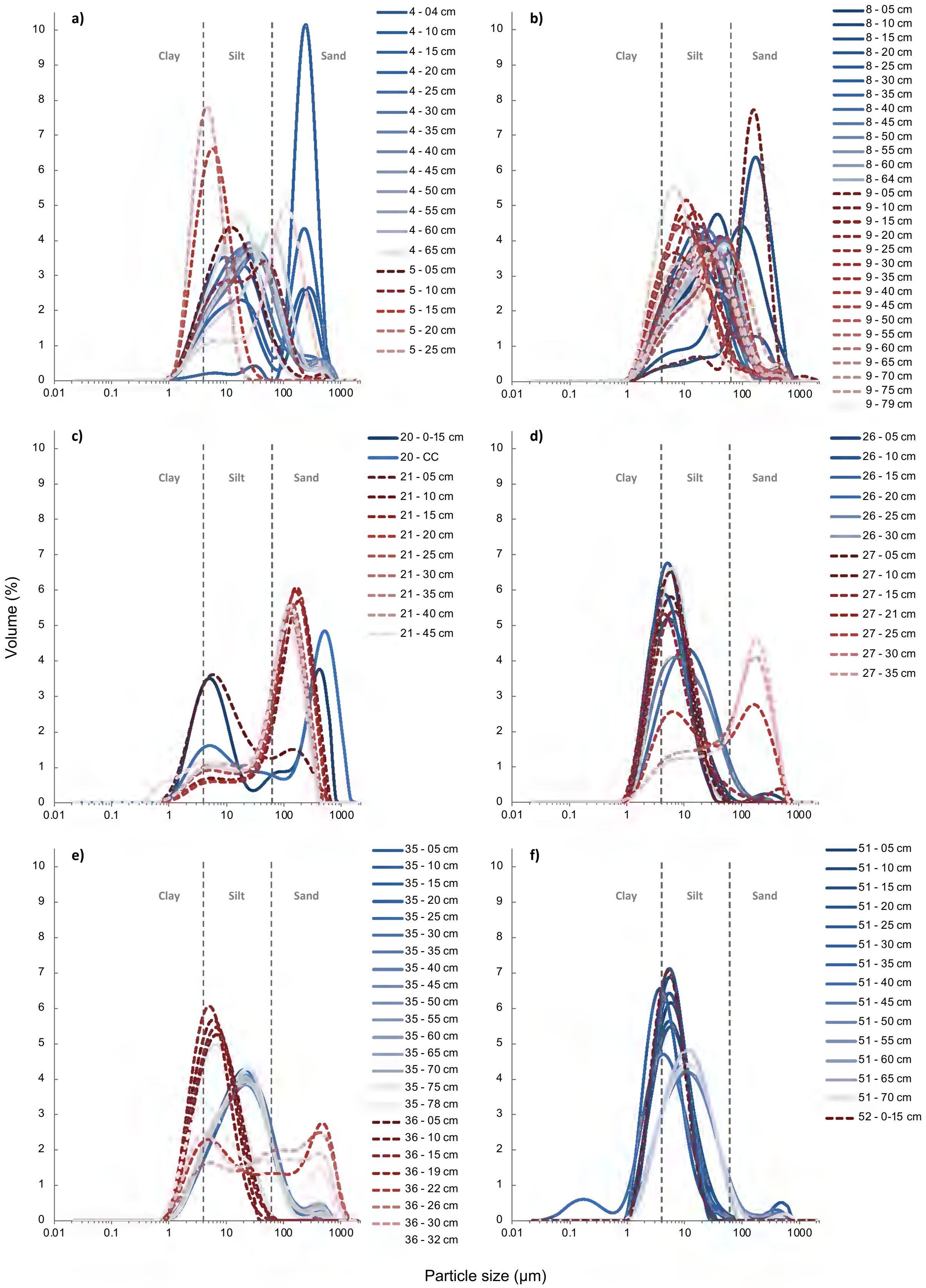

Figure 4.4 Particle-size distributions for samples from selected cores from each section of the reservoir: a) North Burdekin, b) South Burdekin, c) South Suttor, d) North Suttor, e) Central Reservoir, f) Eastern Reservoir. Solid blue lines = samples from cores collected within the river channel; dashed red lines = samples from cores from the outside, or the edge of, the channel. Samples are referred to as 'site - sample depth', e.g., *4 - 04 cm* is a sample from site 4, depth 4 cm. CC = material from the core catcher.

Suttor produced very consistent, unimodal size distributions with modes at 4.5−13 µm except in a few coarse, out-of-channel samples that were classified as pre-dam regolith material (modes of 159−178 µm; see supp. data in Appendix C section C.2 p 187, and section 5.3.2). Likewise, the particle-size distributions of both in- and out-of-channel sediments were very consistent down core in both the Central and Eastern reservoir sections (Figure 4.4e, f). In the Central Reservoir, in-channel sediments were coarser (modes of 17.8−126 µm) than out of channel cores (modes at 4–8 µm). In and out of channel samples from the Eastern Reservoir (Figure 4.4f) produced size-distribution patterns like those for in-channel North Suttor sediments with modes at 3.0–12.6 µm.

Clay, silt and sand size fractions for each sample were plotted on a ternary plot (Figure 4.5). Sediments from both Burdekin sections of the reservoir were relatively high (average 89%) in silt to sand-sized particles and contained <11% clay on average. Sediment from the Central Reservoir was similar in particle size to that from the Burdekin sections (average 88% silt and sand-sized particles) with a small number (7) of samples that had little to no sand (<3%) and a higher clay fraction (26%–37%). Sediments from the South Suttor had ≤ 28% clay and up to 75% sand. Conversely samples from the North Suttor contained <16% sand on average and 2%–49% clay (average 27%). However, samples from within the channel had a maximum of 3.6% sand, while samples from cores collected outside the channel in this section contained up to 89% sand. Almost all (85%) samples from the Eastern Reservoir contained <20% sand (average 8%, dropping to 2% for in-channel samples) and 8%−55% clay. Samples from the North Suttor, South Suttor and Eastern Reservoir sections formed a trend of increasing sand and silt and decreasing clay, but generally had higher proportions of clay than samples of comparable sand content from the Burdekin and Central Reservoir sections (Figure 4.5).

The particle-size distributions of samples from the base of cores interpreted as being of pre-dam regolith (as described in section 5.3.2) followed the same trend of increasing sand and silt and decreasing clay as that formed by the North Suttor, South Suttor and Eastern Reservoir samples (Figure 4.5).

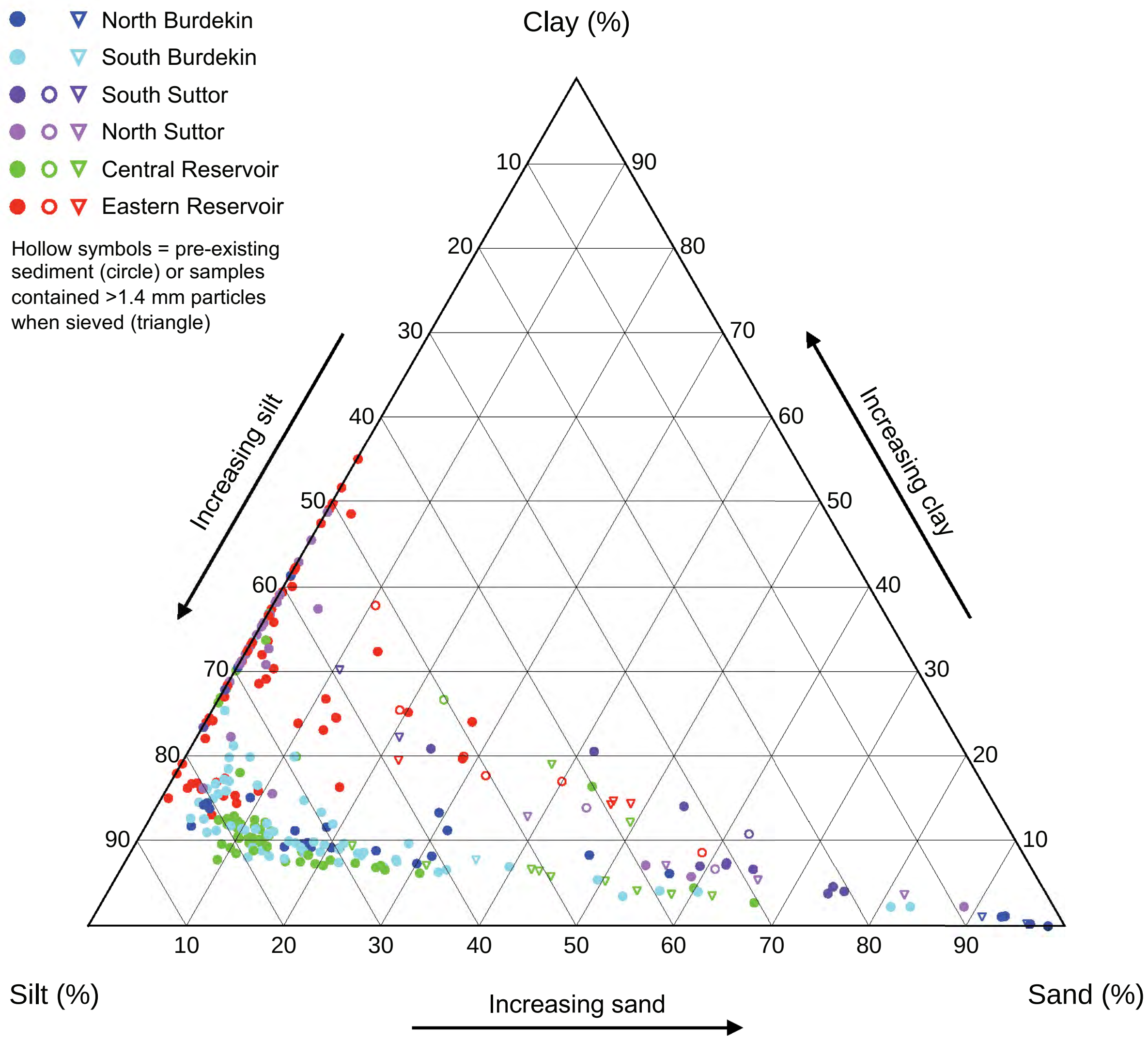

Figure 4.5 Ternary graph indicating the percentage of clay (<3.9 µm), silt (3.9–62.5 µm) and sand (>62.5 µm) in all core and grab sediments. Hollow symbols indicate samples that have been identified as pre-existing sediment (circle) or that contained >1.4 mm particles when sieved prior to laser grainsizing (triangle).

4.3.4. Sediment mineralogy

The minerals identified using XRD in core and grab samples were similar across all sites (Figure 4.6). Every sample contained quartz, muscovite/illite and kaolinite group clays (henceforth referred to as kaolinite) and >95% of samples contained smectite group clays (smectite). All samples also contained alkali and/or plagioclase feldspars. Amphibole minerals were present in 31% of samples, and vermiculite was identified in 42% of samples. A smaller number of samples contained chlorite and goethite (22% and 23% respectively) and phlogopite, a mica associated with ultramafic and/or alkaline igneous rocks, was identified in three samples.

The mineral proportions in samples from the Burdekin sections were variable, with quartz ranging from 14% to 61% and kaolinite from 1% to 52%. Amphibole minerals were predominantly found in Burdekin and Central section sediments (Figure 4.6) and were present in only 18% of samples from the Eastern Reservoir section; a similar distribution was found for vermiculite. Samples from the Burdekin section containing high amounts of quartz did not always produce coarse particle-size distributions (e.g., core *5 - 20 cm*, 61% quartz but a mode of 4–5 μm).

In-channel samples from the Suttor sections had higher proportions of muscovite/illite than samples from out of the channel (median 33% in cf. 10% out, Figure 4.6b). Samples that were higher in muscovite/illite were lower in quartz, with in-channel samples containing 19% quartz (median) and out of channel samples 60% (median). Samples from Suttor sections with coarser particle-size distributions had higher proportions of quartz (e.g., 60%–66% quartz in samples with modes at 112–178 μm). Sample mineralogy proportions varied between cores but were relatively similar for samples from the same core (Figure 4.6b).

Samples from the Central Reservoir had less variable mineralogy than samples from the Burdekin sections (Figure 4.6c). Quartz varied from 13% to 86% but was found in greater proportions in samples from the bottom half of core 36 (62%–86%). These high quartz samples contain almost no muscovite/illite or smectite and were from the same out-of-channel samples that have a very different size distribution (Figure 4.4e) so were designated pre-existing sediment. The mineralogy of in-channel samples was more consistent down core (e.g., core 32, 13%–32% quartz, 37%–51% kaolinite) than in samples from cores on the edge of the channel (e.g., 26%–53% quartz, 12%–40% kaolinite; Figure 4.6c).

The proportions of the four major minerals (quartz, muscovite/illite, kaolinite, and smectite) remained consistent both down core and between in-channel sites in the Eastern Reservoir (Figure 4.6d). Samples from the Eastern Reservoir had higher median values of kaolinite than samples from the other sections (48% cf. 26%–36%) and lower quartz content (median 18%).

Larger proportions of alkali feldspar were observed in samples from upstream areas of the reservoir (median 5%, North Burdekin and South Suttor) compared to the remainder of the reservoir (2%–3%). Samples from the Suttor and Eastern Reservoir sections contained less plagioclase feldspar than samples from the Burdekin and Central Reservoir (3%–6% cf. 8%–10%).

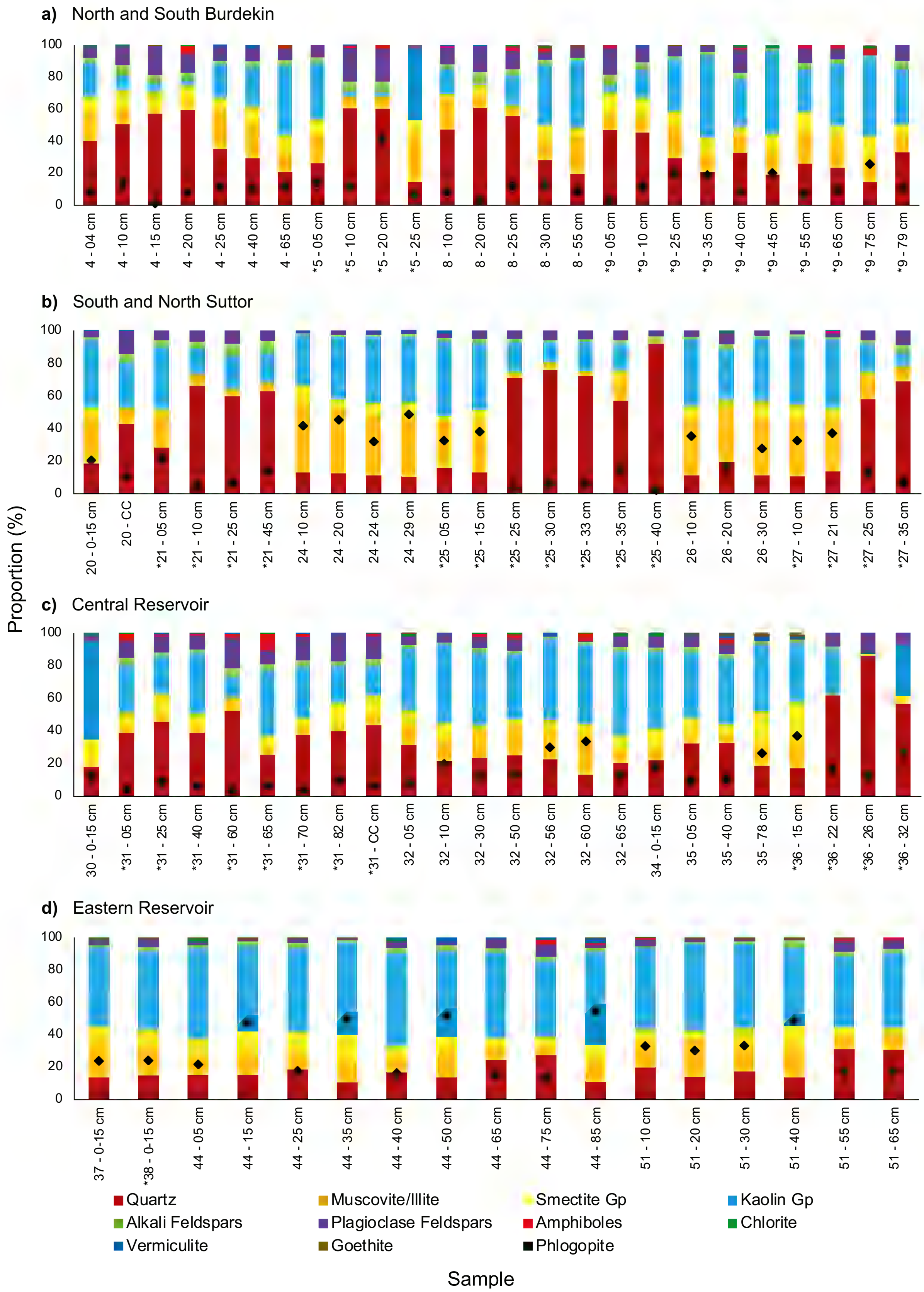

Figure 4.6 Relative proportions of minerals in core sediment and grab samples from the BFD reservoir. Samples are presented in upstream to downstream order. Asterisks indicate samples from out of the channel. Black diamonds indicate percent clay (from granulometry).

4.3.5. Geochemistry of sediments

4.3.5.1. <u>Strontium/Neodymium isotopic results</u>

Benthic sediments were isotopically distinct from SS with higher $^{87}Sr/^{86}Sr$ ratios (0.7211–0.7321), lower Sr concentrations (69–138 ppm) and higher Nd concentrations (32.1–45.4 ppm; Figure 4.7a, b). Suspended sediments had $^{87}Sr/^{86}Sr$ ratios ranging from 0.7138 to 0.7235, higher Sr concentrations (135–433 ppm) and lower Nd concentrations (13.1–34.8 ppm). Detailed results can be found in Appendix C (Table C7).

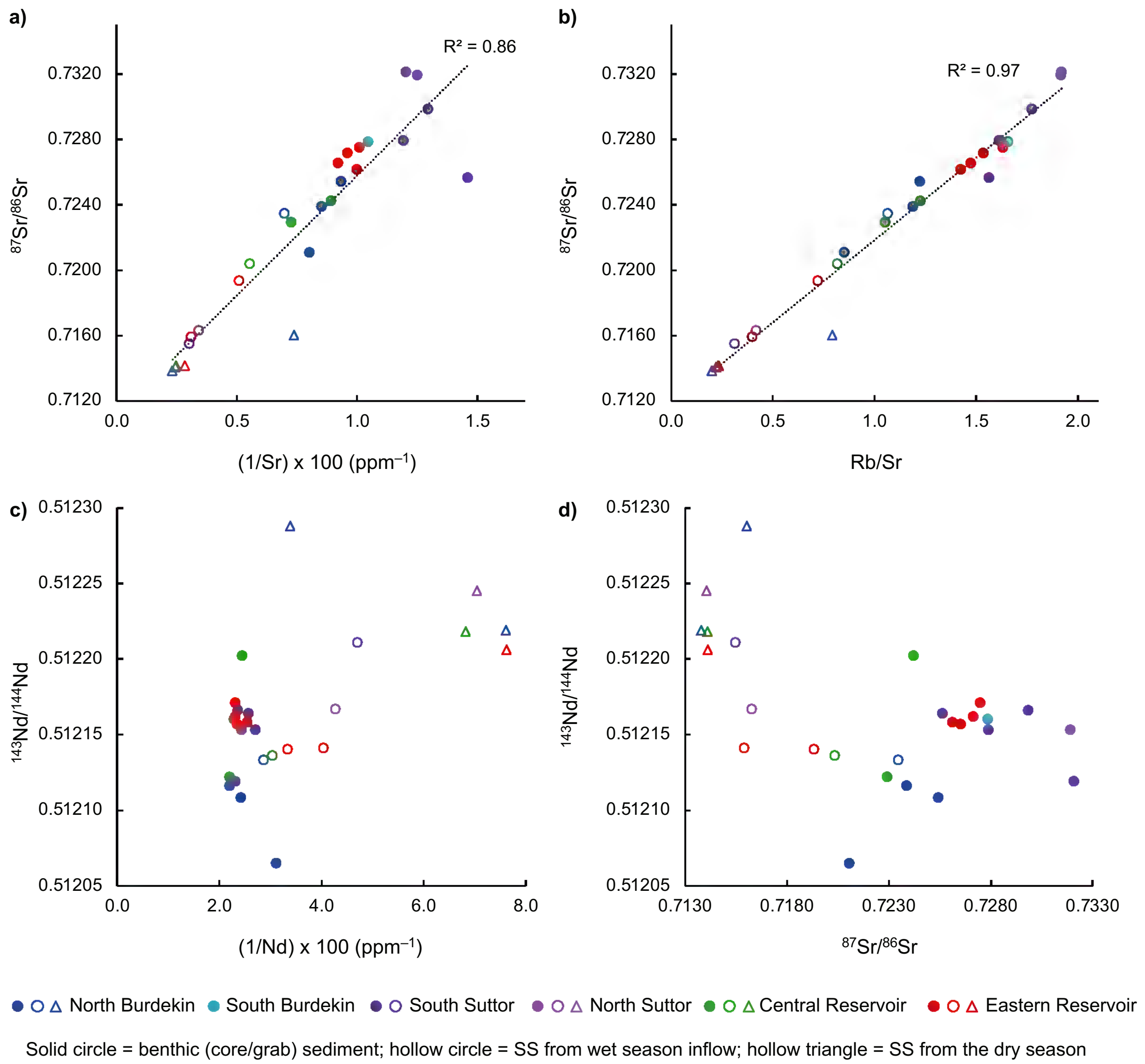

Figure 4.7 a) $^{87}Sr/^{86}Sr$ ratio vs 1/Sr x 100; b) $^{87}Sr/^{86}Sr$ ratio vs Rb/Sr ratio; c) $^{144}Nd/^{143}Nd$ ratio vs 1/Nd x 100; and d) $^{144}Nd/^{143}Nd$ ratio vs $^{87}Sr/^{86}Sr$ ratio for benthic and suspended sediments from the BFD reservoir. Sr and Nd ±2-σ (x10^{-6}) and εNd(0) values can be found in Appendix C (Table C7).

Benthic and SS samples from the BFD reservoir define a Sr isotope mixing line with a strong linear relationship (R^2 = 0.86; Figure 4.7a). Benthic sediments from the Eastern Reservoir define points close to the Sr isotope mixing line (Figure 4.7a) and lie between sediments from the Burdekin and Central Reservoir (lower Sr ratio, higher Sr concentration) and the Suttor section (higher Sr ratio, lower Sr concentration) indicating that the Sr in these samples is a mixture of those two components. The proportion of Sr in the Central and Eastern Reservoir samples that was derived from the Suttor and Burdekin sources was calculated using a simple mixing model (see methods) and is presented in section 4.3.5.3.

Nd data did not exhibit any clear trend (Figure 4.7c). ε^0(Nd) values for all samples were negative (Table D3). Benthic sediment and wet season SS had similar $^{143}Nd/^{144}Nd$ ratios (0.512065–0.512211) but dry season SS displayed slightly higher $^{143}Nd/^{144}Nd$ ratios (0.512206–0.512288).

4.3.5.2. <u>Geochemical determination of end-members</u>

Sr isotopes indicated differences between the two potential sources of sediment to the BFD Reservoir: the Burdekin River, represented by sediment collected from the Burdekin sections, and the combined Suttor, Cape and Belyando rivers, represented by sediment from the Suttor sections. Examination of the geochemical data identified two corresponding end-members (Burdekin and Suttor) for several elements including: Ca, Sr, Cs and Na (Figure 4.8).

Samples from the Burdekin and Central Reservoir sections contained more Sr and less Rb and Cs than samples from the Suttor and Eastern Reservoir sections (medians 96–149 ppm Sr, 158–112 ppm Rb, and 6–11 ppm Cs cf. 69–123 Sr, 76–172 ppm Rb, and 4–14 ppm Cs; Figure 4.8). Samples from the Suttor sections with high Si content (>82%, Figure 4.8c) created outliers with lower Rb (<100 ppm) and Cs (<7 ppm) content.

Concentrations of Ca and Na were higher in North and South Burdekin and Central Reservoir sediments (median 1.1%–1.3% Ca and 1.3% Na) and lower in North and South Suttor and Eastern Reservoir sediments (median 0.5%–0.7% Ca and 0.5%–0.7% Na; Figure 4.8).

4.3.5.3. <u>Contribution of source sediment</u>

A simple mixing model (section 4.2.8) was solved for the percentage contribution of each end-member (Suttor or Burdekin) for several elements, ratios and oxides (Sr, $^{87}Sr/^{86}Sr$, CaO, Cs, Rb; Table 4.2). $^{87}Sr/^{86}Sr$ ratios suggested that samples from the Central Reservoir had a

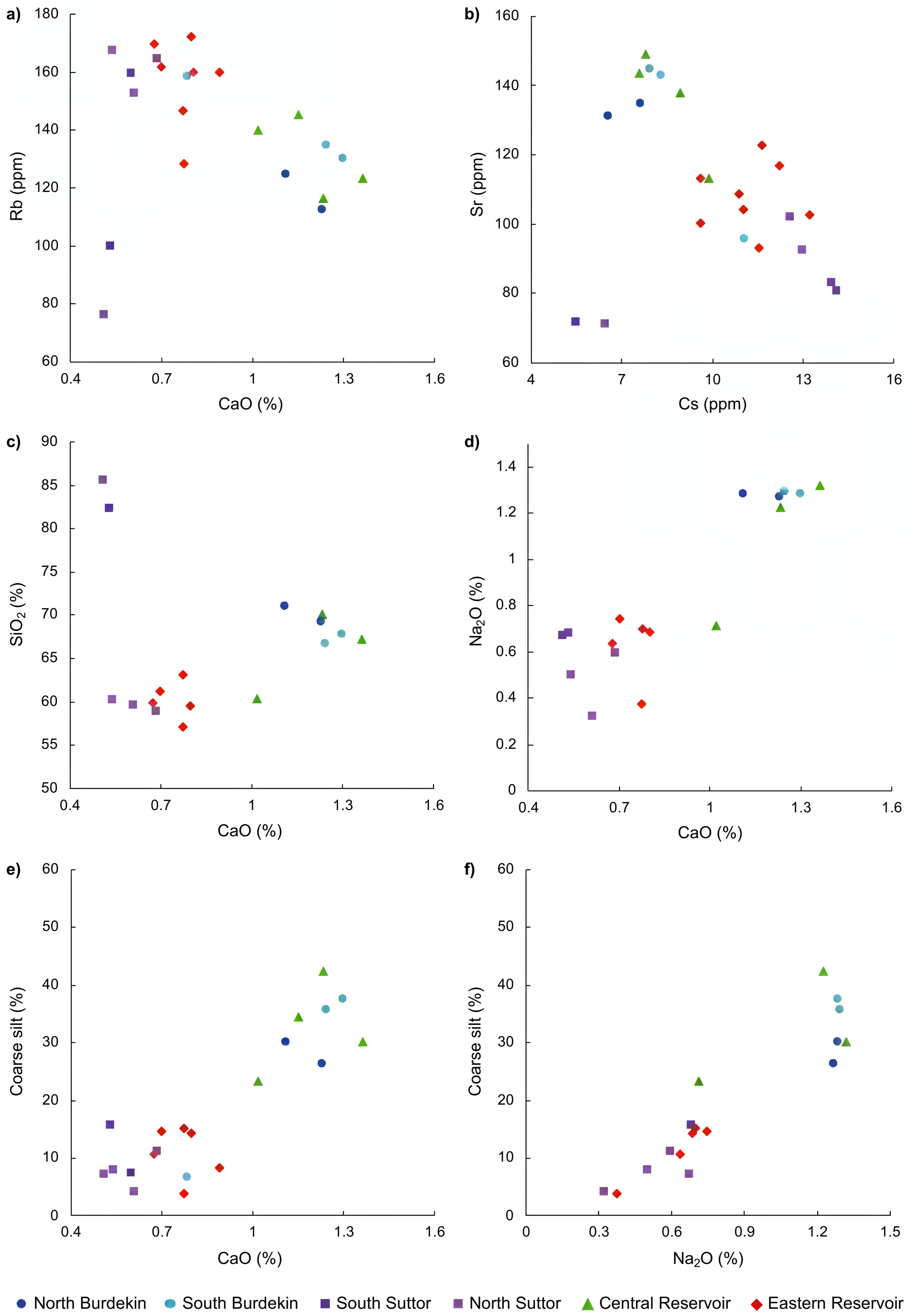

Figure 4.8 Relationship of a) Rb with CaO, b) Sr with Cs, c) SiO_2 with CaO, d) Na_2O with CaO, e) coarse silt (15.6-62.5 µm) with CaO and f) coarse silt with Na_2O in samples from the BFD Reservoir. Data points represent median values for samples from cores from each section of the reservoir and corresponding grab samples.

greater proportion of sediment from the Burdekin source (71%–83%). Samples from the Eastern Reservoir contained a more equal contribution from Burdekin and Suttor sources (46%–58% from the Suttor), however the contribution from the Suttor increased in samples closer to the dam (Table 4.2). Ca and Cs content suggested similar contributions from the Burdekin source to Central Reservoir sediments (55%–87%) and from the Suttor source to the Eastern Reservoir sediments (52%–78%). All the above elements indicated that the contribution to deposited sediments from the Burdekin source decreased as samples got closer to the dam.

Clear end-members were observed for Rb in Suttor and Burdekin sediments (Figure 4.8a) but when the same samples were used to solve the model, estimations of contribution from the Suttor were much higher, exceeding 100% for 3 samples (Table 4.2). This was largely because the Eastern Reservoir samples used contained higher Rb concentrations than the samples used to represent the 'source' material and suggests that the Rb results are not as robust. High percentages notwithstanding, Rb produced a similar trend of increased Suttor contribution with decreasing distance to the dam.

4.4. Discussion

4.4.1. Sediment distribution within the reservoir

Greater accumulation of sediment in the channel compared to the bank indicates that turbidity currents following the relict river channels through the BFD reservoir, coupled with the deeper water over those channels, leads to greater and preferential deposition of sediment within those channels. Although seismic and bathymetry data collected in the reservoir suggest that relict channel features have not been filled or smoothed over by sediment (Cooper et al., 2018 – Chapter 5), the longest cores (60–85 cm) came from within the channel. Density currents will follow the original river channel until the channel has filled with sediments (Fan, 1986). Once the channel has filled with sediment, then the behaviour of turbid flow through the reservoir will likely change as the horizontal flow component would be broadened (van B Weaver & Stone, 1980) leading to greater deposition of sediment outside of the channel. The greater contribution of SS to the reservoir by the Burdekin River (90% of the total; Bainbridge et al., 2014) was reflected in the longer lengths of in-channel cores recovered from the Burdekin sections (median 60 cm) and through the Central and Eastern reservoir sections (median 81.5 m). A similar depth of deposition in and out of the channel in the Suttor section (median 32 cm in vs. 36.5 cm out) may represent easier overtopping by inflow of the narrower channel (~75–250 m c.f. ~190–370 m for the Burdekin River channel within the Burdekin section) within a much wider reservoir area (2–4 km c.f. ~300–400 m). No sediment was observed building up immediately behind the dam wall (Cooper et al., 2018 – Chapter 5) as is often observed in other dams that receive turbid inflow (Annandale, 2006; Samadi & Galay, 2005).

Table 4.2 Estimation of the contribution of sediment from Burdekin and Suttor sources to sediment samples from the Central and Eastern Reservoir using selected elements present in each sample.

Sample	Location	Element	Contribution from Suttor (%)	Contribution from Burdekin (%)
B4-7	Central Reservoir	$^{87}Sr/^{86}Sr$	17%	83%
		Sr (ppm)	-	>100%
		CaO (%)	13%	87%
		Cs (ppm)	43%	57%
		Rb (ppm)	83%	17%
D2-7	Central Reservoir	$^{87}Sr/^{86}Sr$	29%	71%
		Sr (ppm)	28%	72%
		CaO (%)	33%	67%
		Cs (ppm)	45%	55%
		Rb (ppm)	67%	33%
D61	Eastern Reservoir	$^{87}Sr/^{86}Sr$	46%	54%
		Sr (ppm)	55%	45%
		CaO (%)	-	-
		Cs (ppm)	52%	48%
		Rb (ppm)	78%	22%
D59	Eastern Reservoir	$^{87}Sr/^{86}Sr$	50%	50%
		Sr (ppm)	37%	63%
		CaO (%)	55%	45%
		Cs (ppm)	70%	30%
		Rb (ppm)	>100%	-
D58	Eastern Reservoir	$^{87}Sr/^{86}Sr$	50%	50%
		Sr (ppm)	45%	55%
		CaO (%)	68%	32%
		Cs (ppm)	71%	29%
		Rb (ppm)	>100%	-
D1-7	Eastern Reservoir	$^{87}Sr/^{86}Sr$	58%	42%
		Sr (ppm)	57%	43%
		CaO (%)	74%	26%
		Cs (ppm)	78%	22%
		Rb (ppm)	>100%	-

Note: Estimation based on geochemistry of source samples B1-7 (North Burdekin section) and S1-7 (North Suttor section).
'-' indicates that data was not available for that sample.
>100% indicates that the concentration for that element for the combined sample fell outside of the range created by the end-members.

Almost all sediment trapped in the reservoir was >0.5 μm however particles <0.5 μm may be trapped in the reservoir in times of drought, when flow over the dam wall is restricted. This size fraction (<0.5 μm) is predominantly delivered to the reservoir by the Suttor River (Lewis et al., 2013). This study found particles <0.5μm in only six core samples, at percentages of <0.5% in all but two of the samples, supporting the finding of Lewis et al. (2013) that sediment <0.5 μm exclusively passes over the dam spillway, except in years when there is no overflow. Five of the samples containing particles <0.5 μm were in the Eastern reservoir, and two of those samples contained 8%–12% of <0.5 μm particles. It is likely that these samples correspond to times of extremely low inflow into the reservoir such as the 1992–93 water year when water failed to flow over the spillway during the wet season. Sediment particles smaller than 0.9 μm causes persistent turbidity in the reservoir (Cooper et al., 2017 – Chapter 2). While particles <0.9 μm are present in 17% of samples, they contribute <3% of the total of any sample. This scarcity suggests that the conclusion reached by Cooper et al. (2017 – Chapter 2), that resuspension is not the dominant process causing persistent turbidity, remains valid.

4.4.2. Temporal changes recorded in core sediments

Core sediment profiles do not contain a recognisable record of the large flow events that have occurred since the completion of the BFD, e.g. in 1990–91, 2008–09 and 2010–11 (Bainbridge et al., 2012; Fleming & Loofs, 1991; Lewis et al., 2013; Figure 2.2). Dhivert et al. (2015) mapped three major flood events in the Villerest Dam reservoir in France using significant changes in particle size and caesium dating, demonstrating that events could be distinguished even in reservoirs with a short history (26 years, comparable to the age of the BFD). Very fine- to coarse-grained sands (62.5–2000 μm) and gravels (>2mm) characterise the Upper Burdekin river bed around Big Bend (~142 km upstream of the BFD reservoir; Fielding & Alexander, 1996). The above-average flows that have occurred in the BFD reservoir would be expected to transport greater volumes of coarser particles and deposit them further into the reservoir creating identifiable layers (Shotbolt et al., 2005). While an increase in median grainsize was observed in benthic sediments sampled before and after above-average flow events in 2008, 2009 and 2011 (Chapter 3, Figure 3.6) and sandy layers and lamination were preserved in a handful of cores, no distinct layers attributable to those flow events were observable in the sediment cores collected.

Large events are often preserved in reservoir sediment cores as distinctive layers of sand grading upwards into silt and clay (Ambers, 2001; Dhivert et al., 2015). However frequent turbidity currents, such as those observed in the BFD reservoir (Chapter 3), can produce regular sediment layers that are indistinguishable from sediments deposited outside of large flow events (Giovanoli, 1990). Sand was found in cores from the Burdekin sections where particle-size distributions were more variable (Figure 4.4a, b) but the proportions of sand in deposited sediments from the Central and Eastern Reservoir sections remained consistently low (<27% and <18% (in-channel), respectively). Scouring may occur in narrow reaches of a reservoir (Morris & Fan, 1998) so it is possible that large flows have deposited sandy material in-channel in the North and South Burdekin but that the silt–clay fraction that would have deposited on top of that sand has been resuspended and transported downstream by subsequent inflow. Regardless, the consistency of mineralogy (Figure 4.6d) and particle size down-core in the Eastern Reservoir suggest that very coarse material (>1,260 μm) from even the largest flood events does not reach the dam wall. To conclusively correlate sediment from the BFD reservoir with specific flow events would require further analysis of the sediments, possibly using techniques such as Pb dating and diatom records, as were used to document inflow events that deposited sediment over a 20-year period in the Kangaroo Creek Reservoir, South Australia (Tibby et al., 2010).

4.4.3. Spatial variation of sediment characteristics

The differences in particle-size distribution and geochemistry of benthic sediment observed within the reservoir were dominantly spatial and not temporal, with greater differences in geochemistry and particle size observed between locations rather than with depth. All analyses highlighted two populations of sediments that had common characteristics: a population of sediments from the Burdekin and Central Reservoir sections and another comprising sediments from the Suttor and Eastern Reservoir sections. These relationships are documented in the following sections.

Distance from the point at which inflow enters the reservoir determines the bulk particle size of deposited sediment. A decrease in particle size was seen from the northern point of inflow (North Burdekin) to the dam wall (Eastern Reservoir) and a decrease was also seen from the South Suttor to the North Suttor. Coarser particles (>15.6 μm) were found in the North and South Burdekin, South Suttor and Central sections while clay and fine silt-sized particles (<15.6 μm) were dominant in the Eastern and North Suttor sections of the reservoir. When flow enters a reservoir its velocity typically drops and it deposits coarser sediment fractions (Frenette & Julien, 1996). If the reservoir is only partially full, as occurs each year in the BFD reservoir prior to the wet season (Appendix C, Figure C3), sediment will be deposited further into the reservoir (White, 1990). In the Burdekin sections the reservoir is relatively narrow and riverine in nature (Figure 4.1) allowing coarser sediment to be transported further into the reservoir and deposited in the wider Central Reservoir. Although Bainbridge et al. (2014) found that >70% of the SS contributed to the reservoir by the Burdekin River is clay and fine silt (<16 μm), on average core sediment samples from the Burdekin sections contained only 37%–44% of particles that size, suggesting that flows through this section of the reservoir deposit the coarser particles and transport finer material further into the reservoir. While turbidity currents are observed to travel through the reservoir and overflow the dam wall carrying particles of up to 564 μm (Bainbridge et al., 2006b), particles <10 μm dominate wet season flow reaching the wall in average to below-average flow years (Chapter 3).

The greater proportion of silt and sand often observed in out-of-channel sediment samples may represent greater inputs from nearby bank sources coupled with lower levels of deposition of sediment from upstream than occur in-channel. Van B Weaver and Stone (1980) suggested that coarser sediment found in 'quiet water' areas of Howison's Poort Reservoir, South Africa, was contributed to the reservoir by overland flow during storm events; this mechanism could also explain increased amounts of coarse material in sites outside of the river channel in the BFD reservoir. Clay material contributed during these events would remain in suspension and travel further into the reservoir.

Quartz, muscovite/illite, kaolinite and smectite were the predominant minerals present in reservoir sediment. The elemental and mineralogical composition of sediment from the reservoir corresponds to the composition expected for a mix of intensely weathered silicates of varying origin (granites, rhyolites, basalts, metamorphic and sedimentary rocks, Figure 4.2). Kaolinite is typical of well-leached, acid and base-depleted tropical soils and stream sediments (Wilson, 1999). Smectite formation, a stage in the weathering of micas and chlorites to kaolinite and gibbsite, is favoured by poorly drained, mildly alkaline soils, such as those that form on basalts (Borchardt, 1989; Velde & Meunier, 2008). Si, Al and K are the main components of weathered silicates and were found in high concentrations (55%–92%, 3%–28%, <5% respectively) in BFD reservoir sediment. Ca, an element which can be associated with silicates, was found in lower concentrations (<5%).

Mineralogy indicated that sediment deposited in the Eastern Reservoir was dominantly sourced from the Suttor/Belyando/Cape river systems. Samples from the Eastern Reservoir had higher median values of kaolinite than samples from the other sections (48% cf. 26%–36%). Fleming and Loofs (1991) suggested that the Suttor and Belyando River sub-catchments contribute smectite and kaolinite from extensive heavy clay plains with low relief. Bainbridge et al. (2016) showed that SS from the Suttor, Belyando and Cape rivers contain more kaolinite (25%–28%) than SS from the Upper Burdekin River catchment (18%) which is dominated by expandable clays (smectites, 53%) and illite (29%). Sediment from the Suttor sections reflected those proportions containing more kaolinite (median 33%, rising to 38% for in-channel samples) while sediments from Burdekin sections contained less (26%). Median smectite concentrations were similar in sediment from throughout the reservoir (6%–9%), except for the South Suttor (1%) suggesting that the main source of the smectite in Central and Eastern Reservoir sediment was the Burdekin River. Bainbridge et al. (2016) found that BFD overflow sediment reflected the Upper Burdekin's clay mineral signature. This finding coupled with the mineralogical and particle-size data from this study indicates that the fine sediment leaving the reservoir was mostly from the Burdekin River, which dominates reservoir inflow and overflow annually (Bainbridge 2014; Appendix C, Figure C3). While the Suttor/Belyando/Cape rivers contribute relatively lower sediment loads and might be expected to contribute less to the export of SS from the reservoir, these results also suggest that fine sediment from the Suttor remains in the reservoir and contributes to sediment deposits in the Eastern Reservoir. The high quartz content of sediment from the Burdekin and Central Reservoir (median 33%) but low quartz content of Eastern Reservoir sediment (18%) indicates that coarser sediment from the Burdekin was deposited in the Central Reservoir and did not reach the Eastern Reservoir. As a result, the proportion of sediment from the Suttor in Eastern Reservoir sediment increased (discussed further in section 4.4.6).

4.4.4. Fractionation and weathering trends

The mineralogy of BFD reservoir sediment is related to particle size, with less-weathered minerals from the upstream areas of the reservoir associated with coarser particle sizes. Vermiculite forms from the weathering of micas or other Fe- and Mg-rich aluminosilicates like chlorite, hornblende or basalt (Langmuir, 1997) and breaks down to smectites, which in turn weather to kaolinite. Vermiculite was mostly found in Burdekin and Central sediments, as was most chlorite and amphibole (Figure 4.6). Feldspars were found in greater amounts in the North Burdekin and South Suttor sediments (7%–11% and 5% vs. 4% and 2%–3% respectively). Plagioclase concentrations were also higher in South Burdekin and Central section sediments (5%–12%). Samples with a coarser particle-size distribution contained more quartz and feldspar: for example, sediments from core 21 in the Upper Suttor contained 60%–66% quartz and 10%–15% feldspars in samples with primary size distribution modes at 112–178 µm. Coarser material (>15.6 µm) was found in greater concentrations in the Burdekin, South Suttor and Central sections (Figure 4.5). It is likely that in the most upstream areas, coarse sediment is deposited as soon as stream velocity diminishes (Morris & Fan, 1998), which is reflected in the benthic sediment containing lower proportions of kaolinite and smectite (clay-sized) minerals, while less coarse sediment is transported to and deposited in the Eastern Reservoir.

This interesting trend reflects the fractionation and concentration undergone by the sediment as it moves through the reservoir. Sediment transport causes labile mineral grains like feldspars to preferentially be broken down in size and chemically weathered (Bahlburg & Dobrzinski, 2011). High flow, particularly from the Burdekin catchment, can carry coarser, heavier sediment (dominated by quartz), while lighter, finer sediment (dominated by kaolinite and smectite) is able to travel further into the reservoir under lower flow conditions. This sorting leads to the higher proportion of clay minerals observed in Eastern Reservoir and North Suttor sediments. Cracking clay soils predominate throughout the Suttor and Belyando sub-catchments due to the presence of basic igneous rocks and clay-containing sedimentary rocks (Roth et al., 2002) and the deeply weathered geology favours the development of kaolinite, meaning that sediment from the North Suttor and Eastern Reservoir is also more weathered than sediment from the Burdekin and Central reservoir. The greater concentration of Rb in some Eastern Reservoir sediments than in the Suttor and Burdekin sediment end-members (Figure 4.8a) indicates further fractionation towards finer, more clay-rich sediments. This suggests that the fractionation is not just dependent on source but is also complicated by in-reservoir sorting. The lower proportion of kaolinite in the North Suttor, despite the greater overall percentage of fine particles relative to other sections, may indicate the contribution of some mechanically rather than chemically weathered minerals as well as dilution of the average by a few coarser samples (>54% coarse silt and sand, >57% quartz, <18% kaolinite) often collected from outside the channel.

4.4.5. Geochemical character of sediment source

Sediments from the Burdekin sections of the reservoir have a different geochemical signature to sediments from the Suttor sections reflecting their differing catchment sources. All the BFD reservoir sub-catchments are intensely weathered. The Upper Burdekin catchment contains red duplex soils, black and red soils of basaltic origin, sands and sodic duplex soils (Roth et al., 2002). The major clay components of these soil types are kaolinite and smectite with some chlorite and illite (Norrish & Pickering, 1983). Sodic soils have a high Na content and higher Na_2O (>1.2%) was observed in sediment from the Burdekin and Central reservoir sections (Figure 4.8d). The Suttor/Belyando and Cape catchments are characterised by grey/brown clays and red/yellow earths (Roth et al., 2002), soils that contain mainly smectite and kaolinite (Norrish & Pickering, 1983). Compared to the Burdekin section sediments, Suttor sediments contained less alkali and plagioclase feldspars (<6% cf. 8%−10%), minerals that weather to illite, smectite and kaolinite, losing Na, Ca and Sr as they breakdown (Ngon Ngon et al. 2014). In BFD reservoir sediment, Ca and Na also displayed a relationship with particle size, decreasing as the percentage of clay and fine silt increased and increasing as the concentration of coarse silt and sand increased (Figure 4.8e, f). Highly-weathered sediment from the Suttor and Eastern Reservoir sections contained more clay, which led them to contain less Na, Sr, Ca (Figure 4.8b, d). Differences were also observed in the $^{87}Sr/^{86}Sr$ ratios for each section with higher $^{87}Sr/^{86}Sr$ ratios and lower Sr concentrations in Suttor sediment and higher Sr concentrations and lower $^{87}Sr/^{86}Sr$ ratios in Burdekin sediments. The lower $^{87}Sr/^{86}Sr$ ratios in Burdekin sediment probably reflect the contribution from the higher percentage of geologically young basalts in the Upper Burdekin catchment (Figure 4.2), which will have lower Rb/Sr ratios and lower $^{87}Sr/^{86}Sr$ ratios (Faure & Mensing, 2005). The relatively higher $^{87}Sr/^{86}Sr$ ratios in Suttor sediment are also likely to be a function of the higher Sr isotope ratio found in sedimentary material and its greater age (Faure & Mensing, 2005). Two samples from the Suttor formed outliers with respect to Sr, Cs and Rb data. These samples were very high in SiO_2 (>82%; Figure 4.8c) indicating quartz (Si) dilution. The differing geochemical signatures for sediment from the reservoir's sub-catchments allowed sediment from the Burdekin and Suttor to be determined as distinct end-members for several elements (higher Ca, Na and Sr and lower Cs and $^{87}Sr/^{86}Sr$ ratios in the Burdekin, lower Ca, Na and Sr and higher Cs and $^{87}Sr/^{86}Sr$ ratios in the Suttor; Figure 4.8).

4.4.6. Effect of sediment source and character on distribution

Differences in the particle-size distribution of sediments from the two sources to the BFD reservoir lead to greater deposition of sediment from the Burdekin in the Central Reservoir (55%−87%, Table 4.2), while material from the Suttor deposits in the Eastern Reservoir (46%−78%). This trend reflects a decrease in the amount of material deposited by flow from the Burdekin as the flow moves downstream, leading to the systematic increase in the proportion of sediment from the Suttor as sample locations get closer to the dam wall. Sand and silt-sized particles were observed in the sediment deposited in the Central Reservoir, but not in the North Suttor section, suggesting that particles of this size were from the Burdekin, where they were also observed in deposited sediment. Coarse sediment from the Suttor is deposited early in the South Suttor section and only the finer material is transported and deposited downstream. The dominance of the Burdekin as a source of sediment to the BFD reservoir (76–95% in the water years from 2005–06 to 2009–10; Bainbridge et al., 2014) means any deposition of fine material from the Suttor in the Central Reservoir section is diluted. Fine material from both sources travels further towards the dam and is deposited in the Eastern Reservoir section once the reservoir stops overflowing. Despite this, the geochemistry of the sediment deposited near to the dam indicated a greater contribution from the Suttor (>58%). This may be because more of the sediment from the Burdekin exits the reservoir in dam overflow, sediment which was shown to reflect the clay mineral signature of sediment from the Upper Burdekin (Bainbridge et al., 2016). Bedload is unlikely to be a strongly influencing process particularly at the dam wall (Chapter 3) suggesting instead that the Suttor contributes more of the fine material that remains in suspension and deposits slowly after dam overflow has ceased.

The timing and magnitude of inflow contributes to the availability of sediment from each source and potential for deposition within the reservoir. Turbid inflows containing an average of 2.6 million tonnes of sediment enter the BFD reservoir every wet season and form turbidity currents that travel through the reservoir as an interflow (Cooper et al., 2018 – Chapter 5; Chapter 3). In the period between 1987 and 2011, the BFD overflowed every water year but one (1992–93) allowing sediment to exit the reservoir. In most wet seasons (19 of the 24 years to 2011), water entering the reservoir at the beginning of the wet season came from both the Burdekin and Suttor/Cape rivers. However, in most years less water entered the BFD reservoir via the Suttor River as the combined annual discharge from the Suttor and Cape rivers was smaller, (mean annual discharge 2.2 ± 2.6 TL, median 1.2 TL) than that from the Burdekin River (mean 4.3 ± 4.6 TL, median 2.3 TL recorded at the Burdekin River at Sellheim; Chapter 3). In 19 of the 24 years, more than 53% of inflow came from the Burdekin River (Figure S1) and in all but the year it filled (1987) sediment load to the BFD reservoir was dominated by the Burdekin source (median 85%; Cooper et al., 2017 – Chapter 2, Appendix A). As inflow from the Burdekin River continues through the wet season it may carry less sediment because sediment transport in the Burdekin River can be supply limited

(Amos et al., 2004) and because reduced flow leads to deposition of larger particles upstream. As a result, once the dam stops overflowing the sediment remaining in water in the Eastern Reservoir is more likely to be from the clay-particle dominated Suttor source (Bainbridge et al., 2014) and it is this SS that remains behind and may be deposited. Additionally, in some wet seasons (5 of 24, Figure S2) initial flows from the Suttor and Cape rivers occur before flow from the Burdekin. This inflow doesn't always cause the dam to overflow meaning that the sediment transported into the reservoir from the southern catchments is initially trapped and may also be deposited.

The Sr and Nd isotopic data did not indicate the provenance of SS but may indicate the preferential weathering of volcanic and/or sedimentary rocks. Although SS collected during the dry season displayed lower $^{87}Sr/^{86}Sr$ ratios and higher Sr concentrations, it was isotopically homogenous with respect to Sr, which may indicate mixing in the reservoir of the material that remains in suspension throughout the year (Cooper et al., 2017 – Chapter 2). Negative εNd values for all samples indicate that the Nd budget was dominated by rocks that contained recycled crustal material (Faure & Mensing, 2005). Dry season SS displayed slightly higher $^{143}Nd/^{144}Nd$ ratios than benthic sediment and wet season SS (0.512206–0.512288 c.f. 0.512065–0.512211; Figure 4.7b) and were characterised by slightly more radiogenic εNd values (mean -9.0 c.f. means of −9.9 and −10.5 for wet season SS and benthic sediment respectively). Dry season SS from the Burdekin is clay-sized (<0.9 μm) and composed of clay and mica minerals (Cooper et al., 2017 – Chapter 2). River sediments do not generally exhibit any significant grain-size dependent Nd isotopic variability but, in a few river systems, clays can display more radiogenic signatures than associated silts (Bayon et al., 2015). One explanation for the more radiogenic signature of dry season SS is the sorption of Nd from the dissolved load of the river onto clays, because river water tends to have slightly higher radiogenic Nd than corresponding SS in rivers draining mostly sedimentary rocks (Goldstein & Jacobsen, 1987). However, the method used to analyse BFD reservoir samples should have removed the organic component that would host any adsorped Nd.

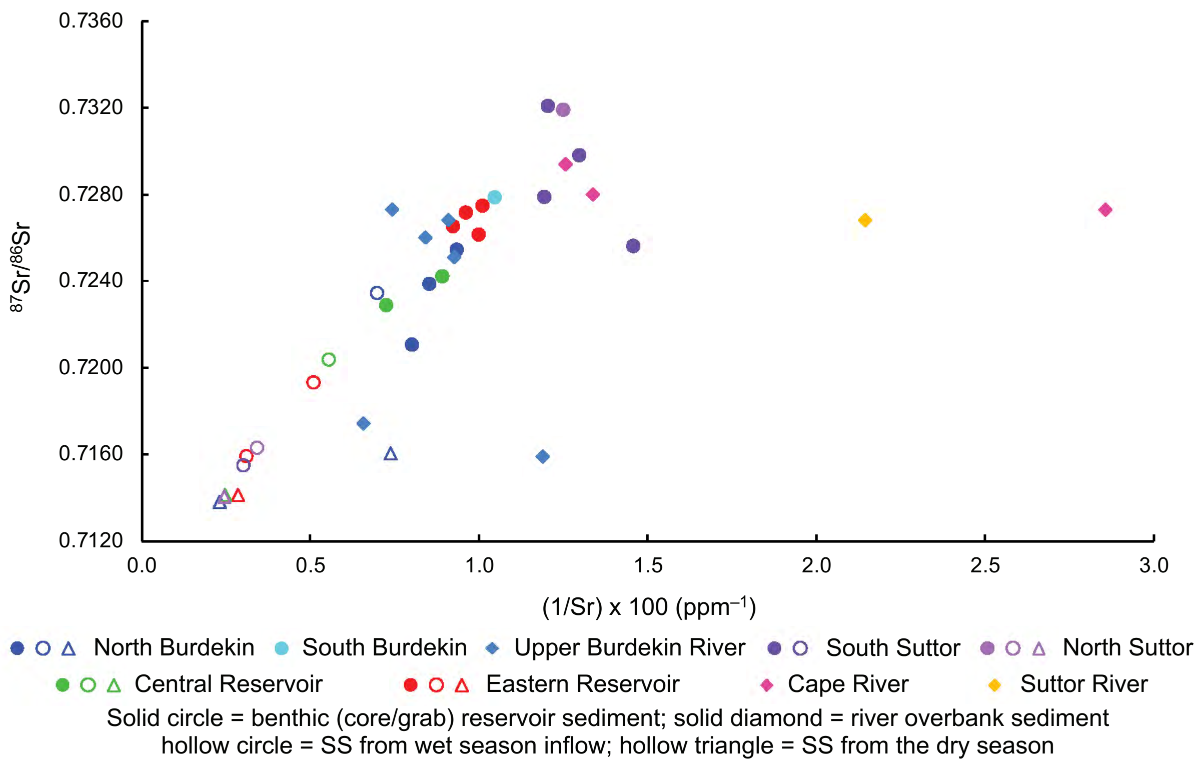

Figure 4.9 $^{87}Sr/^{86}Sr$ ratio vs 1/Sr x 100 for benthic and suspended sediments from the BFD reservoir and overbank sediments from the Upper Burdekin, Suttor and Cape river catchments collected by de Caritat et al. (2022).

Bayon et al. (2015) attribute particle size dependent Nd isotopic variability in clays to preferential weathering of volcanic and/or sedimentary rocks relative to other lithologies during continental weathering, a process that may be occurring throughout the BFD reservoir's catchment.

An effort was made to compare SS data from this study to geochemical data and Sr isotopes for SS collected in the Upper Burdekin (Zoe Bainbridge, unpublished data) but no clear correlations could be drawn. This is because the Bainbridge data was from analysis done on clay separations and only represented the very fine material (<10 µm fraction) present in the SS (Bainbridge et al., 2016) and grainsize exerts a strong control over sediment composition (Collins et al., 2020; von Eynatten & Tolosana-Delgado, 2011). However, a comparison to recently published Sr isotope data from coarse (<2 mm) overbank sediments collected in the Upper Burdekin, Suttor and Cape river catchments (de Caritat et al., 2022) shows good overlap between those sediments and the similarly-sized sediments from this study (Figure 4.9). The overbank sediments are naturally mixed, fine-grained fluvial/alluvial sediments that represent an average of the main soil and rock types contributing sediment from a catchment through weathering (de Caritat et al., 2023). This correlation corroborates the differing geochemistry observed between sediments from the Upper Burdekin and the Suttor and Cape river catchments described in previous sections.

While the geochemistry of the bulk sediment reflects the clear particle size fractionation of SS transported and preferentially deposited in different sections of the reservoir, the use of this bulk fraction to attribute specific source contributions to the deposited sediments has limitations. The fractionation of particle size in the reservoir with the preferential deposition of the coarser sediment particles can present considerable challenges in sediment tracing exercises (e.g., Bainbridge et al., 2024; Gaspar et al., 2022; Laceby et al., 2017), although other studies suggest little influence of particle size on source tracing (B. Fu et al., 2008). Further studies should conduct tracing on the <10 µm fraction and also examine the potential to use elemental ratios to examine the influence of, and potentially better account for, the particle size influence on sediment tracing. Although there is less certainty on the allocation of the proportional contributions from the two upstream river sources from the geochemistry data (considering the sediment monitoring budgets presented in Bainbridge et al., 2014), the data clearly highlight the increasing influence of the Suttor arm on the benthic sediments in the more downstream reaches of the reservoir.

4.5. Conclusions

The differences in geochemistry and particle size observed for sediment core and grab sediments collected in the BFD reservoir were dominantly spatial and not temporal. Although large flow events have occurred since the completion of the BFD, no conclusive evidence of them was found in core sediments from the reservoir. Greater volumes of sediment have been deposited in the relict river channel, but no sediment has built up behind the dam wall. The results of this study largely agreed with the finding of Lewis et al. (2013) that sediment <0.5 µm exclusively passes over the dam spillway, but the presence of some particles of that size in sediments from sites close to the dam wall suggest that these particles can be trapped and deposited in lower velocity and deeper parts of the reservoir in years of extremely low wet season flow, when water does not overtop the dam.

There are two main sources of sediment to the BFD reservoir: the Burdekin River and the Suttor/Belyando/Cape rivers. Sediments from the Burdekin sections of the reservoir have a different geochemical, particle size, and mineralogical signature to sediments from the Suttor sections. Upstream sediments and those from the Burdekin and Central Reservoir were dominated by coarser and less-weathered material while sediments from the North Suttor and closer to the dam wall were finer and contained more mature sediment. The contribution from the Suttor, Belyando and Cape river systems to deposited sediment increases in the samples closer to the dam due to the fine size of the particles transported in flow from those rivers, and to discharge patterns and magnitude. Geochemical models indicate that approximately half the sediment deposited in the Eastern Reservoir comes from the southern rivers via the Suttor River (46%–58%), while most of the sediment deposited in the Central Reservoir came from the Burdekin River system (55%–87%). This trend reflects the fractionation and concentration undergone by the sediment as it moves through the reservoir, however the greater concentration in Eastern Reservoir sediments than in end-member sediments of some elements, such as Rb, suggests that fractionation is not just dependent on source but is also complicated by in-reservoir sorting.

Dry season turbidity in the lake is caused primarily by SS <0.9 μm in size and composed largely of kaolin and smectite group clays and micas. (Cooper et al., 2017 – Chapter 2). This study indicates that both the Burdekin and Suttor rivers contribute the SS that remains in suspension, but the Suttor is likely to contribute a greater portion of this SS as it is contributes a greater proportion of the sediment that deposits in the Eastern Reservoir and is less likely to be carried over the dam wall in overflow.

The geochemical data collected as part of this study provides an environmental baseline for sediment in the BFD reservoir. Additional studies of sediment in the BFD reservoir should focus on dating key sediments through fallout radionuclides, optically stimulated luminescence dating, or diatom records which could determine source variability over time and provide more accurate rates of sediment accumulation. New techniques like high-resolution CT scanning could be used to identify flood layers in sediment cores (Foucher et al., 2020) to investigate the impact of extreme inflow events on sediment transport and accumulation, events that are likely to become more common as the Earth's climate changes.

Chapter 5: Variability of the useful life of reservoirs in tropical locations: A case study from the Burdekin Falls Dam, Australia.

Published as: Cooper, M., Lewis, S. E., Stieglitz, T. C., & Smithers, S. G. (2018). Variability of the useful life of reservoirs in tropical locations: A case study from the Burdekin Falls Dam, Australia. *International Journal of Sediment Research, 33*(2), 93–106. https://doi.org/10.1016/j.ijsrc.2017.11.002

Minor changes have been made for consistency and clarity and to modernise some references. Reviewers will encounter some repetition of information included in the preceding sections of this thesis, particularly in the introduction and methods sections.

Abstract

Large dam construction for irrigation, hydropower, water supply, and flood control in tropical to sub-tropical areas increased markedly after 1950. Many of the dams built during this period have filled with sediment and no longer perform to their original design specifications; in many cases, forecast dam life was greatly overestimated. This study investigates the useful life of Burdekin Falls Dam (BFD), north-eastern Australia and compares the findings with other tropical reservoirs. Using two independent methods it is estimated that between 61 and 65 million m^3 of sediment has been deposited in the reservoir over the 24 years of operation between 1987 and 2011. This sediment volume equates to an average of 0.15% of capacity lost per year since construction was completed. If current sediment loads/climate regimes persist, reservoir capacity will be reduced by 50% after 345 years. However, the useful life of the BFD reduces to just 276 years when drawdown (lowering of the water level) data are considered; these data show reservoir use would be affected once 40% of storage was filled with sediment, with a 60% drawdown return period of 1 in 15 years. When compared to similar large tropical to sub-tropical reservoirs, the BFD has a slightly longer reservoir useful life than dams in India and a much longer half-life than for both similar-sized and larger dams in China, Brazil, and Iran. Properties of the BFD that promote a longer useful life include a lower trap efficiency, relatively low annual sediment load delivered to the reservoir, limited sediment deposition behind the dam wall (and uniform distribution of deposited sediment), and the export of highly turbid annual floodwaters before settling and deposition of any remaining sediment within the reservoir.

Keywords: Reservoir half-life; Lake Dalrymple; Sediment trapping; Trap efficiency; Tropical reservoir; Useful life.

5.1. Introduction

The construction of large (spillway wall >15 m high) dams primarily for irrigation, hydropower, water supply, and flood control markedly increased after 1950 to support rapidly growing human populations (Liu et al., 2013; Syvitski et al., 2022; Syvitski et al., 2005; Vörösmarty et al., 2003; Walling, 2006). Such dams typically have higher sediment trap efficiencies (i.e., higher capacity to inflow ratios) and thus reservoir storage capacity can rapidly decline due to sediment deposition. Sedimentation within many of these reservoirs has been so rapid that they no longer perform to their design specifications (Lahlou, 1996; Palmieri et al., 2001; Pitt & Thompson, 1984; Rãdoane & Rãdoane, 2005; Tamene et al., 2006). For example, the storage capacity of several reservoirs on the Yellow River, China, was reduced 50%–87% within 5–7 years of construction (Zeng & Zhou, 1989). Sediment accumulation in a reservoir is a function of factors including a) reservoir design and operation; b) sediment erosion in the upstream catchment area; c) sediment characteristics including particle size and density; and d) the trap efficiency (TE) of the reservoir which is related to the capacity to inflow ratio, and reservoir shape and age (Brune, 1953; Butt et al., 2010; Nagle et al., 1999; Raudkivi, 1993; Roca, 2012; Verstraeten & Poesen, 2000).

The useful life of a dam is defined as the length of time over which it is safe and operable (Wieland, 2013), and includes the period where sediment deposition reduces storage capacity but does not hamper operations (Frenette & Julien, 1996; Garg & Jothiprakash, 2008; Sumi & Hirose, 2009). Typically reservoirs have a design life of at least 50–100 years (Askew, 1974; Dendy, 1974; Frenette & Julien, 1996; U.S. Bureau of Reclamation, 1987; Vishnoi & Govil, 2007), however, an assessment in 1986 reported the average useful life for reservoirs globally was less than 25 years (Mahmood, 1987). Reservoir half-life is the time taken to reduce capacity by 50% (Morris & Fan, 1998; Murthy, 1977; Pitt & Thompson, 1984), but the reality is that most reservoirs require supplementation or replacement before their half-life has been reached. Understanding the useful life of reservoirs and the factors that influence it is critical to selecting an appropriate location and reservoir design to maximise useful life and economic returns.

The useful lives of reservoirs in Asia, Europe, and North and South America have been investigated, with many studies focussed on reservoirs with extreme sedimentation problems due to large sediment loads delivered from the upstream catchments coupled with relatively high sediment TE (Carvalho et al., 2000; Dendy, 1974; K. D. Fu et al., 2008; Garg & Jothiprakash, 2008; Lee et al., 2022; Rãdoane & Rãdoane, 2005; Roca, 2012). Calculated TE in these studies varied from less than 50% (Lajczak, 1996) to 100% (Shahin, 1993). In comparison, there has been limited research on the useful life of large reservoirs in seasonally dry tropical climates such as in Australia. Many of these reservoirs have relatively high capacity to inflow ratios (>0.5) and hence have high (>70%) sediment TE (Waterhouse et al., 2016). Previous work in Australia has focused on the useful life of small reservoirs (catchment area <100 km^2) in temperate and grassland locations (Chanson, 1998; Chanson & James, 1999) where reservoirs completely filling with sediment has also been documented (Chanson, 2012).

The Burdekin Falls Dam (BFD) is located on the Burdekin River in the seasonally dry tropics of north Queensland, Australia (20.644812°S, 147.139159°E; Figure 5.1). The BFD was constructed to supply the downstream Burdekin River Irrigation Area (BRIA), industry, and to supplement the city of Townsville's water supply (Sunwater Limited, 2024b). The dam was completed in 1987 and its reservoir, Lake Dalrymple, is Australia's 12th largest by capacity with a volume of 1.86 km^3 (Australian National Committee on Large Dams (ANCOLD), 2010). A preliminary scoping study estimated the design life of the BFD would be in the order of hundreds of years assuming that all bedload and 30% of washload sediments were trapped (Fleming, 1981). However, no monitoring data were available at the time to support this assumption and while measured load and TE estimates have since been reported (Lewis et al., 2013) no study has calculated the half-life or useful life of the BFD reservoir since construction. The BFD provides a unique opportunity to investigate the useful life of a large reservoir in a seasonally dry tropical setting, and to contribute to the limited knowledge base for reservoirs in such regions.

In this study the half-life and the useful life of the BFD reservoir are calculated by estimating the total volume of sediment deposition since completion using two independent methods together with historic reservoir drawdown data. (Drawdown is the lowering of the water level in a reservoir and occurs as a result of regular use or for a specific purpose, e.g. dam wall inspection and maintenance.)

5.2. The Burdekin River and the Burdekin Falls Dam

The Burdekin River basin (~130,120 km^2) is situated in north-eastern Australia and 114,220 km^2 (~88%) of the watershed lies upstream of the BFD. The reservoir covers an area of 220 km^2 and receives water from three major sub-catchments formed by the Upper Burdekin, Suttor/Belyando, and Cape/Campaspe rivers (Figure 5.1). The BFD has overflowed every wet season but two since completion (Cooper et al., 2017 – Chapter 2) and has a capacity to inflow ratio of 0.24 (Bainbridge et al., 2014). The Burdekin River is one of Australia's largest rivers by average annual discharge volume (9.18 million ML yr^{-1}) with very high intra- and inter-annual variability, ranging from 0.25 to 54.03 million ML yr^{-1} (Bainbridge et al., 2014; Roth et al., 2002), with greater than 80% of annual rainfall and river discharge occurring during the wet season months, December to April (Lewis et al., 2006; Lough, 1991).

The Burdekin River basin is also the largest contributor of suspended sediment loads (average annual load 3.3 Mt) to the Great Barrier Reef (McCloskey et al., 2021). The relative proportions of sediment export from the catchments above the BFD remain consistent despite variable flow contributions with >75% of the annual mean sediment load delivered from the steep upper Burdekin catchment (average 147 t km^{-2} y^{-1}) and <25% contributed by the southern lowland catchments (averages range from 9 to 17 t km^{-2} y^{-1}; (Bainbridge et al., 2014; Lewis et al., 2013; Roth et al., 2002). Cattle grazing is the dominant land use (90%) in the Burdekin catchment and is the dominant contributor to suspended sediment loads (Dougall et al., 2014).

5.3. Methods

Two independent methods are applied to calculate the volume of sediment deposited in the BFD reservoir since construction to determine its useful life. These include 1) applying annual mean suspended sediment concentration and flow data of the upstream rivers to estimate the amount of incoming sediment load coupled with the sediment TE estimator of Lewis et al. (2013); and 2) extrapolating the depth of deposited sediment in the reservoir using sediment cores. A bathymetric survey within Lake Dalrymple examined sediment accumulation along the pre-dam river channels, providing support for the gravity core data.

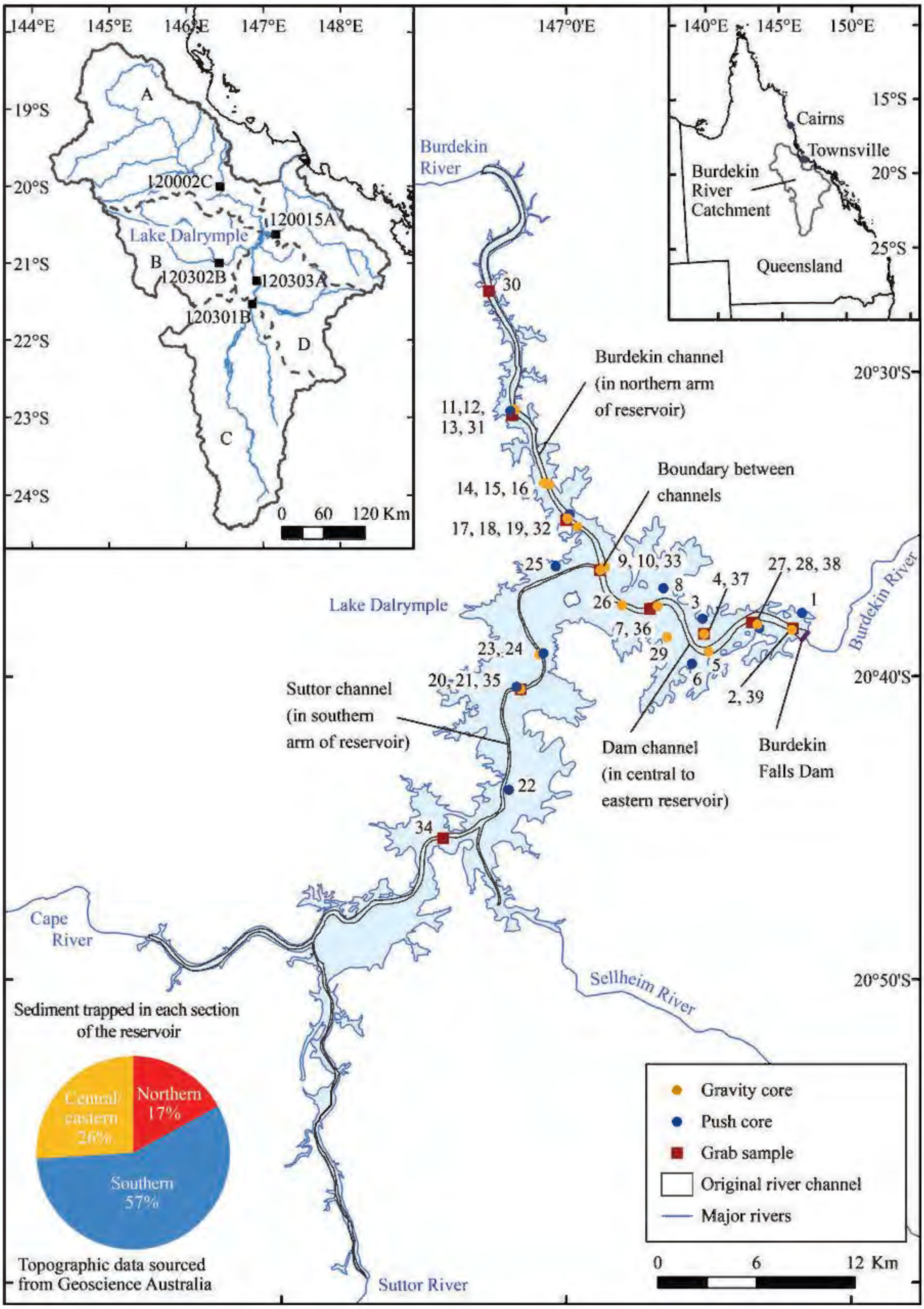

Figure 5.1 Main map: Location of coring and grab sampling sites within Lake Dalrymple, the reservoir of the Burdekin Falls Dam (BFD). Small inset (top right-hand corner): location of the Burdekin River catchment within Queensland, Australia. Large inset (top left-hand corner): location of Lake Dalrymple within the Burdekin River catchment and of water gauging stations: 120002C Burdekin River at Sellheim, 120301B Belyando at Gregory Development Road, 120303A Suttor River at St. Anns, 120302B Cape River at Taemas, and 120015A Burdekin River at Hydro Site. Reservoir sub-catchments are also shown: A, Upper Burdekin River (40,344 km²); B, Cape/Campaspe rivers (20,273 km²); C, Belyando River (35,334 km²); and D, Suttor River (18,143 km²).

5.3.1. Determination of sedimentation volume using calculated trap efficiency

TE is the proportion of sediment delivered by upstream rivers deposited in a reservoir, usually expressed as a percentage (Heinemann, 1981). Importantly, calculated TE can be multiplied by the estimated or measured sediment influx to a reservoir to determine the mass of sediment retained in the reservoir annually. Conversion of sediment mass to volume allows the calculation of the capacity lost in the reservoir over time, which is used to estimate the reservoir's useful life.

The TE of the BFD was measured over the period 2005–2010 which covered a wide range of inflows and sediment loads delivered from different parts of the catchment. Sixty-six percent of the sediment influx was trapped over this period and the range of TE over these water years (1 Oct. to 30 Sept. each year) was 50%–85% (Lewis et al., 2013). Lewis et al. (2013) showed that a modified version (incorporating a daily time step) of the Churchill (1948) equation best predicted the annual TE of the BFD. Lewis et al.’s (2013) equation was used to calculate the annual TE for the water years from 1987–88 to 2014–15. Annual TEs were multiplied by the corresponding annual sediment loads to calculate the mass of sediment trapped by the dam. Annual suspended sediment loads delivered to the dam for the years 1987–88 to 2004–05 (all gauges; Figure 5.1) and 2013–14 to 2014–15 (excluding the Burdekin at Sellheim gauge) were calculated using annual flow gauge measurements (DRDMW, 2021) and the annual mean concentration data from the upstream tributaries measured during the 2005–06 to 2010–11 period. Measured suspended sediment loads for the 2005–06 to 2012–13 years were taken from Lewis et al. (2013; 2005–06 to 2009–10), Turner et al. (2013; 2010–11), and Wallace et al. (2014, 2015; 2011–12 and 2012–13, respectively). Measured suspended sediment loads were only available for the Burdekin at Sellheim gauge for the 2013–14 and 2014–15 years (Garzon-Garcia et al., 2015; Wallace et al., 2016).

The total mass of sediment trapped from 1987 to 2011 (allowing comparison with sediment thickness data) was converted to a volume using sediment density so that the annual mean capacity of the reservoir lost since construction could be determined. The density of trapped sediment was measured using the dry mass of Van Veen grab samples spaced throughout the reservoir and the median used to convert mass to volume (Table 5.1; Figure 5.1). The median density of sediments was calculated using standard equations (Annandale, 1987; Miller, 1953; U.S. Bureau of Reclamation, 1987) and particle-size data (Table 5.1); these standard equations allow the compaction of deposited sediment over time to be taken into account.

Particle-size distributions for grab samples were determined using a Malvern Mastersizer 2000 laser diffraction analyser with a lens range of 0.02–2000 µm. Samples were prepared and analysed using the methods described in Cooper et al. (2017 – Chapter 2).

The equation for fine sediments developed by Gill (1979) was used to provide a comparative reservoir half-life estimate (50% reduction in capacity) because it takes into account the reduction in capacity to inflow ratio as a result of increased sedimentation. Gill's equation uses the pre-compaction median density, calculated using the equation in U.S. Bureau of Reclamation (1987).

The limitations of this approach include the relatively short temporal resolution of the measured load dataset and the assumption of consistent sediment erosion rates over time. The measured TEs that led to the revised TE equation use data from only five years, and the equation is likely to underestimate TE for extreme discharge events as it did for the 2008–09 wet season (Lewis et al., 2013). However, as the measured interval included 1-in-30 to 1-in-50-year flow events in the Belyando/Suttor Rivers (2007–08) and Burdekin River (2008–09; Lewis et al., 2013), respectively, and there has been limited development of the watershed since dam construction the authors are confident that the calculations yield reasonably reliable outputs.

Table 5.1 Average measured dry bulk density and particle-size data for sediment collected by grab sampling. These data were used to calculate sediment density.

Site ID	Location	Date sample collected	Core type	Water depth (m)	Average dry bulk density (kg m^{-3}	Particle size (%)		
						Clay (<4 µm)	Silt (4–62.5 µm)	Sand (62.5–2000 µm)
30	Burdekin	December 2003	Grab	7.5	887	17	77	6
31	Burdekin	December 2003	Grab	15.0	946	23	77	0
32	Burdekin	December 2003	Grab	18.0	812	35	65	0
33	Burdekin	August 2005	Grab	19.0	880	13	80	7
34	Suttor	December 2003	Grab	13.0	876	38	62	0
35	Suttor	August 2005	Grab	19.8	812	37	63	0
36	Dam	August 2005	Grab	23.3	921	19	75	6
37	Dam	August 2005	Grab	11.8	671	32	64	4
38	Dam	August 2005	Grab	25.4	723	32	68	0
39	Dam	August 2005	Grab	28.8	717	35	65	0

Note: See Figure 5.1 for sample locations.

5.3.2. Determination of sediment volume using sediment cores

Eighteen gravity cores and 11 push cores were collected from Lake Dalrymple in August 2011 (Figure 5.1). Gravity cores were collected from within or close to the drowned Burdekin and Suttor river channels in water >3.5 m deep. Push cores were collected from areas outside of these channels in water <10 m deep. All cores were stored and transported in an upright position.

Gravity cores were collected using an 80 kg Ewing Piston Corer mounted on a twin-hulled boat. The corer consisted of a 1 m long metal core barrel with a 10 cm long metal core catcher attached to a weighted head. A hard-plastic inner tube with an internal diameter of 33 mm lined the core barrel. The corer was winched downwards at approximately 20 $cm \cdot s^{-1}$ until a trigger weight caused the corer to drop rapidly when approximately 2 m above the benthic surface. Once penetration ceased the corer was winched back to the boat. The inner tube containing sediment was removed and plugged at both ends and material in the core catcher was collected.

A manual push corer was used to collect push cores. Plastic tubing with an inner diameter of 65 mm and length of up to 1 m was screwed directly onto the core head, which contained a seal activated by a lever. The corer was lowered over the side of the boat and extender rods were progressively attached until the corer was at the required depth. The core tube was pushed into the sediment as far as possible. When core penetration ceased, a rope was pulled to activate the seal before the core was raised to the surface. The internal sample tube was removed and sealed at both ends.

The Burdekin River channel upstream and downstream of the reservoir largely contains silt, sand, and gravel (Alexander & Fielding, 2006) and this was also true of the now-flooded areas of the river channel in the reservoir prior to dam construction; sandy bedforms are clearly seen in aerial photos taken while the dam was under construction (Figure 5.2). The Suttor River channel upstream of the reservoir is braided and vegetated but pre-dam aerial photography shows that the Suttor River channel also contained sand bars and bedforms. Drawing on this information, the following assumptions for the core-based approach to estimate sediment volume were made:

1. Cores that reached gravel or larger-sized material and/or hard, sticky clay were deemed to have reached the pre-reservoir surface. In the few cases where the corer

managed to penetrate this surface, core lengths were adjusted to reflect the sediment that had been deposited after dam construction.

2. Cores collected from the drowned riverbanks occasionally contained a dense layer of leaf material and plant roots at their base; this layer was interpreted as the material that was deposited in the reservoir when submerged trees died and dropped all of their leaves and was preserved in the anoxic bottom water (Faithful & Griffiths, 2000). This was also used as an indication of having reached the pre-dam surface and core lengths were adjusted accordingly.
3. Cores that contained only mud and/or showed no clear evidence of having struck pre-dam material were interpreted to contain only sediment deposited since the construction of the dam and the full length of the core was considered in the calculations. The mud in these cores was relatively homogenous and similar to the mud clearly deposited above the pre-flooding surface collected elsewhere.

Details of sediment cores, including the length adjusted to remove the contribution of pre-dam sediment where inferred, are listed in Table 5.2.

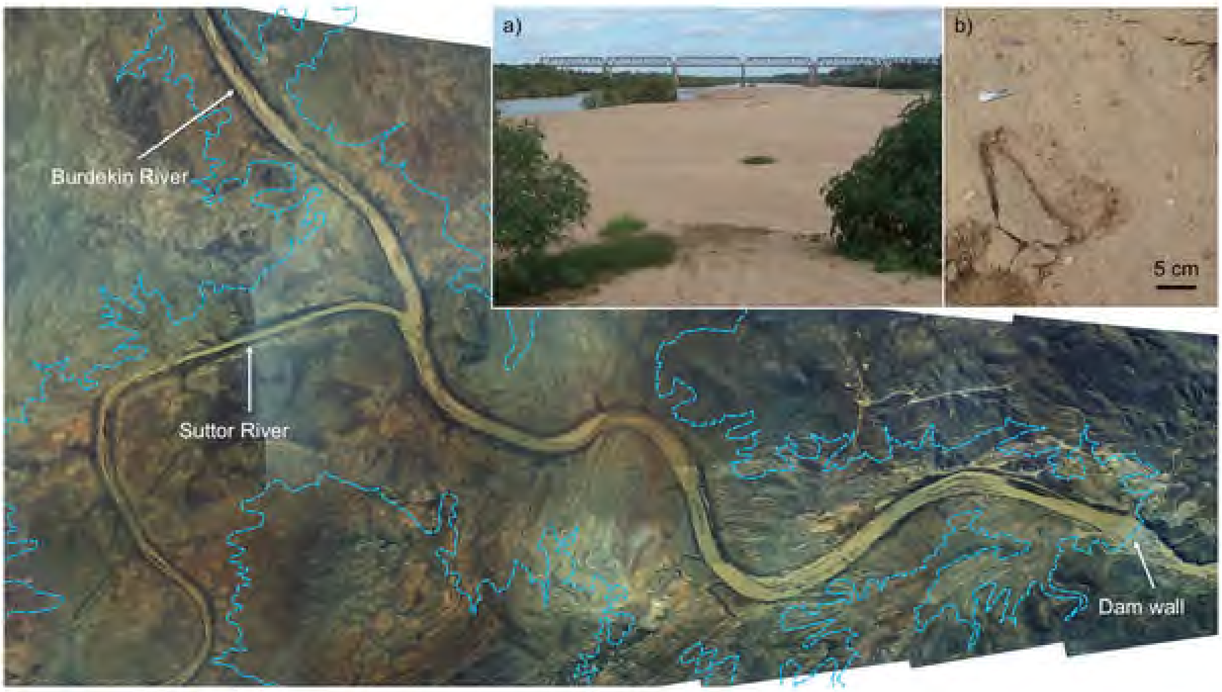

Figure 5.2 Aerial photograph of the Burdekin and Suttor Rivers taken while the BFD was under construction. The dotted line outlines the reservoir. Inset: a) view downstream within Burdekin River channel at the Macrossan Bridge over the Flinders Highway (approx. 100 km upstream of the reservoir), b) Photo of sediment within the channel at the location shown in (a) showing silt, sand, and gravel sized particles overlain with a ~1 mm layer of fine sediment. Inset photos taken by M. Cooper, May 2006.

Table 5.2 Details of core samples collected in the BFD reservoir, Lake Dalrymple.

Site ID	Location	Co-ordinates (decimal degrees)		Date collected	Water depth (m)	Core type	Adjusted sediment depth (cm)*	Relation to channel
1	Dam	-20.632086	147.137673	Aug 2011	3.0	Push	2	Out
2	Dam	-20.641274	147.131612	Aug 2011	32.0	Gravity	71	In
3	Dam	-20.635326	147.079587	Aug 2011	7.0	Push	10 (12)	Out
4	Dam	-20.643734	147.080419	Aug 2011	13.0	Gravity	2.5	Out
5	Dam	-20.653348	147.083097	Aug 2011	27.5	Gravity	88	In
6	Dam	-20.659920	147.073360	Aug 2011	9.2	Push	26	Out
7	Dam	-20.628219	147.053377	Aug 2011	25.0	Gravity	81	In
8	Dam	-20.618459	147.056689	Aug 2011	6.4	Push	20 (15)	Out
9	Dam	-20.608466	147.019929	Aug 2011	18.6	Gravity	85	In
10	Dam	-20.606885	147.022430	Aug 2011	21.0	Gravity	82	In
11	Burdekin	-20.521076	146.968335	Aug 2011	19.4	Gravity	30	In
12	Burdekin	-20.520975	146.969949	Aug 2011	6.5	Gravity	67	In
13	Burdekin	-20.521620	146.967300	Aug 2011	6.2	Push	25	Out
14	Burdekin	-20.560660	146.986922	Aug 2011	19.0	Gravity	66	In
15	Burdekin	-20.561220	146.989483	Aug 2011	13.5	Gravity	82	In
16	Burdekin	-20.561600	146.990073	Aug 2011	3.5	Gravity	60	In
17	Burdekin	-20.577730	147.002044	Aug 2011	2.7	Push	43	Out
18	Burdekin	-20.580224	147.000916	Aug 2011	20.0	Gravity	16	In
19	Burdekin	-20.584666	147.006562	Aug 2011	20.0	Gravity	44	In
20	Suttor	-20.673772	146.973312	Sept 2011	22.2	Gravity	31	In
21	Suttor	-20.672494	146.971075	Sept 2011	8.4	Push	43	Out
22	Suttor	-20.729289	146.966423	Sept 2011	3.7	Push	43	Out
23	Suttor	-20.654864	146.984225	Sept 2011	22.9	Gravity	33	In
24	Suttor	-20.654287	146.986602	Sept 2011	8.3	Push	30 (7)	Out
25	Suttor	-20.606543	146.993903	Sept 2011	7.0	Push	19 (3)	Out
26	Dam	-20.627840	147.032496	Sept 2011	22.0	Gravity	41	In
27	Dam	-20.640326	147.112686	Sept 2011	8.1	Push	26 (1)	Out
28	Dam	-20.638379	147.111498	Sept 2011	18.5	Gravity	19 (3)	Out
29	Dam	-20.645471	147.058809	Sept 2011	13.0	Gravity	24	Out

Note: Burdekin = the Burdekin River (northern) arm of the reservoir, Suttor = the Suttor River (southern) arm of the reservoir, Dam = the central and eastern sections of the reservoir (see Figure 5.1).
*Core lengths were adjusted to remove pre-dam sediment where it was inferred (see section 5.3.2). The length by which a core was reduced is listed in brackets.

The length of cores and their locations were used to calculate a total volume of sediment deposited in the reservoir since construction. The areas of the channels that lie within the reservoir, as mapped on the pre-reservoir Glendon (8356), Harvest Home (8256), and Ravenswood (8257) 1:100 000 topographic map sheets (Australia Division of National Mapping, 1973, 1975a, 1975b), were calculated by digitising the channels using GIS software. The total channel area was divided into three sections (Figure 5.1): Burdekin River (above the confluence with the Suttor River); Suttor/Cape River (upstream of the confluence), and Dam (channel downstream of the confluence, within the eastern section of the reservoir). Cores were classified as in or out of the channel using water depth at the core site, the bathymetry, and topographic maps. Median depth of sediment deposition was calculated for each of the three 'in channel' sections because of the varying lengths of core retrieved from these areas (16–88 cm; Table 5.2). A single median sediment depth was calculated for the whole out-of-channel area due to the more consistent values of sediment deposition recorded throughout the reservoir in non-channel areas (range 2–43 cm; Table 5.2). Median sediment depths were converted to volume using the respective areas for each section.

This method was limited by the number and location of the cores collected. There were only two successful gravity cores from five attempts in the southern arm and they were similar in length to the push cores that were collected from that arm (~30 cm). Additionally, because cores from the southern arm were only collected in the most downstream areas (samples 20–25, Figure 5.1), the average depth of sediment deposition required extrapolation to the remainder of the southern arm.

5.3.3. Bathymetric data acquisition & analysis

Multibeam bathymetry mapping of the reservoir was undertaken from 16–21 February 2004. At the start of the survey, water was flowing 94 cm over the dam spillway, decreasing to 63 cm at completion. Multibeam mapping was undertaken using a RESON SeaBat 8101 echosounder operating at 240 kHz, mounted on a 5 m twin hull catamaran cruising at 4–5 knots along survey lines of 2–3 km in length. The multibeam echosounder has a circular array of 101 beams with an along-track and across-track beam angle of 1.5° to provide a 150-degree swath coverage. Vessel track and heading were concurrently recorded with a digital global positioning system (DGPS) receiver and gyrocompass, and the motion of the vessel was recorded with a motion sensor mounted at the vessel's centre of gravity.

Bathymetric data were processed using *SwathEd* (Ocean Mapping Group of the University of New Brunswick, Canada) software and IVS Fledermaus geo-spatial processing and analysis software. Salinity, temperature, and depth were used to calculate a sound velocity profile in the reservoir. Dynamic sensor offsets were calculated with a small scale (patch) test near the dam wall. Sonar ranges were converted to depth by integrating the range, GPS, heading, and motion data whereby the acoustic data were corrected for refraction using sound velocity profiles representative for water conditions at the time of data collection. Raw soundings were reduced to a bathymetry grid with a horizontal resolution of 1 m, and data were weighted by beam number giving preference to inner beam data. Small artefacts due to imperfect correction of vessel motion were present in the resulting bathymetry data.

Data were collected along and across the Burdekin River's original channel. In most instances, cross-channel transects were not possible because standing timber remaining in the reservoir restricted safe navigation outside of channel boundaries (especially in the southern arm) and due to the narrowness of the northern arm (Figure 5.1). The slow speed of the vessel and the limited availability of equipment and personnel meant that only the central to eastern section of the reservoir could be surveyed. As a result, it was not possible to use this technique to estimate the volume of sediment in the dam; it was instead used to validate the sediment core data.

5.3.4. Dam capacity data analysis

The daily storage volume of the BFD reservoir was examined from 1987 to 2016. The lowest volume recorded in each water year was tabled and arranged in order of magnitude (lowest to highest; Table 5.3). The return period (estimated time interval between events of a similar size or intensity) and annual exceedance probability (probability that a particular capacity minimum will occur in any given year) were calculated using the method in Salas et al. (2014) allowing the frequency of the lowest annual volumes to be determined and used to set a useful life capacity.

5.4. Results

5.4.1. Method 1: Sediment load and TE data

The average annual TE calculated using Lewis et al.'s (2013) modified Churchill equation for all water years between 1987–88 and 2014–15 was 71%. The total amount of sediment trapped in the reservoir from 1987–88 to 2014–15 was 73 million t; to 2010–11, 68 million t was trapped (timeframe reduced to allow comparison with the sediment thickness method; see Appendix D, Table D1). The median measured dry bulk density of sediment samples was 844 kg m^{-3} (range 670–946 kg m^{-3}). Median calculated densities (using particle-size data) were 902 kg m^{-3} (range 850–1058 kg m^{-3}) for pre-compaction sediments and 1045 kg m^{-3} (range 1005–1165 kg m^{-3}) for sediments after 24 years (through 2011). Calculated density that compensated for compaction was preferred to measured density and was used to calculate that

Table 5.3 Minimum capacity recorded in the BFD reservoir since construction.

Water year	Date of minimum volume	Storage level (m AHD)*	Storage volume (ML)	Storage volume (%)	Magnitude ranking	Return period in years	Annual exceedance probability (%)
1987–88	9-Nov-87	144.55	564021	30.32	-	-	-
1993–94	31-Jan-94	146.40	744226	40.01	1	29.00	3.4%
2015–16	4-Jan-16	146.79	743807	40.16	2	14.50	6.9%
1992–93	30-Sep-93	148.06	926929	49.83	3	9.67	10.3%
2002–03	12-Feb-03	148.24	905815	48.91	4	7.25	13.8%
2005–06	14-Jan-06	149.04	1005593	54.29	5	5.80	17.2%
1994–95	26-Jan-95	149.45	1079582	58.04	6	4.83	20.7%
2014–15	30-Sep-15	149.89	1121778	60.57	7	4.14	24.1%
2003–04	13-Dec-03	149.90	1122500	60.61	8	3.63	27.6%
2013–14	30-Jan-14	150.06	1145757	61.86	9	3.22	31.0%
2004–05	11-Dec-04	150.09	1149840	62.08	10	2.90	34.5%
1996–97	10-Dec-96	150.19	1173453	63.09	11	2.64	37.9%
1995–96	20-Nov-95	151.33	1380017	74.19	12	2.42	41.4%
2009–10	1-Jan-10	151.46	1361727	73.52	13	2.23	44.8%
2006–07	23-Jan-07	151.57	1380842	74.55	14	2.07	48.3%
1997–98	14-Dec-97	151.64	1435500	77.18	15	1.93	51.7%
2001–02	17-Nov-01	151.68	1441927	77.52	16	1.81	55.2%
2012–13	24-Jan-13	151.94	1445821	78.06	17	1.71	58.6%
1991–92	7-Feb-92	151.96	1492282	80.23	18	1.61	62.1%
1999–00	7-Nov-99	152.12	1521756	81.81	19	1.53	65.5%
1990–91	25-Dec-90	152.29	1551974	83.44	20	1.45	69.0%
2000–01	30-Sep-01	152.56	1600395	86.04	21	1.38	72.4%
2007–08	5-Dec-07	152.71	1587913	85.73	22	1.32	75.9%
1998–99	30-Sep-99	152.78	1639995	88.17	23	1.26	79.3%
1989–90	10-Nov-89	152.86	1654181	88.93	24	1.21	82.8%
2008–09	27-Nov-08	152.90	1624470	87.71	25	1.16	86.2%
1988–89	20-Nov-88	152.98	1676654	90.14	26	1.12	89.7%
2011–12	1-Dec-11	153.01	1647373	88.94	27	1.07	93.1%
2010–11	1-Oct-10	153.76	1801025	97.24	28	1.04	96.6%

The minimum capacity of 30.3% observed in the 1987–88 water year was excluded from probability calculations as this is the year in which the reservoir first started to fill. Capacity data obtained from the then Queensland Department of Natural Resources and Mines (V. Manley, personal communication, 1 August 2016; October 1987–July 2002) and Sunwater Limited ACN 131034985 (M. Ali, Bureau of Meteorology, personal communication, 25 July 2016; July 2002–July 2016).
Note that there is slight difference in the storage volume to storage level relation between sources.
*AHD = Australian Height Datum; the mean sea level for 1966–1968 was assigned a value of 0.000 m AHD

65 million m^3 of sediment was deposited in the reservoir over the 24-year period (i.e., 1987–88 to 2010–11; Table 5.4). This equates to a capacity reduction of 3.5%. Without detailed data covering the whole reservoir and identifying deposition hotspots, it might be assumed that sediment was deposited evenly over the 220 km^2 area, making the mean depth

of the sediment in the reservoir 30 cm, an average of 1.2 cm yr^{-1} (Table 5.4). This method could be improved over time by incorporating additional load data collected in the Burdekin catchment.

5.4.2. Method 2: Post-construction sediment thickness using sediment cores

Post-dam sediment deposits collected in cores varied between 2 and 88 cm thick. All 11 push cores and two gravity cores were collected from outside of the river channel and sediment recovered had a median thickness of 24.5 cm. The thickness of deposits typically decreased with distance from the drowned river channel. Depth of sediment in push cores from the southern arm increased with distance from the dam wall, ranging from 43 cm at the most upstream site (site 22) to 19 cm at the site furthest downstream (site 25; Figure 5.1). Push cores collected in the northern arm showed the opposite trend; cores closer to the dam wall had thicker post-dam sediment deposits (from 25 cm upstream at site 13 to 43 cm downstream at site 17). Sediment depth was <30 cm in all cores collected in the out-of-channel areas of the central/eastern section of the reservoir.

The combined areas of the drowned river channels within the reservoir totalled 27 km^2 (Burdekin channel 9 km^2, Suttor channel 12 km^2, Dam channel 6 km^2). The thickness of sediment deposited in the channel post-dam construction varied from 16 cm (site 18) to 88 cm (site 5; Figure 5.1, Table 5.2). All cores with >60 cm of sediment were collected from within the channel in the northern and central/eastern sections of the reservoir; the two gravity cores in the southern section each contained ≤33 cm of sediment (Table 5.2; Figure 5.1).

Core samples indicate that a total volume of 61 million m^3 of sediment was deposited in the reservoir between 1987 and September 2011 (Table 5.4). This equates to a capacity reduction

Table 5.4 Calculation of the total volume of sediment entering the dam over the 24-year period 1987–2011.

	Median measured dry bulk density	**Median calculated density after 24 years**	**Core-based calculation**
Density (kg m^{-3})	844	1039	N/A
Volume of sediment entering dam (m3)	80 x 10^6	65 x 10^6	61 x 10^6
Average depth deposited (m)	0.37	0.30	0.28
Deposition depth per year (cm)	1.5	1.2	1.2
Percentage of reservoir filled	4.3	3.5	3.3
Percentage of reservoir filled per year	0.18	0.15	0.14
Years to fill dam 50%/100%	279/557	345/690	363/727

Note: Calculated density takes compaction into consideration.

of 3.3% since construction. More sediment was deposited within channels, but the channel makes up only 12% of the total reservoir area. If it is again assumed that this sediment volume was deposited evenly over the 220 km^2 area then the mean depth of the sediment in the reservoir would be 27.9 cm, or accumulation equal to 1.2 cm yr^{-1}. Using maximum in-channel depths for each area (Burdekin, 82 cm; Suttor, 33 cm, Dam, 88 cm) and the out-of-channel median for the remainder of the reservoir would only increase average sediment depth to 29.1 cm (still an average of 1.2 cm yr^{-1}). This method would be greatly strengthened by the collection of additional cores from the reservoir.

5.4.3. Geophysical survey

Bathymetric data were collected from an area of 9.78 km^2 (4% of the reservoir; Figure 5.3). In the surveyed area the benthic surface is 24–34 m below the water surface in drowned river channels but shallows to just 4 m elsewhere. Bathymetric data clearly depict small-scale pre-dam features such as small creeks and gullies visible in aerial photographs taken prior to dam construction (Figure 5.2), suggesting that limited sediment deposition (i.e., <1 m) has occurred.

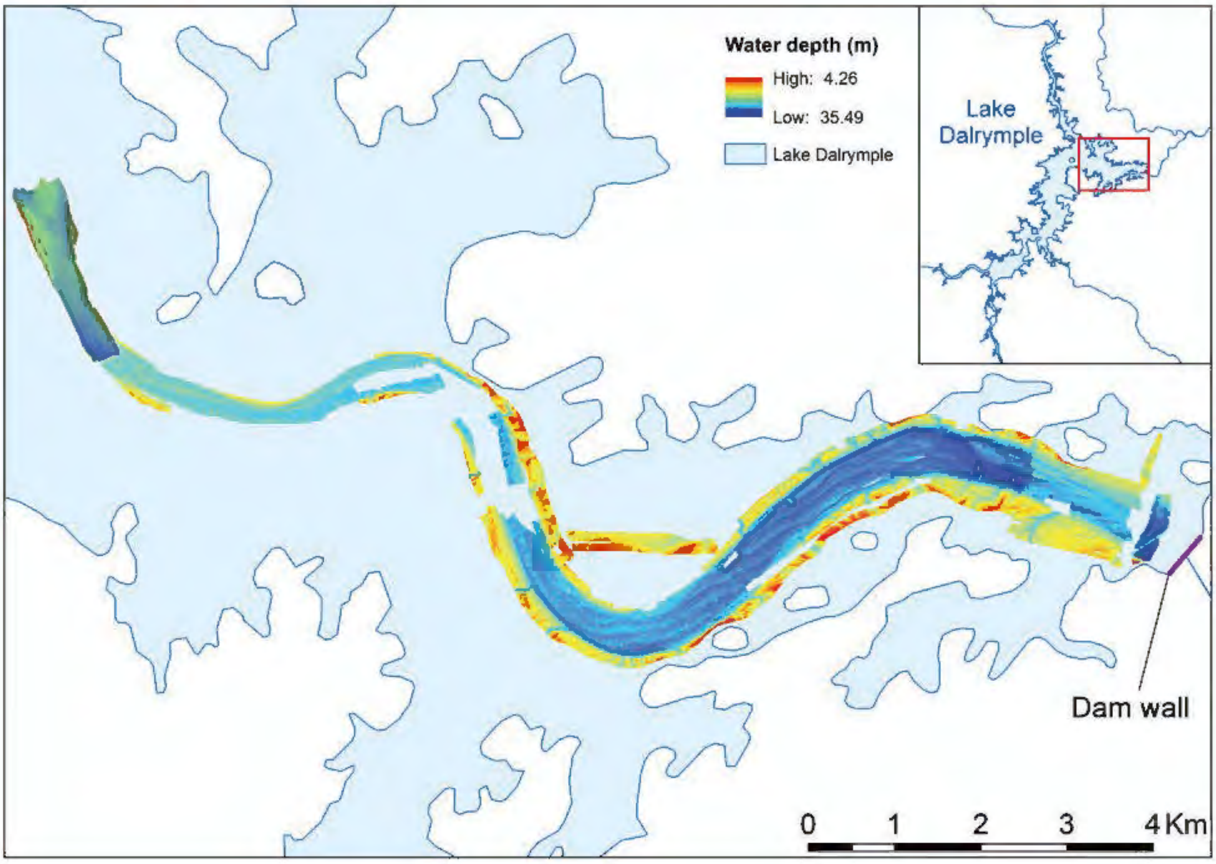

Figure 5.3 Location of bathymetric data collected in Lake Dalrymple.

5.4.4. Capacity analysis of the Burdekin Falls Dam reservoir

The volume of the BFD reservoir fell to a minimum of ~40% of full capacity during two water years in the 30 years since construction (excluding the year in which the reservoir first filled). The probability of a capacity <40.2% in any given year is 6.9%, representing a return period of 1 in 15 years (Table 5.3). This return interval may be used as an additional measure of useful life as if the capacity of the BFD reservoir is reduced by 40%, based on historic data, the dam would be unable to meet demand in 1 in 15 years.

5.5. Discussion

5.5.1. The useful life of the Burdekin Falls Dam

Both techniques used to determine the volume of sediment trapped by the BFD through 2011 provided similar results: 65 million m^3 of sediment using the annual load and TE technique and 61 million m^3 using the extrapolation of sediment deposit depths. Given the difficulty collecting cores within the reservoir due to its size and depth, it is believed that method one provided a more reliable estimation of the amount of sediment currently residing in the reservoir (65 million m^3), while the sediment core data provided insight into the distribution of sediment within the reservoir. Although Lewis et al.'s (2013) modified version of the Churchill (1948) equation combined with the mean suspended sediment concentration data potentially underestimates TE during extreme inflow events, the application of this equation over a longer period (>20 years) incorporates inflow (and sediment load) variability thereby providing a reasonable estimate. It is also likely that Lewis et al.'s (2013) use of daily TE data improves the accuracy of the results. Issa et al. (2015) tested a range of methods for calculating TE and found that using monthly TE data produced better results than long-term data, and that estimated sedimentation volumes were comparable to measured sedimentation rates.

Bathymetric survey data from the BFD reservoir complement the sediment load/trapping calculations and coring results, suggesting that <1 m of sediment deposition has occurred across broad areas of the reservoir. Bathymetric surveys are used to measure deposition at many dams (Carvalho et al., 2000; Samadi Boroujeni et al., 2009), however surveys need to be combined with traditional engineering survey techniques (e.g., fixed points) and run at regular intervals to be effective at measuring sediment accumulation (Furnans & Austin, 2008).

The data presented here show that 0.15% of the BFD reservoir capacity has been lost per year since construction. If similar sediment loads/climate regimes prevail, the storage capacity of the BFD reservoir would be halved in 345 years. Gill's (1979) equation for fine sediments produced an identical reservoir half-life estimate (50% reduction in capacity) for the BFD of 345 years.

To accurately calculate a reservoir's useful life, capacity data must also be examined (or modelled) to capture climate variability. In seasonally dry tropical locations, it is not unusual for reservoirs to drawdown to <20% capacity during drier periods (e.g., Ross River Dam, Townsville; City of Townsville, 2016) meaning a 'reservoir half-life' will not be relevant. The lowest drawdown of the BFD reservoir was in January 1994 when the volume reached a minimum of 40% (146.4 m AHD; Table 5.3). At current rates of sedimentation, it would take 276 years for the BFD to lose 40% of its storage capacity. Hence it is estimated the useful life of the BFD is 276 years – 69 years shorter than the reservoir half-life. The operators of the BFD have an Interim Resource Operations License that provides for total water allocations of 1.12 million ML (Queensland Competition Authority, 2003); this amount is equal to 60% of the reservoir's capacity, supporting the use of a ~40% capacity loss threshold for estimating the useful life of the BFD.

The Burdekin Basin Draft Water Resource Plan 2006 (Department of Natural Resources Mines and Water, 2006) provides for future developments such as a raising of the BFD by 2 m. This increase in wall height would expand the dam's storage capacity by 574,240 ML (31%) to 2,434,240 ML (Sunwater Limited, 2024a). At current incoming sediment loads and with an estimated average annual TE increasing from 71% to 74% (due to increased capacity to inflow ratio and using 1987–2011 flow data), that expansion would increase the reservoir's half-life from 345 to 427 years and the reservoir's useful life from 276 to 342 years.

The estimate of 0.15% of capacity lost annually in the BFD reservoir is comparable to values reported by the Burdekin Project Ecological Study (Fleming, 1981) and Prosser et al. (2002), which both predicted annual sediment trapping equivalent to only 0.1% of reservoir volume. The minimum withdrawal level for the BFD reservoir is 129.9 m AHD, equal to a capacity of 3% or 56 million m^3 (T. Bailey, Sunwater, personal communication, 5 February 2016); below this level is dead storage (the volume below the intake of the lowest-level outlet and which cannot be drained by gravity; live storage is the total volume below full reservoir level less dead storage (Morris & Fan, 1998). The calculated loss of volume after 24 years of operation (65 million m^3) is greater than the volume of dead storage but it is unlikely that all sedimentation has occurred within the dead storage area. Regular dam operations draw water from the top 6 m of the reservoir (148 to 154 m AHD), so the current loss of storage is unlikely to affect dam operation.

Of the 61 million m^3 of sediment estimated to be trapped using the sediment thickness method, 57% (35 million m^3) is trapped in the southern section of the reservoir and only 17% and 26% is trapped in the northern and central/eastern sections, respectively (Figure 5.1). The large percentage attributed to the southern section is due to the much larger area over which sediment is distributed (approx. 139 km^2 or 63% of the reservoir's area). However, only 10 million m^3 of sediment was contributed by the Cape and Suttor/Belyando rivers from 1987 to 2011 (Appendix D, Table D1). In 19 of the 24 years since dam construction >50% of inflow came from the Burdekin River (DRDMW, 2021). Water from the Burdekin River will back-flow into the southern section while the reservoir is filling, and when the Cape and Suttor/Belyando rivers are not flowing. Suspended sediment concentration peaks early in the flow event (Bainbridge et al., 2006a) so the net effect will be to distribute sediment from the Burdekin River into the southern section.

There is no evidence in the sediment recovered by coring or the bathymetry to indicate that sediment is building up immediately behind the BFD. It is common for sediment to deposit in deltas that form at the head of a reservoir (Frenette & Julien, 1996; White, 1990) and turbidity currents in particular may cause the deposition of sediment immediately behind a dam wall (Annandale, 2006; Samadi & Galay, 2005). High turbidity inflow has been observed travelling through the BFD reservoir at a depth of 15 m, however, once the dam overflows suspended sediment is transported through the reservoir and over the dam wall (Faithful & Griffiths, 2000). Turbidity currents will usually move in the original river channel within a reservoir until that channel fills with sediment (Fan, 1986). The drowned Burdekin and Suttor river channels are clearly delineated in the bathymetry, so it is likely that these channels direct water flow through the reservoir.

Greater sediment depth in the channel in the Burdekin (median 60 cm) and Dam (median 81cm) sections compared to out-of-channel depths (medians of 34 cm and 19.5 cm, respectively) indicates that sediment is being preferentially deposited within the channel in these sections. These data may be explained by one, or all, of the following mechanisms:

1) Turbid density currents formed during periods of inflow transport and deposit sediment along the length of reservoirs (Morris & Fan, 1998). Because those currents

follow the original river channels in the BFD reservoir sediment is preferentially deposited in those channels.

2) Sediment is resuspended (or remains in suspension) and is distributed throughout the reservoir. When the water becomes calm enough, more sediment deposits in deeper areas because the mass of particles above any part of the benthic surface is a linear function of depth (Hilton et al., 1986).
3) Sediment resuspended from shallower areas is slowly mixed and transported to deeper, calmer water where it redeposits (Hilton et al., 1986).

Sediment deposited in deeper areas like the relict channel is more likely to remain relatively undisturbed, particularly as it contains clay minerals that tend to be sticky and cohesive and lead to low erodibility (Grabowski et al., 2011).

5.5.2. The useful life of reservoirs—a comparison with reservoirs around the world

There are numerous parameters that affect the useful life of a dam. These include:

- The annual drawdown capacity of a reservoir (i.e., climate variability and water allocation)
- the sediment load of inflow, which is in turn affected by catchment-related factors such as vegetation, rainfall, gradient, geology, degree of weathering, and size; capacity to inflow ratio and TE; texture and size of incoming sediment deposited and its distribution within the reservoir
- the method of reservoir operation and how sediment is transported through the reservoir
- the reservoir's size and shape, including depth (Brune, 1953; Nagle et al., 1999; Raudkivi, 1993).

Structural and engineering factors also contribute to the overall life of any dam; while that aspect of dam life is beyond the scope of this paper, a useful summary of the engineering issues that affect the life-span of dams is provided by Wieland (2013).

Table 5.5 compares sedimentation in the BFD reservoir to that of other large tropical to sub-tropical reservoirs around the world. The BFD has the longest useful life even though it shares similar physical characteristics with many of them. The half-life calculated for the BFD reservoir (345 years) is similar to that for Indian dams (169–240 years) but longer than for both similar-sized and larger dams in China, Brazil, and Iran (12–200 years; discussed further in sections 5.5.2.2–5.5.2.6 below).

5.5.2.1. Reservoir drawdown capacity

When calculating reservoir useful life, it is critical to determine the inter-annual drawdown variability of the reservoir because dam capacity needs to exceed maximum annual drawdown to be useful. In some reservoirs in wet tropical areas, annual drawdowns may be small before replenishment meaning that the useful life may only be compromised when >50% of the dam capacity is reduced by sedimentation. Conversely, in dry areas, annual drawdown and water lost to evaporation may regularly comprise a larger proportion of total capacity, with some reservoir volumes decreasing to as little as 9% (Helfer et al., 2012; Reynolds, 2012). In these cases, reservoirs will have a much lower useful life than the half-life (50% capacity). For example, Koga reservoir in Ethiopia decreases to 9% of capacity in the dry season and Reynolds (2012) demonstrated that a decrease in reservoir volume as low as 11% could result in the reservoir drying out for at least one month a year and could occur in as little as 11–22 years post-construction. Drawdown information for many reservoirs is limited, so in this study reservoir half-lives are compared as these are more commonly reported in the literature.

5.5.2.2. Annual sediment load of inflow

A key reason for the longer reservoir half-life of the BFD is the relatively low sediment load entering the reservoir annually (average 2.6 x 10^6 t; Appendix D, Table D1) relative to other locations (>26.9 x 10^6 t yr^{-1}). For example, the Manwan Dam reservoir, China, has a very similar TE (60.5%), volume (1060 x 10^6 m^3), and upstream watershed area (114,500 km^2) to the BFD, but has a much shorter reservoir half-life (predicted to lose 50% of its volume in 25 years; Table 5.5). This is chiefly because of the much larger volume (i.e. order of magnitude higher) of sediment entering the reservoir: 26.9–28.5 x 10^6 t yr^{-1} including bedload (K. D. Fu et al., 2008). The Sefid-Roud Reservoir in Iran, also similar in volume (1760 x 10^6 m^3), climate (dry, semi-arid), and TE (73%) to the BFD (TE 71%; Morris & Fan, 1998), likewise has a much shorter half-life (27 years) than the BFD, and this is again due to the much higher sediment load (48 x 10^6 t yr^{-1}) entering the reservoir (Shokri et al., 2013). Were the same amount of sediment to enter the BFD as is deposited in the Manwan and Sefid-Roud reservoirs then the reservoir half-life of the BFD would drop to 20–34 years. Several of the dams listed in Table 5.5 are in areas that are highly prone to erosion including within steep mountainous ranges and strong undulating terrain where reservoirs receive high amounts of bedload material and from mass wasting such as landslips (Nagle et al., 1999). Sediment yields in the Burdekin River watershed are much lower (generally 4–10 times) than other tropical rivers around the world (Bainbridge et al., 2014) and most bedload sediments are deposited upstream of the BFD reservoir (Lewis et al., 2013).

5.5.2.3. Capacity to inflow ratio and TE

The BFD has a much lower TE (70%) than dams with comparable reservoir half-lives (Table 5.5), e.g., Tehri Dam, India (TE 95%, 169 years) and Bhakra Dam, India (TE 99.6%, 240 years). This is due to the relatively low capacity to inflow ratio of the BFD (0.24; Bainbridge et al., 2014) where nearly a third of the sediment that enters the reservoir during the wet season is commonly transported through the dam and over the wall. In comparison, the Tehri Dam reservoir has twice the volume of the BFD reservoir (3540 x 10^6 m^3) but covers a much smaller area (52 km^2) and is much deeper (max depth 230 m). Like the BFD, it receives most of its inflow during monsoonal rainfall events that transport highly turbid water into the reservoir with an average annual sediment load of 15.4 x 10^6 t (Vishnoi & Govil, 2007). The average annual loss in capacity of the Tehri Dam, based on the predicted loss of live storage of 35% in 169 years (Vishnoi & Govil, 2007), is 0.21%, only slightly higher than the BFD's 0.15%. But this loss only applies to live storage; the remainder of the sediment entering the reservoir is being deposited in dead storage, which comprises 26% of the reservoir (Vishnoi & Govil, 2007), allowing the Tehri Dam to trap more sediment before reducing its useful life. In contrast, only 3% of the BFD capacity is dead storage (T. Bailey, Sunwater, personal communication, 24 March 2013) meaning that more of the dam's capacity is available for use but sediment deposition will more quickly deplete the live storage.

5.5.2.4. Texture, size and distribution of sediment

Bathymetric and sediment core data from the BFD reservoir indicate that sediment has not formed a delta in the central/eastern section and as indicated earlier, there is no evidence that sediment is accumulating immediately behind the dam wall. The location of sediment deposition within a reservoir can have a major effect on the useful life. Sediment deposited against a dam wall can impede its function particularly if it has deep-water outlets or is used for hydropower (Oehy & Schleiss, 2007). The Dez Dam reservoir in Iran is twice the volume of, and deeper (mean depth 51 m) than, the BFD reservoir (mean depth 8.5 m) but has a much shorter useful life (~50 years, extrapolated). The Dez Dam reservoir has lost 19% capacity in 40 years (meaning it will take 105 years to fill 50% with sediment) but the sediment level near the dam has risen at a rate of ~2 m yr^{-1} and in 2007 sediment was only 10 m below the intake level for power generation (Samadi Boroujeni et al., 2009). This is because fine sediment (55% clay, 45% silt) is re-entrained from deposits at the upstream end of the reservoir and transported to the face of Dez Dam in highly concentrated turbidity currents, which occur four to six times a year (Samadi & Galay, 2005). Although the BFD experiences turbidity currents, these may travel as mid-water column flows and exit the dam as overflow (Faithful & Griffiths, 2000), transporting sediment out of the reservoir instead of depositing it behind the dam wall. Additionally, some of the fine sediment that is trapped by the BFD reservoir, remains in suspension causing persistent turbidity (Cooper et al., 2017 – Chapter 2; Griffiths & Faithful, 1996); importantly, this sediment remains mobile and may exit the dam as part of regular releases for irrigation.

5.5.2.5. Method of reservoir operation and sediment transport through the reservoir

The BFD may release water from multiple depths allowing for siltation problems to be addressed. Operational water discharges are presently released from the top 6 m of the reservoir. However, should sediment start to build up behind the dam then it would be possible to alter the operation of the BFD to flush the sediment (T. Bailey, Sunwater, personal communication, 5 February 2013). Flushing involves significantly drawing down a reservoir to create a scouring effect and remove sediment in outflow (Atkinson, 1996). It is an effective and inexpensive sediment removal method that has been used successfully in both small and large reservoirs around the world (Lai & Shen, 1996). For example, the operation of the Sefid-Roud Dam is regularly modified to open low-level water outlets in an effort to scour and flush sediment from the reservoir (Khosronejad, 2009). Changes to the operation of the Sanmenxia Dam on the Yellow River in China (mean sediment load 1.6 x 10^9 t; Wang et al., 2005) allow for medium and minor floods to transit the reservoir reducing retention time and decreasing sedimentation in the reservoir, while large discharges are used to flush sediment from the dam (Wu et al., 2007). The BFD naturally manages turbid floodwater the same way by overflowing during large inflow events, allowing sediment to pass through the reservoir, reducing TE (Faithful & Griffiths, 2000; Lewis et al., 2013).

5.5.2.6. Reservoir size and shape

The large volume of the BFD reservoir contributes to its long useful life as worldwide the highest rates of loss of storage are found in the smallest reservoirs (storage volume <1233 m^3) and the lowest storage rate losses occur in the largest reservoirs (White, 2001). Although Mahmood (1987) reported that the global average for reservoir useful life was <25 years, for larger dams this is only true where they trap extremely large volumes of sediment such as the

Sanmenxia Dam (Table 5.5). Extreme siltation rates of >200 m^3 km^{-2} $year^{-1}$ have been observed in Australia (Chanson, 2012) but sedimentation problems have predominantly been in reservoirs with a watershed area of <100 km^2 while larger reservoirs have generally been less affected (Chanson & James, 1999; Jones et al., 2000).

The shape of the BFD reservoir largely explains the even distribution of sediment deposited within it (outside of the channels). The reservoir is generally broad, dendritic, and moderately shallow (max. depth 40 m; mean depth 8.5 m) so sediment entering the reservoir may disperse and be deposited relatively evenly across a wide area (220 km^2). The area of the reservoir also remains large even when the reservoir is drawn down. Conversely, the TE of the Tarbela Reservoir in Pakistan is higher because its shape leads to the trapping of almost all the incoming sediment (Roca, 2012). Reservoir drawdowns as part of regular operation have allowed the sediment delta to progress closer to the dam wall, as when water levels are low, the sediment deposited in the upper reaches is reworked and transported downstream within the reservoir (Roca, 2012). Progression of a delta in the upstream reaches of the BFD reservoir has not been observed but cannot be ruled out by the sampling done as a part of this study.

5.6. Conclusions

This study found that ~68 million t of sediment (equivalent to 65 million m^3 of sediment) was deposited in the BFD reservoir over 24 years between 1987 and 2011. If this deposition rate persists the reservoir's half-life (50% capacity lost) will be ~345 years. Based on drawdown data for the BFD reservoir collected since construction, if capacity was reduced by just 40% the dam could not service existing demand approximately once in every 15 years. Adjusting for drawdown, the useful life of the BFD is 276 years which is generally much longer than other similar, large reservoirs in tropical locations around the world.

The longer useful life of the BFD can be attributed to a lower TE (71%), lower annual sediment load entering the reservoir (2.6 x 10^6 t), and the ability of the BFD to pass highly turbid (up to 620 mg L^{-1}) annual flood waters (Bainbridge et al., 2008; Lewis et al., 2009). The BFD catchment is highly weathered, but its lower gradient allows for trapping of sediment including bedload upstream of the reservoir. Further, the large surface area of the reservoir allows relatively even deposition of the trapped sediment to occur prior to reaching the dam wall where it could otherwise begin to impede dam operation. Finally, the persistent turbidity present in the reservoir indicates that a portion of the sediment trapped by the BFD reservoir is never deposited, instead remaining mobile and exiting the dam. The longevity of dams around the world could be improved by choosing dam sites on rivers with lower sediment yields, highlighting the importance of constructing accurate sediment budgets during planning stages. Where that is not possible, it is important to incorporate sediment transport mechanisms like low-level outlets that allow for scouring and the discharge of turbidity currents. For some reservoirs the construction of secondary trapping structures such as another dam upstream can prolong the useful life of the reservoir. Importantly, the estimation of the useful life of a dam should incorporate measured or modelled data of the predicted drawdown of the reservoir over a period of >30 years.

Most reservoirs are designed and operated on the concept of a finite life which will ultimately be terminated by sediment accumulation rather than structural failure (Morris & Fan, 1998). China and India are continuing to build dams while dam construction in Europe and North America has essentially ceased (Farnsworth & Milliman, 2003). These areas already have dams that have been losing capacity continuously since construction due to high sediment loads entering the reservoirs and flushing and other sediment removal techniques are applied that didn't originally feature in the design of those dams. Accurately predicting and understanding the key processes that influence the useful life of reservoirs are key components to better plan, develop, and manage dam construction.

Table 5.5 Examples of the useful life of reservoirs in tropical to semi-arid environments

Reservoir/ dam	Country	Year finished	Reservoir volume ($x10^6$ m^3)	Area (km^2)	TE (%)	Siltation %	Average annual capacity lost (calculated; %)	Useful life[a] (years)	Reference	Köppen-Geiger climate classification[b]
Lake Dalrymple (Burdekin Falls Dam)	Australia	1987	1,860	220	70	3.5% in 24 years	0.15	345 (to 50% total storage; 276 to 40%)	(Lewis et al., 2013; This study)	Dry, semi-arid
Itiquira Dam and reservoir	Brazil	2002	4.8	2.1	46	-	-	12 (to fill to intake sill)	(Carvalho et al., 2000)	Continental
Manwan Dam and reservoir	China	1993	1,060	23.6	60.5	21.5%–22.8% in 11 years	2.0	25[c] (to 50% total storage); 29–31 to fill dead storage	(K. D. Fu et al., 2008); (Kummu & Varis, 2007)	Humid, mid-latitude (parts are Continental or Dry, semi-arid)
Sanmenxia Dam	China	1960	9,750	2,350	93[d]	To 1964 lost 41.5%[d]	Was 10.4 (now 1.7 yr^{-1})	~23[c] (to 50% total storage)	(Morris & Fan, 1998)	Dry, arid and Dry, semi-arid
Tehri Dam and reservoir	India	2006	3,540	42	95	35.7% of live storage predicted lost after 169 years	0.21 (in live storage)	169 (241 to 50% total storage)	(Vishnoi & Govil, 2007)	Humid, mid-latitude
Gobindsagar Reservoir (Bhakra Dam)	India	1963	9,868	168	99.6	1546 x 10^6 m^3 in 40 years (~15%)	0.39	240 (to 50% live storage)	(Garg & Jothiprakash, 2008)	Humid, mid-latitude (parts are Dry, semi-arid)
Sefid-Roud Dam	Iran	1962	1,760	52	73	35.7% in 17 years (to 1979)	2.1	~23[e] (to 50% total storage)	(Morris & Fan, 1998; Smith, 1984)	Dry, semi-arid
Dez Dam and reservoir	Iran	1963	3,315	64.9	-	19% in 40 years	0.48	~50[c] to level of power generation intake (calc.); 105 to 50% total storage	(Samadi Boroujeni et al., 2009)	Dry, arid and Dry, semi-arid
Mosul Dam and reservoir	Iraq	1986	11,110	380	95.3	10.29% in 25 years	0.41	125 (to 50% total storage)	(Issa et al., 2013, 2015)	Humid, mid-latitude and Dry, semi-arid
Tarbela Reservoir	Pakistan	1974	11,600	250	95	~20% lost in 21 years; in 2009 live storage loss estimated at 30%	0.86	85; 58[c] (to 50% total storage)	(Munir, 2011; Roca, 2012)	Humid, mid-latitude
Mangla Dam Reservoir	Pakistan	1967	7,254	251	-	20.5% in 38 years (to 2005)	0.54	93[c] (to 50% total storage)	(Butt et al., 2011)	Dry, semi-arid and Humid, mid-latitude

[a]Useful life: the period during which the capacity occupied by sediment does not prevent the reservoir from serving its intended primary purpose; is reservoir specific.
[b]Climate classification for the catchment (Peel et al., 2007).
[c]Extrapolated from published data; assumes a constant sedimentation rate.
[d]During first four years of operation. Post-construction work was subsequently carried out to allow greater discharge of sediment-laden water and remove deposited sediment. Since 1973 the reservoir has been used to store clear water from non-flood seasons and discharge turbid water during flood events.
[e]Initial life based on first 17 years of operation. In 1980 sediment control was initiated which included dredging and flushing of sediments.

Chapter 6: Conclusions and further research

Hundreds of thousands of dams have been built around the world to supply water for drinking, irrigation, hydropower and recreation. However, despite their benefits, dams may reduce water quality downstream, modify the timing, magnitude and frequency of high and low flows, negatively impact on flora, fauna and society, and inhibit the movement of sediment and reduce sediment delivery to the sea (Ansar et al., 2014; Benchimol & Peres, 2015; Friedl & Wuest, 2002; Syvitski et al., 2022; Syvitski et al., 2005). Reservoirs may also experience problems with sedimentation, turbidity, poor water quality and damage to infrastructure (de Cesare et al., 2001; Raudkivi, 1993). Previous research into reservoirs in Australia has focussed mainly on water quality and physical processes within water supply reservoirs. Research into sediment within Australian reservoirs has commonly focussed on seasonal turbidity, identification of sediment source, and dating of sediments to estimate sediment accumulation rates (Douglas et al., 2003; Rahman & Bakri, 2010; Tibby et al., 2010; Townsend, 2002). Further, research into sediment relationships in large reservoirs in tropical to semi-arid regions of Australia has been limited, with little to no detailed examination of the composition and sources of sediment. Hence, the primary aim of this thesis was to investigate the character, dynamics and sources of suspended and benthic sediment in the BFD reservoir, Lake Dalrymple, to provide insight and understand the implications for ecosystem management.

6.1. Conclusions

This thesis used a multidisciplinary approach to determine the key behaviours of sediment in the BFD reservoir and determine the primary sources of that sediment. This study created a large, integrated suspended and benthic sediment dataset including particle size, mineralogy and geochemical data collected over three consecutive median to below-median rainfall and discharge water years (1 October to 30 September; Fig 2.2), and again five years later, allowing analysis with both spatial and temporal resolution. The research had five objectives which are outlined below, together with key conclusions:

Objective one: *Physically and chemically characterise suspended and benthic sediment from the BFD reservoir and describe any intra- and inter-annual variability* (Chapters 2, 3 and 4)

- The mineralogy of dry season SS was consistent throughout the BFD reservoir and remained consistent across multiple sampling years. Wet season SS mineralogy also remained relatively consistent across sampling years.

- Wet and dry season SS samples collected from the BFD reservoir contained the same minerals: quartz, micas (muscovite/illite), kaolin group clays (kaolinite) and smectite group (expandable) clays. Wet season SS samples also contained feldspar minerals and chlorite. All benthic sediment samples (grab and core) contained the same minerals as SS with addition of small amounts of amphiboles (<2%) and occasional vermiculite and goethite (<1.4%). Feldspars were more abundant in benthic sediment (2%–16% c.f. <4%), particularly in samples from the Burdekin section of the BFD reservoir.
- Quartz and feldspars were associated with coarse sediment and deposited in greater percentages in upstream parts of the BFD reservoir while smectite and kaolinite group clays were observed in greater proportions in the fine sediment (<62.5 µm) deposited in sections of the reservoir closest to the dam wall.
- The particle-size distribution of SS at all four sites was bi-modal in both the wet and dry seasons. In dry season SS the dominant fractions centred on 0.1–0.2 µm (range 0.04–1 µm) with smaller secondary peaks at 4–10 µm, although samples closest to the dam wall produced an almost unimodal distribution (peak at 0.1–0.2 µm). Peaks of 0.1–0.3 µm and 2–6 µm were observed in wet season SS samples, which primarily contained sediment <62.5µm in diameter. Where particles >62.5 µm diameter were found they comprised <3% of those samples and less than 1.3% of SS was >126 µm in diameter. Samples from depths where turbidity data indicated turbid inflow typically contained more silt- than clay-sized particles.
- The particle-size distribution of benthic sediments varied from unimodal to bimodal. The minimum particle size of almost all samples was 0.9 µm (3 samples had less than 0.2% <0.9 µm). Sediment distributions were coarser and more variable in the Burdekin and upstream Suttor sections than they were in the eastern sections of the BFD reservoir, where very uniform distributions and finer peak particle sizes were observed.

Objective two: *Determine the cause of persistent turbidity in the BFD reservoir and identify the processes contributing to the intra- and inter-annual variability of minerogenic turbidity* (Chapters 2 and 3)

- Turbidity provides a reliable proxy for suspended sediment concentration ($r^2 = 0.97$) in the BFD reservoir system, allowing the spatial and temporal relationships between turbidity, particle size and mineralogy to be investigated.

- Turbidity caused by high concentrations of SS (up to 1507 mg/L) increased with wet season inflow, ranging from 46 to 2080 NTU.
- Turbidity in the BFD reservoir decreased following the wet season but remained relatively high during the dry season (>45 NTU), predominantly due to colloidal particles (<0.9 µm) composed largely of kaolin and smectite group clays and micas. Benthic sediments ranged from 1 to 30 µm in size, suggesting that resuspension of lake bottom sediments had little effect on turbidity.
- Dry season turbidity levels were strongly affected by the magnitude and duration of inflow waters from the preceding wet season, reflecting the limited availability of suspended particles delivered from the upstream catchment.
- This study emphasised the importance of reservoir flushing by extended periods of high flow as a major control of turbidity and provided evidence that even a persistently turbid reservoir may clarify naturally. Persistent turbidity caused by colloidal SS (<0.9 µm) that does not settle out will be reduced by prolonged and above-average reservoir inflow that has depleted its sediment sources continuing to move through the reservoir. Turbidity in the dry season will remain elevated in years where wet season flow events are below median to median.

Objective three: *Examine the effect of thermal stratification on turbid inflow and investigate the influence of turbidity currents on sediment transport and deposition in the BFD reservoir* (Chapter 3)

- The BFD reservoir stratified thermally in the spring and summer, developing a thermocline between 5 and 15 m that was shallowest in upstream areas of the reservoir.
- Turbid inflows entered the BFD reservoir every wet season (summer-autumn) and formed turbidity currents that entered the reservoir as under- and interflows.
- During these events, turbid interflows in deeper parts of the reservoir (>20 m) transitioned into underflows, temporarily disrupting stratification, a process rarely documented in the literature.
- Overflow of the dam occurred even during most below-average to average flow events (dependent on reservoir volume prior to each wet season and the frequency of wet season inflow events), discharging turbid flows carrying fine-grained sediment (97%

of particles <62.5 µm) that extended through the BFD reservoir to the dam wall and limiting the amount of fine sediment deposited in the reservoir.

- The location of turbid flows within the water column through the BFD reservoir was dependent on the density of the inflow and the density of the water column in the reservoir.
- Examination of the particle size of turbid inflow and benthic sediments from sample sites located throughout the BFD reservoir found that sediment >126 µm was largely absent from wet season inflow in below-average flow events and was moved through the reservoir as bedload (a process restricted to the uppermost reaches) or deposited in the upper reaches of the reservoir.
- An increase in the particle size of benthic sediments collected after above-average inflow events between 2008 and 2011 indicated that these larger events transported coarser particles from the northern Burdekin sections of the BFD reservoir further into the impoundment.
- This understanding of turbidity current behaviour in the BFD reservoir will allow dam managers to manipulate water releases in the future to discharge turbid water from targeted depths and facilitate sediment removal should sedimentation near the dam wall become a problem or if turbidity currents threaten to damage proposed hydroelectric infrastructure.

Objective four: *Examine the potential of geochemical and physical characteristics of sediment deposited in the BFD reservoir to identify discrete sediment sources within a large geologically complex catchment* (Chapter 4)

- The two primary sources of sediment to the reservoir, the northern Burdekin River and the southern and western Suttor/Belyando/Cape rivers, can be distinguished based on their geochemical, particle size, and mineralogical characteristics.
- The elemental and mineralogical composition of the sediments was dominated by quartz, muscovite/illite, kaolinite and smectite. The younger and more variable geology of the Upper Burdekin catchment provides sediment to the reservoir that has a higher proportion of quartz and feldspars, while the basic igneous and clay-containing sedimentary rocks and deeply weathered geology of the southern catchments create sediment with a greater proportion of kaolinite.

- Differences in sediment geochemistry and particle size within the BFD reservoir were dominantly spatial and not temporal, with greater differences in geochemistry occurring between locations rather than with depth.
- Particle size decreased from the point of inflow toward the dam wall, with coarser particles able to travel further into the reservoir along the narrower, more riverine, Burdekin arm.
- The mineralogy and geochemistry of BFD reservoir sediment is related to the source materials and particle size fractionation processes through the reservoir. Less-weathered minerals (quartz and feldspars) are deposited in the upstream North and South Burdekin, South Suttor and Central Reservoir areas of the reservoir and are associated with coarser particle sizes (>15.6 µm). Fine (<15.6 µm) highly-weathered minerals (kaolinite, smectite) are deposited in the North Suttor and Eastern Reservoir sections.
- Sr ratios indicated that 71%–83% of sediment deposited in the Central Reservoir comes from the Burdekin River system, while 46%–58% of sediment deposited in the Eastern Reservoir comes from the Suttor River system.
- The fractionation and sorting of sediment as it travels through the reservoir is complicated by in-reservoir sorting.
- Sediment preferentially deposits in the relict river channel, particularly in the northern Burdekin arm and central to eastern sections of the BFD reservoir, but no sediment has built up immediately behind the dam wall.
- Although large flow events have occurred since the completion of the BFD, clear evidence of them was not identified in cores from the reservoir.
- Data collected creates an environmental baseline for sediment in the BFD reservoir that can be used for future evaluations of sediment composition in this reservoir and will contribute to the ongoing management strategy for this system.

Objective five: *Spatially and temporally quantify sediment deposition in Lake Dalrymple to determine the useful life of the BFD and identify where that life sits in a global context* (Chapters 4 and 5)

- Using two independent methods it was estimated that between 61 and 65 million m^3 (~68 million t) of sediment was deposited in the BFD reservoir between the completion of dam construction (1987) and September 2011. This sediment volume equates to an average of 0.15% of capacity lost per year since construction was completed.

- If current sediment loads/climate regimes persist, reservoir capacity will be reduced by 50% after 345 years. However, the useful life of the BFD reduces to just 276 years when drawdown data are considered; these data show reservoir use would be affected once 40% of storage was filled with sediment, with a 60% drawdown return period of 1 in 15 years.
- When compared to similar large tropical to sub-tropical reservoirs, the BFD has a slightly longer reservoir useful life than dams in India and a much longer half-life than similar-sized and larger dams in China, Brazil, and Iran. Properties of the BFD that promote a longer useful life include a lower trap efficiency, relatively low annual sediment load delivered to the reservoir, limited sediment deposition behind the dam wall (and relatively uniform distribution of deposited sediment), and the export of highly turbid annual floodwaters before settling and deposition of any remaining sediment within the reservoir.
- Most reservoirs are designed and operated on the concept of a finite life that will ultimately be terminated by sediment accumulation rather than structural failure (Morris & Fan, 1998). Given the likelihood that the BFD reservoir will not fill with sediment, further life research might need to focus on engineering aspects to ensure the dam infrastructure remains strong.

6.2. Future research directions

Dams continue to be seen as a way to ensure water and power supply for growing populations including in locations like northern Australia, Africa and Asia (Zarfl et al., 2015). This study has relevance for reservoir managers and ecologists responsible for reservoir planning, development and management in tropical to sub-tropical regions worldwide. The insights arising from this thesis have provided a solid foundation for further research in the following areas:

- The data presented in Chapter 3 discussed the behaviour of turbidity currents in the reservoir and their role in sediment transport and deposition. However, this study was only able to sample below average flow events and focussed on the flow peak. Further sampling of above-average flow events is needed to understand the impact of larger flows on the formation and position of turbidity currents, and the potential for homogenisation of the entire water column, influencing water quality within the dam and in discharged waters. Turbidity currents could also be monitored for longer periods of time after peak inflow/overflow to better understand how those currents evolve throughout the entire flow event and the resultant effect on sediment transport and deposition and water quality within the BFD reservoir. Additional monitoring techniques such as acoustic Doppler current profiling could also be used to gain a better understanding of flow within the reservoir, as measuring water current velocities would allow more detailed modelling of flow and sediment carrying capacity throughout the reservoir.

- Bathymetry should be collected further upstream within the reservoir, targeting river deltas to confirm the presence of sediment fans in those areas. This would allow the deposition or erosion of sediment in those deltas to be monitored and provide a baseline for future bathymetric studies, particularly if reservoir volume is increased.
- Dating of core sediments using ^{210}Pb or biostratigraphy (e.g., pollen or diatoms) or new techniques like high-resolution CT scanning should be undertaken to quantify the amount of sediment deposited each year and identify the relationship between sediment volume and flow characteristics. Dating of sediment deposits would also allow the effects of above and below-average flow events on sediment transport, particle size and the location of deposition to be better understood.
- Clays <0.9 µm cause year-round turbidity in the BFD reservoir. Clay-sized particles (<3.9 µm) are supplied to the reservoir from all of its sub-catchments, but the lack of mineralogical distinction between SS from the sites sampled means that the present study was not able to confirm the hypothesis that the southern sub-catchments (Suttor/Belyando, Cape rivers) supply the clays causing the persistent turbidity. (Fleming & Loofs, 1991). Additional geochemical tracing of the SS using clay mineral fingerprinting and trace element geochemistry should be undertaken to better constrain the origin of clays in the BFD reservoir enabling targeted catchment management to improve water quality.
- The presence of some heavy metals in concentrations greater than Australian Interim Sediment Quality Guidelines (ISQG) ‘High’ values (ANZECC & ARMCANZ, 2000) in core sediments throughout the reservoir indicates that further investigation of heavy metals in the BFD reservoir is required, starting with an assessment of background concentrations. Concentrations of Ni exceeded ISQG-High values putting them above

the threshold at which adverse effects on biota are probable while Cr and Cu values fell within a transition zone where toxicity effects on biota cannot be reliably predicted (Santos et al., 2013). The ISQG recommend a comparison with background metal concentrations and for a site-specific study to be conducted to determine whether this exceedance poses a risk to the ecosystem. The impact of increased drawdown associated with greater water demands, leading to larger areas of sediment exposure or increased sediment overturn which can remobilise or make bioavailable previously trapped heavy metals (Hahn et al., 2018), should also be investigated.

- Modelling of the BFD reservoir's response to future flow changes will also be required to adequately manage sediment within the reservoir. The Burdekin Falls Dam Improvement and Raising projects are being progressed by dam owners Sunwater Limited, who plan to raise the BFD by 2 m to increase water supply and bring the dam in line with modern engineering design standards (Sunwater Limited, 2024a). Although turbidity currents travel through the BFD reservoir in a similar way in below-average flow years, changes to the reservoir's volume, depth and surface area could change future stratification patterns and the sediment transfer and depositional characteristics of the reservoir and would need to be monitored. Any reduction in the frequency and volume of dam overtopping could lead to less frequent venting of turbidity currents from the reservoir potentially increasing sediment deposition within the reservoir or leading to deposition in new locations. Upstream dams, such as the Hells Gates Dam previously planned for a site on the Burdekin River approx. 270 km upstream of the reservoir (Townsville Enterprise, 2017), would alter flow regimes in the Upper Burdekin River and have the potential to reduce flows into the BFD reservoir. Coupled with climate variability and drought, reduced flows could lead to greater drawdown of the reservoir potentially causing resuspension and transport of sediment closer to the dam wall where it could become problematic.
- More research is needed in lakes and reservoirs globally to inform the development of management policies that are urgently needed to reduce plastic pollution in freshwater lakes. Plastic debris is thought to be widespread in terrestrial environments globally (Rochman & Hoellein, 2020) and Nava et al. (2023) have found plastics in 38 lakes and reservoirs around the world, including one in Australia. While Lake Dalrymple does not fall in the categories of reservoirs most likely to be vulnerable to plastic contamination (those located in densely populated and urbanized areas and large lakes and reservoirs with elevated deposition areas, long water-retention times, and high

levels of anthropogenic influence; (Nava et al., 2023)), plastic pollution is a growing problem and has been identified in lakes and reservoirs in even remote areas. Plastics can harm ocean and aquatic life and contaminate water used by humans, so it is important to understand if plastics are present in the Burdekin River system, including Lake Dalrymple, to help prevent plastics from entering downstream waterways and ending up in the Great Barrier Reef.

References

Abraham, J. (1998). Spatial distribution of major and trace elements in shallow reservoir sediments: an example from Lake Waco, Texas. *Environmental Geology, 36*(3), 349–363. http://dx.doi.org/10.1007/s002540050351

Ajaaj, A. A., Khan, A. A., Mishra, A. K., & Alhathloul, S. H. (2024). Estimation of incoming sediments and useful life of Haditha Reservoir with limited measurements using hydrological modeling. *Hydrology, 11*(8). https://doi.org/10.3390/hydrology11080128

Akhurst, E. G. J., & Breen, C. M. (1988). Ionic content as a factor influencing turbidity in two floodplain lakes after a flood. *Hydrobiologia, 160*(1), 19–31. http://dx.doi.org/10.1007/BF00014275

Alexander, J., & Fielding, C. (1997). Gravel antidunes in the tropical Burdekin River, Queensland, Australia. *Sedimentology, 44*(2), 327–337. http://dx.doi.org/10.1111/j.1365-3091.1997.tb01527.x

Alexander, J., & Fielding, C. R. (2006). Coarse-grained floodplain deposits in the seasonal tropics: Towards a better facies model. *Journal of Sedimentary Research, 76*(3), 539–556. http://dx.doi.org/10.2110/jsr.2006.029

Alexander, J., Fielding, C. R., & Pocock, G. D. (1999a). Flood behaviour of the Burdekin River, tropical north Queensland, Australia. In S. B. Marriot & J. Alexander (Eds.), *Floodplains: Interdisciplinary Approaches* (Vol. 163, pp. 27-40). Geological Society of London, Special Publications.

Alexander, J., Herbert, C. M., Fielding, C. R., & Amos, K. J. (2020). Controls on channel deposits of highly variable rivers: Comparing hydrology and event deposits in the Burdekin River, Australia. *Sedimentology, 67*(5), 2721–2746. https://doi.org/10.1111/sed.12717

Allanson, B. R., & Jackson, P. B. (1983). *Limnology and fisheries potential of Lake le Roux*. http://researchspace.csir.co.za/dspace/handle/10204/2323

Ambers, R. K. R. (2001). Using the sediment record in a western Oregon flood-control reservoir to assess the influence of storm history and logging on sediment yield. *Journal of Hydrology, 244*(3-4), 181–200. https://doi.org/10.1016/S0022-1694(01)00331-6

Amos, K. J., Alexander, J., Horn, A., Pocock, G. D., & Fielding, C. R. (2004). Supply limited sediment transport in a high-discharge event of the tropical Burdekin River, North Queensland, Australia. *Sedimentology, 51*, 145–162. https://doi.org/10.1111/j.1365-3091.2004.00616.x

An, S., & Julien, P. Y. (2014). Three-dimensional modeling of turbid density currents in Imha Reservoir, South Korea. *Journal of Hydraulic Engineering, 140*(5), 05014004-05014001–05014004-05014015. http://dx.doi.org/10.1061/(ASCE)HY.1943-7900.0000851

Annandale, G. W. (1987). *Reservoir sedimentation* (Vol. 29). Elsevier Science. https://www.elsevier.com/books/reservoir-sedimentation/annandale/978-0-444-42729-8

Annandale, G. W. (2006). Reservoir sedimentation. In M. G. Anderson (Ed.), *Encyclopedia of Hydrological Sciences* (pp. Part 7. Erosion and sedimentation). John Wiley & Sons, Ltd. https://doi.org/http://dx.doi.org/10.1002/0470848944.hsa086

Ansar, A., Flyvbjerg, B., Budzier, A., & Lunn, D. (2014). Should we build more large dams? The actual costs of hydropower megaproject development. *Energy Policy, 69*, 43–56. https://doi.org/10.1016/j.enpol.2013.10.069

ANZECC, & ARMCANZ. (2000). *Australian and New Zealand guidelines for fresh and marine water quality. Volume 1, The guidelines* (National Water Quality Management Strategy, Issue. https://www.waterquality.gov.au/anz-guidelines/resources/previous-guidelines/anzecc-armcanz-2000

APHA. (1998). *Standard Methods for the Examination of Water and Wastewater* (20th ed.). Prepared and published jointly by American Public Health Association, American Water Works Association and Water Environment Federation.

Askew, A. J. (1974). Optimum reservoir operating policies and the imposition of a reliability constraint. *Water Resources Research, 10*(1), 51–56. http://dx.doi.org/10.1029/WR010i001p00051

ASTM. (2000). Standard test methods for determining sediment concentration in water samples: D 3977-97. In *ASTM Book of Standards* (Vol. 11.02 Water (II). pp. 395–400). American Society for Testing and Materials International, West Conshohocken, PA, USA.

Atkinson, E. (1996). *The feasibility of flushing sediment from reservoirs* (HR Wallingford Report OD 137, Wallingford, UK). https://assets.publishing.service.gov.uk/media/57a08dbde5274a31e00019fa/R5839-od137.pdf

Atobatele, O. E., & Ugwumba, O. A. (2008). Seasonal variation in the physicochemistry of a small tropical reservoir (Aiba Reservoir, Iwo, Osun, Nigeria). *African Journal of Biotechnology, 7*(12), 1962–1971. http://dx.doi.org/10.5897/AJB2008.000-5043

Australia Division of National Mapping. (1973). *Glendon, 8356, Edition 1. Australia 1:100 000 National Topographic Map Series. [cartographic material]* [Part of the national mapping programme]. Canberra, Division of National Mapping under the direction of the Minister for Minerals and Energy. http://pid.geoscience.gov.au/dataset/ga/46841

Australia Division of National Mapping. (1975a). *Harvest Home 1:100 000 topographic map. Edition 1. Record 8256 [cartographic material]* [Part of the national mapping programme]. Canberra, Geoscience Australia. http://pid.geoscience.gov.au/dataset/ga/46813

Australia Division of National Mapping. (1975b). *Ravenswood 1:100 000 topographic map. Edition 1. Record 8257. [cartographic material]* [Part of the national mapping programme]. Geoscience Australia, Canberra, Division of National Mapping under the direction of the Minister for Minerals and Energy. http://pid.geoscience.gov.au/dataset/ga/46814

Australian National Committee on Large Dams (ANCOLD). (2010). *Register of large dams in Australia*. Australian National Committee on Large Dams Incorporated. Retrieved Last accessed 2 April 2018 from https://www.ancold.org.au/?page_id=24

Bahlburg, H., & Dobrzinski, N. (2011). Chapter 6: A review of the Chemical Index of Alteration (CIA) and its application to the study of Neoproterozoic glacial deposits and climate transitions. *Geological Society, London, Memoirs, 36*(1), 81–92. https://doi.org/10.1144/M36.6

Bainbridge, Z. T. (2015). *Tracing the sources, transport and dispersal of suspended sediment from the Burdekin River catchment into the Great Barrier Reef lagoon* [PhD, James Cook University]. Townsville, Australia.

Bainbridge, Z. T., Brodie, J., Lewis, S. E., Duncan, I., Post, D., Faithful, J., & Furnas, M. (2006a). *Event-based water quality monitoring in the Burdekin Dry Tropics Region – 2004/2005 Wet season* (ACTFR Report No. 06/01 for the Burdekin Dry Tropics NRM). Australian Centre for Tropical Freshwater Research. https://www.dropbox.com/s/5ypaupf8p3bdu7m/06%2001_Burdekin%200405%20Wet%20Season%20Water%20Monitoring%20Report%2022Sept06.pdf?dl=0

Bainbridge, Z. T., Lewis, S. E., Brodie, J., Faithful, J., Maughan, M., Post, D., O'Reagain, P., Bartley, R., Ross, S., Schaffelke, B., McShane, T., & Baynes, L. (2006b). *Monitoring of sediments and nutrients in the Burdekin Dry Tropics region: Interim Report for the 2005/06 wet season*. J. C. U. Australian Centre for Tropical Freshwater Research, Townsville. https://www.dropbox.com/s/j0uhcq8uv79qovg/06%2013%200506%20Wet%20Season%20Burdekin%20Report_130307-1.pdf?dl=0

Bainbridge, Z. T., Lewis, S. E., Davis, A. M., & Brodie, J. (2008). *Event-based community water quality monitoring in the Burdekin Dry Tropics Region: 2007-2008 wet season update*. Australian Centre for Tropical Freshwater Research. https://www.dropbox.com/s/h3gilbyttngp5ur/08%2019%20BDT%20WQ%20Monitoring%200708%20Wet%20Season%20Update.pdf?dl=0

Bainbridge, Z. T., Lewis, S. E., Smithers, S., Wilkinson, S., Douglas, G., Hillier, S., & Brodie, J. (2016). Clay mineral source tracing and characterisation of Burdekin River (NE Australia) and flood plume fine sediment. *Journal of Soils and Sediments, 16*(2), 687–706. https://doi.org/10.1007/s11368-015-1282-4

Bainbridge, Z. T., Lewis, S. E., Smithers, S. G., Kuhnert, P. M., Henderson, B. L., & Brodie, J. E. (2014). Fine-suspended sediment and water budgets for a large, seasonally dry tropical catchment: Burdekin River catchment, Queensland, Australia. *Water Resources Research, 50*(11), 9067–9087. http://dx.doi.org/10.1002/2013WR014386

Bainbridge, Z. T., Olley, J. M., Lewis, S. E., Stevens, T., & Smithers, S. G. (2024). Tracing sources of inorganic suspended particulate matter in the Great Barrier Reef lagoon, Australia. *Scientific Reports, 14*(1), 15651. https://doi.org/10.1038/s41598-024-66561-5

Bainbridge, Z. T., Wolanski, E., Álvarez-Romero, J. G., Lewis, S. E., & Brodie, J. E. (2012). Fine sediment and nutrient dynamics related to particle size and floc formation in a Burdekin River flood plume, Australia. *Marine Pollution Bulletin, 65*(4-9), 236–248. http://dx.doi.org/10.1016/j.marpolbul.2012.01.043

Batalla, R. J., & Vericat, D. (2009). Hydrological and sediment transport dynamics of flushing flows: implications for management in large Mediterranean Rivers. *River Research and Applications, 25*(3), 297–314. https://doi.org/10.1002/rra.1160

Bayon, G., Toucanne, S., Skonieczny, C., André, L., Bermell, S., Cheron, S., Dennielou, B., Etoubleau, J., Freslon, N., Gauchery, T., Germain, Y., Jorry, S. J., Ménot, G., Monin, L., Ponzevera, E., Rouget, M. L., Tachikawa, K., & Barrat, J. A. (2015). Rare earth elements and neodymium isotopes in world river sediments revisited. *Geochimica et Cosmochimica Acta, 170*(Supplement C), 17–38. https://doi.org/10.1016/j.gca.2015.08.001

Bayram, A., & Kenanoğlu, M. (2016). Variation of total suspended solids versus turbidity and Secchi disk depth in the Borçka Dam Reservoir, Çoruh River Basin, Turkey. *Lake and Reservoir Management, 32*(3), 209–224. https://doi.org/10.1080/10402381.2016.1160168

Bellinger, E. G., & Sigee, D. C. (2010). *Freshwater algae: Identification and use as bioindicators*. Wiley-Blackwell. https://doi.org/https://doi.org/10.1002/9780470689554

Benchimol, M., & Peres, C. A. (2015). Predicting local extinctions of Amazonian vertebrates in forest islands created by a mega dam. *Biological Conservation, 187*, 61–72. https://doi.org/10.1016/j.biocon.2015.04.005

Bertone, E., Stewart, R. A., Zhang, H., & O'Halloran, K. (2015). Analysis of the mixing processes in the subtropical Advancetown Lake, Australia. *Journal of Hydrology, 522*, 67–79. http://dx.doi.org/10.1016/j.jhydrol.2014.12.046

Bilotta, G. S., & Brazier, R. E. (2008). Understanding the influence of suspended solids on water quality and aquatic biota. *Water Research, 42*(12), 2849–2861. https://doi.org/10.1016/j.watres.2008.03.018

Bloesch, J. (1994). Editorial: Sediment resuspension in lakes. *Hydrobiologia, 284*(1), 1–3. https://doi.org/10.1007/bf00005726

Bloesch, J. (1995). Mechanisms, measurement and importance of sediment resuspension in lakes. *Marine and Freshwater Research, 46*(1), 295–304. https://doi.org/10.1071/MF9950295

Blott, S. J., & Pye, K. (2012). Particle size scales and classification of sediment types based on particle size distributions: Review and recommended procedures. *Sedimentology, 59*(7), 2071–2096. https://doi.org/10.1111/j.1365-3091.2012.01335.x

Borchardt, G. (1989). Smectites. In J. B. Dixon & S. B. Weed (Eds.), *Minerals in soil environments* (pp. 675–727). Soil Science Society of America. https://doi.org/https://doi.org/10.2136/sssabookser1.2ed.c14

Bristow, K. L., Charlesworth, P. B., McMahon, G. A., Arunakumaren, J., Bajracharya, K., Ham, G., Sutherland, P., Laidlow, G., Lowis, B., & Nielson, G. (2000). *Towards a more integrated approach to water management in the Burdekin Delta irrigation area* ANCID 2000 Conference, 11–13 September, 2000, Toowoomba, Queensland. https://citeseerx.ist.psu.edu/viewdoc/download?doi=10.1.1.114.9363&rep=rep1&type=pdf

Brizga, S. O., Kaitzke, R., Butler, B., Cappo, M. C., Connolly, N., Lait, R., Pearson, R. J., Pusey, B., Smithers, S., & Werren, G. L. (2006). *Burdekin Basin draft water resources plan: Phase I – current environmental condition report.* https://qldgov.softlinkhosting.com.au:443/liberty/OpacLogin?mode=BASIC&openDetail=true&corporation=DERM&action=search&queryTerm=uuid%3D%22675e6f46c0a81431000907bb23d97868%22&operator=OR&url=%2Fopac%2Fsearch.do

Brown and Root. (2001). *Fluvial supply of sediments to the Queensland coast: Final report.* https://qldgov.softlinkhosting.com.au:443/liberty/OpacLogin?mode=BASIC&openDetail=true&corporation=DERM&action=search&queryTerm=uuid%3D%225ab4a245c0a814100122cacf42aefdf2%22&operator=OR&url=%2Fopac%2Fsearch.do

Brune, G. M. (1953). Trap efficiency of reservoirs. *Transactions, American Geophysical Union, 34*(3), 407–418. http://dx.doi.org/10.1029/TR034i003p00407

Burdekin Project Assessment Committee. (1978). *Report on Burdekin River Project*.

Burdekin Shire Rivers Trust. (2000). *Burdekin River extraction and sediment management plan (including environmental assessment); Final report*.

Bureau of Meteorology. (2016). *Climate data online*. http://www.bom.gov.au/jsp/ncc/cdio/weatherData/av?p_nccObsCode=136&p_display_type=dailyDataFile&p_startYear=&p_c=&p_stn_num=34085 Sellheim, Station number 034085. Last accessed: 11 July 2016. Retrieved 11 July 2016 from http://www.bom.gov.au/climate/data/index.shtml (Sellheim = Station number 034085)

Bureau of Meteorology. (2017). *Rainfall variability*. http://www.bom.gov.au/jsp/ncc/climate_averages/rainfall-variability/index.jsp Last accessed: 20 May 2017. Retrieved 20 May 2017 from http://www.bom.gov.au/jsp/ncc/climate_averages/rainfall-variability/index.jsp

Burford, M. A., Green, S. A., Cook, A. J., Johnson, S. A., Kerr, J. G., & O'Brien, K. R. (2012). Sources and fate of nutrients in a subtropical reservoir. *Aquatic Sciences, 74*(1), 179–190. https://doi.org/10.1007/s00027-011-0209-4

Burford, M. A., McNeale, K., Krogh, C., O'Donohue, M., Packer, T., & McAlister, T. (2004). Water quality monitoring in reservoirs in southeast Queensland. *Water, 31*(8), 64–67. http://www98.griffith.edu.au/dspace/bitstream/10072/7743/1/27745_1.pdf

Burger, R. L. (2003). El Nino, early Peruvian civilization, and human agency: Some thoughts from the Lurin Valley. *Fieldiana Botany, 43*, 90–107.

Burrows, D., & Butler, B. (2007). Determining end-point goals and effective strategies for rehabilitation of coastal wetlands: examples from the Burdekin River, North Queensland. Proceedings of the 5th Australian Stream Management Conference. Australian rivers: making a difference. 21–25 May, 2007, Charles Sturt University, Albury, New South Wales.

Burrows, D., Maughan, M., Butler, B., & Lymburner, L. (2007). *Assessing the condition of wetlands in the Burdekin Catchment using existing GIS data and field knowledge, for the Coastal Catchments Initiative*. TropWATER. https://www.dropbox.com/s/bxzx8c90lly4tbi/06%2020%20Assessing%20the%20condition%20of%20wetlands%20in%20the%20Burdekin%20catchment.pdf?dl=0

Burrows, D. M., & Faithful, J. W. (2003, 6–11 July 2003). From blue to brown: Persistently elevated turbidity resulting from damming of the tropical Burdekin River. 9th International Conference on River Research and Applications, Albury, Australia.

Butt, M. J., Mahmood, R., & Waqas, A. (2011). Sediments deposition due to soil erosion in the watershed region of Mangla Dam. *Environmental Monitoring and Assessment, 181*(1-4), 419–429. http://dx.doi.org/10.1007/s10661-010-1838-0

Butt, M. J., Waqas, A., & Mahmood, R. (2010). The combined effect of vegetation and soil erosion in the water resource management. *Water Resources Management, 24*(13), 3701–3714. http://dx.doi.org/10.1007/s11269-010-9627-7

Campbell, G., Phinn, S. R., & Daniel, P. (2011a). The specific inherent optical properties of three sub-tropical and tropical water reservoirs in Queensland, Australia. *Hydrobiologia, 658*(1), 233–252. https://doi.org/10.1007/s10750-010-0476-4

Campbell, G., Phinn, S. R., Dekker, A. G., & Brando, V. E. (2011b). Remote sensing of water quality in an Australian tropical freshwater impoundment using matrix inversion and MERIS images. *Remote Sensing of Environment, 115*(9), 2402–2414. http://dx.doi.org/10.1016/j.rse.2011.05.003

Cao, Z., Li, J., Pender, G., & Liu, Q. (2015). Whole-process modeling of reservoir turbidity currents by a double layer-averaged model. *Journal of Hydraulic Engineering, 141*(2), 04014069. http://dx.doi.org/10.1061/(ASCE)HY.1943-7900.0000951

Carvalho, N. d. O., Filizola Júnior, N. P., dos Santos, P. M. C., & Lima, J. E. F. W. (2000). *Reservoir sedimentation assessment guideline* (Brazilian Electricity Regulatory Agency - ANEEL, Hydrological Studies and Information Department, Brasilia, Brazil). http://www.aneel.gov.br/documents/656835/14876406/2000_ReservoirSedimentationAssessmentGuideline/13dd9d40-211e-67ce-7edb-1b663f755a76

Cattanéo, F., Guillard, J., Diouf, S., O'Rourke, J., & Grimardias, D. (2021). Mitigation of ecological impacts on fish of large reservoir sediment management through controlled flushing – The case of the Verbois dam (Rhône River, Switzerland). *The Science of The Total Environment, 756*, 144053. https://doi.org/10.1016/j.scitotenv.2020.144053

Chamoun, S., De Cesare, G., & Schleiss, A. J. (2016). Managing reservoir sedimentation by venting turbidity currents: A review. *International Journal of Sediment Research, 31*(3), 195–204. http://dx.doi.org/10.1016/j.ijsrc.2016.06.001

Chanson, H. (1998). Extreme reservoir sedimentation in Australia: A review. *International Journal of Sediment Research, 13*(3), 55–63. https://espace.library.uq.edu.au/view/UQ:9341

Chanson, H. (2012). Reservoir sedimentation in Australia under extreme conditions. In L. Bengtsson, R. W. Herschy, & R. W. Fairbridge (Eds.), *Encyclopedia of Lakes and Reservoirs* (pp. 649–656). Springer Netherlands. https://doi.org/http://dx.doi.org/10.1007/978-1-4020-4410-6_193

Chanson, H., & James, D. P. (1999, 22–27 August 1999). Siltation of Australian reservoirs: Some observations and dam safety implications. Proceedings, 28th IAHR Congress: Hydraulic engineering for sustainable water resources management at the turn of the millenium, Graz, Austria.

Chaudhuri, D. (2017). Empirical approaches in prediction of reservoir sediment distribution—An experience of 57 reservoirs in the USA and India. *International Journal of Sediment Research, 32*(2), 260–276. https://doi.org/10.1016/j.ijsrc.2017.04.001

Chivers, D. P., Al-Batati, F., Brown, G. E., & Ferrari, M. C. O. (2013). The effect of turbidity on recognition and generalization of predators and non-predators in aquatic ecosystems. *Ecology and Evolution, 3*(2), 268–277. https://doi.org/10.1002/ece3.454

Chou, F. N. F., & Wu, C. (2010). Reducing the impacts of flood-induced reservoir turbidity on a regional water supply system. *Advances in Water Resources, 33*(2), 146–157. https://doi.org/10.1016/j.advwatres.2009.10.011

Chudek, E., Horn, A. M., Joo, M., & McLaren, S. (1998). *Stratification behaviour of Queensland dams*. Department of Natural Resources, Resource Sciences Centre, Water Resources Group.

Chung, S. W., Hipsey, M. R., & Imberger, J. (2009). Modelling the propagation of turbid density inflows into a stratified lake: Daecheong Reservoir, Korea. *Environmental Modelling & Software, 24*(12), 1467–1482. http://dx.doi.org/10.1016/j.envsoft.2009.05.016

Churchill, M. A. (1948, May 6-8, 1947). Discussion of paper “Analysis and use of reservoir sedimentation data” by L.C. Gottschalk. Proceedings, Federal Interagency Sedimentation Conference, Denver, Colorado, 1947.

City of Townsville. (2016). *Dam Levels. Last accessed 20 November 2016.* Retrieved 20 November 2016 from https://www.townsville.qld.gov.au/water-waste-and-environment/water-supply-and-dams/dam-levels

Clark, E. H. (1985). The off-site costs of soil erosion. *Journal of Soil and Water Conservation, 40*(1), 19–22. https://www.jswconline.org/content/40/1/19/tab-article-info

Collins, A. L., Blackwell, M., Boeckx, P., Chivers, C.-A., Emelko, M., Evrard, O., Foster, I., Gellis, A., Gholami, H., Granger, S., Harris, P., Horowitz, A. J., Laceby, J. P., Martinez-Carreras, N., Minella, J., Mol, L., Nosrati, K., Pulley, S., Silins, U., da Silva, Y. J., Stone, M., Tiecher, T., Upadhayay, H. R., & Zhang, Y. (2020). Sediment source fingerprinting: benchmarking recent outputs, remaining challenges and emerging themes. *Journal of Soils and Sediments, 20*(12), 4160–4193. https://doi.org/10.1007/s11368-020-02755-4

Cooper, M., Lewis, S. E., & Smithers, S. G. (2017). Spatial and temporal dynamics of suspended sediment causing persistent turbidity in a large reservoir: Lake Dalrymple, Queensland, Australia. *Marine and Freshwater Research, 68*(7), 1377–1390. https://doi.org/10.1071/MF16316

Cooper, M., Lewis, S. E., Stieglitz, T. C., & Smithers, S. G. (2018). Variability of the useful life of reservoirs in tropical locations: A case study from the Burdekin Falls Dam, Australia. *International Journal of Sediment Research, 33*(2), 93–106. https://doi.org/10.1016/j.ijsrc.2017.11.002

Cossu, R., Forrest, A. L., Roop, H. A., Dunbar, G. B., Vandergoes, M. J., Levy, R. H., Stumpner, P., & Schladow, S. G. (2016). Seasonal variability in turbidity currents in Lake Ohau, New Zealand, and their influence on sedimentation. *Marine and Freshwater Research, 67*(11), 1725–1739. http://dx.doi.org/10.1071/MF15043

Croke, J., Bartley, R., Chappell, J., Austin, J. M., Fifield, K., Tims, S. G., Thompson, C. J., & Furuichi, T. (2015, 2015/07/15/). ^{10}Be-derived denudation rates from the Burdekin catchment: The largest contributor of sediment to the Great Barrier Reef. *Geomorphology, 241*, 122–134. https://doi.org/10.1016/j.geomorph.2015.04.003

Csiki, S., & Rhoads, B. L. (2010). Hydraulic and geomorphological effects of run-of-river dams. *Progress in Physical Geography: Earth and Environment, 34*(6), 755–780. http://dx.doi.org/10.1177/0309133310369435

CSIRO Division of Water Resources. (1994). *Nutrient and sediment sources in Chaffey Reservoir catchment*. CSIRO Division of Water Resources. https://doi.org/10.4225/08/594eb7c820218

Dallimore, C. J., Imberger, J., & Hodges, B. R. (2004). Modeling a plunging underflow. *Journal of Hydraulic Engineering, 130*(11), 1068–1076. http://dx.doi.org/10.1061/(ASCE)0733-9429(2004)130:11(1068)

Davies-Colley, R. J., & Smith, D. G. (2001). Turbidity, suspended sediment, and water clarity: A review. *Journal of the American Water Resources Association, 37*(5), 1085–1101. https://doi.org/10.1111/j.1752-1688.2001.tb03624.x

Davis, A. M., Lewis, S. E., O'Brien, D. S., Bainbridge, Z. T., Bentley, C., Mueller, J. F., & Brodie, J. E. (2014). Water resource development and high value coastal wetlands on the Lower Burdekin Floodplain, Australia. In E. Wolanski (Ed.), *Estuaries of Australia in 2050 and beyond* (pp. 223–245). Springer Netherlands. https://doi.org/https://doi.org/10.1007/978-94-007-7019-5_13

Davis, J. R., & Koop, K. (2006). Eutrophication in Australian rivers, reservoirs and estuaries – A Southern Hemisphere perspective on the science and its implications. *Hydrobiologia, 559*(1), 23–76. https://doi.org/10.1007/s10750-005-4429-2

de Caritat, P., Bloch, J., & Hutcheon, I. (1994). LPNORM: A linear programming normative analysis code. *Computers & Geosciences, 20*(3), 313–347. http://dx.doi.org/10.1016/0098-3004(94)90045-0

de Caritat, P., & Cooper, M. (2011). *National Geochemical Survey of Australia: Data Quality Assessment*. https://pid.geoscience.gov.au/dataset/ga/71971

de Caritat, P., Cooper, M., Pappas, W., Thun, C., & Webber, E. (2010). *National Geochemical Survey of Australia: Analytical methods manual*. http://pid.geoscience.gov.au/dataset/ga/70369

de Caritat, P., Dosseto, A., & Dux, F. (2022). *A strontium isoscape of northern Australia (dataset)*. https://dx.doi.org/10.26186/147473

de Caritat, P., Dosseto, A., & Dux, F. (2023). A strontium isoscape of northern Australia. *Earth Syst. Sci. Data, 15*(4), 1655–1673. https://doi.org/10.5194/essd-15-1655-2023

De Cesare, G., Boillat, J.-L., & Schleiss, A. J. (2006). Circulation in stratified lakes due to flood-induced turbidity currents. *Journal of Environmental Engineering, 132*(11), 1508–1517. http://dx.doi.org/10.1061/(ASCE)0733-9372(2006)132:11(1508)

de Cesare, G., Schleiss, A., & Hermann, F. (2001). Impact of turbidity currents on reservoir sedimentation. *Journal of Hydraulic Engineering, 127*(1), 6–16. http://dx.doi.org/10.1061/(asce)0733-9429(2001)127:1(6)

DEHP. (2009). *Queensland Water Quality Guidelines, Version 3*. https://qldgov.softlinkhosting.com.au:443/liberty/OpacLogin?mode=BASIC&openDetail=true&corporation=DERM&action=search&queryTerm=uuid%3D%2204fc3f72c0a862fe49ed47710017669f%22&operator=OR&url=%2Fopac%2Fsearch.do

Dendy, F. E. (1974). Sediment trap efficiency of small reservoirs. *Transactions of the American Society of Agricultural Engineers, 17*(5), 899–901. http://dx.doi.org/10.13031/2013.36994

Department of Natural Resources Mines and Water. (2006). *Burdekin Basin draft water resource plan – Overview report and draft plan*. Department of Natural Resources, Mines and Water. https://qldgov.softlinkhosting.com.au:443/liberty/OpacLogin?mode=BASIC&openDetail=true&corporation=DERM&action=search&queryTerm=uuid%3D%22675e7486c0a8143101f1a6a641d041a0%22&operator=OR&url=%2Fopac%2Fsearch.do

Dhivert, E., Grosbois, C., Coynel, A., Lefèvre, I., & Desmet, M. (2015). Influences of major flood sediment inputs on sedimentary and geochemical signals archived in a reservoir core (Upper Loire Basin, France). *Catena, 126*, 75–85. http://dx.doi.org/10.1016/j.catena.2014.10.030

Donohue, I., & Garcia Molinos, J. (2009). Impacts of increased sediment loads on the ecology of lakes. *Biological Reviews, 84*(4), 517–531. https://doi.org/10.1111/j.1469-185X.2009.00081.x

Dougall, C., Ellis, R., Waters, D., & Carroll, C. (2014). *Modelling reductions of pollutant loads due to improved management practices in the Great Barrier Reef catchments - Burdekin NRM Region* (Technical Report Volume 4, Issue. https://www.reefplan.qld.gov.au/__data/assets/pdf_file/0012/46002/burdekin-catchment-modelling-report.pdf

Douglas, G., Ford, P., Jones, G., & Palmer, M. (2003). Identification of sources of sediment to Lake Samsonvale (North Pine Dam), southeast Queensland, Australia. In D. H. DeBoer, W. Froehlich, T. Mizuyama, & A. Pietroniro (Eds.), *Erosion Prediction in Ungauged Basins: Integrating Methods and Techniques (Proceedings of symposium HS01 held during IUGG2003 at Sapporo, July 2003)* (pp. 33–42). International Association of Hydrological Sciences. https://iahs.info/uploads/dms/12616.09-33-42-HS1-8-G-Douglas.pdf

Douglas, G., Palmer, M., Caitcheon, G., & Orr, P. (2007). Identification of sediment sources to Lake Wivenhoe, south-east Queensland, Australia. *Marine and Freshwater Research, 58*(9), 793–810. http://dx.doi.org/10.1071/MF05175

DRDMW. (2021). *Streamflow discharge data provided by the State of Queensland (Department of Regional Development, Manufacturing and Water).* Formerly published by the Department of Natural Resources and Mines. Retrieved 25 June 2021 from https://water-monitoring.information.qld.gov.au/

Droppo, I., G. (2001). Rethinking what constitutes suspended sediment. *Hydrological Processes, 15*(9), 1551–1564. https://doi.org/10.1002/hyp.228

Duan, D., Ran, Y., Cheng, H., Chen, J. a., & Wan, G. (2014). Contamination trends of trace metals and coupling with algal productivity in sediment cores in Pearl River Delta, South China. *Chemosphere, 103*, 35–43. http://dx.doi.org/10.1016/j.chemosphere.2013.11.011

Effler, S. W., Gelda, R. K., Johnson, D. L., & Owens, E. M. (1998). Sediment resuspension in Cannonsville Reservoir. *Lake and Reservoir Management, 14*(2-3), 225–237. https://doi.org/10.1080/07438149809354333

Effler, S. W., & Matthews, D. A. (2004). Sediment resuspension and drawdown in a water supply reservoir. *Journal of the American Water Resources Association, 40*(1), 251–264. https://doi.org/10.1111/j.1752-1688.2004.tb01023.x

Effler, S. W., Matthews, D. A., Kaser, J. W., Prestigiacomo, A. R., & Smith, D. G. (2006a). Runoff event impacts on a water supply reservoir: Suspended sediment loading, turbid plume behaviour, and sediment deposition. *Journal of the American Water Resources Association, 42*(6), 1697–1710. http://dx.doi.org/10.1111/j.1752-1688.2006.tb06030.x

Effler, S. W., O'Donnell, D. M., Matthews, D. A., Perkins, M., O'Donnell, S. M., Gelda, R. K., Prestigiacomo, A. R., Peng, F., Smith, D. G., Bader, A. P., & Mayfield, J. D. (2008). Insights for the structure of a reservoir turbidity model from monitoring and process studies. *Lake and Reservoir Management, 24*(1), 69–86. http://dx.doi.org/10.1080/07438140809354052

Effler, S. W., Prestigiacomo, A. R., Peng, F., Bulygina, K. B., & Smith, D. G. (2006b). Resolution of turbidity patterns from runoff events in a water supply reservoir, and the advantages of in situ beam atenuation measurements. *Lake and Reservoir Management, 22*(1), 79–93. https://doi.org/10.1080/07438140609353886

Eggins, S. M., Woodhead, J. D., Kinsley, L. P. J., Mortimer, G. E., Sylvester, P., McCulloch, M. T., Hergt, J. M., & Handler, M. R. (1997). A simple method for the precise determination of ≥ 40 trace elements in geological samples by ICPMS using enriched isotope internal standardisation. *Chemical Geology, 134*(4), 311–326. http://dx.doi.org/10.1016/S0009-2541(96)00100-3

Elçi, Ş. (2008). Effects of thermal stratification and mixing on reservoir water quality. *Limnology, 9*(2), 135–142. http://dx.doi.org/10.1007/s10201-008-0240-x

Emamgholizadeh, S., Bateni, S. M., & Nielson, J. R. (2018). Evaluation of different strategies for management of reservoir sedimentation in semi-arid regions: a case study (Dez Reservoir). *Lake and Reservoir Management, 34*(3), 270–282. https://doi.org/10.1080/10402381.2018.1436624

Environment Australia. (2001). *A Directory of Important Wetlands in Australia, Third Edition*. https://www.environment.gov.au/water/wetlands/publications/directory-important-wetlands-australia-third-edition

Espa, P., Brignoli, M. L., Crosa, G., Gentili, G., & Quadroni, S. (2016). Controlled sediment flushing at the Cancano Reservoir (Italian Alps): Management of the operation and downstream environmental impact. *Journal of Environmental Management, 182*, 1–12. http://dx.doi.org/10.1016/j.jenvman.2016.07.021

Espitalie, J., Deroo, G., & Marquis, F. (1985). La pyrolyse Rock-Eval et ses applications. Première partie. *Oil & Gas Science and Technology - Rev. IFP, 40*(5), 563–579. http://dx.doi.org/10.2516/ogst:1985035

Faithful, J. W., & Griffiths, D. J. (2000). Turbid flow through a tropical reservoir (Lake Dalrymple, Queensland, Australia): Responses to a summer storm event. *Lakes and*

Reservoirs: Research and Management, 5(4), 231–247. http://dx.doi.org/10.1046/j.1440-1770.2000.00123.x

Fan, J. (1986). Turbid density currents in reservoirs. *Water International, 11*(3), 107–116. http://dx.doi.org/10.1080/02508068608686404

Fan, J. (2008). Stratified flow through outlets. *Journal of Hydro-environment Research, 2*(1), 3–18. http://dx.doi.org/10.1016/j.jher.2008.04.001

Farnsworth, K. L., & Milliman, J. D. (2003). Effects of climatic and anthropogenic change on small mountainous rivers: The Salinas River example. *Global and Planetary Change, 39*(1-2), 53–64. http://dx.doi.org/10.1016/S0921-8181(03)00017-1

Faure, G., & Mensing, T. M. (2005). *Isotopes: principles and applications* (3rd ed.). Wiley.

Fergusson, C. L., & Henderson, R. A. (2013). Thomson Orogen. In P. A. Jell (Ed.), *Geology of Queensland* (pp. 113–224). Geological Survey of Queensland.

Fernandez, R. L., & Imberger, J. (2006). Bed roughness induced entrainment in a high Richardson number underflow. *Journal of Hydraulic Research, 44*(6), 725–738. https://doi.org/10.1080/00221686.2006.9521724

Fielding, C. R., & Alexander, J. (1996). Sedimentology of the Upper Burdekin River of North Queensland, Australia—an example of a tropical, variable discharge river. *Terra Nova, 8*(5), 447–457. http://dx.doi.org/10.1111/j.1365-3121.1996.tb00770.x

Filstrup, C. T., & Lind, O. T. (2010). Sediment transport mechanisms influencing spatiotemporal resuspension patterns in a shallow, polymictic reservoir. *Lake and Reservoir Management, 26*(2), 85–94. https://doi.org/10.1080/07438141.2010.490771

Finlayson, C. M., Farrell, T. P., & Griffiths, D. J. (1980). Studies of the hydrobiology of a tropical lake in north-western Queensland. II. Seasonal changes in thermal and dissolved oxygen characteristics. *Marine and Freshwater Research, 31*(5), 589–596. http://dx.doi.org/10.1071/MF9800589

Fleming, P. M. (1981). Hydrology and sediment transport. In P. M. Fleming, R. H. Gunn, A. M. Reece, & J. R. McAlpine (Eds.), *Burdekin project ecological study* (pp. 143–180). CSIRO and Department of National Development and Energy. https://doi.org/https://doi.org/10.4225/08/586d396c3664b

Fleming, P. M., & Loofs, M. (1991). *Flood generation and transmission in the Burdekin and Haughton Rivers, North Queensland.* https://publications.csiro.au/rpr/download?pid=procite:e2c0e7d0-8862-420f-a4ce-e2153b19959d&dsid=DS1

Foucher, A., Evrard, O., Cerdan, O., Chabert, C., Lecompte, F., Lefevre, I., Vandromme, R., & Salvador-Blanes, S. (2020). A quick and low-cost technique to identify layers associated with heavy rainfall in sediment archives during the Anthropocene. *Sedimentology, 67*(1), 486–501. https://doi.org/10.1111/sed.12650

Frenette, M., & Julien, P. Y. (1996). *Physical processes governing reservoir sedimentation.* Proceedings, International Conference on Reservoir Sedimentation, Fort Collins, Colorado, USA. https://www.engr.colostate.edu/~pierre/ce_old/resume/Paperspdf/Frenette-Julien%20reservoir96.pdf

Friedl, G., & Wuest, A. (2002). Disrupting biogeochemical cycles – consequences of damming. *Aquatic Science, 64*(1), 55–65. https://doi.org/10.1007/s00027-002-8054-0

Fu, B., Newham, L. T., & Field, J. B. (2008). *Influence of particle size on geochemical suspended sediment tracing in Australia.* Sediment Dynamics in Changing Environments, (Proceedings of a conference in Christchurch, New Zealand, December 2008). https://iahs.info/uploads/dms/14491.07-23-30-02-325-Fu.pdf

Fu, K. D., He, D. M., & Lu, X. X. (2008). Sedimentation in the Manwan Reservoir in the Upper Mekong and its downstream impacts. *Quaternary International, 186*(1), 91–99. http://dx.doi.org/10.1016/j.quaint.2007.09.041

Fukumoto, Y., Li, X., Yasuda, Y., Okamura, M., Yamada, K., & Kashima, K. (2015). The Holocene environmental changes in southern Indonesia reconstructed from highland caldera lake sediment in Bali Island. *Quaternary International, 374*, 15–33. http://dx.doi.org/10.1016/j.quaint.2015.03.020

Furnans, J., & Austin, B. (2008). Hydrographic survey methods for determining reservoir volume. *Environmental Modelling & Software, 23*(2), 139–146. http://dx.doi.org/10.1016/j.envsoft.2007.05.011

Gao, B., Wei, X., Zhou, H. D., Lu, J., Hao, H., & Wang, X. H. (2014). Pollution characteristics and possible sources of seldom monitored trace elements in surface sediments collected from Three Gorges Reservoir, China [Article]. *Scientific World Journal, 2014*, 170639, Article 170639. https://doi.org/10.1155/2014/170639

Gao, F., Guo, W., Wang, J., & Zhao, X. (2015). Historical record of trace elements input and risk in the shallow freshwater lake, North China. *Journal of Geochemical Exploration, 155*, 26–32. http://dx.doi.org/10.1016/j.gexplo.2015.04.002

Garg, V., & Jothiprakash, V. (2008). Estimation of useful life of a reservoir using sediment trap efficiency. *Journal of Spatial Hydrology, 8*(2), 1–14. https://scholarsarchive.byu.edu/josh/vol8/iss2/2

Garzon-Garcia, A., Wallace, R., Huggins, R., Turner, R. D. R., Smith, R. A., Orr, D., Ferguson, B., Gardiner, R., Thomson, B., & Warne, M. S. J. (2015). *Total suspended solids, nutrient and pesticide loads (2013–2014) for rivers that discharge to the Great Barrier Reef – Great Barrier Reef Catchment Loads Monitoring Program*. https://www.reefplan.qld.gov.au/__data/assets/pdf_file/0033/45987/2013-2014-gbr-catchment-loads-technical-report.pdf

Gaspar, L., Blake, W. H., Lizaga, I., Latorre, B., & Navas, A. (2022). Particle size effect on geochemical composition of experimental soil mixtures relevant for unmixing modelling. *Geomorphology, 403*, 108178. https://doi.org/10.1016/j.geomorph.2022.108178

Geddes, M. C. (1984). Limnology of Lake Alexandrina, River Murray, South Australia, and the effects of nutrients and light on the phytoplankton. *Marine and Freshwater Research, 35*(4), 399–415. http://dx.doi.org/10.1071/MF9840399

Geddes, M. C. (1988). The role of turbidity in the limnology of Lake Alexandrina, River Murray, South Australia; comparisons between clear and turbid phases. *Marine and Freshwater Research, 39*(2), 201–209. http://dx.doi.org/10.1071/MF9880201

Gelda, R. K., & Effler, S. W. (2007). Modeling turbidity in a water supply reservoir: Advancements and issues. *Journal of Environmental Engineering, 133*(2), 139–148. http://dx.doi.org/10.1061/(ASCE)0733-9372(2007)133:2(139)

Gelda, R. K., Effler, S. W., Prestigiacomo, A. R., Peng, F., Effler, A. J. P., Wagner, B. A., Perkins, M., O'Donnell, D. M., O'Donnell, S. M., & Pierson, D. C. (2013). Characterizations and modeling of turbidity in a water supply reservoir following an extreme runoff event. *Inland Waters, 3*(3), 377–390. http://dx.doi.org/10.5268/iw-3.3.581

Georgoulas, A. N., Kopasakis, K. I., Angelidis, P. B., & Kotsovinos, N. E. (2012). Numerical investigation of continuous, high density turbidity currents response, in the variation of fundamental flow controlling parameters. *Computers & Fluids, 60*, 21–35. http://dx.doi.org/10.1016/j.compfluid.2012.02.025

Gill, M. A. (1979). Sedimentation and useful life of reservoirs. *Journal of Hydrology, 44*(1-2), 89–95. http://dx.doi.org/10.1016/0022-1694(79)90148-3

Gilvear, D. J., & Petts, G. E. (1985). Turbidity and suspended solids variations downstream of a regulating reservoir. *Earth Surface Processes and Landforms, 10*(4), 363–373. https://doi.org/10.1002/esp.3290100408

Giovanoli, F. (1990). Horizontal transport and sedimentation by interflows and turbidity currents in Lake Geneva. In M. M. Tilzer & C. Serruya (Eds.), *Large Lakes* (pp. 175–195). Springer Berlin Heidelberg. https://doi.org/https://doi.org/10.1007/978-3-642-84077-7_9

Gippel, C. J. (1995). Potential of turbidity monitoring for measuring the transport of suspended solids in streams. *Hydrological Processes, 9*(1), 83-97. https://doi.org/10.1002/hyp.3360090108

Gladstone, C., & Pritchard, D. (2010). Patterns of deposition from experimental turbidity currents with reversing buoyancy. *Sedimentology, 57*(1), 53–84. http://dx.doi.org/10.1111/j.1365-3091.2009.01087.x

Goldstein, S. J., & Jacobsen, S. B. (1987). The Nd and Sr isotopic systematics of river-water dissolved material: Implications for the sources of Nd and Sr in seawater. *Chemical Geology: Isotope Geoscience section, 66*(3-4), 245–272. https://doi.org/10.1016/0168-9622(87)90045-5

Gomboš, M., Tall, A., Trpčevská, J., Kandra, B., Pavelkova, D., & Balejčíková, L. (2018). Sedimentation rate of soil microparticles. *Arabian Journal of Geosciences, 11*(20), 635. https://doi.org/10.1007/s12517-018-4002-8

Grabowski, R. C., Droppo, I. G., & Wharton, G. (2011). Erodibility of cohesive sediment: The importance of sediment properties. *Earth-Science Reviews, 105*(3), 101–120. https://doi.org/10.1016/j.earscirev.2011.01.008

Gray, J. R., Glysson, G. D., Turcios, L. M., & Schwarz, G. E. (2000). *Comparability of suspended-sediment concentration and total suspended solids data* (Water-Resources Investigations Report 00-4191, Issue. https://water.usgs.gov/osw/pubs/WRIR00-4191.pdf

Griffiths, D. J., & Faithful, J. W. (1996). Effects of the sediment load of a tropical North-Australian river on water column characteristics in the receiving impoundment. *Archiv Fur Hydrobiologie: Large Rivers, 10*(1-4), 147–157. http://dx.doi.org/10.1127/lr/10/1996/147

Griffiths, D. J., & Farrell, P. D. (1991). Turbidity and water quality in tropical reservoirs in Northern Australia. *Internationale Vereinigung fuer Theoretische und Angewandte Limnologie: Verhandlungen, 24*(3), 1465–1470. https://doi.org/10.1080/03680770.1989.11899003 (Reprint of: Proceedings of the International Association for Theoretical and Applied Limnology, Congress in Munich 1989)

Gu, R., McCutcheon, S. C., & Wang, P.-F. (1996). Modeling reservoir density underflow and interflow from a chemical spill. *Water Resources Research, 32*(3), 695–705. http://dx.doi.org/10.1029/95WR03486

Guo, C., Jin, Z., Guo, L., Lu, J., Ren, S., & Zhou, Y. (2020). On the cumulative dam impact in the upper Changjiang River: Streamflow and sediment load changes. *Catena, 184*, 104250. https://doi.org/10.1016/j.catena.2019.104250

Hach Company. (2004). *Portable turbidimeter Model 2100P – Instrument and Procedure Manual*. https://www.manualslib.com/manual/1279581/Hach-2100p.html

Hahn, J., Opp, C., Evgrafova, A., Groll, M., Zitzer, N., & Laufenberg, G. (2018). Impacts of dam draining on the mobility of heavy metals and arsenic in water and basin bottom sediments of three studied dams in Germany. *Science of The Total Environment, 640-641*, 1072–1081. https://doi.org/10.1016/j.scitotenv.2018.05.295

Hart, R. C. (1986). Zooplankton abundance, community structure and dynamics in relation to inorganic turbidity, and their implications for a potential fishery in subtropical Lake le Roux, South Africa. *Freshwater Biology, 16*(3), 351–371. https://doi.org/10.1111/j.1365-2427.1986.tb00976.x

Hart, R. C. (1999). On the limnology of Spioenkop, a turbid reservoir on the upper Thukela River, with particular reference to the structure and dynamics of its plankton community. *Water S. A., 25*(4), 519–528. http://www.wrc.org.za/wp-content/uploads/mdocs/WaterSA_1999_04_oct99_p519.pdf

Hawkins, P. R., & Griffiths, D. J. (1993). Artificial destratification of a small tropical reservoir: Effects upon the phytoplankton. *Hydrobiologia, 254*(3), 169–181. https://doi.org/10.1007/BF00014111

Hebbert, B., Imberger, J., Loh, I., & Patterson, J. (1979). Collie River underflow into the Wellington Reservoir. *Journal of the Hydraulics Division, ASCE, 105*(5), 533–545. https://doi.org/10.1061/JYCEAJ.0005206

Heinemann, H. G. (1981). A new sediment trap efficiency curve for small reservoirs. *Water Resources Bulletin, 17*(5), 825–830. http://dx.doi.org/10.1111/j.1752-1688.1981.tb01304.x

Helfer, F., Lemckert, C., & Zhang, H. (2012). Impacts of climate change on temperature and evaporation from a large reservoir in Australia. *Journal of Hydrology, 475*, 365–378. http://dx.doi.org/10.1016/j.jhydrol.2012.10.008

Hickel, W. (1984). Seston retention by Whatman GF/C glass-fiber filters. *Marine ecology. Progress series, 16*(1-2), 185–191. https://www.int-res.com/articles/meps/16/m016p185.pdf

Hilton, J., Lishman, J. P., & Allen, P. V. (1986). The dominant processes of sediment distribution and focusing in a small, eutrophic, monomictic lake. *Limnology and Oceanography, 31*(1), 125–133. http://dx.doi.org/10.4319/lo.1986.31.1.0125

Hu, C., Hu, W., Zhang, F., Hu, Z., Li, X., & Chen, Y. (2006). Sediment resuspension in the Lake Taihu, China. *Chinese Science Bulletin, 51*(6), 731–737. https://doi.org/10.1007/s11434-006-0731-2

Huang, T., Li, X., Rijnaarts, H., Grotenhuis, T., Ma, W., Sun, X., & Xu, J. (2014, 7/1/). Effects of storm runoff on the thermal regime and water quality of a deep, stratified reservoir in a temperate monsoon zone, in Northwest China. *Science of The Total Environment, 485–486*, 820-827. http://dx.doi.org/10.1016/j.scitotenv.2014.01.008

Hubble, D. S., & Harper, D. M. (2001). Impact of light regimen and self-shading by algal cells on primary productivity in the water column of a shallow tropical lake (Lake Naivasha, Kenya). *Lakes and Reservoirs: Research and Management, 6*(2), 143–150. https://doi.org/10.1046/j.1440-1770.2001.00133.x

Hydrolab Corporation. (2002). *Hydrolab Quanta Operating Manual*. Hydrolab Corporation. http://www.ott.com/download/hydrolab-quanta-manual/

Imberger, J. (1985a). The diurnal mixed layer. *Limnology and Oceanography, 30*(4), 737–770. https://doi.org/10.4319/lo.1985.30.4.0737

Imberger, J. (1985b). Thermal characteristics of standing waters: An illustration of dynamic processes. *Hydrobiologia, 125*(1), 7–29. https://doi.org/10.1007/BF00045923

Imtiyaz, N., Lee, F.-Z., Lin, G.-F., & Lai, J.-S. (2024). Modeling and analysis of turbidity currents in a reservoir with the dredged guiding channel. *KSCE Journal of Civil Engineering, 28*(8), 3257–3269. https://doi.org/10.1007/s12205-024-1054-z

International Atomic Energy Agency. (2003). *Collection and preparation of bottom sediment samples for analysis of radionuclides and trace elements.* (IAEA-TECDOC-1360, Issue. I. A. E. Agency. http://www-pub.iaea.org/MTCD/Publications/PDF/te_1360_web.pdf

Issa, I. E., Al-Ansari, N., Knutsson, S., & Sherwany, G. (2015). Monitoring and evaluating the sedimentation process in Mosul Dam Reservoir using trap efficiency approaches. *Engineering, 7*(4), 190–202. https://doi.org/10.4236/eng.2015.74015

Jansen, R. B. (1980). *Dams and public safety*. Water resources technical publication, U.S. Department of the Interior, Water and Power Resources Service. https://www.usbr.gov/tsc/techreferences/mands/mands-pdfs/AZ1130.pdf

Jones, G. J., & Poplawski, W. (1998). Understanding and management of cyanobacterial blooms in sub-tropical reservoirs of Queensland, Australia. *Water Science and Technology, 37*(2), 161–168. http://dx.doi.org/10.1016/S0273-1223(98)00020-1

Jones, P. A., Loughran, R. J., & Elliott, G. L. (2000). Sedimentation in a semi-arid zone reservoir in Australia determined by 137Cs [Article]. *Acta Geologica Hispanica, 35*(3-4), 329–338. https://www.ars.usda.gov/ARSUserFiles/80420510/Cesium137/Jones.pdf

Juracek, K. E. (2015). The aging of America's reservoirs: In-reservoir and downstream physical changes and habitat implications. *JAWRA Journal of the American Water Resources Association, 51*(1), 168–184. https://doi.org/10.1111/jawr.12238

Kerr, S. J. (1995). *Silt, turbidity and suspended sediments in the aquatic environment: An annotated bibliography and literature review*. http://www.ontarioriversalliance.ca/silt-turbidity-and-suspended-sediments-in-the-aquatic-environment-an-annotated-bibliography-and-literature-review/

Khakzad, H., & Elfimov, V. I. (2015). Environmental reviews and case studies: A review of environmental characteristics and effects of Dez Dam flushing operation on downstream. *Environmental Practice, 17*(3), 211–232. http://dx.doi.org/10.1017/S1466046615000198

Khosronejad, A. (2009). Optimization of the Sefid-Roud Dam desiltation process using a sophisticated one-dimensional numerical model. *International Journal of Sediment Research, 24*(2), 189–200. http://dx.doi.org/10.1016/S1001-6279(09)60026-3

Kinhill Cameron McNamara. (1996). *Strategic plan for managment and improvement of the lower Burdekin River*.

Kondolf, G. M., Gao, Y., Annandale, G. W., Morris, G. L., Jiang, E., Zhang, J., Cao, Y., Carling, P., Fu, K., & Guo, Q. (2014). Sustainable sediment management in reservoirs and regulated rivers: Experiences from five continents. *Earth's Future, 2*(5), 256–280. https://doi.org/10.1002/2013EF000184

Kroon, F. J., Kuhnert, P. M., Henderson, B. L., Wilkinson, S. N., Kinsey-Henderson, A., Abbott, B., Brodie, J. E., & Turner, R. D. R. (2012). River loads of suspended solids, nitrogen, phosphorus and herbicides delivered to the Great Barrier Reef lagoon. *Marine Pollution Bulletin, 65*(4-9), 167–181. http://dx.doi.org/10.1016/j.marpolbul.2011.10.018

Kuhnert, P. M., Henderson, B. L., Lewis, S. E., Bainbridge, Z. T., Wilkinson, S. N., & Brodie, J. E. (2012). Quantifying total suspended sediment export from the Burdekin River catchment using the loads regression estimator tool. *Water Resources Research, 48*(4), W04533. https://doi.org/10.1029/2011WR011080

Kuhnert, P. M., Pagendam, D. E., Bartley, R., Gladish, D. W., Lewis, S. E., & Bainbridge, Z. T. (2018). Making management decisions in the face of uncertainty: A case study using the Burdekin catchment in the Great Barrier Reef. *Marine and Freshwater Research, 69*(8), 1187–1200. https://doi.org/10.1071/MF17237

Kummu, M., & Varis, O. (2007). Sediment-related impacts due to upstream reservoir trapping, the Lower Mekong River. *Geomorphology, 85*(3-4), 275–293. http://dx.doi.org/10.1016/j.geomorph.2006.03.024

LaBounty, J. F., & Horn, M. J. (1997). The influence of drainage from the Las Vegas Valley on the limnology of Boulder Basin, Lake Mead, Arizona-Nevada. *Lake and Reservoir Management, 13*(2), 95–108. http://dx.doi.org/10.1080/07438149709354301

Laceby, J. P., Evrard, O., Smith, H. G., Blake, W. H., Olley, J. M., Minella, J. P. G., & Owens, P. N. (2017, 6//). The challenges and opportunities of addressing particle size effects in sediment source fingerprinting: A review. *Earth-Science Reviews, 169*, 85-103. https://doi.org/10.1016/j.earscirev.2017.04.009

Laceby, J. P., McMahon, J., Evrard, O., & Olley, J. (2015). A comparison of geological and statistical approaches to element selection for sediment fingerprinting. *Journal of Soils and Sediments, 15*(10), 2117–2131. https://doi.org/10.1007/s11368-015-1111-9

Lahlou, A. (1996). Environmental and socio-economic impacts of erosion and sedimentation in North Africa. Erosion and sediment yield: Global and regional perspectives (Proceedings of the Exeter Symposium, July 1996), Exeter, UK, 1996.

Lai, J.-S., & Shen, H. W. (1996). Flushing sediment through reservoirs. *Journal of Hydraulic Research, 34*(2), 237–255. http://dx.doi.org/10.1080/00221689609498499

Lai, Y. G., Huang, J., & Wu, K. (2015). Reservoir turbidity current modeling with a two-dimensional layer-averaged model. *Journal of Hydraulic Engineering, 141*(12), 04015029. http://dx.doi.org/10.1061/(ASCE)HY.1943-7900.0001041

Lajczak, A. (1996). Modelling the long-term course of non-flushed reservoir sedimentation and estimating the life of dams. *Earth Surface Processes and Landforms, 21*(12), 1091–1107. http://dx.doi.org/10.1002/(sici)1096-9837(199612)21:12<1091::aid-esp653>3.0.co;2-2

Land & Water Australia. (2002). *National River Contaminants Program...integrated management of nutrients, sediment and salt in Australian rivers. Program Plan 2001/02–2004/05*. https://www.insidecotton.com/sites/default/files/article-files/pr020226.pdf

Langmuir, D. (1997). *Aqueous environmental geochemistry*. Prentice Hall.

Lee, F.-Z., Lai, J.-S., & Sumi, T. (2022). Reservoir sediment management and downstream river impacts for sustainable water resources—case study of Shihmen Reservoir. *Water, 14*(3), 479. https://www.mdpi.com/2073-4441/14/3/479

Lee, F.-Z., Lai, J.-S., Tan, Y.-C., & Sung, C.-C. (2014). Turbid density current venting through reservoir outlets. *KSCE Journal of Civil Engineering, 18*(2), 694–705. http://dx.doi.org/10.1007/s12205-014-0275-y

Lee, H.-Y., & Yu, W.-S. (1997). Experimental study of reservoir turbidity current. *Journal of Hydraulic Engineering, 123*(6), 520–528. https://doi.org/10.1061/(ASCE)0733-9429(1997)123:6(520)

Lei, Y., Du, X., Wang, Y., Chen, Q., Tang, H., & Jiang, S. (2018). Diatom succession dynamics controlled by multiple forces in a subtropical reservoir in southern China. *Quaternary International, 493*, 227–244. https://doi.org/10.1016/j.quaint.2018.05.048

Lewis, S., Bainbridge, Z., & Smithers, S. (2021). *A synthesis of the changing sources, transport and delivery of sand to the Burdekin River Delta: implications for the stability of the Bowling Green spit* (A Report for Water Planning Ecology, Science and Technology Division, Department of Environment and Science). TropWATER James Cook University. https://researchonline.jcu.edu.au/79692/

Lewis, S. E., Bainbridge, Z. T., Kuhnert, P. M., Sherman, B. S., Henderson, B., Dougall, C., Cooper, M., & Brodie, J. E. (2013). Calculating sediment trapping efficiencies for reservoirs in tropical settings: A case study from the Burdekin Falls Dam, NE Australia. *Water Resources Research, 49*(2), 1017–1029. http://dx.doi.org/10.1002/wrcr.20117

Lewis, S. E., Bainbridge, Z. T., Sherman, B. S., Brodie, J. E., & Cooper, M. (2009). *Trapping efficiency of the Burdekin Falls Dam, north Queensland: Estimates from a three-year monitoring program. Report to the Marine and Tropical Sciences Research Facility*. http://rrrc.org.au/wp-content/uploads/2014/06/372-JCU-Lewis-S-et-al-2009-Burdekin-Dam-trapping-efficiency.pdf

Lewis, S. E., Brodie, J. E., Ledee, E., & Alewijnse, M. (2006). *The spatial extent of delivery of terrestrial materials from the Burdekin region in the Great Barrier Reef lagoon* (ACTFR 06/02). (ACTFR Technical Report 06/02 to North Queensland Dry Tropics, Issue 1). James Cook University. https://www.dropbox.com/s/wvg2tbgxn84xyfq/06%2002%20Burdekin%20Receiving%20Waters%20Report.pdf?dl=0

Lewis, W. M. (1987). Tropical limnology. *Annual Review of Ecology and Systematics, 18*, 159–184. https://www.jstor.org/stable/2097129

Li, B., Chen, N., Wang, W., Wang, C., Schmitt, R. J. P., Lin, A., & Daily, G. C. (2021). Eco-environmental impacts of dams in the Yangtze River Basin, China. *The Science of The Total Environment*(774), 145743. https://doi.org/10.1016/j.scitotenv.2021.145743

Li, B.-P., Zhao, J.-X., Greig, A., Collerson, K. D., Feng, Y.-X., Sun, X.-M., Guo, M.-S., & Zhuo, Z.-X. (2006). Characterisation of Chinese Tang sancai from Gongxian and Yaozhou kilns using ICP-MS trace element and TIMS Sr–Nd isotopic analysis. *Journal of Archaeological Science, 33*(1), 56–62. http://dx.doi.org/10.1016/j.jas.2005.06.007

Li, W., Chen, X., Xu, S., Wang, T., Han, D., & Xiao, Y. (2024). Effects of storm runoff on the spatial–temporal variation and stratified water quality in Biliuhe Reservoir, a drinking water reservoir. *Environmental science and pollution research international, 31*(13), 19556–19574. https://doi.org/10.1007/s11356-024-32431-w

Lick, W., Lick, J., & Kirk Ziegler, C. (1994). The resuspension and transport of fine-grained sediments in Lake Erie. *Journal of Great Lakes Research, 20*(4), 599–612. https://doi.org/10.1016/s0380-1330(94)71181-3

Lietman, P. L. (1997). *Evaluation of agricultural best-management practices in the Conestoga River Headwaters, Pennsylvania: A summary report, 1982–1990* (U.S. Geological Survey Water-supply Paper 2493, Issue. U.S. Government Printing Office.

Lind, O. T., Chrzanowski, T. H., & Dávalos-Lind, L. (1997). Clay turbidity and the relative production of bacterioplankton and phytoplankton. *Hydrobiologia, 353*(1-3), 1–18. https://doi.org/10.1023/A:1003039932699

Lind, O. T., Doyle, R., Vodopich, D. S., Trotter, B. G., Limon, J. G., & Davalos-Lind, L. (1992). Clay turbidity: Regulation of phytoplankton production in a large, nutrient-rich tropical lake. *Limnology and Oceanography, 37*(3), 549–565. https://doi.org/10.4319/lo.1992.37.3.0549

Liu, C., Sui, J., He, Y., & Hirshfield, F. (2013). Changes in runoff and sediment load from major Chinese rivers to the Pacific Ocean over the period 1955–2010. *International Journal of Sediment Research, 28*(4), 486–495. http://dx.doi.org/10.1016/S1001-6279(14)60007-X

Liu, W., Wu, J., Zeng, H., & Ma, L. (2014). Geochemical evidence of human impacts on deep Lake Fuxian, southwest China. *Limnologica - Ecology and Management of Inland Waters, 45*, 1–6. http://dx.doi.org/10.1016/j.limno.2013.09.003

Liu, W. C., & Chen, W. B. (2013). Modeling hydrothermal, suspended solids transport and residence time in a deep reservoir. *International Journal of Environmental Science and Technology, 10*(2), 251–260. http://dx.doi.org/10.1007/s13762-012-0147-2

Long, E. R., Macdonald, D. D., Smith, S. L., & Calder, F. D. (1995). Incidence of adverse biological effects within ranges of chemical concentrations in marine and estuarine sediments. *Environmental Management, 19*(1), 81–97. https://doi.org/10.1007/bf02472006

Lough, J. M. (1991). Rainfall variations in Queensland, Australia: 1891–1986. *International Journal of Climatology, 11*(7), 745–768. http://dx.doi.org/10.1002/joc.3370110704

Lough, J. M. (2007). Tropical river flow and rainfall reconstructions from coral luminescence: Great Barrier Reef, Australia. *Paleoceanography, 22*(2), PA2218. http://dx.doi.org/10.1029/2006PA001377

Lymburner, L., Botha, E., Hestir, E., Anstee, J., Sagar, S., Dekker, A., & Malthus, T. (2016). Landsat 8: Providing continuity and increased precision for measuring multi-decadal time series of total suspended matter. *Remote Sensing of Environment, 185*, 108–118. http://dx.doi.org/10.1016/j.rse.2016.04.011

Macías, J. G. L., & Lind, O. T. (1990). The management of Lake Chapala (México): Considerations after significant changes in the water regime. *Lake and Reservoir Management, 6*(1), 61–70. https://doi.org/10.1080/07438149009354696

MacKinnon, M. R., & Herbert, B. W. (1996). Temperature, dissolved oxygen and stratification in a tropical reservoir, Lake Tinaroo, Northern Queensland, Australia. *Marine and Freshwater Research, 47*(7), 937–949. http://dx.doi.org/10.1071/MF9960937

Mahmood, K. (1987). *Reservoir sedimentation: impact, extent, and mitigation* (World Bank Technical Paper WTP-71). (Technical paper no. 71, Issue. http://documents.worldbank.org/curated/en/888541468762328736/Reservoir-sedimentation-impact-extent-and-mitigation

Majoro, F., Wali, U. G., Munyaneza, O., Naramabuye, F.-X., Bugenimana, E. D., & Mukamwambali, C. (2020). Sediment transport and its impacts on Lake Kivu, Gihira Water Treatment Plant and various hydropower plants along Sebeya River in Rwanda. *Journal of water resource and protection, 12*(11), 934–950. https://doi.org/10.4236/jwarp.2020.1211055

Malvern Instruments Ltd. (1999). *Mastersizer 2000 Operators Guide* (Vol. MAN0247 Issue 2.0, October 1999). Malvern Instruments Ltd., Malvern, United Kingdom.

Marosi, M., Ghomeshi, M., & Sarkardeh, H. (2015). Sedimentation control in the reservoirs by using an obstacle. *Sadhana, 40*(4), 1373–1383. http://dx.doi.org/10.1007/s12046-015-0333-2

Marti, C. L., Mills, R., & Imberger, J. (2011). Pathways of multiple inflows into a stratified reservoir: Thomson Reservoir, Australia. *Advances in Water Resources, 34*(5), 551–561. http://dx.doi.org/10.1016/j.advwatres.2011.01.003

Matthews, M. D. (1991). The effect of grain shape and density on size measurement. In J. P. M. Syvitski (Ed.), *Principles, Methods, and Application of Particle Size Analysis* (pp. 22–33). Cambridge University Press. https://doi.org/https://doi.org/10.1017/CBO9780511626142.004

Mazhar, N., Mirza, A. I., Butt, Z. S., Nawaz, M., & Akram, M. A. N. (2021). Advancement of the pivot point of underwater delta: A study of Tarbela Reservoir, Haripur, Pakistan. *Journal of Himalayan Earth Sciences, 54*(2), 40–46. http://nceg.uop.edu.pk/GeologicalBulletin/Vol-54(2)-2021/Vol-54(2)-2021-Paper4.pdf

McCloskey, G. L., Baheerathan, R., Dougall, C., Ellis, R., Bennett, F. R., Waters, D., Darr, S., Fentie, B., Hateley, L. R., & Askildsen, M. (2021). Modelled estimates of fine sediment and particulate nutrients delivered from the Great Barrier Reef catchments. *Marine Pollution Bulletin, 165*, 112163. https://doi.org/10.1016/j.marpolbul.2021.112163

McCullough, G. K., Barber, D., & Cooley, P. M. (2007). The vertical distribution of runoff and its suspended load in Lake Malawi. *Journal of Great Lakes Research, 33*(2), 449–465. http://dx.doi.org/10.3394/0380-1330(2007)33[449:TVDORA]2.0.CO;2

Miller, C. R. (1953). *Determination of the unit weight of sediment for use in sediment volume computations* (US Department of the Interior, Bureau of Reclamation, Project Planning Division, Denver, USA). https://www.usbr.gov/library/

Mindat.org. (2023). *Montmorillonite*. Hudson Institute of Mineralogy. Retrieved 4 June 2023 from https://www.mindat.org/min-2821.html

Mitchell, A., Furnas, M., De'ath, G., Brodie, J., & Lewis, S. (2006). *A report into water quality condition of the Burdekin River and surrounds based on the AIMS end-of-catchment sampling program*. https://drive.google.com/file/d/0B2eYGb5_l-addWtYR2djQmVQVkU/view?resourcekey=0-XreLlO1EC32hfYFv1utslg

Moore, D. M., & Reynolds, R. C. (1997). *X-ray diffraction and the identification and analysis of clay minerals* (2nd ed.). Oxford University Press.

Moore, J. W., & Ramamoorthy, S. (2012). *Heavy metals in natural waters: applied monitoring and impact assessment* (1st ed.). Springer, New York, NY. https://doi.org/https://doi.org/10.1007/978-1-4612-5210-8

Morris, G. L., & Fan, J. (1998). *Reservoir sedimentation handbook: Design and management of dams, reservoirs, and watersheds for sustainable use*. McGraw-Hill Book Co. https://www.reservoirsedimentation.com/

Mueller, P., Thoss, H., Kaempf, L., & Güntner, A. (2013). A buoy for continuous monitoring of suspended sediment dynamics. *Sensors (Basel, Switzerland), 13*(10), 13779–13801. http://dx.doi.org/10.3390/s131013779

Müller, M., De Cesare, G., & Schleiss, A. J. (2017). Experiments on the effect of inflow and outflow sequences on suspended sediment exchange rates. *International Journal of Sediment Research, 32*(2), 155–170. https://doi.org/10.1016/j.ijsrc.2017.02.001

Munir, S. (2011). *Role of sediment transport in operation and maintenance of supply and demand based irrigation canals: Application to Machai Maira branch canals* [PhD dissertation, Hydraulic Engineering-Land and Water Development Core, UNESCO-IHE, Institute for Water Education, Delft, the Netherlands]. Purchasable through CRC

Press of Boca Raton, Florida. https://books.google.com.au/books?id=dvvRBQAAQBAJ

Murthy, B. N. (1977). *Life of reservoir* (Central Board of Irrigation and Power Technical Report 19, New Delhi, India). (Issue 19 of Technical Report, Central Board of Irrigation and Power), Issue. http://books.google.com.au/books?id=jSp7GwAACAAJ

Nagle, G. N., Fahey, T. J., & Lassoie, J. P. (1999). Management of sedimentation in tropical watersheds. *Environmental Management, 23*(4), 441–452. http://dx.doi.org/10.1007/s002679900199

Nava, V., Chandra, S., Aherne, J., Alfonso, M. B., Antão-Geraldes, A. M., Attermeyer, K., Bao, R., Bartrons, M., Berger, S. A., Biernaczyk, M., Bissen, R., Brookes, J. D., Brown, D., Cañedo-Argüelles, M., Canle, M., Capelli, C., Carballeira, R., Cereijo, J. L., Chawchai, S., Christensen, S. T., Christoffersen, K. S., de Eyto, E., Delgado, J., Dornan, T. N., Doubek, J. P., Dusaucy, J., Erina, O., Ersoy, Z., Feuchtmayr, H., Frezzotti, M. L., Galafassi, S., Gateuille, D., Gonçalves, V., Grossart, H. P., Hamilton, D. P., Harris, T. D., Kangur, K., Kankılıç, G. B., Kessler, R., Kiel, C., Krynak, E. M., Leiva-Presa, À., Lepori, F., Matias, M. G., Matsuzaki, S. S., McElarney, Y., Messyasz, B., Mitchell, M., Mlambo, M. C., Motitsoe, S. N., Nandini, S., Orlandi, V., Owens, C., Özkundakci, D., Pinnow, S., Pociecha, A., Raposeiro, P. M., Rõõm, E. I., Rotta, F., Salmaso, N., Sarma, S. S. S., Sartirana, D., Scordo, F., Sibomana, C., Siewert, D., Stepanowska, K., Tavşanoğlu Ü, N., Tereshina, M., Thompson, J., Tolotti, M., Valois, A., Verburg, P., Welsh, B., Wesolek, B., Weyhenmeyer, G. A., Wu, N., Zawisza, E., Zink, L., & Leoni, B. (2023). Plastic debris in lakes and reservoirs. *Nature, 619*(7969), 317–322. https://doi.org/10.1038/s41586-023-06168-4

Newham, M., Moss, A. J., Moulton, D., & Thames, D. (2017). *Draft environmental values and water quality guidelines: Burdekin River Basin fresh and estuarine waters*. https://qldgov.softlinkhosting.com.au:443/liberty/OpacLogin?mode=BASIC&openDetail=true&corporation=DERM&action=search&queryTerm=uuid%3D%22cf2c6a9f0a0200f074e58699001e0a09%22&operator=OR&url=%2Fopac%2Fsearch.do

NHMRC, & NRMMC. (2011). *Australian Drinking Water Guidelines Paper 6, National Water Quality Management Strategy*. National Health and Medical Research Council, National Resource Management Ministerial Council, Commonwealth of Australia, Canberra. https://www.nhmrc.gov.au/about-us/publications/australian-drinking-water-guidelines

Norrish, K., & Pickering, J. G. (1983). Clay minerals. In Division of Soils CSIRO (Ed.), *Soils, an Australian viewpoint* (pp. 281–308).

Oehy, C. D., & Schleiss, A. J. (2007). Control of turbidity currents in reservoirs by solid and permeable obstacles. *Journal of Hydraulic Engineering, 133*(6), 637–648. http://dx.doi.org/10.1061/(ASCE)0733-9429(2007)133:6(637)

Olive, L. J., & Olley, J. M. (1997, 312 + viii pages). River regulation and sediment transport in a semiarid river – the Murrumbidgee River, New South Wales, Australia. Human Impact on Erosion and Sedimentation, Proceedings of Symposium S6 during the Fifth IAHS Scientific Assembly, Rabat, Morocco, 23 April - 3 May 1997.

Olive, L. J., & Walker, P. H. (1982). Processes in overland flow – erosion and production of suspended material. Prediction in Water Quality: Proceedings of a Symposium on the Prediction in Water Quality, Canberra.

Oliver, R. L., & Ganf, G. G. (1988). The optical properties of a turbid reservoir and its phytoplankton in relation to photosynthesis and growth (Mount Bold Reservoir, South Australia). *Journal of Plankton Research, 10*(6), 1155–1177. https://doi.org/10.1093/plankt/10.6.1155

Padhy, M. K., & Saini, R. P. (2011). Study of silt erosion on performance of a Pelton turbine. *Energy, 36*(1), 141–147. http://dx.doi.org/10.1016/j.energy.2010.10.060

Palmieri, A., Shah, F., & Dinar, A. (2001). Economics of reservoir sedimentation and sustainable management of dams. *Journal of Environmental Management, 61*(2), 149–163. http://dx.doi.org/10.1006/jema.2000.0392

Peel, M. C., Finlayson, B. L., & McMahon, T. A. (2007). Updated world map of the Köppen-Geiger climate classification. *Hydrology and Earth System Sciences, 11*(5), 1633–1644. http://dx.doi.org/10.5194/hess-11-1633-2007

Perera, D., Williams, S., & Smakhtin, V. (2023). Present and future losses of storage in large reservoirs due to sedimentation: A country-wise global assessment. *Sustainability, 15*(1), 219. https://doi.org/10.3390/su15010219

Perkins, M. G., Effler, S. W., Peng, F., Pierson, D., Smith, D. G., & Agrawal, Y. C. (2007). Particle characterization and settling velocities for a water supply reservoir during a turbidity event. *Journal of Environmental Engineering, 133*(8), 800–808. https://doi.org/10.1061/(ASCE)0733-9372(2007)133:8(800)

Perna, C., & Burrows, D. (2005). Improved dissolved oxygen status following removal of exotic weed mats in important fish habitat lagoons of the tropical Burdekin River floodplain, Australia. *Marine Pollution Bulletin, 51*(1-4), 138–148. https://doi.org/10.1016/j.marpolbul.2004.10.050

Petheram, C., Tickell, S., O'Gara, F., Bristow, K. L., Smith, A., & Jolly, P. (2008). *Analysis of the Lower Burdekin, Ord and Katherine-Douglas-Daly irrigation areas: Implications to future design and management of tropical irrigation*. http://www.clw.csiro.au/publications/science/2008/sr19-08.pdf

Pitt, J. D., & Thompson, G. (1984). Impact of sediment on reservoir life. Challenges in African Hydrology and Water Resources: Proceedings of the Harare Symposium July 1984, Harare, Zimbabwe, 1984.

Pringle, A. W. (1991). Fluvial sediment supply to the North-east Queensland Coast, Australia. *Australian Geographical Studies, 29*(1), 114–138. https://doi.org/10.1111/j.1467-8470.1991.tb00710.x

Prosser, I. P., Moran, C. J., Lu, H., Scott, A., Rustomji, P., Stevenson, J., Priestly, G., Roth, C. H., & Post, D. (2002). *Regional patterns of erosion and sediment transport in the*

Burdekin River Catchment (CSIRO Land and Water Technical Report no.5/02, Townsville, Australia). http://www.clw.csiro.au/publications/technical2002/tr5-02.pdf

Prosser, I. P., Rutherfurd, I. D., Olley, J. M., Young, W. J., Wallbrink, P. J., & Moran, C. J. (2001). Large-scale patterns of erosion and sediment transport in river networks, with examples from Australia. *Marine and Freshwater Research, 52*(1), 81–99. https://doi.org/10.1071/MF00033

Pyke, J. (2000). Minerals laboratory staff develops new ICP-MS preparation method. *AGSO Research Newsletter,* 12–14. http://www.ga.gov.au/webtemp/image_cache/GA12208.pdf

Queensland Competition Authority. (2003). *Burdekin Haughton Water Supply Scheme: Assessment of certain pricing matters relating to the Burdekin River irrigation area – Final report* (Queensland Competition Authority, Brisbane, Australia). https://www.qca.org.au/wp-content/uploads/2019/05/4535_BurdekinFinalReport_April03-1.pdf

Queensland Government. (2017, 30 April 2017). *Burdekin Falls Dam hydro-electricity to power North Queensland: Premier* https://statements.qld.gov.au/statements/80954

Ra, K., Bang, J.-H., Lee, J.-M., Kim, K.-T., & Kim, E.-S. (2011). The extent and historical trend of metal pollution recorded in core sediments from the artificial Lake Shihwa, Korea. *Marine Pollution Bulletin, 62*(8), 1814–1821. http://dx.doi.org/10.1016/j.marpolbul.2011.05.010

Rãdoane, M., & Rãdoane, N. (2005). Dams, sediment sources and reservoir silting in Romania. *Geomorphology, 71*(1-2), 112–125. http://dx.doi.org/10.1016/j.geomorph.2004.04.010

Rahman, A. K. M., Al Bakri, D., Ford, P., & Church, T. (2005). Limnological characteristics, eutrophication and cyanobacterial blooms in an inland reservoir, Australia. *Lakes and Reservoirs: Research and Management, 10*(4), 211–220. https://doi.org/10.1111/j.1440-1770.2005.00279.x

Rahman, A. K. M. M., & Bakri, D. A. (2010). Contribution of diffuse sources to the sediment and phosphorus budgets in Ben Chifley Catchment, Australia. *Environmental Earth Sciences, 60*(3), 463–472. https://doi.org/10.1007/s12665-009-0187-1

Raudkivi, A. J. (1993). *Sedimentation: Exclusion and removal of sediment from diverted water*. CRC Press. https://doi.org/https://doi.org/10.1201/9781003077619

Raymond, O. L., Liu, S., Gallagher, R., Zhang, W., & Highet, L. M. (2012). *Surface Geology of Australia 1:1 million scale dataset 2012 edition.* Geoscience Australia, Canberra. https://dx.doi.org/10.26186/74619

Reynolds, B. (2012). *Variability and change in Koga Reservoir volume, Blue Nile, Ethiopia* [Masters thesis, Department of Earth Sciences, Uppsala University]. Uppsala, Sweden. http://uu.diva-portal.org/smash/record.jsf?pid=diva2%3A621607&dswid=9524

Roach, A. C. (2005). Assessment of metals in sediments from Lake Macquarie, New South Wales, Australia, using normalisation models and sediment quality guidelines. *Marine Environmental Research, 59*(5), 453–472. http://dx.doi.org/10.1016/j.marenvres.2004.07.002

Roca, M. (2012, 5-7 September 2012). Tarbela Dam in Pakistan. Case study of reservoir sedimentation. River Flow 2012: Proceedings of the International Conference on Fluvial Hydraulics, San José, Costa Rica, San José, Costa Rica, 2012.

Rochman, C. M., & Hoellein, T. (2020). The global odyssey of plastic pollution. *Science, 368*(6496), 1184–1185. https://doi.org/10.1126/science.abc4428

Roth, C. H., Lawson, G., & Cavanagh, D. (2002). *Overview of key natural resource management issues in the Burdekin Catchment, with particular reference to water quality and salinity: Burdekin Catchment condition study phase I.* http://www.clw.csiro.au/publications/consultancy/2003/Burdekin_Catchment_Report_Condition_Study_Phase_1-2003.pdf

Routh, J., Meyers, P. A., Hjorth, T., Baskaran, M., & Hallberg, R. (2007). Sedimentary geochemical record of recent environmental changes around Lake Middle Marviken, Sweden. *Journal of Paleolimnology, 37*(4), 529–545. https://doi.org/10.1007/s10933-006-9032-7

Rueda, F., Cortés, A., de Vicente, I., Escobar, M. A., Hoyer, A. B., Fleenor, W., & Moreno, E. (2010). River inflow mixing in a stratified reservoir. In *Environmental Hydraulics, Two Volume Set* (pp. 391–396). CRC Press. https://doi.org/https://doi.org/10.1201/b10553

Russell, D. J. (1987). Aspects of the limnology of tropical lakes in Queensland, Australia – with notes on their suitability for recreational fisheries. *Proceedings of the Royal Society of Queensland, 98*, 83–91.

Sabbatini, M. R., Murphy, K. J., & Irigoyen, J. H. (1998). Vegetation–environment relationships in irrigation channel systems of southern Argentina. *Aquatic Botany, 60*(2), 119–133. http://dx.doi.org/10.1016/S0304-3770(97)00086-7

Salas, J. D., Govindaraju, R. S., Anderson, M., Arabi, M., Francés, F., Suarez, W., Lavado-Casimiro, W. S., & Green, T. R. (2014). Introduction to hydrology. In L. K. Wang & C. T. Yang (Eds.), *Modern water resources engineering* (pp. 1–126). Humana Press. https://doi.org/http://dx.doi.org/10.1007/978-1-62703-595-8_1

Samadi Boroujeni, H., Fathi-Moghadam, M., & Shafaei-Bejestan, M. (2009). Investigation on bulk density of deposited sediments in Dez Reservoir. *Trends in Applied Sciences Research, 4*(3), 148–157. https://dx.doi.org/10.3923/tasr.2009.148.157

Samadi, H., & Galay, V. J. (2005). Turbidity current measurements within the Dez reservoir, Iran. Proceedings, Hydrotechnical Engineering: Cornerstone of a Sustainable Environment. 17th Canadian Hydrotechnical Conference, Edmonton, Alberta, 2005.

Santos, I. S., Garcia, C. A. B., Passos, E. A., & Alves, J. P. H. (2013). Distributions of trace metals in sediment cores from a hypertrophic reservoir in northeast Brazil. *Journal of the Brazilian Chemical Society, 24*(2), 246–255. https://doi.org/10.5935/0103-5053.20130032

Schladow, S. G., & Hamilton, D. P. (1995). Effect of major flow diversion on sediment nutrient release in a stratified reservoir. *Marine and Freshwater Research, 46*(1), 189–195. http://dx.doi.org/10.1071/MF9950189

Schleiss, A. J., Franca, M. J., Juez, C., & De Cesare, G. (2016). Reservoir sedimentation. *Journal of Hydraulic Research, 54*(6), 595–614. http://dx.doi.org/10.1080/00221686.2016.1225320

Shahin, M. M. A. (1993). An overview of reservoir sedimentation in some African river basins. Sediment Problems: Strategies for Monitoring, Prediction and Control (Proceedings of the Yokohama Symposium, July 1993), Yokohama, Japan, 1993.

Shaw, J., & Sutcliffe, J. (2003). Ancient dams, settlement archaeology and Buddhist propagation in central India: The hydrological background. *Hydrological Sciences Journal, 48*(2), 277–291. https://doi.org/10.1623/hysj.48.2.277.44695

Sherman, B., Whittington, J., & Oliver, R. (2000). The impact of artificial destratification on water quality in Chaffey Reservoir.*Advances in Limnology* Kinneret Symposium on Limnology and Lake Management 2000+, Ginnosar, Israel.

Sherman, B. S., Lemckert, C., & Zhang, H. (2010). *The impact of artificial destratification on reservoir evaporation*. Urban Water Security Research Alliance Technical Report No. 35. http://www.urbanwateralliance.org.au/publications/UWSRA-tr35.pdf

Shokri, A., Haddad, O. B., & Mariño, M. A. (2013). Reservoir operation for simultaneously meeting water demand and sediment flushing: Stochastic dynamic programming approach with two uncertainties. *Journal of Water Resources Planning and Management, 139*(3), 277–289. https://doi.org/10.1061/(ASCE)WR.1943-5452.0000244

Shotbolt, L. A., Thomas, A. D., & Hutchinson, S. M. (2005). The use of reservoir sediments as environmental archives of catchment inputs and atmospheric pollution. *Progress in Physical Geography: Earth and Environment, 29*(3), 337–361. https://doi.org/10.1191/0309133305pp452ra

Shoup, D. E., & Wahl, D. H. (2009). The effects of turbidity on prey selection by piscivorous largemouth bass. *Transactions of the American Fisheries Society, 138*(5), 1018–1027. https://doi.org/10.1577/T09-015.1

Simms, A. D., Woodroffe, C., Jones, B. G., Heijnis, H., Mann, R. A., & Harrison, J. (2008). Use of 210Pb and 137Cs to simultaneously constrain ages and sources of post-dam sediments in the Cordeaux reservoir, Sydney, Australia. *Journal of Environmental Radioactivity, 99*(7), 1111–1120. http://dx.doi.org/10.1016/j.jenvrad.2008.01.002

Skene, T. M., & Oades, J. M. (1995). The effects of sodium adsorption ratio and electrolyte concentration on water quality: Laboratory studies. *Soil Science, 159*(1), 65–73. http://ovidsp.ovid.com/ovidweb.cgi?T=JS&PAGE=reference&D=ovftb&NEWS=N&AN=00010694-199501000-00008.

Smith, K. V. H. (1984). A three years experience in sediment removal from Sefid Rud Reservoir by Chasse Method. In K. V. H. Smith (Ed.), *Channels and channel control structures* (pp. 235–247). Springer. https://doi.org/http://dx.doi.org/10.1007/978-3-662-11300-4_19

Souza, V. A., & Wasserman, J. C. (2015). Distribution of heavy metals in sediments of a tropical reservoir in Brazil: Sources and fate. *Journal of South American Earth Sciences, 63*, 208–216. http://dx.doi.org/10.1016/j.jsames.2015.07.014

Sperazza, M., Moore, J. N., & Hendrix, M. S. (2004). High-resolution particle size analysis of naturally occurring very fine-grained sediment through laser diffractometry. *Journal of Sedimentary Research, 74*(5), 736–743. http://dx.doi.org/10.1306/031104740736

Steane, M. S., & Tyler, P. A. (1982). Anomalous stratification behaviour of Lake Gorden, headwater reservoir of the lower Gorden River, Tasmania. *Marine and Freshwater Research, 33*(5), 739–760. http://dx.doi.org/10.1071/MF9820739

Sumi, T., & Hirose, T. (2009). Accumulation of sediments in reservoirs. In Y. Takahasi (Ed.), *Water storage, transportation and distribution* (Vol. 1, pp. 224–252). EOLSS Publishers. https://www.eolss.net/ebooklib/bookinfo/water-storage-transportation-distribution.aspx#

Sunwater Limited. (2009). *Sunwater dam portfolio*.

Sunwater Limited. (2024a). *Burdekin Falls Dam Raising and Improvement project. Project overview September 2024*. https://www.sunwater.com.au/wp-content/uploads/2024/07/20240930_BFD%20update_Sept24.pdf?_t=1727733891

Sunwater Limited. (2024b). *Burdekin Haughton Scheme*. Retrieved 20 November 2024 from http://www.sunwater.com.au/schemes/burdekin-haughton

Syvitski, J., Ángel, J. R., Saito, Y., Overeem, I., Vörösmarty, C. J., Wang, H., & Olago, D. (2022). Earth’s sediment cycle during the Anthropocene. *Nature Reviews Earth & Environment, 3*(3), 179–196. https://doi.org/10.1038/s43017-021-00253-w

Syvitski, J. P. M., Vorosmarty, C. J., Kettner, A. J., & Green, P. (2005). Impact of humans on the flux of terrestrial sediment to the global coastal ocean. *Science, 308*(5720), 376–380. http://dx.doi.org/10.1126/science.1109454

Szyczewski, P., Siepak, J., Niedzielski, P., & Sobczynski, T. (2009). Research on heavy metals in Poland. *Polish Journal of Environmental Studies, 18*(5), 755–768. http://www.pjoes.com/Research-on-Heavy-Metals-in-Poland,88292,0,2.html

Tamene, L., Park, S. J., Dikau, R., & Vlek, P. L. G. (2006). Reservoir siltation in the semi-arid highlands of northern Ethiopia: Sediment yield–catchment area relationship and a semi-quantitative approach for predicting sediment yield. *Earth Surface Processes and Landforms, 31*(11), 1364–1383. http://dx.doi.org/10.1002/esp.1338

Tammeorg, O., Niemistö, J., Horppila, J., Haldna, M., & Kangur, K. (2013). Sedimentation and resuspension dynamics in Lake Vesijärvi (Finland): Comparison of temporal and spatial variations of sediment fluxes in deep and shallow areas. *Fundamental and Applied Limnology, 182*(4), 297–307. https://doi.org/10.1127/1863-9135/2013/0423

Tarela, P. A., & Menéndez, A. N. (1999). A model to predict reservoir sedimentation. *Lakes and Reservoirs: Research and Management, 4*(3-4), 121–133. http://dx.doi.org/10.1046/j.1440-1770.1999.00087.x

Thornton, K. W. (1984). Regional comparisons of lakes and reservoirs: Geology, climatology, and morphology. *Lake and Reservoir Management, 1*(1), 261–265. https://doi.org/10.1080/07438148409354521

Thornton, K. W., Kimmel, B. L., & Payne, F. E. (1990). Perspectives on reservoir limnology. In *Reservoir limnology: ecological perspectives* (pp. 1–13). John Wiley and Sons.

Tibby, J., Gell, P., Hancock, G., & Clark, M. (2010). Complex reservoir sedimentation revealed by an unusual combination of sediment records, Kangaroo Creek Reservoir, South Australia. *Journal of Paleolimnology, 43*(3), 535–549. https://doi.org/10.1007/s10933-009-9349-0

Tonguç Uysal, I., Zhao, J.-X., Golding, S. D., Lawrence, M. G., Glikson, M., & Collerson, K. D. (2007). Sm–Nd dating and rare-earth element tracing of calcite: Implications for fluid-flow events in the Bowen Basin, Australia. *Chemical Geology, 238*(1-2), 63–71. http://dx.doi.org/10.1016/j.chemgeo.2006.10.014

Townsend, S. A. (1998, Feb). The influence of retention time and wind exposure on stratification and mixing in two tropical Australian reservoirs [Article]. *Archiv Fur Hydrobiologie, 141*(3), 353–371. https://doi.org/10.1127/archiv-hydrobiol/141/1998/353

Townsend, S. A. (2002). Seasonal evaporative concentration of an extremely turbid water-body in the semiarid tropics of Australia. *Lakes and Reservoirs: Research and Management, 7*(2), 103–107. https://doi.org/10.1046/j.1440-169X.2002.00173.x

Townsend, S. A., Boland, K. T., & Luongvan, J. T. (1997). Wet and dry season heat loss in two tropical Australian reservoirs. *Archiv Fur Hydrobiologie, 139*(1), 51–68. https://doi.org/10.1127/archiv-hydrobiol/139/1997/51

Townsville Enterprise. (2017). *Hell's Gates Dam opportunity overview*. https://s3-ap-southeast-2.amazonaws.com/os-data-2/townsvilleenterprise-com-au/documents/hellsgatesdamfeasibilitystudyoverview.pdf

Tundisi, J. G., & Tundisi, T. M. (2011). *Limnology* (1st ed.). CRC Press. https://doi.org/https://doi.org/10.1201/b11386

Turner, R., Huggins, R., Wallace, R., Smith, R., & Warne, M. St J. (2013). *Total suspended solids, nutrient and pesticide loads (2010–2011) for rivers that discharge to the Great Barrier Reef – Great Barrier Reef Catchment Loads Monitoring 2010–2011*. https://www.reefplan.qld.gov.au/__data/assets/pdf_file/0028/45982/2010-2011-gbr-catchment-loads-report.pdf

U.S. Bureau of Reclamation. (1987). *Design of small dams* (3rd ed.). U.S. Government Printing Office. https://www.usbr.gov/tsc/techreferences/mands/mands-pdfs/SmallDams.pdf

Uhlmann, D., Paul, L., Hupfer, M., & Fischer, R. (2011). 2.08 - Lakes and reservoirs. In P. Wilderer (Ed.), *Treatise on Water Science* (pp. 157–213). Elsevier. https://doi.org/https://doi.org/10.1016/b978-0-444-53199-5.00034-8

Valipour, R., Boegman, L., Bouffard, D., & Rao, Y. R. (2017). Sediment resuspension mechanisms and their contributions to high-turbidity events in a large lake. *Limnology and Oceanography, 62*(3), 1045–1065. https://doi.org/10.1002/lno.10485

van B Weaver, A., & Stone, A. W. (1980). Distinguishing sub-environments of sediment distribution in reservoirs using particle size distribution parameters. *Journal of the Limnological Society of Southern Africa, 6*(1), 59–65. https://doi.org/10.1080/03779688.1980.9633210

Velde, B., & Meunier, A. (2008). *The origin of clay minerals in soils and weathered rocks* (Vol. 1. Aufl.). Springer. https://doi.org/https://doi.org/10.1007/978-3-540-75634-7

Verstraeten, G., & Poesen, J. (2000). Estimating trap efficiency of small reservoirs and ponds: Methods and implications for the assessment of sediment yield. *Progress in Physical Geography, 24*(2), 219–251. http://dx.doi.org/10.1177/030913330002400204

Vilhena, L. C., Hillmer, I., & Imberger, J. (2010). The role of climate change in the occurrence of algal blooms: Lake Burragorang, Australia. *Limnology and Oceanography, 55*(3), 1188–1200. https://doi.org/10.4319/lo.2010.55.3.1188

Villacorta-Rath, C., Espinoza, T., Cockayne, B., Schaffer, J., & Burrows, D. (2022). Environmental DNA analysis confirms extant populations of the cryptic Irwin's turtle within its historical range. *BMC Ecology and Evolution, 22*(1), 57. https://doi.org/10.1186/s12862-022-02009-6

Vishnoi, R. K., & Govil, R. (2007). Sedimentation and life of the reservoir. *Water and Energy International, 64*(1), 99–107. https://www.indianjournals.com/ijor.aspx?target=ijor:wei&volume=64&issue=1&article=020

von Eynatten, H., & Tolosana-Delgado, R. (2011). Geochemistry versus grain-size relations of sediments in the light of comminution, chemical alteration, and contrasting source rocks. In J. J. Egozcue, R. Tolosana-Delgado, & M. I. Ortego, Proceedings of the 4th International Workshop on Compositional Data Analysis, Girona, Spain.

Vörösmarty, C. J., Meybeck, M., Fekete, B., Sharma, K., Green, P., & Syvitski, J. P. M. (2003). Anthropogenic sediment retention: Major global impact from registered river impoundments. *Global and Planetary Change, 39*(1-2), 169–190. http://dx.doi.org/10.1016/s0921-8181(03)00023-7

Wallace, R., Huggins, R., King, O., Gardiner, R., Thomson, B., Orr, D., Ferguson, B., Taylor, C., Severino, Z., Smith, R. A., Warne, M. S. J., Turner, R. D. R., & Mann, R. M. (2016). *Total suspended solids, nutrient and pesticide loads (2014–2015) for rivers that discharge to the Great Barrier Reef – Great Barrier Reef Catchment Loads Monitoring Program.* (Department of Science, Information Technology and Innovation, Brisbane, Australia). https://www.reefplan.qld.gov.au/__data/assets/pdf_file/0035/45989/2014-2015-gbr-catchment-loads-technical-report.pdf

Wallace, R., Huggins, R., Smith, R. A., Turner, R. D. R., Garzon-Garcia, A., & Warne, M. S. J. (2015). *Total suspended solids, nutrient and pesticide loads (2012–2013) for rivers that discharge to the Great Barrier Reef – Great Barrier Reef Catchment Loads Monitoring Program 2012–2013* (Department of Science, Information Technology and Innovation, Brisbane, Australia). https://www.reefplan.qld.gov.au/__data/assets/pdf_file/0031/45985/2012-2013-gbr-catchment-loads-technical-report.pdf

Wallace, R., Huggins, R., Smith, R. A., Turner, R. D. R., Vardy, S., & Warne, M. S. J. (2014). *Total suspended solids, nutrient and pesticide loads (2011–2012) for rivers that discharge to the Great Barrier Reef – Great Barrier Reef Catchment Loads Monitoring Program 2011–2012* (Department of Science, Information Technology and Innovation, Brisbane, Australia). https://www.reefplan.qld.gov.au/__data/assets/pdf_file/0029/45983/2011-2012-gbr-catchment-loads-report.pdf

Walling, D. E. (2006). Human impact on land–ocean sediment transfer by the world's rivers. *Geomorphology, 79*(3-4), 192–216. http://dx.doi.org/10.1016/j.geomorph.2006.06.019

Walling, D. E., & Moorehead, P. W. (1989). The particle size characteristics of fluvial suspended sediment: An overview. *Hydrobiologia, 176-177*(1), 125–149. http://dx.doi.org/10.1007/bf00026549

Walling, D. E., Wilkinson, S. N., & Horowitz, A. J. (2011). 2.12 - Catchment erosion, sediment delivery, and sediment quality. In P. Wilderer (Ed.), *Treatise on Water Science* (pp. 305–338). Elsevier. https://doi.org/https://doi.org/10.1016/b978-0-444-53199-5.00039-7

Wang, G., Wu, B., & Wang, Z.-Y. (2005). Sedimentation problems and management strategies of Sanmenxia Reservoir, Yellow River, China. *Water Resources Research, 41*(9), W09417. http://dx.doi.org/10.1029/2004wr003919

Wang, J., Wu, J., & Zeng, H. (2015). Sediment record of abrupt environmental changes in Lake Chenpu, upper reaches of Yellow River Basin, north China. *Environmental Earth Sciences, 73*(10), 6355–6363. https://doi.org/10.1007/s12665-014-3857-6

Wang, S., Qian, X., Han, B.-P., Wang, Q.-H., & Ding, Z.-F. (2011). Physical limnology of a typical subtropical reservoir in south China. *Lake and Reservoir Management, 27*(2), 149–161. https://doi.org/10.1080/07438141.2011.573613

Wang, S., Qian, X., Wang, Q. H., & Xiong, W. (2012). Modeling turbidity intrusion processes in flooding season of a canyon-shaped reservoir, South China. *Procedia Environmental Sciences, 13*, 1327–1337. http://dx.doi.org/10.1016/j.proenv.2012.01.125

Wasson, R. J., Caitcheon, G., Murray, A. S., McCulloch, M., & Quade, J. (2002). Sourcing sediment using multiple tracers in the catchment of Lake Argyle, Northwestern Australia. *Environmental Management, 29*(5), 634–646. https://doi.org/10.1007/s00267-001-0049-4

Wasson, R. J., Clark, R. L., Nanninga, P. M., & Waters, J. (1987). 210Pb as a chronometer and tracer, Burrinjuck Reservoir, Australia. *Earth Surface Processes and Landforms, 12*(4), 399–414. https://doi.org/10.1002/esp.3290120406

Waterhouse, J., Brodie, J., Lewis, S., & Audas, D.-m. (2016). Land-sea connectivity, ecohydrology and holistic management of the Great Barrier Reef and its catchments: time for a change. *Ecohydrology & Hydrobiology, 16*(1), 45–57. http://dx.doi.org/10.1016/j.ecohyd.2015.08.005

Waterhouse, J., Lønborg, C., Logan, M., Petus, C., Tracey, D., Lewis, S., Howley, C., Harper, E., Tonin, H., Skuza, M., Doyle, J., Costello, P., Davidson, J., Gunn, K., Wright, M., Zagorskis, I., Kroon, F., & Gruber, R. (2018). *Marine Monitoring Program: Annual Report for inshore water quality monitoring 2016–2017*. Great Barrier Reef Marine Park Authority. http://hdl.handle.net/11017/3396

Wells, M. G., & Sherman, B. (2001). Stratification produced by surface cooling in lakes with significant shallow regions. *Limnology and Oceanography, 46*(7), 1747–1759. https://doi.org/10.4319/lo.2001.46.7.1747

White, W. R. (1990). Reservoir sedimentation and flushing. Proceedings, Hydrology in mountainous regions. II – Artificial reservoirs; water and slopes (Proceedings of two Lausanne Symposia), Lausanne, Switzerland, 1990.

White, W. R. (2001). *Evacuation of sediments from reservoirs*. Thomas Telford Services Limited. https://www.icevirtuallibrary.com/isbn/9780727737748

Wieland, M. (2013). Safety aspects of sustainable storage dams. In *Life-Cycle and Sustainability of Civil Infrastructure Systems* (pp. 1876–1883). CRC Press. https://doi.org/http://dx.doi.org/10.1201/b12995-290

Wildman Jr., R. A., Pratson, L. F., DeLeon, M., & Hering, J. G. (2011). Physical, chemical, and mineralogical characteristics of a reservoir sediment delta (Lake Powell, USA) and implications for water quality during low water level. *Journal of Environmental Quality, 40*(2), 575–586. https://doi.org/10.2134/jeq2010.0323

Williams, G. P., & Wolman, M. G. (1984). *Downstream effects of dams on alluvial rivers*. Geological Survey Professional Paper 1286. United States Government Printing Office. https://pubs.usgs.gov/pp/1286/report.pdf

Wilson, M. J. (1999). The origin and formation of clay minerals in soils; past, present and future perspectives. *Clay Minerals, 34*(1), 7–25. http://claymin.geoscienceworld.org/content/34/1/7.abstract

Wolanski, E., & Hopper, C. (2022). Dams and climate change accelerate channel avulsion and coastal erosion and threaten Ramsar-listed wetlands in the largest Great Barrier Reef watershed. *Ecohydrology & Hydrobiology, 22*(2), 197–212. https://doi.org/10.1016/j.ecohyd.2022.01.001

Woodyer, K. D. (1978). Sediment regime of the Darling River. Proceedings of the Royal Society of Victoria, November 1978, Melbourne, Australia.

Wu, B., Wang, G., & Xia, J. (2007). Case study: Delayed sedimentation response to inflow and operations at Sanmenxia Dam. *Journal of Hydraulic Engineering, 133*(5), 482–494. http://dx.doi.org/10.1061/(ASCE)0733-9429(2007)133:5(482)

Yao, F., Livneh, B., Rajagopalan, B., Wang, J., Crétaux, J.-F., Wada, Y., & Berge-Nguyen, M. (2023). Satellites reveal widespread decline in global lake water storage. *Science, 380*(6646), 743–749. https://doi.org/10.1126/science.abo2812

Yu, W.-S., Lee, H.-Y., & Hsu, S. M. (2000). Experiments on deposition behavior of fine sediment in a reservoir. *Journal of Hydraulic Engineering, 126*(12), 912–920. http://dx.doi.org/10.1061/(ASCE)0733-9429(2000)126:12(912)

Zarfl, C., Lumsdon, A. E., Berlekamp, J., Tydecks, L., & Tockner, K. (2015). A global boom in hydropower dam construction. *Aquatic Sciences, 77*(1), 161–170. https://doi.org/10.1007/s00027-014-0377-0

Zeng, Q., & Zhou, W. (1989). Soil erosion in the Yellow River basin and its impacts on reservoir sedimentation and the lower Yellow River. Sediment and the Environment, Proceedings of the Baltimore Symposium, May 1989, Baltimore, USA, 1989.

Zhang, Y., Liu, X., Qin, B., Shi, K., Deng, J., & Zhou, Y. (2016). Aquatic vegetation in response to increased eutrophication and degraded light climate in Eastern Lake Taihu: Implications for lake ecological restoration. *Scientific Reports, 6*, 23867. https://doi.org/10.1038/srep23867

Zhao, Q., Ding, S., Lu, X., Liang, G., Hong, Z., Lu, M., & Jing, Y. (2022). Water-sediment regulation scheme of the Xiaolangdi Dam influences redistribution and accumulation of heavy metals in sediments in the middle and lower reaches of the Yellow River. *Catena, 210*, 105880. https://doi.org/10.1016/j.catena.2021.105880

Appendices

Appendix A: Chapter 2 supplementary material

Additional sampling location and sample collection details have been provided, along with water monitoring station numbers. Regression statistics are provided for the turbidity, TSS and baseflow relationships presented in Figure 2.5 and Figure 2.8. The likely relationship between high turbidity and localised rainfall is briefly discussed.

A.1 Introduction

Table A1 Distance from sampling locations to the dam wall, river inflow point (boundary of the gazetted reservoir at 100% capacity) and water monitoring gauges

Sample Site	Distance from dam (km)	Distance from inflowing river(s) (km)	Distance from water monitoring station(s) (km)
Burdekin	26	18 (Burdekin River)	113 (Burdekin Sellheim)
Suttor	25	56 (Suttor River)	76 (Suttor St Anns)
		35 (Cape River)	92 (Cape Taemas)
Dam 2	10	34 (Burdekin River)	129 (Burdekin Sellheim)
		71 (Suttor River)	90 (Suttor St Anns)
		50 (Cape River)	107 (Cape Taemas)
Dam 1	0.8	44 (Burdekin River)	139 (Burdekin Sellheim)
		80 (Suttor River)	100 (Suttor St Anns)
		59 (Cape River)	116 (Cape Taemas)

Table A2 Sample collection details for each site

Sample site	Date	Time (24-h clock)	Latitude (decimal degrees)	Longitude (decimal degrees)
Burdekin	29-Jun-04	12:05	146.96826	-20.52081
	16-Dec-04	15:30	146.96834	-20.52124
	03-Aug-05	8:39	146.96863	-20.52106
	11-Oct-06	9:57	146.96849	-20.52130
	06-Sep-11	11:57	146.96807	-20.52100
Suttor	29-Jun-04	11:13	146.97418	-20.67348
	16-Dec-04	17:43	146.97321	-20.67375
	03-Aug-05	11:33	146.97336	-20.67402
	11-Oct-06	12:00	146.97343	-20.67386
	06-Sep-11	15:26	146.97310	-20.67409
Dam 2	29-Jun-04	10:00	147.04939	-20.62979
	17-Dec-04	7:15	147.04921	-20.62994
	03-Aug-05	15:46	147.04910	-20.62986
	11-Oct-06	14:23	147.04909	-20.62988
	07-Sep-11	12:41	147.04930	-20.62989
Dam 1	29-Jun-04	8:42	147.13251	-20.64054
	17-Dec-04	8:27	147.13242	-20.64065
	04-Aug-05	7:50	147.13231	-20.64058
	11-Oct-06	15:57	147.13222	-20.64083
	07-Sep-11	9:33	147.13291	-20.64064

A.2 Additional methods

Rainfall and hydrological data

Rainfall records for the following meteorological stations were downloaded from the Bureau of Meteorology (BOM) website (http://www.bom.gov.au/climate/data/):

• 34085 – Sellheim (equivalent to the Burdekin River water monitoring station)

• 34022 – Mount Douglas (Suttor; 32 km south of the St Anns water monitoring station)

• 34094 – Taemas (equivalent to the Cape River gauging station)

• 34029 – Burdekin Falls Dam (located at the dam, 5 km upstream of the Burdekin hydro monitoring station).

A.3 Additional results and discussion

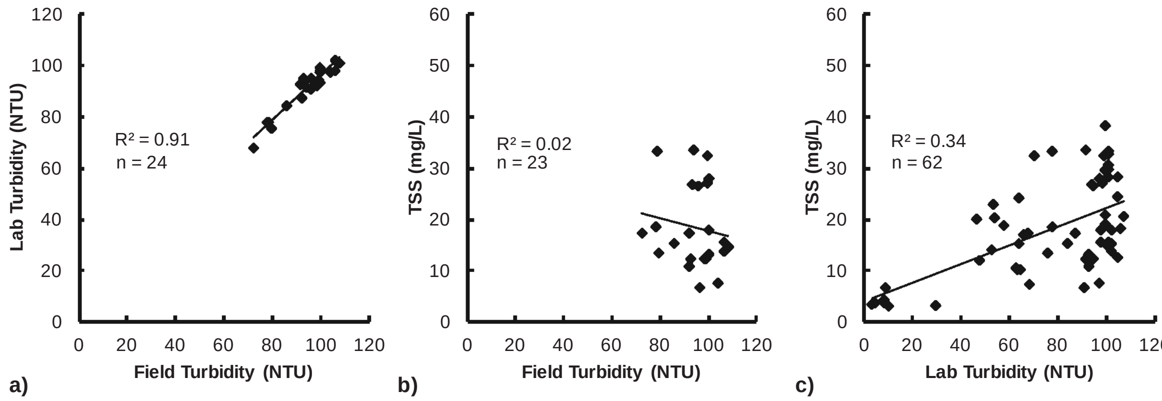

Figure A1 (Equiv. to Figure 2.4 in the paper). (*a*) Turbidity data collected in situ and in the laboratory; (*b*) in situ turbidity data *v*. total suspended solids; c) laboratory turbidity data *v*. total suspended solids. The line $y = mx + c$ was estimated from the available data. Estimates were: (*a*) $m = 0.877$ (s.e. = 0.059, null hypothesis that slope = 1 has a *P*-value of 0.048) and $c = 8.706$ (s.e. = 5.556, null hypothesis that intercept = 0 has *P*-value of 0.131); (*b*) $m = -0.125$ (s.e. = 0.183, null hypothesis that slope = 0 has a *P*-value of 0.502) and $c = 30.316$ (s.e. = 17.315, null hypothesis that intercept = 0 has *P*-value of 0.095); (*c*) $m = 0.181$ (s.e. = 0.033, null hypothesis that slope = 1 has a *P*-value of <0.0001) and $c = 4.130$ (s.e. = 2.720, null hypothesis that intercept = 0 has *P*-value of 0.134).

Regression statistics for the turbidity and TSS relationships have been calculated and are presented above. For figure a, Field *v*. laboratory turbidity, modelling a null hypothesis of a slope = 1, the *P* = value is <0.05 (statistically significant at the 5% level of significance) indicating that there is not a 1:1 relationship between laboratory and field turbidity. However, the *P*-value for the null hypothesis intercept = 0 was >0.05 which indicates that there is no evidence to suggest that the intercept is not zero. When the model was run again assuming an intercept of zero, a Pearson's r^2 value of 0.999 was produced however the p-value was still <0.05. This indicates that the slope is still significantly statistically different from 1, but that the difference is not very large. So, although there is not a 1:1 relationship between laboratory and field turbidity (even if intercept was zero), the relationship is still very close to one.

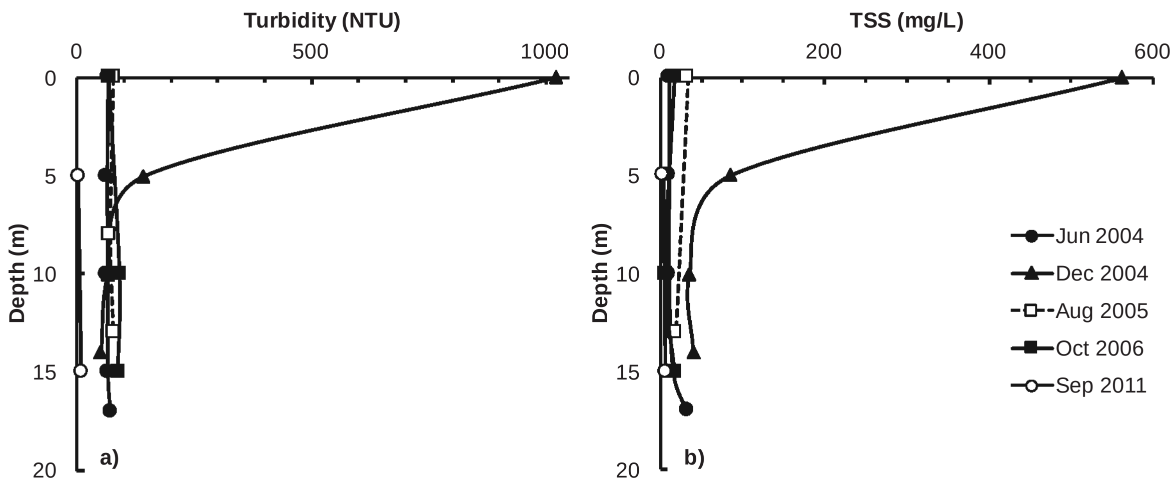

Figure A2 (*a*) Dry season turbidity and (*b*) TSS with depth at the Burdekin site. These graphs include the samples excluded from Figure 2.5 in the paper as turbidity was extremely high in these samples because of localised rainfall in the days before sampling.

High turbidity (1020 NTU in surface water) was observed at the Burdekin Site in December 2004. The turbidity was most likely due to inflow caused by localised rainfall in the days before sampling. In total, 68 mm, equivalent to the monthly median rainfall for December (67.8 mm; Bureau of Meteorology, climate data online, see http://www.bom.gov.au/climate/data/index.shtml, Sellheim = Station number 034085, accessed 11 July 2016; Tables A3, A4) was recorded at Sellheim, 113 km upstream of the Burdekin sampling site in the 10 days before sampling in the reservoir.

Although rainfall in the catchments has the ability to cause turbid inflow, the effects of rainfall as measured at upstream gauges on turbidity in the reservoir is not straightforward. The Mount Douglas gauge, 108 km from the Suttor site also recorded 46 mm of rain in the 6–31 days before sampling in December 2004 (Table S3) but no corresponding increase in turbidity was observed at the Suttor site. In the 15 days before sampling in August 2005, 82 and 56 mm of rain were recorded at the Sellheim and Burdekin Falls Dam gauges respectively (Table S3); however, no corresponding increase in turbidity was observed at the Burdekin site.

Rainfall in the vicinity of most sampling sites was not recorded. The closest rainfall gauge to all sites is at the dam wall, 26 km from the Burdekin Site. Prior to the December 2004 sampling 18 mm of rain was received at the dam wall in the 2–27 days before sampling. Although the two Dam sites are closer to the wall and rainfall was also recorded at the Suttor River gauge (Mount Douglas) no increase in turbidity was observed.

I acknowledge that localised rainfall events during the dry season may temporarily elevate turbidity in isolated areas of the reservoir, but this study does not have the data to quantify how long turbidity may be elevated nor where it may be located (e.g., proximal to the reservoir's banks).

Table A3 Rainfall in the 2 weeks before sampling at each location (Bureau of Meteorology, climate data online, see http://www.bom.gov.au/climate/data/index.shtml, accessed 11 July 2016)

Sampled date	Sellheim (Burdekin)		Mount Douglas (Suttor)		Taemas (Cape)		Burdekin Falls Dam	
	Rainfall (mm)	Number of days before	Rainfall (mm)	Number of days before	Rainfall (mm)	Number of days before	Rainfall (mm)	Number of days before
29 Jun 04	0	-	0	-	0	-	0	-
16 Dec 04	68.1	4–23	46.4	6–31	18	2–24	18	2–27
3 Aug 05	82.2	0–15	38	1–15	49	0–15	56	0–15
11 Oct 06	0	-	0	-	0	-	0	-
6 Sep 11	0	-	0	-	18	8–9	1.5	7–8

Table A4 Monthly median rainfall in millimetres for each location (Bureau of Meteorology, climate data online, see http://www.bom.gov.au/climate/data/index.shtml, accessed 11 July 2016)

Gauge	Jan	Feb	Mar	Apr	May	Jun	Jul	Aug	Sep	Oct	Nov	Dec
Sellheim (Burdekin)	114.8	114.1	84.8	18.9	9.5	11.4	0	0	0	9.4	30.0	67.8
Mount Douglas (Suttor & Belyando)	93.5	92.4	49.4	10.9	12.2	16.0	2.2	5.0	1.9	15.7	44.6	64.0
Taemas (Cape)	112.1	103.4	52.4	11.0	6.3	8.2	0	5.8	0	5.5	27.7	42.0
Burdekin Falls Dam	123.5	97.0	48.2	21.0	18.0	11.5	2.0	1.2	2.5	9.5	34.0	78.2

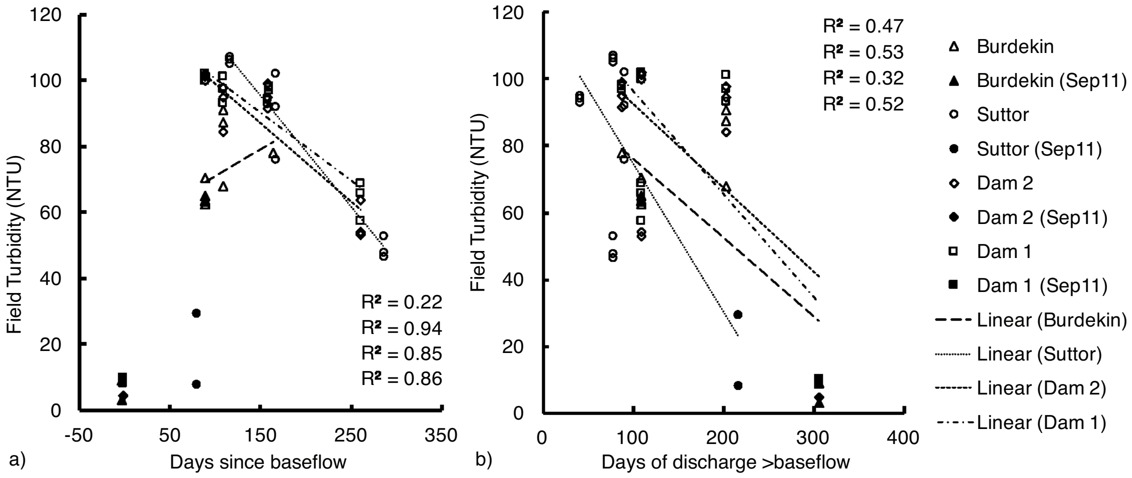

Figure A3 (Equiv. to Figure 2.8 in the paper). (a) Plot of the number of days since baseflow was last reached vs. turbidity at each location. (b) Plot of the duration of discharge recorded that was above baseflow vs. turbidity at each location.

Plot a) September 2011 samples were excluded from the regression calculations as outliers whose turbidity values are greatly affected by the above-average discharge and low flow duration of that water year. The line $y = mx + c$ was estimated from the available data for each set of samples from each location.

Burdekin: $m = 0.163$ (s.e. = 0.108, hypothesis that slope = 0 has a P-value of 0.168) and $c = 54.791$ (s.e. = 12.196, hypothesis that intercept = 0 has P-value of 0.002). Note that Burdekin site samples from December 2004 have not been included as discussed above.

Suttor: $m = -0.335$ (s.e. = 0.024, hypothesis that slope = 0 has a P-value of <0.0001) and $c = 145.386$ (s.e. = 4.467, hypothesis that intercept = 0 has P-value of <0.0001).

Dam 2: $m = -0.240$ (s.e. = 0.028, hypothesis that slope = 0 has a P-value of <0.0001) and $c = 122.910$ (s.e. = 4.293, hypothesis that intercept = 0 has P-value of <0.0001).

Dam 1: $m = -0.204$ (s.e. = 0.022, hypothesis that slope = 0 has a P-value of <0.0001) and $c = 120.784$ (s.e. = 3.312, hypothesis that intercept = 0 has P-value of <0.0001).

Plot b) The line $y = mx + c$ was estimated from the available data for each set of samples from each location.

Burdekin: $m = -0.235$ (s.e. = 0.079, hypothesis that slope = 0 has a P-value of 0.014) and $c = 99.581$ (s.e. = 0.113, hypothesis that intercept = 0 has P-value of <0.0001).

Suttor: $m = -0.448$ (s.e. = 0.024, hypothesis that slope = 0 has a P-value of 0.002) and $c = 119.711$ (s.e. = 11.760, hypothesis that intercept = 0 has P-value of <0.0001).

Dam 2: $m = -0.251$ (s.e. = 0.098, hypothesis that slope = 0 has a P-value of 0.022) and $c = 117.714$ (s.e. = 14.389, hypothesis that intercept = 0 has P-value of <0.0001).

Dam 1: $m = -0.310$ (s.e. = 0.074, hypothesis that slope = 0 has a P-value of 0.001) and $c = 127.786$ (s.e. = 11.723, hypothesis that intercept = 0 has P-value of <0.0001).

Appendix B: Chapter 3 supplementary material

B.1 Additional methods

Hydrological data

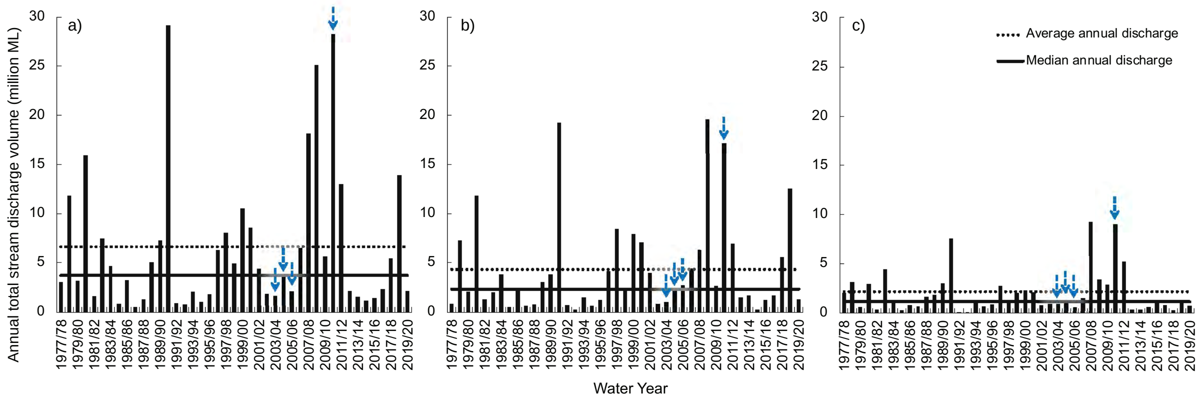

Figure B1 Annual discharge at the flow gauges at the (a) Burdekin River at the Hydro Site (120015A), (b) Burdekin River at Sellheim (120002C) and (c) combined Suttor River at St Anns (120303A) and Cape River at Taemas (120302B). Arrows indicate the 2003–04, 2004–05, 2005–06, and 2010–11 water years sampled. Average and median annual discharge are calculated for the period from the water year of gauge installation (1977–78 for the Burdekin River at Hydro Site, 1968–69 for the Burdekin River at Sellheim and 1968–69 for the combined Suttor River at St Anns and Cape River at Taemas, based on the Cape River gauge date) to the end of the 2019–20 water year (Data source: https://water-monitoring.information.qld.gov.au/, accessed June 2021). Mean ± s.d. discharge was 6.6 ± 7.7 TL (median 3.7 TL) for the Burdekin River at the Hydro Site, 4.3 ± 4.9 TL (median 2.3 TL) for the Burdekin River at Sellheim and 2.2 ± 2.6 TL (median 1.2 TL) for the combined Suttor River at St Anns and Cape River.

The median total annual discharge (3.7 TL) received at the Burdekin Hydro gauging station is 2.1 times the volume of the reservoir (1.8 TL).

Inflow

Most inflowing water in most years came from the Burdekin River (Table B2). However, in 2007–08 the Suttor and Cape rivers contributed more discharge to the reservoir and prior to sampling in 2004 slightly more water (52% c.f. 48%) was received from the Suttor/Cape Rivers (Table B2).

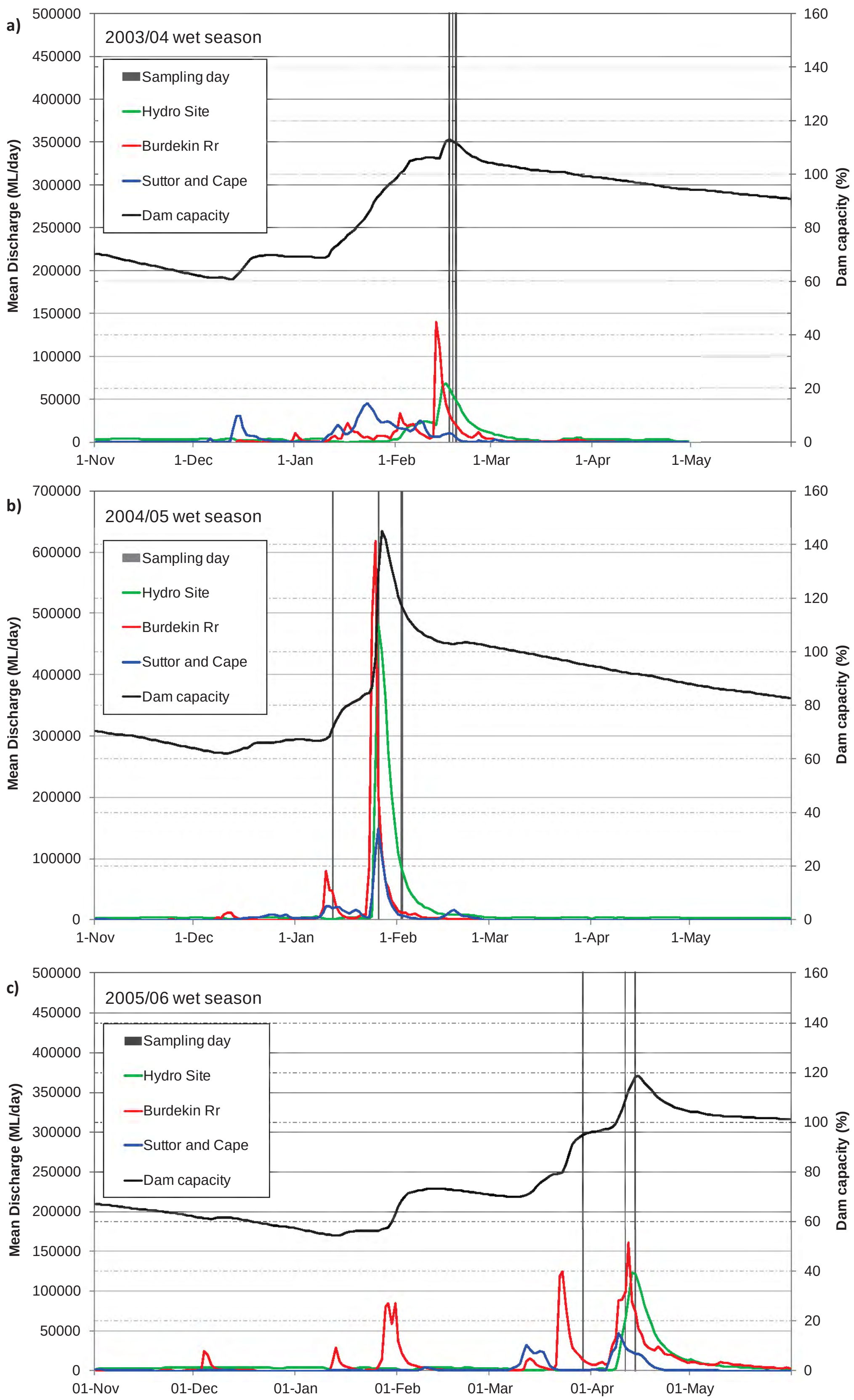

Figure B2 Wet season discharge through the Burdekin River at the Hydro Site (gauge 120015A), Burdekin River at Sellheim (120002C), and combined Suttor River at St Anns/Cape River at Taemas (120303A and 120302B) water monitoring stations. (Note differing Y-axis scale for 2004/2005 graph.) Burdekin Falls Dam reservoir volume is shown (black) and sampling days are marked by vertical lines. Burdekin Falls Dam reservoir volume data obtained from Sunwater Limited ACN 131034985 (M. Ali, Bureau of Meteorology, pers. comm., 25 July 2016; July 2002–July 2016).

Table B1 Water depth at Full Supply Level (FSL) at each site, and distance from sampling locations to the dam wall (as measured along the relict river channel), river inflow point (boundary of the gazetted reservoir at 100% capacity) and water monitoring gauges.

Sample Site	Water depth at FSL (m)	Distance from dam (km)	Distance from inflowing river(s) (km)	Distance from water monitoring station(s) (km)
Burdekin	19	26	18 (Burdekin River)	113 (Burdekin Sellheim)
Suttor	22	25	56 (Suttor River)	76 (Suttor St Anns)
			35 (Cape River)	92 (Cape Taemas)
Central	26	10	34 (Burdekin River)	129 (Burdekin Sellheim)
			71 (Suttor River)	90 (Suttor St Anns)
			50 (Cape River)	107 (Cape Taemas)
Eastern	31	0.8	44 (Burdekin River)	139 (Burdekin Sellheim)
			80 (Suttor River)	100 (Suttor St Anns)
			59 (Cape River)	116 (Cape Taemas)

Table B2 Percentage of total discharge from the Burdekin Sellheim, Suttor St Anns and Cape River at Taemas gauges recorded at each gauge prior to sampling.

Year	Total annual discharge (%)		Discharge from 1 Nov* to final sampling day (%)		Max height of water over dam wall (m)
	Burdekin Sellheim	Suttor/Cape	Burdekin Sellheim	Suttor/Cape	
2003–04	53%	47%	48%	52%	0.93
2004–05	67%	33%	69%	31%	3.04
2005–06	81%	19%	78%	22%	1.31
2007–08	40%	60%	N/A	N/A	5.02
2008–09	85%	15%	N/A	N/A	6.61
2010–11	65%	35%	66%	34%	4.21

*1 November is the start of the wet season.

Table B3 Sample collection details for each site.

Sample site	Date	Time	Latitude (decimal degrees)	Longitude (decimal degrees)
Burdekin	17-Feb-04	17:03	146.96841	-20.52119
	16-Dec-04	15:30	146.96834	-20.52124
	12-Jan-05	11:41	146.96799	-20.52108
	26-Jan-05	09:52	146.96893	-20.52155
	2-Feb-05	08:55	146.96857	-20.52132
	3-Aug-05	08:39	146.96863	-20.52106
	29-Mar-06	10:09	146.96855	-20.52131
	11-Apr-06	10:18	146.96863	-20.52153
	14-Apr-06	11:02	146.96870	-20.52148
	6-Sep-11	11:57	146.96807	-20.52100
Suttor	17-Feb-04	11:10	146.97356	-20.67356
	16-Dec-04	17:43	146.97321	-20.67375
	12-Jan-05	08:44	146.97346	-20.67391
	2-Feb-05	11:38	146.97305	-20.67392
	3-Aug-05	11:33	146.97336	-20.67402
	29-Mar-06	12:23	146.97327	-20.67385
	11-Apr-06	12:23	146.97357	-20.67408
	14-Apr-06	12:16	146.97356	-20.67402
	6-Sep-11	15:26	146.97310	-20.67409
Central	19-Feb-04	14:57	147.04933	-20.62979
	17-Dec-04	07:15	147.04921	-20.62994
	12-Jan-05	14:52	147.04916	-20.62978
	2-Feb-05	14:39	147.04947	-20.62970
	3-Aug-05	15:46	147.04910	-20.62986
	29-Mar-06	14:54	147.04932	-20.62991
	11-Apr-06	14:51	147.04933	-20.92970
	14-Apr-06	09:40	147.04939	-20.62992
	7-Sep-11	12:41	147.04930	-20.62989
Eastern	18-Feb-04	08:30	147.13235	-20.64063
	17-Dec-04	08:27	147.13242	-20.64065
	12-Jan-05	17:02	147.13246	-20.64030
	26-Jan-05	13:22	147.13257	-20.64051
	2-Feb-05	17:08	147.13280	-20.64077
	4-Aug-05	07:50	147.13231	-20.64058
	29-Mar-06	17:07	147.13287	-20.64070
	11-Apr-06	16:22	147.13266	-20.64095
	14-Apr-06	08:12	147.13275	-20.64052
	7-Sep-11	09:33	147.13291	-20.64064

Appendix C: Chapter 4 supplementary material

Additional sampling location and sample collection and particle-size analysis details have been provided, along with details of annual discharge at relevant flow gauges. Further information on the analytical precision and bias for both the XRF and ICP-MS analyses and detailed Sr and Nd isotopic ratio data are also included.

C.1 Additional methods

Table C4 Sample site co-ordinates and sampling dates for all grab and core samples collected in the BFD reservoir.

Site ID	Study site ID	Location	Latitude	Longitude	Collection date
1	B04	Burdekin River	-20.391500	146.936040	18/12/2003
2	B02	North Burdekin	-20.419050	146.973390	17/12/2003
3	DAM14	North Burdekin	-20.521076	146.968335	31/08/2011
4	DAM16	North Burdekin	-20.520975	146.969949	31/08/2011
5	DAM17	North Burdekin	-20.521620	146.967300	31/08/2011
6	B1-7	North Burdekin	-20.521060	146.968630	03/08/2005
7	B1-12	North Burdekin	-20.521001	146.968072	06/09/2011
8	DAM18	South Burdekin	-20.560660	146.986922	31/08/2011
9	DAM19A	South Burdekin	-20.561220	146.989483	31/08/2011
10	DAM20	South Burdekin	-20.561600	146.990073	31/08/2011
11	B10-12	South Burdekin	-20.579542	147.000407	06/09/2011
12	DAM21	South Burdekin	-20.577730	147.002044	31/08/2011
13	DAM22A	South Burdekin	-20.580224	147.000916	31/08/2011
14	B08	South Burdekin	-20.581000	146.999880	18/12/2003
15	DAM23	South Burdekin	-20.584666	147.006562	31/08/2011
16	S3	Suttor River	-20.918070	146.853320	28/03/2004
17	S03	South Suttor	-20.815870	146.839000	18/12/2003
18	S01	South Suttor	-20.775290	146.954380	18/12/2003
19	S06	South Suttor	-20.726030	146.964190	18/12/2003
20	DAM26	South Suttor	-20.727156	146.963174	01/09/2011
21	DAM27	South Suttor	-20.729289	146.966423	01/09/2011
22	S1-7	North Suttor	-20.674020	146.973360	03/08/2005
23	S1-12	North Suttor	-20.674087	146.973097	06/09/2011
24	DAM24	North Suttor	-20.673772	146.973312	01/09/2011
25	DAM25	North Suttor	-20.672494	146.971075	01/09/2011
26	DAM28	North Suttor	-20.654864	146.984225	01/09/2011
27	DAM29	North Suttor	-20.654287	146.986602	01/09/2011
28	DAM30	North Suttor	-20.617549	146.979747	06/09/2011
29	DAM32	North Suttor	-20.606543	146.993903	01/09/2011
30	B4-7	Central Reservoir	-20.608510	147.019530	03/08/2005
31	DAM12	Central Reservoir	-20.608466	147.019929	30/08/2011
32	DAM13	Central Reservoir	-20.606885	147.022430	30/08/2011
33	DAM33	Central Reservoir	-20.627840	147.032496	01/09/2011

Site ID	Study site ID	Location	Latitude	Longitude	Collection date
34	D2-7	Central Reservoir	-20.629860	147.049100	03/08/2005
35	DAM10A	Central Reservoir	-20.628219	147.053377	30/08/2011
36	DAM11	Central Reservoir	-20.618459	147.056689	30/08/2011
37	DAM37	Eastern Reservoir	-20.637271	147.069344	07/09/2011
38	DAM38	Eastern Reservoir	-20.637756	147.066480	07/09/2011
39	DAM39	Eastern Reservoir	-20.645471	147.058809	02/09/2011
40	D61	Eastern Reservoir	-20.648700	147.073030	04/08/2005
41	DAM06	Eastern Reservoir	-20.635326	147.079587	30/08/2011
42	DAM07	Eastern Reservoir	-20.643734	147.080419	30/08/2011
43	DAM09	Eastern Reservoir	-20.659920	147.073360	30/08/2011
44	DAM08	Eastern Reservoir	-20.653348	147.083097	30/08/2011
45	D59	Eastern Reservoir	-20.643310	147.095430	04/08/2005
46	DAM34	Eastern Reservoir	-20.633770	147.111022	07/09/2011
47	DAM35	Eastern Reservoir	-20.640326	147.112686	02/09/2011
48	DAM36	Eastern Reservoir	-20.638379	147.111498	02/09/2011
49	D58	Eastern Reservoir	-20.634520	147.119350	04/08/2005
50	DAM02	Eastern Reservoir	-20.636476	147.133916	29/08/2011
51	DAM03	Eastern Reservoir	-20.641274	147.131612	29/08/2011
52	DAM04	Eastern Reservoir	-20.638194	147.133828	07/09/2011
53	DAM05	Eastern Reservoir	-20.637799	147.133854	30/08/2011
54	D1-7	Eastern Reservoir	-20.640580	147.132310	04/08/2005

Note: Location refers to reservoir sections marked in Figure 4.1.

Particle-size analyses

Samples were wet sieved using a 1.4 mm sieve prior to analysis to remove any coarse particles that would damage the Mastersizer. Twelve percent of samples (n=34) contained organic or inorganic fragments >1.4 mm that were removed from the aliquot.

Table C5 Benthic sediment samples that contained material >1.4 mm removed before particle sizing.

Site ID	Study site ID	Sample Name	Location	Water Depth (m)	Sample Type	Relation to channel
3	DAM14	Dam14-15cm	North Burdekin	19.4	Gravity	In
3	DAM14	Dam14-20cm	North Burdekin	19.4	Gravity	In
15	DAM23	Dam23-38cm	South Burdekin	20	Gravity	In
17	S03	S03SED	South Suttor	6	Grab	In
20	DAM26	Dam26-cc	South Suttor	18.6	Gravity	In
21	DAM27	Dam27-of	South Suttor	3.7	Push	Out
25	DAM25	Dam25-25cm	North Suttor	8.4	Push	Out
25	DAM25	Dam25-33cm	North Suttor	8.4	Push	Out
27	DAM29	Dam29-25cm	North Suttor	8.3	Push	Out
27	DAM29	Dam29-30cm	North Suttor	8.3	Push	Out
27	DAM29	Dam29-35cm	North Suttor	8.3	Push	Out
29	DAM32	Dam32-21cm	North Suttor	7	Push	Out

Site ID	Study site ID	Sample Name	Location	Water Depth (m)	Sample Type	Relation to channel
31	DAM12	Dam12-05cm	Central Reservoir	18.6	Gravity	In
31	DAM12	Dam12-45cm	Central Reservoir	18.6	Gravity	In
31	DAM12	Dam12-50cm	Central Reservoir	18.6	Gravity	In
31	DAM12	Dam12-55cm	Central Reservoir	18.6	Gravity	In
31	DAM12	Dam12-60cm	Central Reservoir	18.6	Gravity	In
31	DAM12	Dam12-65cm	Central Reservoir	18.6	Gravity	In
31	DAM12	Dam12-70cm	Central Reservoir	18.6	Gravity	In
31	DAM12	Dam12-82cm	Central Reservoir	18.6	Gravity	In
31	DAM12	Dam12cc	Central Reservoir	18.6	Gravity	In
36	DAM11	Dam11-26cm	Central Reservoir	6.4	Push	Out
36	DAM11	Dam11-30cm	Eastern Reservoir	7	Push	Out
41	DAM06	Dam06-10cm	Eastern Reservoir	7	Push	Out
41	DAM06	Dam06-15cm	Eastern Reservoir	7	Push	Out
41	DAM06	Dam06-20cm	Eastern Reservoir	7	Push	Out
42	DAM07	Dam07cc	Eastern Reservoir	13	Gravity	Out
43	DAM09	Dam09-26cm	Eastern Reservoir	9.2	Push	Out
47	DAM35	Dam35-25cm	Eastern Reservoir	8.1	Push	Out
48	DAM36	Dam36-09cm	Eastern Reservoir	18.5	Gravity	Out
48	DAM36	Dam36-19cm	Eastern Reservoir	18.5	Gravity	Out
48	DAM36	Dam36-cc	Eastern Reservoir	18.5	Gravity	Out
50	DAM02	Dam02	Eastern Reservoir	N/A	Gravity	Out
53	DAM05	Dam05cc	Eastern Reservoir	19	Gravity	Out

X-Ray diffraction (XRD) analyses

A cross-check of the mineralogical results using software developed by de Caritat et al. (1994) indicated that the identified mineralogy and calculated mineral percentages were appropriate. Compared with XRF major oxide data (data not shown), the quantified mineralogy matched the generated mineral percentages well, although iron was often unable to be fully accounted for.

Loss on ignition

Loss on ignition (LOI; weight percent) was measured gravimetrically for core and grab samples to provide an indication of the combined organic material and carbonate content present; in clay-rich sediment the water of hydration will also have been lost. The LOI was the mass lost from a sample (initial weight 2–5 g, pre-dried at 110°C for one hour to remove pore-water) placed into a pre-weighed porcelain crucible, ignited to 1000°C for four hours, subsequently cooled in a desiccator, and re-weighed, expressed as a percentage.

Assessment of analytical precision and bias for XRF and ICP-MS analyses

Analytical precision of XRF and ICP-MS analyses was assessed using the standard deviation (SD) from a series of repeat analyses of a stable standard (CRM). The relative standard deviation (RSD, in %) was obtained by dividing the SD by the average result of the repeat analyses. Bias was assessed by dividing the average laboratory results for CRMs by the recommended values for that CRM. Bias is expressed as a percentage, where 100% means a perfect match between laboratory results and recommended values (i.e. no bias; de Caritat & Cooper, 2011). Table C3 shows the precision and bias obtained for both analyses.

The ICP-MS calibrations obtained were verified against a range of blanks and CRMs: AGV-2 (andesite, USGS), GSP-2 (granodiorite, USGS), STM-2 (syenite, USGS), and Jlk-1 and STSD-4 (as for XRF). The analytical method divided the elements into four groups. The counts obtained for each analyte were ratioed against one of four isotopes introduced to the solution as internal standards (nickel-61, samarium-147, thullium-169 and thallium-205), one for each of the analyte groups. Inter-element interference factors were determined using a range of single element solutions.

Table C6 Summary data quality assessment for XRF and ICP-MS analyses. LLD = Lower level of detection, RSD = Relative standard deviation, RV = Recommended values.

Parameter/ Element	Unit	LLD	JLK-1 (Japanese Lake sediment) n=4				STSD-4 (Canadian stream sediment) n=3			
			Average	RSD (CRM)	RV	Bias	Average	RSD (CRM)	RV	Bias
XRF										
LOI	%	0	11.69	9%	12	97%	11.65	6%	11.6	100%
Al_2O_3	%	0.005	16.63	1%	16.73	99%	12.01	1%	12.1	99%
As	mg/kg		28.88	4%	26.8	108%	13.20	5%	15	88%
Ba	mg/kg		580.50	3%	574	101%	1933.00	1%	2000	97%
CaO	%	0.002	0.67	2%	0.686	98%	4.02	1%	4	101%
Ce	mg/kg		71.25	19%	87.9	81%	31.33	85%	44	71%
Cl	mg/kg	10	76.00	49%	N/A	N/A	174.00	24%	N/A	N/A
Cr	mg/kg		70.00	18%	69	101%	92.33	9%	93	99%
Cs	mg/kg		24.25	40%	10.9	222%	9.67	32%	N/A	N/A
Cu	mg/kg	10	61.65	2%	62.9	98%	62.33	8%	65	96%
F	mg/kg	50	684.75	29%	589	116%	514.33	45%	380	135%
Fe_2O_3	%	0.005	6.73	1%	4.251	158%	5.58	1%	5.7	98%
K_2O	%	0.005	2.78	1%	2.805	99%	1.60	1%	1.6	100%
La	mg/kg		38.50	32%	40.6	95%	24.00	22%	24	100%
MgO	%	0.01	1.73	2%	1.736	99%	2.13	0%	2.13	100%
MnO	%	0.005	0.26	1%	0.266	96%	0.19	1%	0.19	101%
Mo	mg/kg		-1.45	-78%	2.19	-66%	4.30	21%	N/A	N/A

Parameter/ Element	Unit	LLD	JLK-1 (Japanese Lake sediment) n=4				STSD-4 (Canadian stream sediment) n=3			
			Average	**RSD (CRM)**	**RV**	**Bias**	**Average**	**RSD (CRM)**	**RV**	**Bias**
Na_2O	%	0.01	1.09	2%	1.051	103%	2.73	1%	2.7	101%
Nb	mg/kg		18.23	16%	15.8	115%	7.00	32%	9	78%
Nd	mg/kg		32.00	17%	35.7	90%	14.33	36%	21	68%
Ni	mg/kg	10	39.08	20%	35	112%	36.57	14%	30	122%
P_2O_5	%	0.005	0.21	2%	0.208	100%	0.22	3%	0.22	98%
Pb	mg/kg		38.10	9%	43.7	87%	18.43	22%	18	102%
Rb	mg/kg	10	138.25	2%	147	94%	44.43	2%	39	114%
Sc	mg/kg		10.58	21%	15.9	67%	12.27	43%	14	88%
SiO_2	%	0.01	57.06	1%	57.16	100%	58.56	1%	58.9	99%
SO_3	mg/kg	10	0.25	4%	0.26	97%	0.23	3%	N/A	N/A
Sr	mg/kg	10	65.95	11%	67.5	98%	360.57	1%	350	103%
Th	mg/kg		26.23	13%	19.5	134%	5.70	143%	N/A	N/A
TiO_2	%	0.005	0.68	1%	0.668	101%	0.70	1%	0.76	93%
U	mg/kg		5.05	34%	3.83	132%	5.60	8%	N/A	N/A
V	mg/kg		105.80	6%	117	90%	102.83	10%	106	97%
Y	mg/kg		45.13	11%	40	113%	23.90	19%	24	100%
Zn	mg/kg	10	146.10	1%	152	96%	95.90	3%	107	90%
Zr	mg/kg	10	130.25	4%	137	95%	201.80	6%	190	106%
ICP-MS										
Ag	mg/kg	0.03	0.05	14%	0.198	28%	0.07	9%	<0.5	N/A
As	mg/kg	0.4	20.38	5%	26.8	76%	10.43	4%	15	70%
Ba	mg/kg	0.5	571.84	2%	574	100%	1902.79	1%	2000	95%
Be	mg/kg	1.1	3.15	9%	3.31	95%	1.74	26%	1.7	102%
Bi	mg/kg	0.02	1.73	2%	N/A	N/A	0.33	4%	N/A	N/A
Cd	mg/kg	0.1	0.22	30%	0.572	39%	0.18	49%	N/A	N/A
Ce	mg/kg	0.03	86.35	5%	87.9	98%	42.09	5%	44	96%
Co	mg/kg	0.1	18.06	4%	18	100%	13.85	1%	13	107%
Cr	mg/kg	0.5	66.05	8%	69	96%	89.01	3%	93	96%
Cs	mg/kg	0.1	13.35	1%	10.9	122%	1.75	2%	1.9	92%
Cu	mg/kg	0.2	65.46	5%	62.9	104%	71.39	5%	65	110%
Dy	mg/kg	0.1	7.83	5%	6.57	119%	4.33	1%	3.8	114%
Er	mg/kg	0.03	4.21	2%	3.59	117%	2.39	4%	N/A	N/A
Eu	mg/kg	0.03	1.35	1%	1.27	107%	1.31	3%	1.2	109%
Ga	mg/kg	0.1	23.81	3%	21.4	111%	14.46	8%	N/A	N/A
Gd	mg/kg	0.03	7.64	0%	6.02	127%	4.47	4%	N/A	N/A
Ge	mg/kg	0.04	1.21	2%	N/A	N/A	0.97	6%	N/A	N/A
Hf	mg/kg	0.04	3.75	2%	3.78	99%	5.15	6%	5.5	94%
Ho	mg/kg	0.02	1.54	4%	1.06	146%	0.86	0%	N/A	N/A
La	mg/kg	0.1	40.58	5%	40.6	100%	20.98	6%	24	87%
Lu	mg/kg	0.02	0.62	1%	0.571	109%	0.36	0%	0.5	73%
Mo	mg/kg	0.3	3.31	13%	2.19	151%	3.15	31%	2.5	126%
Nb	mg/kg	0.03	16.32	0%	15.8	103%	7.96	2%	9	88%

Parameter/ Element	Unit	LLD	JLK-1 (Japanese Lake sediment) n=4				STSD-4 (Canadian stream sediment) n=3			
			Average	RSD (CRM)	RV	Bias	Average	RSD (CRM)	RV	Bias
Nd	mg/kg	0.1	36.38	1%	35.7	102%	22.06	1%	21	105%
Ni	mg/kg	0.5	49.54	36%	35	142%	32.63	13%	30	109%
Pb	mg/kg	0.1	46.71	1%	43.7	107%	18.68	2%	16	117%
Pr	mg/kg	0.02	9.02	1%	8.53	106%	5.24	2%	N/A	N/A
Rb	mg/kg	0.2	142.02	3%	147	97%	37.97	1%	39	97%
Sb	mg/kg	0.4	1.68	32%	1.68	100%	5.38	47%	7.3	74%
Sc	mg/kg	0.3	17.26	4%	15.9	109%	13.18	7%	14	94%
Sm	mg/kg	0.04	8.07	3%	7.87	103%	4.53	4%	5	91%
Sn	mg/kg	0.2	4.52	7%	5.7	79%	1.46	26%	2	73%
Sr	mg/kg	0.2	69.93	4%	67.5	104%	380.16	2%	350	109%
Ta	mg/kg	0.02	1.31	1%	1.57	83%	0.52	2%	0.6	86%
Tb	mg/kg	0.02	1.18	1%	1.23	96%	0.66	0%	0.8	82%
Th	mg/kg	0.02	19.31	4%	19.5	99%	3.74	21%	4.3	87%
U	mg/kg	0.02	3.99	0%	3.83	104%	3.16	12%	3	105%
V	mg/kg	0.1	117.19	1%	117	100%	110.23	4%	106	104%
W	mg/kg	0.1	2.00	10%	3.99	50%	0.52	10%	2	26%
Y	mg/kg	0.05	45.52	8%	40	114%	24.36	12%	24	101%
Yb	mg/kg	0.04	4.34	2%	3.99	109%	2.37	0%	2.6	91%
Zn	mg/kg	0.9	143.59	4%	152	94%	95.08	1%	107	89%
Zr	mg/kg	0.2	132.68	5%	137	97%	200.64	1%	190	106%

C.2 Additional results

Detailed particle-size results

Particle-size distributions of benthic sediment from the BFD reservoir were predominantly unimodal to bimodal (Figure 4.4). The secondary population in bimodal samples was mostly minor, contributing a peak with a mode <4%. Most sediment particles were >0.9 µm. 17% of samples contained particles <0.9 µm; in all but two samples the <0.9 µm component was <3% of the total (core samples *51 - 40 cm*, 10.5% and *44 - 85 cm*, 15.6%). Particles <0.5 µm were found in only six core samples and comprised <0.5% of all but two of those samples (the two exceptions contained 8%–12% of <0.5 µm particles and were from the Eastern Reservoir).

Sediment samples from North and South Burdekin reservoir cores displayed variable particle-size distributions (Figure 4.4a, b). The primary modes of sediment from both in and out of the channel varied from 8 to 251 µm. North Burdekin in-channel core samples from 15 to 20 cm depth were coarser (modes at 224–251 µm), while samples from below 25 cm displayed consistent particle-size distributions with modes at 18–63 µm and small secondary modes

(<0.7%) at 447–500 μm. A similar distribution was seen in in-channel cores from the South Burdekin where samples from 15 to 20 cm depths displayed coarser modes (100–159 μm), with all other samples producing modes at 15–56 μm. Core samples from out of the channel had modes from 5 to 112 μm (Figure 4.4a, b). In the North Burdekin, samples from the top (5–10 cm) and bottom (25 cm) of the out of channel core were coarser (modes at 11–112 μm) than the intermediate depth samples (15–20 cm, 5–7 μm).

Samples from the South Suttor produced distributions with coarse modes (126–400 μm) in all but the shallowest samples (Figure 4.4c). The in-channel samples consisted of one sample of combined core sediment (equivalent to a grab sample) and one of material from the core catcher. Core sediment was evenly bimodal (5 and 400 μm at 3.5%–3.8%) but sediment from the core catcher was sand to coarse gravel in size (63 to 8,000 μm) and only the <2 mm fraction was grainsized; this sample was considered pre-existing material. Material collected outside of the channel was uniform in size (primary mode at 112–159 μm, secondary mode at 5–7 μm) except for the top 5 cm, which was much finer (primary mode at 5.6 μm, secondary mode at 141 μm).

Core sediments from the North Suttor produced very consistent size distributions with modes at 4.5–13 μm although the distributions of some deeper sediments were broader with a lower volume (4%–4.3%, Figure 4.4d). In-channel samples from further upstream in the North Suttor section (site 24, not shown) had similar unimodal distributions centred on 3.5–5.6 μm. Out-of-channel samples from above 25 cm depth produced primarily unimodal peaks at 4–6 μm. Samples from ≥25 cm depth were coarser with modes at 159–178 μm and were classified as pre-existing material due to the variation in particle size and the presence of organic material (leaves, clumps of plant roots).

The particle-size distribution of both in- and out-of-channel sediments were very consistent down core in the Central and Eastern reservoir sections (Figure 4.4e, f). In the Central Reservoir, in-channel sediments produced modes of 22–28 μm and minor secondary modes (<0.3%) at 447 μm. The size distribution for the sample from the very bottom of core 35 (78 cm) matched those for samples from the top 20 cm of the out-of-channel core (36) which were unimodal with a peak at 5–8 μm. The out-of-channel core was collected in a shallow water (6.4 m) embayment (Figure 4.1, site 11). Out-of-channel samples from below 20 cm depth had very different size distribution (Figure 4.4e) and contained granule-sized particles (2–4 mm) prior to analysis; these samples were designated pre-existing sediment.

Samples from the core collected in-channel in the Eastern Reservoir nearest to the dam wall (Figure 4.4f) produced size distribution patterns like those for in-channel North Suttor sediments with modes at 4–6 µm and, secondary modes at 0.2 µm and 447−563 µm (Figure 4.4f). Samples from the lower section of the core (below 45 cm) were slightly coarser (mode at 10–13 µm). The same distribution was observed for core samples from site 44, with modes at 3−20 µm and 447−563 µm (not shown). Samples from out-of-channel grab samples (Figure 4.4f) and cores (Figure 4.1, sites 43 and 47; not shown) produced similar distributions with modes at 4−7 µm.

Loss on ignition

The median measured LOI for benthic (core and grab) sediment was 11.3% (range 1.3%–37.4%). The ranges for sediments from the Burdekin and Suttor sections were similar (1.3%–18.9% and 1.3%−15.2% respectively). Central Reservoir samples had the largest range of LOI values, 4.8%–37.4%, but this dropped to 4.8%−14.3% when the five samples from core 31 that were rich in leaf material were excluded. Eastern Reservoir samples had a slightly smaller range of LOI (3.8%–15.1%).

Table C7 The Sr and Nd isotopic ratios of benthic and suspended sediments from Lake Dalrymple.

Sample Site ID	Date	Sediment type	Location	Sr (ppm)	Nd (ppm)	$^{87}Sr/^{86}Sr$	±2-σ ($x10^{-6}$) (Sr)	$^{143}Nd/^{144}Nd$	±2-σ ($x10^{-6}$) (Nd)	εNd
1	Dec '03	Benthic	Burdekin River	107	41.2	0.7254	8.7	0.512108	9.2	-11.2
2	Dec '03	Benthic	North Burdekin	117	45.4	0.7239	1.0	0.512116	9.2	-11.1
6	Aug '05	Benthic	North Burdekin	125	32.1	0.7211	7.2	0.512065	9.2	-12.0
14	Dec '03	Benthic	South Burdekin	96	43.7	0.7278	8.7	0.512160	1.3	-10.2
16	Mar '04	Benthic	Suttor River	77	42.3	0.7298	8.8	0.512166	8.2	-10.1
17	Dec '03	Benthic	South Suttor	84	36.9	0.7279	7.3	0.512153	5.1	-10.3
18	Dec '03	Benthic	South Suttor	69	38.8	0.7256	8.7	0.512164	1	-10.1
19	Dec '03	Benthic	South Suttor	83	43.1	0.7321	8.8	0.512119	9.2	-11.0
22	Aug '05	Benthic	North Suttor	80	41.1	0.7319	7.3	0.512153	4.9	-10.3
30	Aug '05	Benthic	Central Reservoir	138	45.4	0.7229	8.7	0.512122	1	-11.0
34	Aug '05	Benthic	Central Reservoir	112	40.9	0.7242	7.2	0.512202	1	-9.4
40	Aug '05	Benthic	Eastern Reservoir	100	39.3	0.7261	8.7	0.512158	5	-10.2
45	Aug '05	Benthic	Eastern Reservoir	109	42.6	0.7265	7.3	0.512157	7.2	-10.3
49	Aug '05	Benthic	Eastern Reservoir	104	43.2	0.7272	8.7	0.512162	8.2	-10.2
54	Aug '05	Benthic	Eastern Reservoir	99	43.2	0.7275	8.7	0.512171	21.5	-10.0
1	Dec '03	Suspended	Burdekin River	135	29.5	0.7160	8.6	0.512288	13	-7.7
6*	Mar/Apr '06	Suspended	North Burdekin	143	34.8	0.7235	7.2	0.512133	16	-10.7
6*	Oct '06	Suspended	North Burdekin	433	13.1	0.7138	10	0.512219	8.6	-9.1
16	Mar '04	Suspended	Suttor River	330	21.3	0.7155	8.6	0.512211	10	-9.2
22*	Mar/Apr '06	Suspended	South Suttor	293	23.4	0.7163	10	0.512167	7.2	-10.1
22*	Oct '06	Suspended	North Suttor	408	14.2	0.7141	10	0.512245	7.2	-8.6
34*	Mar/Apr '06	Suspended	Central Reservoir	180	32.9	0.7204	8.6	0.512136	10	-10.7
34*	Oct '06	Suspended	Central Reservoir	404	14.7	0.7141	10	0.512218	10	-9.1
54	Feb '04	Suspended	Eastern Reservoir	196	30.0	0.7193	8.6	0.512140	7.2	-10.6
54*	Mar/Apr '06	Suspended	Eastern Reservoir	322	24.7	0.7159	10	0.512141	8.2	-10.6
54*	Oct '06	Suspended	Eastern Reservoir	351	13.1	0.7141	10	0.512206	11	-9.3

* = A combination of water samples collected at this location (at varying depths) during three sampling trips between 29 March and 14 April 2006 (wet) or of samples collected on 11 October 2006 (dry).

Figure C3 (next page) Daily discharge through the Burdekin River at the Hydro Site (gauge 120015A), Burdekin River at Sellheim (120002C), Suttor River at St Anns (120303A) and Cape River at Taemas (120302B) water monitoring stations. Note: Y-axis scale does not show maximum discharge values to accentuate smaller discharges from the Suttor and Cape rivers. Burdekin Falls Dam reservoir volume is shown (black) and wet season months are marked by vertical grey bars. Burdekin Falls Dam reservoir volume data obtained from Sunwater Limited ACN 131034985 (M. Ali, Bureau of Meteorology, pers. comm.; July 2002–July 2016).

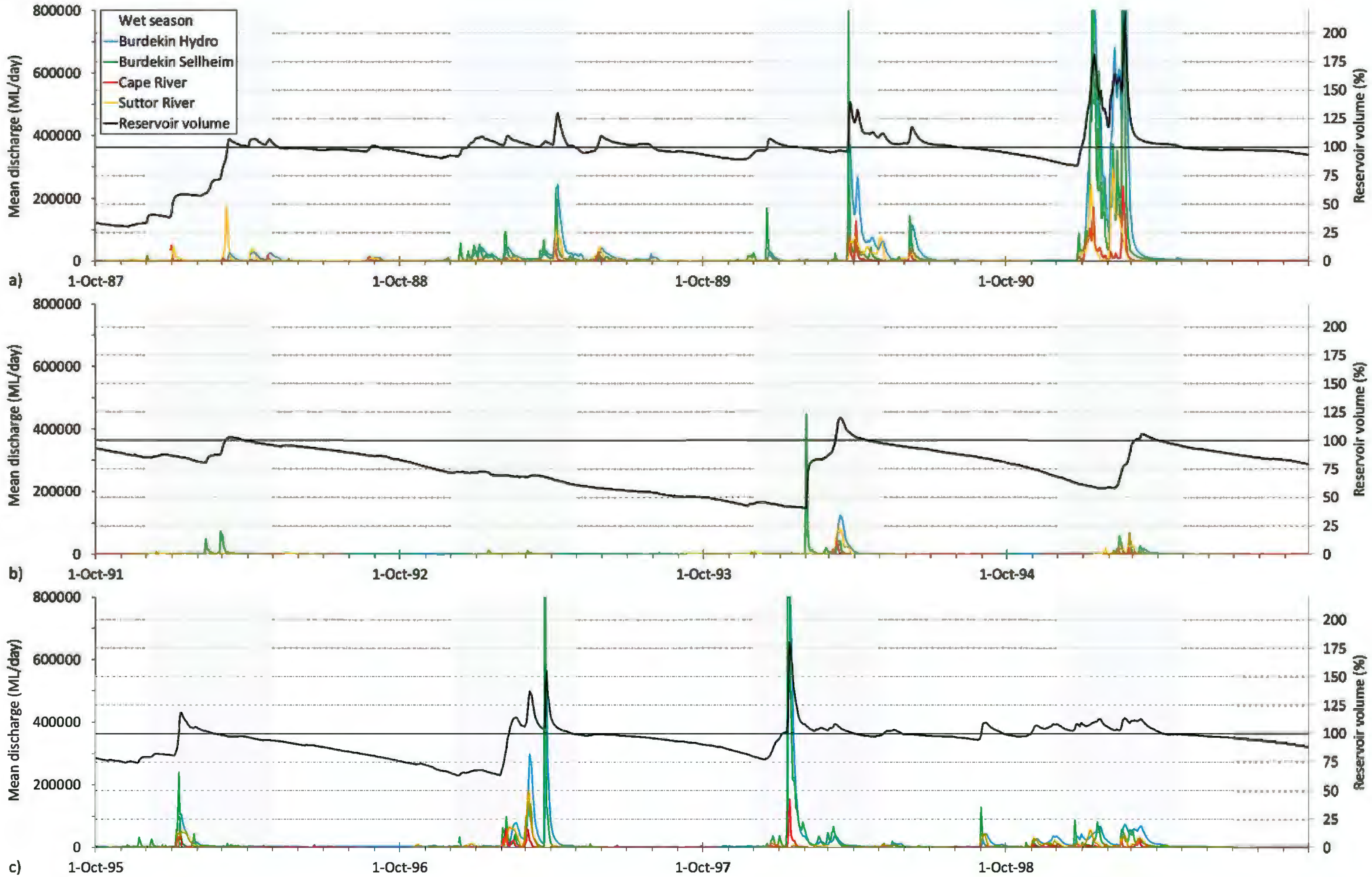

Wet season
Burdekin Hydro
Burdekin Sellheim
Cape River
Suttor River
Reservoir volume
Mean discharge (ML/day)
Reservoir volume (%)
800000
600000
400000
200000
0
200
175
150
125
100
75
50
25
0
a)
1-Oct-87
1-Oct-88
1-Oct-89
1-Oct-90
b)
1-Oct-91
1-Oct-92
1-Oct-93
1-Oct-94
c)
1-Oct-95
1-Oct-96
1-Oct-97
1-Oct-98

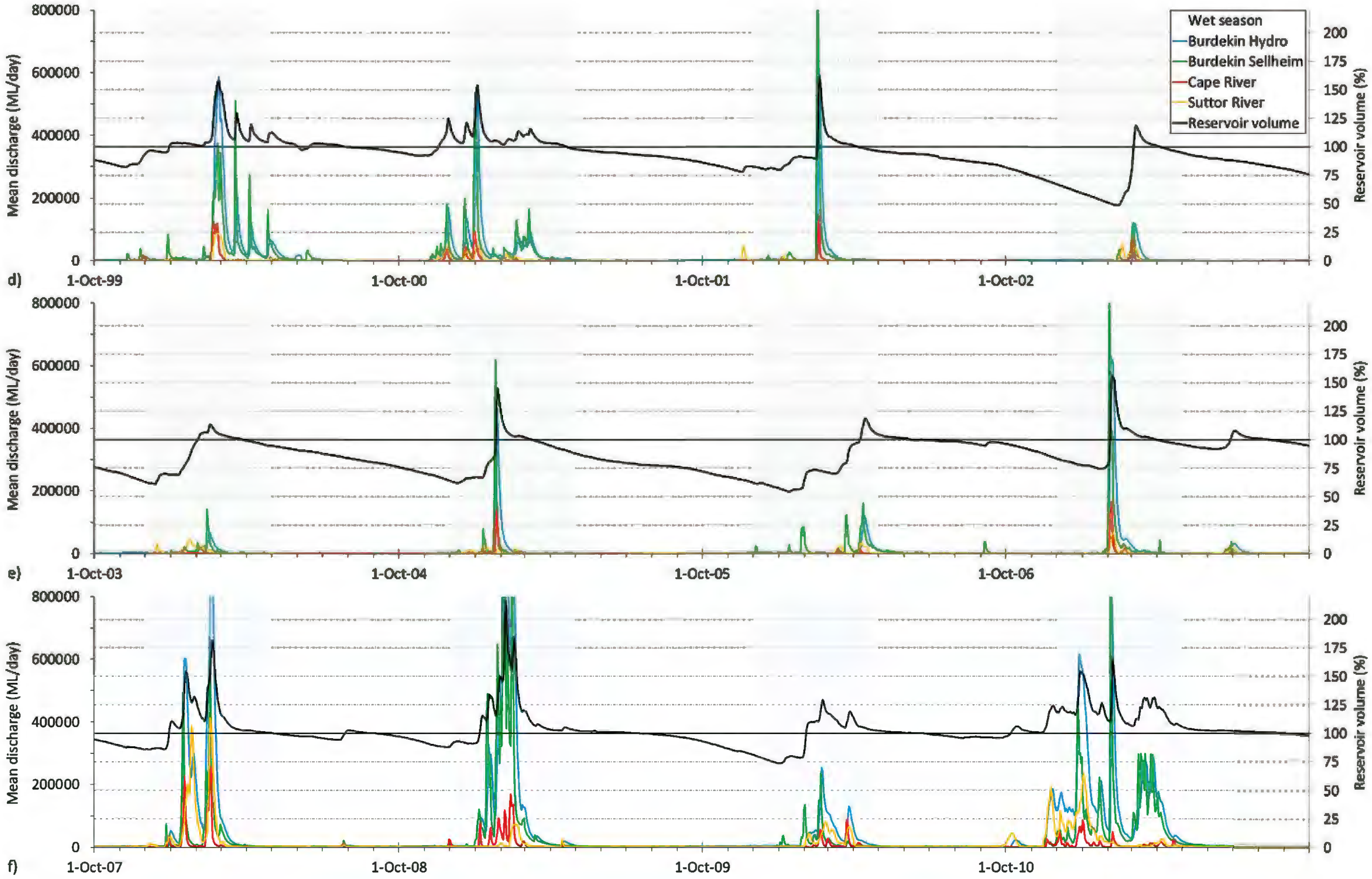

Wet season
Burdekin Hydro
Burdekin Sellheim
Cape River
Suttor River
Reservoir volume
Mean discharge (ML/day)
Reservoir volume (%)
800000
600000
400000
200000
0
200
175
150
125
100
75
50
25
0
d)
1-Oct-99
1-Oct-00
1-Oct-01
1-Oct-02
e)
1-Oct-03
1-Oct-04
1-Oct-05
1-Oct-06
f)
1-Oct-07
1-Oct-08
1-Oct-09
1-Oct-10

Appendix D: Chapter 5 supplementary material

Discharge and annual sediment load data for each of the key water monitoring stations upstream of the Burdekin Falls Dam plus calculated annual trap efficiencies.

Table D1 Discharge and annual sediment load data for each of the key water monitoring stations upstream of the Burdekin Falls Dam (locations in Figure **5.1**). These values multiplied by the calculated annual trap efficiencies give the volume of sediment trapped in the reservoir annually.

Water Year	Discharge - Burdekin at Sellheim gauge (ML)	Burdekin at Sellheim load (tonnes)	Discharge - Cape at Taemas gauge (ML)	Cape at Taemas load (tonnes)	Discharge - Belyando at Gregory Develop-mental Rd gauge (ML)	Belyando at Gregory Develop-mental Rd load (tonnes)	Discharge - Suttor at St Anns (minus Belyando River) gauge (ML)	Suttor at St Anns load (tonnes)	Sub-total flow	Discharge - Burdekin River at Hydro Site gauge (ML)	Discharge - Hydro Site gauge minus sub-total (ungauged above the dam estimate)	Ungauged load (tonnes)	Total suspended sediment load into Burdekin Dam	% Trapping each year (based on revised Churchill)	Sediment trapped (tonnes)	% Trapping each year - increased reservoir volume	Sediment trapped (tonnes)
1987–88	249,397	184,554	229,656	49,376	400,747	56,105	1,017,297	152,595	1,897,097	1,272,777	0	0	442,629	100.0%	442,629	100.0	442,629
1988–89	3,011,879	2,228,791	464,379	99,841	684,372	95,812	668,606	100,291	4,829,237	5,086,303	257,067	61,696	2,586,431	90.3%	2,335,547	92.6	2,395,032
1989–90	3,784,310	2,800,390	774,113	166,434	1,294,274	181,198	911,156	136,673	6,763,854	7,255,462	491,608	117,986	3,402,682	81.9%	2,786,796	85.0	2,892,680
1990–91	19,226,559	14,227,654	2,882,649	619,769	1,367,741	191,484	3,285,364	492,805	26,762,313	29,088,744	2,326,430	558,343	16,090,055	53.9%	8,672,540	59.9	9,645,943
1991–92	655,269	484,899	9,275	1,994	71,763	10,047	39,106	5,866	775,412	848,315	72,903	17,497	520,303	100.0%	520,303	100.0	520,303
1992–93	189,871	140,504	2,064	444	49,604	6,945	0	0	241,539	698,676	457,137	109,713	257,606	100.0%	257,606	100.0	257,606
1993–94	1,410,312	1,043,631	214,177	46,048	556,933	77,971	424,444	63,667	2,605,865	2,018,725	0	0	1,231,316	92.9%	1,143,892	94.9	1,168,219
1994–95	589,066	435,909	107,524	23,118	332,378	46,533	212,617	31,893	1,241,585	1,029,686	0	0	537,452	100.0%	537,452	100.0	537,452
1995–96	1,232,287	911,892	153,244	32,947	240,824	33,715	474,025	71,104	2,100,380	1,779,867	0	0	1,049,659	96.3%	1,010,822	98.0	1,028,349
1996–97	4,148,440	3,069,845	568,079	122,137	1,157,007	161,981	1,054,113	158,117	6,927,639	6,276,542	0	0	3,512,080	78.7%	2,764,007	82.2	2,885,360
1997–98	8,455,085	6,256,763	584,268	125,618	275,906	38,627	267,416	40,112	9,582,676	8,041,380	0	0	6,461,120	67.1%	4,335,411	71.8	4,638,637
1998–99	2,288,784	1,693,700	315,108	67,748	494,934	69,291	1,175,628	176,344	4,274,454	4,932,552	658,098	157,944	2,165,027	93.3%	2,019,970	95.2	2,061,621
1999–00	7,869,179	5,823,193	1,117,271	240,213	599,237	83,893	557,723	83,658	10,143,410	10,499,391	355,982	85,436	6,316,393	73.3%	4,629,916	77.3	4,882,939
2000–01	6,982,992	5,167,414	946,001	203,390	350,189	49,026	786,772	118,016	9,065,954	8,570,716	0	0	5,537,847	80.0%	4,430,277	83.4	4,617,486
2001–02	3,900,067	2,886,050	419,131	90,113	249,113	34,876	109,690	16,454	4,678,002	4,387,513	0	0	3,027,492	73.5%	2,225,207	77.5	2,346,070
2002–03	830,434	614,521	256,645	55,179	323,088	45,232	335,493	50,324	1,745,660	1,833,243	87,583	21,020	786,276	96.3%	757,184	97.9	769,900
2003–04	1,034,601	765,605	58,567	12,592	473,145	66,240	386,738	58,011	1,953,050	1,661,578	0	0	902,447	99.0%	893,423	100.0	902,447
2004–05	2,177,518	1,611,363	550,819	118,426	264,831	37,076	218,144	32,722	3,211,312	3,682,938	471,626	113,190	1,912,778	78.8%	1,507,269	82.2	1,573,108
2005–06	2,713,715	2,144,300	92,402	33,500	279,580	182,200	247,676	96,070	3,333,373	2,078,214	0	10,000	2,466,070	94.6%	2,332,902	96.4	2,377,849
2006–07	4,403,239	3,068,700	781,832	189,200	259,810	128,300	456,616	100,380	5,901,497	6,458,807	557,311	360,000	3,846,580	70.7%	2,719,532	75.0	2,885,229
2007–08	6,236,149	4,663,100	2,324,162	502,700	3,372,544	210,650	3,598,665	706,354	15,531,519	18,070,058	2,538,539	150,000	6,232,804	61.5%	3,833,174	66.7	4,159,577
2008–09	19,499,167	15,006,800	2,330,970	473,200	357,799	106,705	665,839	137,325	22,853,775	25,092,557	2,238,782	300,000	16,024,030	53.3%	8,540,808	59.4	9,519,007
2009–10	2,608,895	1,706,100	774,415	161,400	936,976	162,550	1,133,858	223,390	5,454,143	5,597,646	143,503	200,000	2,453,440	85.9%	2,107,505	88.7	2,175,263
2010–11	17,096,589	7,588,188	1,805,449	359,291	2,585,284	506,684	4,679,010	701,851	26,166,332	28,225,547	2,059,215	494,212	9,650,226	70.9%	6,842,011	75.2	7,257,970
2011–12	6,589,000	2,400,000	1,515,000	220,000	1,861,000	160,000	1,720,024	118,947	11,685,024	13,047,343	1,362,319	326,957	3,225,903	70.0%	2,258,132	74.4	2,399,845
2012–13	1,932,000	610,000	117,000	12,000	56,000	19,000	305,787	67,693	2,410,787	2,179,788	0	0	708,693	97.2%	688,850	98.7	699,661
2013–14	1,800,000	2,100,000	5,347	1,150	195,276	27,339	78,652	11,798	2,079,275	1,605,693	0	0	2,140,286	100.0%	2,140,286	100.0	2,140,286
2014–15	260,000	56,000	41,521	8,927	211,606	29,625	380,609	57,091	893,736	1,158,535	264,799	63,552	215,195	100.0%	215,195	100.0	215,195

Trapping Efficiency and sediment trapped – to end water year 2010–11	69.7%	67,646,183 t
Trapping Efficiency and sediment trapped – to end water year 2014–15	70.5%	72,948,647 t
Trapping Efficiency and sediment trapped after dam wall raised 2 m – to end water year 2010–11	74.1%	71,940,678 t
Trapping Efficiency and sediment trapped after dam wall raised 2 m – to end water year 2014–15	74.8%	77,395,665 t
Average annual sediment load – to end water year 2014–15		2,605,309 t

Note: 2011–12 and 2012–13 data from Wallace et al. (2014) and Wallace et al. (2015) – excluding Suttor discharge volume values which were taken from the water monitoring portal (https://water-monitoring.information.qld.gov.au/)
References in the main manuscript.